Quantitative and functional significance of novel organic nanoparticles in aquatic food webs

Maxime Fuster

École doctorale 65 : Sciences de la Vie, Santé, Agronomie, Environnement

THÈSE

Pour obtenir le grade de
Docteur de l'Université Clermont Auvergne
Spécialité Microbiologie

Présentée et soutenue publiquement le 01-07-2022 par
Maxime Fuster

Importance quantitative et fonctionnelle de nanoparticules organiques inédites dans les réseaux trophiques aquatiques

Jury

Patricia Bonin	Examinatrice	Université Aix-Marseille
Claire Geslin	Rapportrice	Université Bretagne Occidentale
Olivier Pringault	Rapporteur	Institut de Recherche pour le Développement
Cécile Lepère	Examinatrice	Université Clermont Auvergne
Jonathan Colombet	Co-encadrant de thèse	Université Clermont Auvergne
Télesphore Sime-Ngando	Directeur de thèse	Université Clermont Auvergne

Laboratoire Microorganismes : Génome Environnement
LMGE
UMR CNRS 6023, F-63000, Clermont-Ferrand

Remerciements

Tout d'abord un grand merci au Dr Claire Geslin et au Dr Olivier Pringault d'avoir accepté d'être les rapporteurs de ce manuscrit. Merci également au Dr Patricia Bonin et au Dr Cécile Lepère d'avoir accepté de faire partie de mon jury de thèse. Je tenais également à remercier le Dr Isabelle Batisson, le Dr Guillaume Borrel et le Dr Karim Benzerara d'avoir fait partie de mon comité de thèse et d'avoir apporté leur expertise scientifique à ce sujet.

Je tenais à remercier mon directeur de thèse, Télesphore Sime-Ngando de m'avoir fait confiance depuis le départ pour réaliser en toute sérénité cette thèse. Ce fut un plaisir pour moi d'échanger avec vous tout au long de ces quatre années. Je tiens également à remercier ici l'équipe BioAdapt de m'avoir accueilli durant ce temps.

Un grand merci à mon encadrant Jonathan ainsi qu'à Hermine pour ces années. Je ne sais pas par où commencer tellement je pourrais citer d'anecdotes… les proverbes mémorables de Jo, nos sorties terrains et le fameux ponton de Lapeyrouse, mes cascades en salle cyto ou dans les barbelés, la spécialité des Vosges… En tout cas, travailler à vos côtés m'a énormément appris et m'as permis de grandir, tant d'un point de vue scientifique qu'humain et je ne pourrai jamais assez vous remercier pour tout ce que vous avez fait pour moi durant ces quatre années.

Une pensée également pour l'équipe MEB qui m'a accueilli durant mon M2 et qui a su me donner envie de me lancer dans cette aventure. Collaborer avec toi Gisèle fut un vrai plaisir, merci à toi. Agnès, Anne, Cécile et Corinne qui ont toujours été là, même durant cette thèse pour discuter autour d'un café ou d'un verre et sur qui j'ai toujours pu compter. Je suis sûr que sans vous, je n'aurais jamais pu me lancer dans cette aventure. Encore merci à vous du fond du cœur.

Merci également à tous les collègues pour ces moments de convivialité et de discussion autour d'un repas, d'un café ou au détour d'un couloir. Tous vous citer serait beaucoup trop long mais cette thèse n'aurait certainement pas eu la même saveur sans ces moments. Une pensée notamment pour les membres de l'équipe IRTA qui m'ont gentiment intégré et surtout supporté pendant ces quatre années ! Ces moments passés avec vous ont toujours été mémorables ! Une pensée spéciale notamment pour Clacla, j'ai énormément apprécié de collaborer avec toi.

Fanny, merci de m'avoir supporté dans le bureau, je sais que cela n'a pas dû être chose facile tout le temps…. (mais je te rassure c'était réciproque :D). Tous ces fous rires et ces bons moments passés ont contribué au bon déroulement de cette thèse. Marine, je cherche un mot gentil à t'écrire mais bizarrement je ne trouve rien… Je ne pensais pas que l'on pouvait à la fois détester mais aussi apprécier quelqu'un comme ça ! En vrai, merci à toi d'avoir toujours été là et d'avoir toujours su m'écouter. Tu sais très bien que quoi qu'il arrive, je serai derrière toi pour te mettre une soufflante ou pour te féliciter ; merci pour tout. Thomas, te supporter toi en revanche fut un véritable plaisir (solidarité…) ! Toujours avec moi pour faire des blagues de « mauvais goût » ou des « conneries » dans le labo mais également toujours là pour me conseiller, je ne te remercierai jamais assez. Peut-être qu'un jour nos parties de pêche seront fructueuses… En attendant on se consolera à BeerLand ou autour d'un bon barbecue comme toujours.

Merci également à vous Max, Alex, Arthur, Laura, Hélène, Nasta et Martial. Vous savez que je vous considère comme ma famille et sans vous je n'aurais jamais été capable d'être celui que je suis aujourd'hui. Ju et Maé, Camille et Bérenger, malgré la distance vous avez toujours été là pour moi. Toujours présents dans les bons moments comme dans ceux qui l'étaient moins, je sais que je pourrai toujours compter sur vous tous. Un simple merci ne suffit pas…

Merci également à ceux qui me supportent et me soutiennent dans tous mes choix depuis presque 28 ans maintenant, ma famille. Mes parents, mon frère, mais également tous les autres, je vous aime. Enfin, merci à toi de me supporter et de me soutenir depuis 9 ans maintenant. Sans toi, tout cela n'aurait jamais existé. SUMUSUPUTUBULU.

Il y aura certainement des oublis durant ces remerciements mais sachez que je remercie vraiment du fond du cœur chaque personne qui de près ou de loin m'a permis d'être devenu celui que je suis aujourd'hui.

Abréviations

ALNs: Aster Like Nanoparticles

ATP: Adenosine TriPhosphate

BMOPs: Biomimetic Mineral–Organic Particles

CPR: *Candidate Phyla Radiation*

DNA: Deoxyribonucleic Acid

DPANN: *Diapherotrites, Parvarchaeota, Aenigmarchaeota, Nanoarchaeota, Nanohaloarchaea*

EVs: Extracellular Vesicles

GTAs: Gene Transfer Agents

HGT: Horizontal Gene Transfer

LUCA: Last Universal Common Ancestor

OTU: Operational Taxonomic Unit

RNA: Ribonucleic Acid

TMCV: Theoretical Minimal Cell Volume

VLPs: Viral Like Particles

Table des matières

INTRODUCTION GÉNÉRALE 1

ÉTAT DE L'ART / DÉCOUVERTE DES ALNs 13

2.1 Le compartiment femtoplanctonique : source de nouvelles connaissances en biologie et en écologie 15

Femtoplankton: What's New? 15

2.1.1 Abstract 15

2.1.2 Introduction 17

2.1.3 From Mineral to Biotic Entities: A Path Toward the Living Being? 19

2.1.4 Quantitative and Functional Significances of Femtoplankton 45

2.1.5 Conclusions 59

2.2 Découverte de nouvelles entités femtoplanctoniques : les Aster-Like Nanoparticles 61

Discovery of High Abundances of Aster-Like Nanoparticles in Pelagic Environments: Characterization and Dynamics 61

2.2.1 Abstract 61

2.2.2 Introduction 63

2.2.3 Materials and Methods 65

2.2.4 Results 77

2.2.5 Discussion 87

2.2.6 Conclusion 97

2.2.7 Supplemental materials 101

2.3 Conclusions 103

CHAPITRE 1 : ÉTUDE DE LA VARIABILITÉ SPATIALE DES ALNs 105

Trophic Conditions Influence Widespread Distribution of Aster-Like Nanoparticles Within Aquatic Environments 107

3.1 Abstract 109

3.2 Note 109

3.3 Supplemental materials 117

3.4 Conclusions 123

CHAPITRE 2 : ÉTUDE *IN-SITU* DE LA VARIABILITÉ TEMPORELLE DES ALNs 125

Occurrence and seasonal dynamics of ALNs in freshwater lakes are influenced by their biological environment 129

4.1 Abstract 129

4.2 Introduction 129

4.3 Materials and methods 133

4.4 Results 139

4.5 Discussion 147

4.6 Supplemental materials 151

4.7 Conclusions 155

CHAPITRE 3 : INTERACTIONS ENTRE ALNs ET PROCARYOTES EN CONDITIONS CONTROLÉES 157

5.1 Interactions between concentration of prokaryotes and concentration of ALNs in *in-vitro* conditions 161

5.1.1 Introduction 161

5.1.2 Materials and methods 163

5.1.3 Results 167

5.1.4. Discussion and conclusion 173

5.1.5 Supplemental materials 177

5.2 Long-term incubation of ALNs in lake water: Development of specific communities 179

Long-Term Incubation of Lake Water Enables Genomic Sampling of Consortia Involving Planctomycetes and Candidate Phyla Radiation Bacteria 179

5.2.1 Abstract 179

5.2.2 Note 181

5.2.4 Discussion and conclusion 187

5.2.5 Supplemental materials 189

DISCUSSION ET CONCLUSIONS GÉNÉRALES, PERSPECTIVES 201

6.1 Les ALNs : un nouvel acteur du femtoplancton 203

6.2 Écologie des ALNs et importance putative 207

6.3 Perspectives d'études 209

Utilisation de la modélisation comme outil d'étude de la dynamique des ALNs dans les environnements 209

Etude de l'écologie fonctionnelle des ALNs 211

Utilisations d'approches moléculaires 213

Table des Figures et Tableaux

Figure 1 : Concept simplifié de chaîne trophique aquatique. 2

Figure 2 : Représentation schématique des différentes classes de taille planctoniques. 4

Figure 3 : Images d'entités femtoplanctoniques en microscopie électronique à transmission. 6

Figure 4 : Images d'Aster Like Nanoparticles en microscopie électronique en transmission. 8

Figure 5: Transmission electron micrographs of biomimetic mineral–organic- (BMOPs) and/or nanobe-like particles (A–H) and vesicle-like particles (I–S). 20

Figure 6: Transmission electron micrographs of different morphotypes of virus-like particles (VLPs). 30

Figure 7: Transmission electron micrographs of attached (A–Q) or free (R–T) femtoplankton-like prokaryotes. 38

Figure 8: Transmission electron micrographs of different morphotypes of aster-like nanoparticles. 40

Figure 9: Schematic overview of the main components and of organizational complexity (increase in complexity from left to right) of the femtoplankton entities mentioned in this review. 42

Figure 10: Significance of femtoplankton entities in prebiotic evolution: a potential pathway to the cellular and viral world. 44

Figure 11: Schematic overview of the specific and major ecological roles of femtoplankton entities mentioned in this review. 56

Figure 12: Electromicrographs showing heterogeneity of pelagic communities (A) in lakewater collected on March 15th 2017 and ALN-enriched culture (B) obtained from this sampling. 66

Figure 13: Transmission electron microscopy (TEM) micrographs of different morphotypes of aster-like nanoparticles. 76

Figure 14: Electromicrographs of aster-like nanoparticles. 76

Figure 15: Energy-filtered transmission electron microscopy (EFTEM) (A) and electron energy loss spectroscopy (EELS) analyses (B,C) of aster-like nanoparticles. 78

Figure 16: Flow cytometry analysis of aster-like nanoparticle-enriched preparations (E-ALNs). 80

Figure 17: Taxonomic affiliation of the 233 contigs from ALN-enriched DNA templates. 82

Figure 18: Sensitivity of the particles to heat, antibiotics or lysosyme treatments. 82

Figure 19: Development monitoring of aster-like nanoparticles in prokaryote-free medium. 84

Figure 20: Abundance of aster-like nanoparticles in situ (Neuville-France) and ratios (in %) of different morphotypes over a 15-month period. 84

Figure 21:(A) Distribution of aster-like nanoparticles and bacteria abundances in 16 selected stations of a tropical coastal ecosystem (Ha Long Bay-Vietnam), and (B) analyses of correlations (Spearman's product-moment correlation coefficient) between ALNs and environmental parameters which compile all sampling points. 86

Figure 22: (A–C), Electromicrographs documenting a putative interaction between aster-like nanoparticles and microbial cells. 96

Figure 23: Sampling site locations (1–25) and distribution of ALNs in different aquatic environments along the watershed of Loire River (France). 110

Figure 24: Relationships between ALNs and physical-chemical and biological environment. 112

Figure 25: Transmission electron microscopy (TEM) micrographs of different morphotypes of aster-like nanoparticles (ALNs). 130

Figure 26: Dynamics of Aster Like Nanoparticles concentrations (A) and their different forms (B). 142

Figure 27: Principal Component Analysis of individuals (sampling points) in function of lakes (A) or seasons (B). 142

Figure 28: Linear regression between ALNs concentration and concentration of prokaryotes. 144

Figure 29: Experimental design for the preparation of inoculums. 162

Figure 30: Transmission electron micrographs of different morphotypes of aster-like nanoparticles (ALNs). 164

Figure 31: Monitoring of the concentration of ALNs over time, function of medium culture and inoculum. 168

Figure 32: Monitoring of the concentration of prokaryotes (A) in inoculum B over time, function medium culture. 168

Figure 33: Dynamic of ALNs different forms function of culture medium. 170

Figure 34: Bacterial composition of the incubations of inoculum B, according to the culture medium. 172

Figure 35: Long-term incubation enriched for members of the Planctomycetes and CPR bacteria. 182

Figure 36: TEM imaging and viral genomics in the enrichment culture. 184

Figure 37 : Evolution de la concentration en ALNs et en procaryotes entre 2017 et 2021 dans le lac Fargettes. 210

Figure 38 : Images d'ALNs en microscopie électronique à transmission (A,B) ou en microscopie à force atomique (C,D) détaillant la structure des ALNs. 212

Table 1: Comparison of morphologies, some main constitutional elements and development strategies of femtoplankton entities. *42*

Table 2: Physicochemical characteristics of the lakewater on February 2017. ..... *64*

Table 3: Mean ± SD of physico-chemical and biological characteristics according to the lakes (A) or the seasons (B). *138*

Table 4: Pearson correlation between Aster Like Nanoparticles and the environmental variables in the 3 lakes. *144*

Table 5: Significant Spearman correlation coefficients between the presence of ALNs and the presence of microbial OTUs. *146*

Résumé

Face au changement global et notamment à l'augmentation de la température des eaux de surface (Whitehead *et al*., 2009), il est devenu indispensable de comprendre et d'anticiper l'évolution des écosystèmes aquatiques. Le bon fonctionnement et l'évolution de ces écosystèmes ont toujours été intimement liés au fonctionnement du compartiment biologique et notamment microbien (Lalli and Parsons, 1997). Les avancées technologiques des dernières décennies ont permis de mettre en évidence un véritable réseau d'interactions microbiennes (Pomeroy *et al.,* 2007), intégrant une diversité jusqu'alors insoupçonnée d'entités sub-micrométriques pouvant avoir une importance fonctionnelle majeure (Mostajir *et al.*, 2012). Pour comprendre le fonctionnement global des écosystèmes aquatiques, il semble donc nécessaire de concentrer des efforts de recherche sur les plus petites fractions de taille, notamment sur les particules nanoplanctoniques appartenant au femtoplancton jusqu'alors sous-considérées (< 0.2 µm ou 200 nm).

Dans ce contexte, la découverte d'une nouvelle catégorie de particules organiques appartenant au femtoplancton, nommées « *Aster Like Nanoparticles* » (ALNs) (Colombet *et al.,* 2019), soulève de nombreuses questions et notamment celle de leur importance fonctionnelle au sein des écosystèmes aquatiques. L'objectif principal de cette thèse est donc d'approfondir nos connaissances sur les fonctionnalités des ALNs, en se focalisant particulièrement sur l'étude écologique de ces entités afin de pouvoir, à terme, expliquer leur présence et appréhender leurs interactions avec leur environnement physico-chimique et microbien. Pour cela, différentes échelles d'intégration seront considérées : de l'échelle écosystémique à l'échelle expérimentale, en conditions contrôlées.

Nos résultats ont, dans un premier temps, permis de mettre en évidence la présence des ALNs dans un large spectre d'habitats aux caractéristiques différentes (Fuster *et al.,* 2020). Ces résultats ont permis de prouver l'ubiquité des ALNs, capables de se développer dans des environnements physico-chimiques variés. Une étude complémentaire a permis de dresser la dynamique temporelle des ALNs dans différents écosystèmes aquatiques, suggérant que les ALNs sont un acteur majeur à intégrer dans les modèles de successions écologiques (Fuster *et al*., 2022). Cette étude, menée dans trois lacs du Puy-de-Dôme, a permis de démontrer l'importance des paramètres biologiques dans la distribution des ALNs, et notamment l'importance potentielle des procaryotes. Finalement, des études en microcosmes ont permis de confirmer l'importance des procaryotes, avec des résultats montrant un développement jusqu'à 20 fois plus important des ALNs en présence d'une forte concentration de procaryotes. De façon générale, nos résultats ont démontré l'importance des ALNs en tant que nouveaux acteurs dans les écosystèmes aquatiques, d'une part par leur dynamique écosystémique marquée et, d'autre part, par leurs interactions avec les procaryotes, principaux régulateurs des flux de matière et d'énergie. Les ALNs sont donc de nouvelles entités planctoniques qu'il faudra désormais prendre en compte dans l'étude des écosystèmes aquatiques. Enfin, l'ensemble de nos résultats soulève des perspectives de recherche sur la nature et l'écologie des ALNs et leur place dans les schémas évolutifs du monde organique.

Abstract

With global change and especially the increase of surface water temperature (Whitehead *et al.*, 2009), it has become essential to understand and anticipate the evolution of aquatic ecosystems. The proper functioning and evolution of these ecosystems have always been linked to the functioning of the biological compartment, and especially the microbial compartment (Lalli and Parsons, 1997). Over the last few decades, technological advances have revealed a complex network of microbial interactions (Pomeroy *et al.*, 2007), including a previously unsuspected diversity of sub-micrometric entities that may have major functional importance (Mostajir *et al.*, 2012). To understand the global functioning of aquatic ecosystems, it therefore seems necessary to focus research on the smallest size fractions, especially on the previously under-considered nanoplanktonic particles belonging to femtoplankton (< 0.2 µm or 200 nm).

The discovery of a new type of organic particles belonging to femtoplankton, named "*Aster Like Nanoparticles*" (ALNs) (Colombet *et al.*, 2019), raises many questions, especially about their functional importance in aquatic ecosystems. The principal objective of this thesis is therefore to deepen our knowledge on the functionalities of ALNs, focusing especially on the ecological study of these entities to be able, in the future, to explain their presence and understand their interactions with their physico-chemical and microbial environment. To this, different scales of integration will be considered: from the ecosystemic to the experimental scale, under controlled conditions.

Our results allowed us to demonstrate the presence of ALNs in a wide range of habitats with different characteristics (Fuster *et al.*, 2020). These results proved the ubiquity of ALNs, which can develop in various physico-chemical environments. A complementary study has shown the temporal dynamics of ALNs in different aquatic ecosystems, suggesting that ALNs are a major player to be integrated in models of ecological succession (Fuster *et al.*, 2022). This study, performed in three lakes of the Puy-de-Dôme, demonstrated the importance of biological parameters in the distribution of ALNs, and the potential importance of prokaryotes. Eventually, microcosm studies confirmed the importance of prokaryotes, with results showing a development of up to 20 times more ALNs in the presence of a high prokaryotes concentration. Altogether, our results showed the importance of ALNs as new actors in aquatic ecosystems by their strong ecosystemic dynamics and by their interactions with prokaryotes, the main regulators of matter and energy flows. ALNs are therefore new planktonic entities that should be considered in the study of aquatic ecosystems. All our results raise research perspectives on the nature and ecology of ALNs and their position in the evolutionary patterns of the organic world.

INTRODUCTION GÉNÉRALE

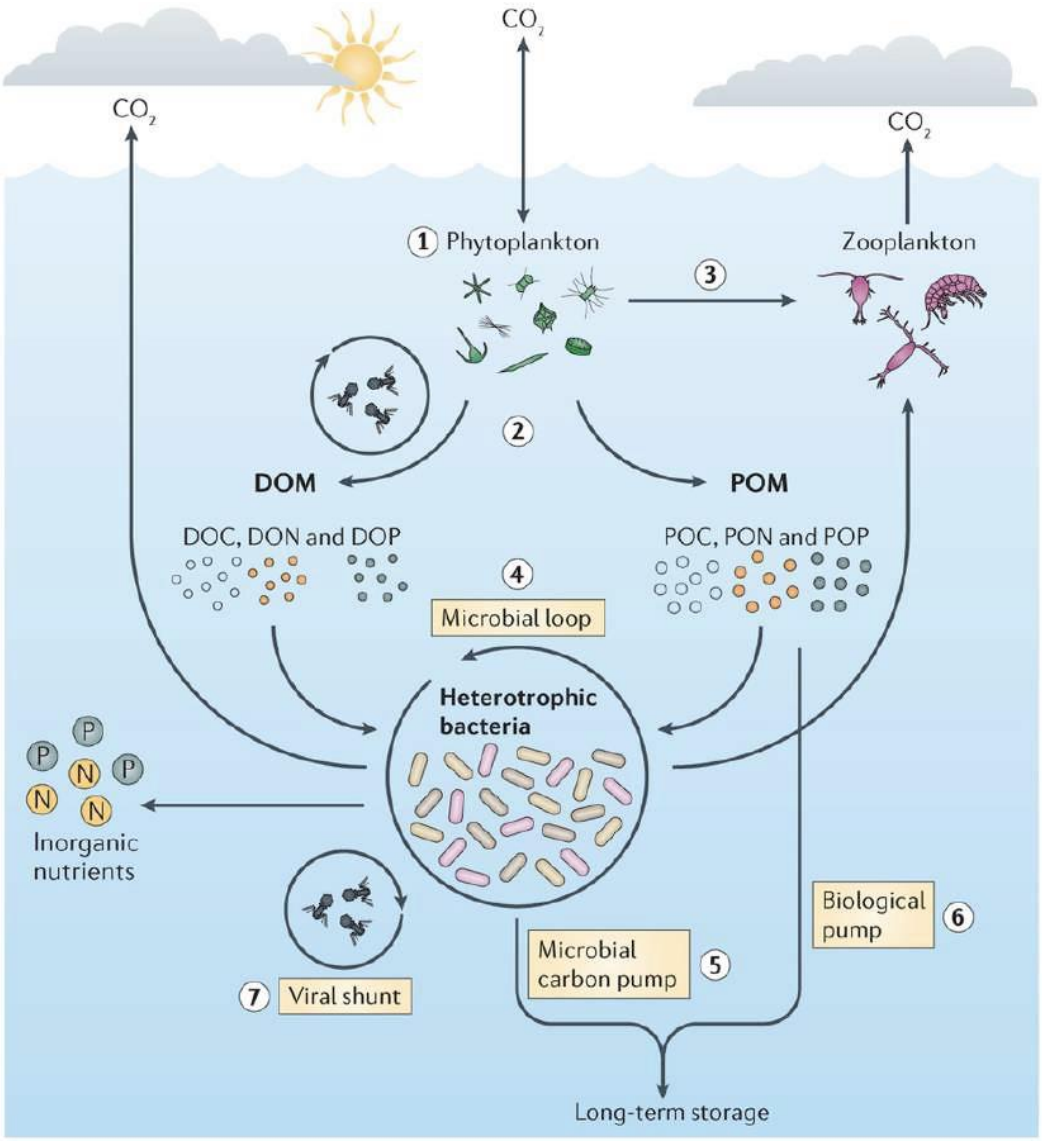

Figure 1 : Concept simplifié de chaîne trophique aquatique.
Cette représentation intègre les concepts de boucle microbienne et virale, jouant un rôle essentiel dans le transfert de matière et d'énergie.
D'après [11]

Il est désormais avéré qu'un changement climatique d'origine anthropique est inévitable. Dans ce contexte de changement global, l'un des impacts est l'augmentation moyenne de la température des eaux de surface, entrainant une modification de l'équilibre chimique et biologique des écosystèmes aquatiques [1]. Prédire les changements de ces écosystèmes afin d'anticiper leurs impacts est donc devenu un défi majeur pour la communauté scientifique. Pour cela, il est nécessaire de comprendre leur fonctionnement, notamment en étudiant

(i) Les flux de matière et d'énergie transitant par ces écosystèmes.

(ii) La diversité des entités et leurs activités biochimiques, régulateurs biologiques de ces flux.

À l'origine, le fonctionnement des écosystèmes et notamment les interactions entre les différents microorganismes et les flux associés étaient appréhendés de manière simplifiée [2]. Les premiers modèles de chaînes trophiques aquatiques étaient donc structurés autour de deux concepts différenciés [2] :

(i) La chaine trophique des brouteurs (reposant sur l'assimilation photosynthétique des producteurs primaires -phytoplancton-, consommé -broutage- par le zooplancton, lui-même consommé par les poissons).

(ii) Le recyclage de la matière organique (provenant des déchets produits par la chaine trophique des brouteurs) par les procaryotes, notamment les bactéries hétérotrophes.

Dû aux limitations techniques, ce concept de chaînes trophiques dissociées ne prenait en compte qu'une part minime de la diversité des organismes aquatiques, excluant notamment les entités sub-micrométriques et les métabolismes et interactions biologiques potentiels associés. La diversité de ces entités s'est par la suite montrée beaucoup plus importante que ce que l'on croyait [3, 4], contribuant de manière tout aussi importante aux flux de matière et d'énergies de la chaîne trophique que les groupes identifiés initialement [5]. L'importance quantitative et fonctionnelle de cette nouvelle diversité biologique, auparavant non considérée, a donc conduit à une reconsidération des modèles d'organisation trophique des écosystèmes aquatiques. Aujourd'hui, nous sommes passés d'une simple chaîne trophique à un véritable réseau complexe d'interactions, intégrant cette nouvelle diversité aux flux de matière et d'énergie à travers les concepts de boucle microbienne [6, 7], virale et de réseaux trophiques microbiens [8–10] (**Figure 1**).

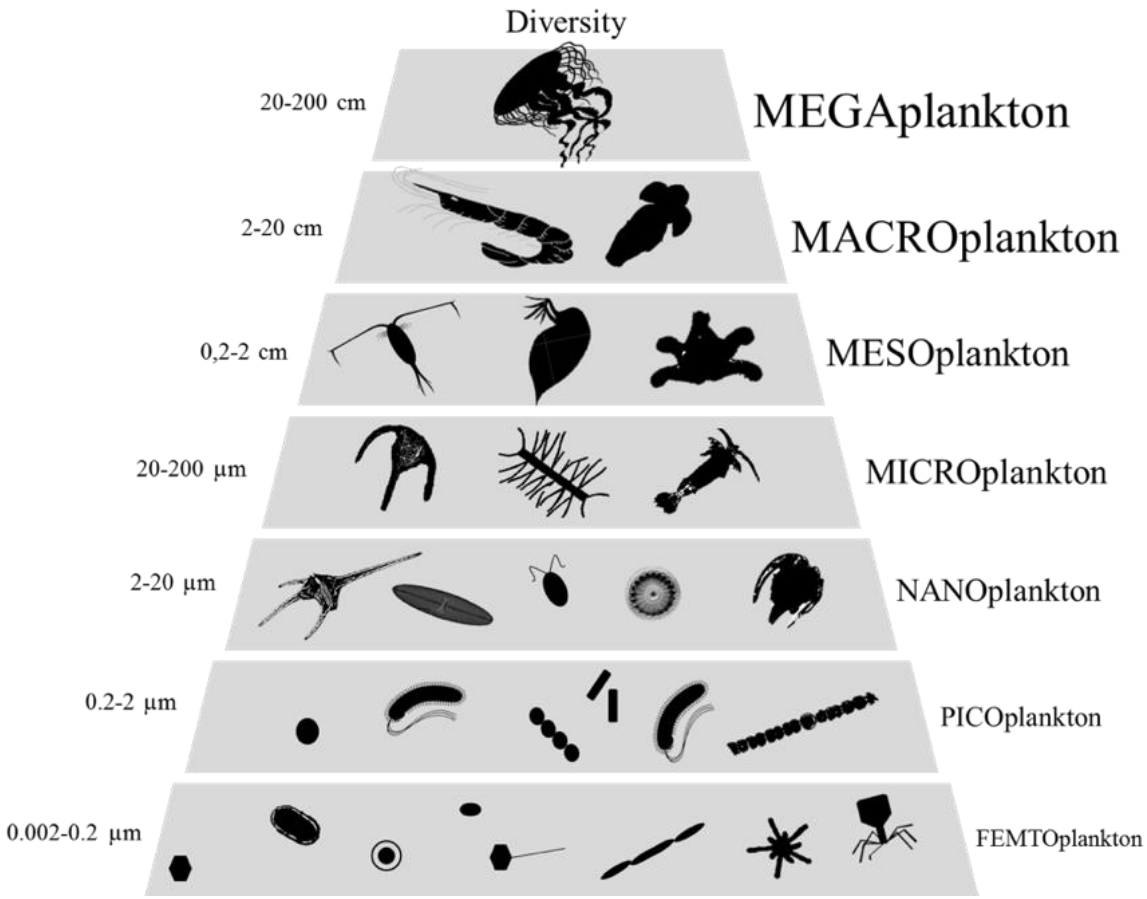

Figure 2 : Représentation schématique des différentes classes de taille planctoniques.
D'après [16]

La boucle microbienne est connectée de manière directe et indirecte au réseau trophique classique, *via* les processus de prédation, parasitisme, excrétion, recyclage des éléments nutritifs, *etc… [12]* (**Figure 1**). La mise en évidence d'une diversité sub-micrométrique importante a permis d'améliorer les modélisations de flux qui, jusqu'ici, n'expliquaient qu'en partie les transferts énergétiques et de biomasse [13, 14]. Les modélisations actuelles font donc une part de plus en plus importante aux entités de petite taille dans les écosystèmes aquatiques (*i.e.* nano, pico et femtoplancton) [9, 15], lesquelles ont jusqu'à maintenant été sous considérées [16]. L'intégration de toutes les composantes du plancton, y compris celles de plus petite taille, semble donc essentielle dans la compréhension du fonctionnement des écosystèmes. Le terme plancton a été introduit pour la première fois par Hensen (1887), pour définir tout organisme vivant en suspension dans l'eau, ayant un pouvoir locomoteur réduit. Le plancton a d'abord été divisé en grands groupes fonctionnels en fonction de leurs modes trophiques (*e.g.* producteurs primaires, consommateurs primaires, *etc*…), mais des raisons pratiques liées à leur étude ont conduit à la création d'une classification par taille où différentes modes trophiques sont confondus [17] (**Figure 2**).

Si les fractions de tailles supérieures sont aujourd'hui largement considérées, les fractions de plus petites tailles ont été ignorées ou sous-estimées durant des décennies, notamment à cause de limitations technologiques. Pour comprendre le fonctionnement global des écosystèmes aquatiques, il semble donc important de concentrer des efforts de recherche sur les plus petites fractions de taille, notamment sur les particules nanoplanctoniques appartenant au femtoplancton (< 0.2 µm ou 200 nm).

Le développement des nouvelles méthodes analytiques, notamment en microscopie, a permis d'améliorer nos connaissances sur les particules nanométriques vivantes ou non (*e.g.* les particules femtoplanctoniques : 2 - 200 nm). Ces techniques ont permis de mettre en évidence une diversité insoupçonnée, les milieux aquatiques étant des réservoirs importants d'entités femtoplanctoniques jusqu'alors négligées. Le femtoplancton n'est donc pas uniquement composé de virus, comme considéré durant des décennies, mais aussi de nombreux autres types de particules. La diversité de ces nanoparticules peut être classée selon un gradient progressif de complexité, allant d'entités minéralo-organiques à des entités biotiques [16] (**Figure 3**).

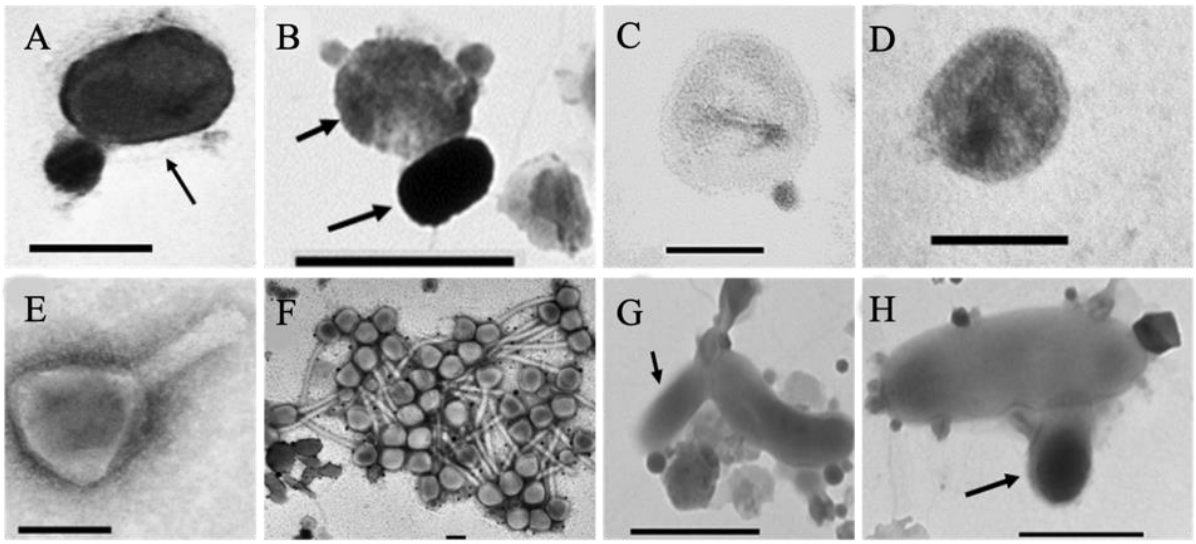

Figure 3 : Images d'entités femtoplanctoniques en microscopie électronique à transmission.

D’après [16].

Les progrès scientifiques ont donc permis d'identifier différentes entités femtoplanctoniques :

- Les particules minéralo-organiques biomimétiques (BMOPs), dérivées de processus physico-chimiques pouvant associer des minéraux et des molécules d'origine organique [18] (**Figure 3 A-B**).
- Les vésicules extracellulaires (EVs) (**Figure 3 C-D**). Les EVs sont universellement produites par les membres de toutes les branches de l'arbre de la vie [19, 20] ; ces vésicules peuvent avoir des fonctions biologiques ou écosystémiques potentiellement importantes [16, 21].
- Les virus ou particules d'allure virale (VLPs) (**Figure 3 E-F**). Les virus ont longtemps été considérés comme la seule composante du femtoplancton. II s'agit d'entités biologiques acellulaires, incapables de se reproduire sans leurs cellules hôtes. Ayant un génome constitué d'ADN ou d'ARN, les virus se trouvent partout où la vie cellulaire est présente ; ils sont très abondants en milieu aquatique et représentent un grand réservoir de biodiversité sur terre [22].
- Les nanobactéries ou nanoarchées (plus petits procaryotes décrits à ce jour). Parmi ces nanoprocaryotes, la découverte des CPR (*Candidate Phyla Radiation*) et DPANN (acronyme des cinq premiers phyla, « *Candidatus Diapherotrites* », « *Candidatus Parvarchaeota* », « *Candidatus Aenigmarchaeota* », *Nanoarchaeota* et « *Candidatus Nanohaloarchaeota* ») a généré de nouvelles connaissances concernant la place des procaryotes dans l'arbre de la vie (**Figure 3 G-H**) [23].

La découverte de toutes ces entités a largement complexifié la compréhension de la fraction femtoplanctonique, impliquant une reconsidération de la diversité et de l'importance écologique du femtoplancton. À travers le spectre de leurs activités et de leurs hôtes potentiels, les entités femtoplanctoniques ont la capacité d'interagir avec tous les composants du plancton. Étant donné leur forte concentration, le femtoplancton peut jouer un rôle majeur dans la circulation, la disponibilité et le transfert de matière et d'énergie dans l'environnement [18]. Leurs interactions avec les autres entités influencent et peuvent contrôler la structure des communautés microbiennes, avec un impact direct ou indirect sur des cycles majeurs tel que le cycle du carbone [24–26].

La diversité méconnue et l'abondance de toutes ces entités ont donc nécessairement un impact sur la circulation des éléments et les cycles biogéochimiques dans les écosystèmes aquatiques. Ces nanoparticules représentent encore aujourd'hui une source potentielle de nouvelles

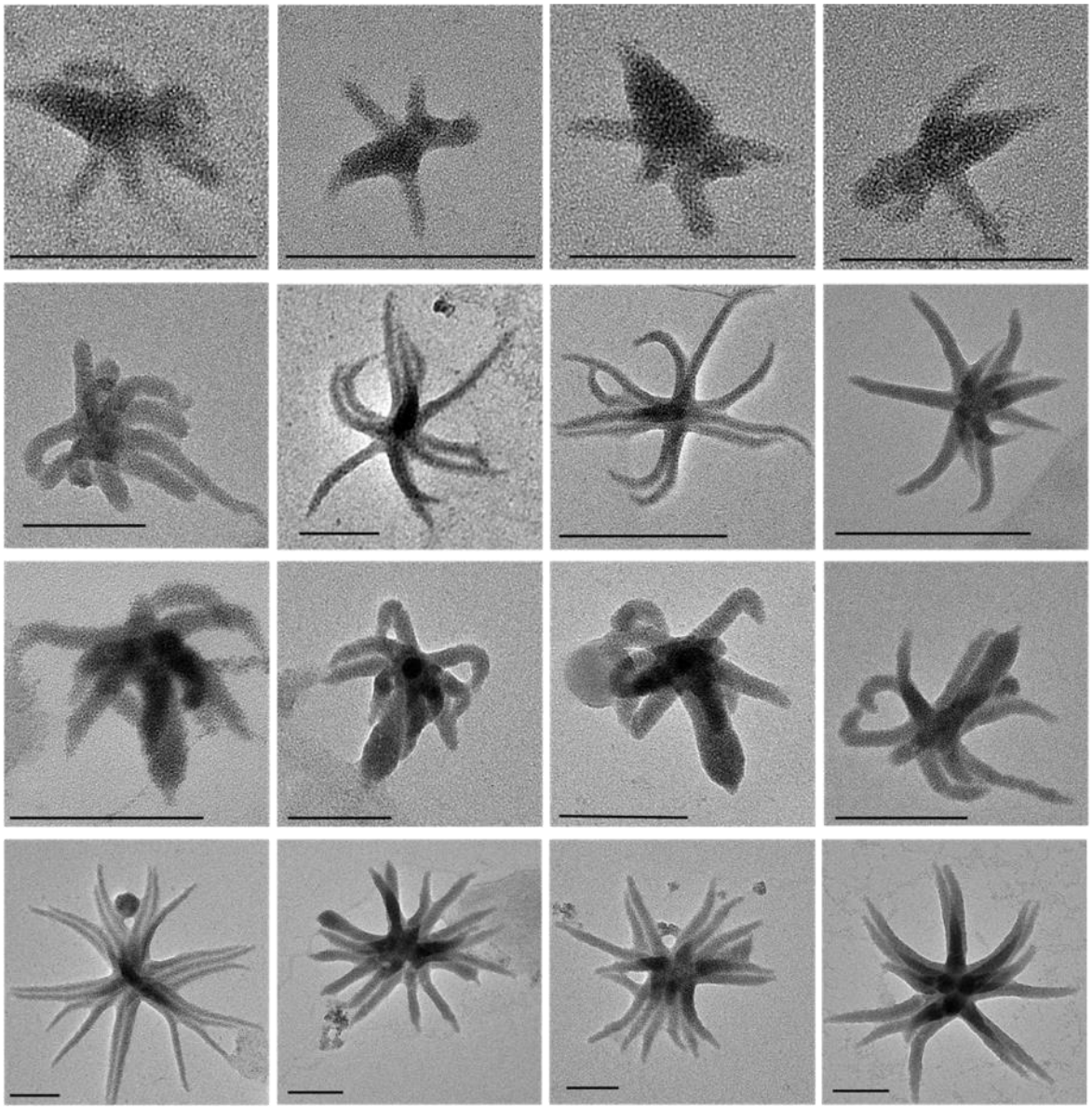

Figure 4 : Images d'Aster Like Nanoparticles en microscopie électronique en transmission. Ces images ont été obtenues lors d'observations d'échantillons issus de milieux naturels. Crédits photos : J.Colombet – plateforme CYSTEM. Échelles = 100 nm

fonctions écologiques jamais décrites auparavant. C'est dans ce contexte scientifique que Colombet et collaborateurs (2019) ont récemment découvert une nouvelle catégorie de particules appartenant au femtoplancton, nommée Aster Like Nanoparticles (ALNs), en raison de leur forme étoilée (**Figure 4**).

Les ALNs ont des caractéristiques phénotypiques et développementales uniques, avec des volumes jusqu'à 200 fois inférieurs au volume minimum théorique pour une entité biologiquement viable (*i.e.* estimé à 0,008 μm^3 par des experts scientifiques). Ils sont sensibles aux traitements biocides et leur concentration fluctue dans des conditions dépourvues d'hôtes potentiels. Ces nouvelles entités sont encore méconnues mais soulèvent de nombreuses questions, notamment sur leur origine, leur nature, ainsi que leur impact sur les flux de matière et d'énergie.

Tout comme les autres entités femtoplanctoniques, les ALNs sont des interactants potentiels des procaryotes [27]. Ajouté à leur capacité de développement et de colonisation du milieu avec des abondances pouvant atteindre 10^8 particules.mL^{-1}, ces ALNs seraient des acteurs méconnus dans le fonctionnement des écosystèmes aquatiques [27].

Aujourd'hui, la compréhension de l'évolution des écosystèmes aquatiques est un défi majeur, notamment face au changement global. La découverte des ALNs soulève de nombreuses questions sur leurs rôles potentiels dans les cycles d'éléments conservés régissant le fonctionnement des écosystèmes. Comprendre ce fonctionnement nécessite donc une meilleure appréhension des entités nanométriques tel que le femtoplancton. L'objectif principal de cette thèse vise à approfondir nos connaissances sur les ALNs. Cet objectif est particulièrement centré sur l'étude écologique de ces entités, en lien avec leurs rôles potentiels dans les écosystèmes aquatiques.

Organisation du mémoire de thèse

Après l'introduction générale de ce manuscrit, l'état de l'art analysera dans un premier temps la diversité et le rôle écologique potentiel des particules femtoplanctoniques dans un contexte évolutif, allant de particules minérales aux particules biologiques, en passant par des particules bio-minérales. La seconde partie de l'état de l'art abordera la découverte et la description du modèle d'étude des travaux de cette thèse : les ALNs.

Suite à l'état de l'art, le corps du manuscrit s'articulera autour des objectifs de la thèse visant à explorer l'écologie des ALNs afin de pouvoir, à terme, expliquer leur présence, appréhender leurs interactions et leurs rôles dans les écosystèmes aquatiques. Pour cela, différentes échelles d'intégration seront considérées : de l'échelle écosystémique à l'échelle expérimentale, en conditions plus ou moins contrôlées.

(i) Le chapitre 1 a pour objectif spécifique de déterminer les conditions préférentielles de développement des ALNs. Pour ce faire nous avons réalisé une étude géographique sur le bassin versant de la Loire, afin de déterminer la distribution des ALNs dans différents écosystèmes aquatiques.

(ii) Le chapitre 2 permettra de vérifier les facteurs putatifs de contrôle des ALNs identifiés dans le chapitre 1, en étudiant leur trophodynamique saisonnière dans 3 écosystèmes lacustres.

(iii) Le chapitre 3 s'intéressera aux interactions potentielles que les ALNs peuvent avoir avec les autres communautés présentes dans l'écosystème, abordées via des expériences en conditions contrôlées. Ces études expérimentales viseront à valider les hypothèses retenues lors des suivis écosystémiques précédents.

Pour finir, un dernier chapitre viendra conclure les travaux réalisés durant cette thèse. L'objectif de ce chapitre sera de mener une analyse intégrative des résultats obtenus, afin de faire ressortir les éléments marquants permettant de mieux comprendre l'écologie des ALNs. Cela permettra également de dresser de nouvelles perspectives de recherche, sources de réflexions pour généraliser les rôles potentiels des ALNs dans le fonctionnement des écosystèmes aquatiques.

ÉTAT DE L'ART / DÉCOUVERTE DES ALNs

Le femtoplancton est devenu en quelques années un compartiment essentiel dans la compréhension du fonctionnement des écosystèmes aquatiques. Si les progrès technologiques ont permis des avancées significatives dans l'exploration de sa diversité et de son rôle, cette fraction reste largement méconnue dans les écosystèmes aquatiques. Son étude est indubitablement une source de nouvelles connaissances tant sur les plans de la biologie, de l'évolution que de l'écologie. L'objectif de ce chapitre qui a fait l'objet de publications parues, est de faire un état de l'art des connaissances sur ce compartiment encore méconnu et d'introduire la découverte des ALNs. Nous aborderons dans ce chapitre la composante femtoplanctonique sous différents aspects : diversité, importances quantitatives et fonctionnelles, origine évolutive. Une attention particulière sera donnée au modèle d'étude de ces travaux de thèse, les ALNs. Leur découverte sera abordée ici en les plaçant dans le contexte de la diversité structurelle et fonctionnelle du femtoplancton.

2.1 Le compartiment femtoplanctonique : source de nouvelles connaissances en biologie et en écologie

Femtoplankton: What's New?

Jonathan COLOMBET[1], Maxime FUSTER[1], Hermine BILLARD[1], Télesphore SIME-NGANDO[1]

[1] Université Clermont Auvergne, CNRS, LMGE, Clermont-Ferrand F-63000, France

Publié dans *Viruses* – Aout 2020
doi:10.3390/v12080881

2.1.1 Abstract

Since the discovery of high abundances of virus-like particles in aquatic environment, emergence of new analytical methods in microscopy and molecular biology has allowed significant advances in the characterization of the femtoplankton, *i.e.*, floating entities filterable on a 0.2 µm pore size filter. The successive evidence in the last decade (2010–2020) of high abundances of biomimetic mineral–organic particles, extracellular vesicles, CPR/DPANN (Candidate phyla radiation/Diapherotrites, Parvarchaeota, Aenigmarchaeota, Nanoarchaeota and Nanohaloarchaeota), and very recently of aster-like nanoparticles (ALNs), show that aquatic ecosystems form a huge reservoir of unidentified and overlooked femtoplankton entities. The purpose of this review is to highlight this unsuspected diversity. Herein, we focus

on the origin, composition, and the ecological potentials of organic femtoplankton entities. Particular emphasis is given to the most recently discovered ALNs. All the entities described are displayed in an evolutionary context along a continuum of complexity, from minerals to cell-like living entities.

2.1.2 Introduction

Victor Hensen first introduced the term "plankton" in 1887 to define all organisms that live in suspension in water and have limited locomotion power to maintain their position against currents. Plankton was first divided into broad functional groups according to their trophic levels but practical reasons related to their study has led to a classification by size classes [17]. Thus, Sieburth classified plankton into size ranges covering eight orders of magnitude from femto- (0.02–0.2 µm) to mega-plankton (>20 cm) [28] (**Figure 2**).

While the largest size fraction has proved to be very diversified, with the occurrence of various phylogenetic groups, the smallest one, *i.e.*, femtoplankton, has long been considered to be exclusively composed of virus-like particles (VLPs) [9, 28]. Over the last two decades, technical advances in molecular and microscopic sciences have revealed an unexpected and underestimated diversity of femtoplankton entities other than viruses, including, for example, various tiny prokaryotes CPR (Candidate phyla radiation), DPANN (Diapherotrites, Parvarchaeota, Aenigmarchaeota, Nanoarchaeota and Nanohaloarchaeota) [23] and, more recently, intriguing aster-like nanoparticles (ALNs) that we have reported in various aquatic systems [27].

These discoveries lead to a necessary reconsideration of the femtoplankton compartment in terms of diversity and associated ecological potentials. We refer here to "femtoplankton entities" as those that (i) are totally or partially organic, (ii) can be filterable on a 0.2 µm pore size filter, (iii) are bounded by an outer membrane, "membrane-like" or wall structure and (iv) have the ability to multiply or divide independently or not. Fully inorganic or non-biotic nanoparticles (from 1 to 100 nm) and molecular colloids (from 1 to 1000 nm) populating aquatic systems have been the subject of excellent reviews and will not be discussed here [29, 30]. In addition, miniaturized prokaryotes and Candidatus Pelagibacter ubique that are on the border between femto- and nanoplankton are also excluded from this review [31–34].

This review focuses on the diversity of femtoentities in aquatic ecosystems, with an emphasis on the origin and composition of their different representatives and the associated ecological potentials. The femtoplankton entities treated in this review are presented in an evolutionary context, along a gradient of progressive increase in complexity, ranging from mineral–organic entities (biomimetic mineral–organic particles/nanobes) to fully biotic entities (VLPs—*i.e.*, viruses, subviral, agents and gene transfer agents—extracellular vesicles and prokaryotes). Particular attention is given to the recently discovered aster-like nanoparticles [27].

2.1.3 From Mineral to Biotic Entities: A Path Toward the Living Being?

Biomimetic Mineral–Organic Particles and Nanobes

The discovery and characterization of new femtoplankton entities collides with the concept of the origin and emergence of a cell life form. Two major theories ("The RNA world" *vs*. "The metabolism-first") and two approaches ("top-down biology" *vs*. "bottom-up chemistry") have historically competed over the research of the starting point of life on the primitive Earth and the primordial stages of life evolution [35–42]. Many scenarios to explain the emergence of the first cell life form arise from these lines of research and from the possible location where life appeared (*e.g.*, submarine hydrothermal vents, pumice rafts, volcanic-hosted splash pools, subaerial geysers, *etc*., reviewed in [43, 44]). However, at present, there is no experimental evidence of a consensus scenario (discussed in [40, 45–47] and references herein). A recurring feature in the evolutionary process that could lead to the first life form is the gradual increase in complexity from inorganic nanoparticles to the emergence of the cell. Baum [48] resumed that the cell could find its origin with the creation of chemical consortia adsorbed on mineral surfaces. The selection processes would eventually give rise to limited entities reproducing independently, such as cells.

Biomimetic mineral–organic particles (BMOPs), including the majority of controversial "nanobes" also known as "nanobacteria", "nanobacteria" or "calcifying nanoparticles" [18, 49–56], could be considered as a first step in complexification leading to the genesis of a cell type structure, known as a protocell. The formation of the majority of BMOPs/nanobes could be the result of physico-chemical processes (*e.g.*, aggregation) that are entirely abiotic, or

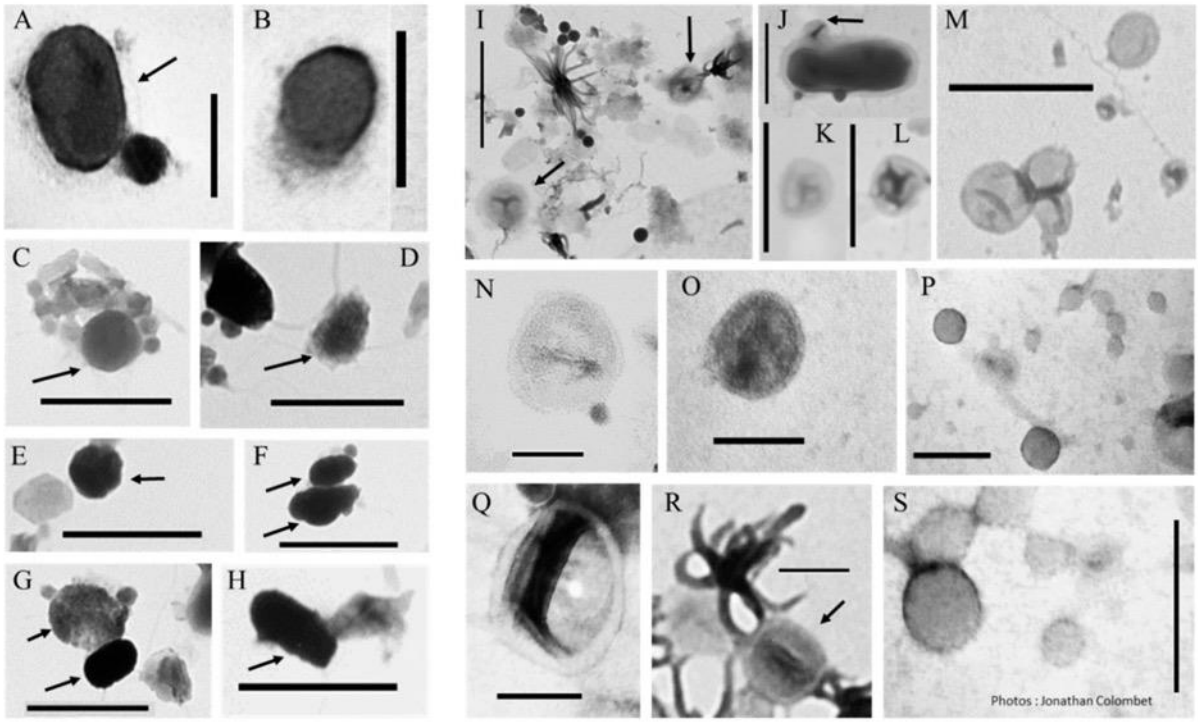

Figure 5: Transmission electron micrographs of biomimetic mineral–organic- (BMOPs) and/or nanobe-like particles (A–H) and vesicle-like particles (I–S).

Arrows indicate the target particles when the samples are heterogeneous. (A,B,N–S) scale bar: 100 nm, (C–H,I–M) scale bar: 500 nm.).

combinations of minerals and molecules derived from biological entities [18, 50, 54]. Nevertheless, these entities present intriguing features. They have the potential to generate mineral–organic amalgams that are able to replicate themselves via cell-like processes, such as symmetrical fission and they have the ability to mimic various life forms (*e.g.*, coccoid, amoeboid, ovoid, filamentous, *etc*.), such as microscopic fungi (Actinomycetes) and prokaryotes [52, 55, 57–59]. However, their tiny size (between 20 and 1000 nm in diameter, like those in **Figure 5 A–H**) results, in most cases, in volumes largely under the theoretical minimal cell volume (TMCV, *i.e.*, 0.008 µm3) required to house nucleic acids and the associated biosynthetic machinery required for a self-sufficient form of life [18, 52, 55, 60]. The origin and characteristics of some of these biomimetic amalgams, mainly those known as "nanobes", remain poorly understood.

The composition of these aggregates of minerals and organic particles is representative of the environment in which they evolved, including human and cow blood, terrestrial minerals, extraterrestrial meteorites, and aquatic environments [18, 50, 52, 55, 58, 61–63]. Since these entities are ubiquitous, we speculate that their diversity is likely at least as great as the number of possible mineral–organic combinations in the environment and is similar or greater than the known biological diversity of the past and contemporary living world.

Carbon, oxygen, nitrogen, calcium, phosphorus, silicon, iron, sodium, magnesium, manganese, fluorine, aluminum, barium, sulfur, zinc, potassium, terbium, chlorine and cobalt are examples of elements that may be included in BMOP and nanobe composition [18, 64]. This non-exhaustive list may combine mineral phases dominated by several compounds (*e.g.*, calcium and iron sulfates, silicon and aluminum oxides, sodium carbonate, iron sulfide and hydroxides containing iron, manganese, aluminum) with organic phases of complex composition (*e.g.*, humic materials, peptides, proteins, lipids, peptidoglycans, polysaccharides) [18, 64] and references herein). It is interesting to note that BMOPs from human samples can include a wide range of proteins with complex biological functions, such as coagulation factors, calcification inhibitors, complement proteins, protease inhibitors, or lipid carriers [65]. The presence of nucleic acids in BMOPs and nanobes remains a controversial issue. Some authors have reported positive detection of nucleic acid using various markers [54, 55]. Raoult *et al*.[54] suggested that BMOPs and nanobes do not contain nucleic acid and that this positive detection could be the result of the labeling of contaminating nucleic acids trapped on the target particle. These results strongly suggest that environmental BMOPs and nanobes are potential carriers of genetic

information and associated biological functions. It is therefore very important to strengthen the research efforts on their origin, composition, diversity, and ecological potentials through their interactions with biotic and abiotic environments.

Many authors, in agreement with the origin, composition and the theoretical formation pattern of BMOPs and nanobes, have classified them as non-living forms [18, 50, 54, 57]. However, some controversial "nanobes" remain mysterious and further work is needed to clearly elucidate their exact nature and to understand the potential role of BMOPs and nanobes in the evolution of life [52, 55, 56, 63]. Indeed, if they are not living entities, BMOPs and nanobes can be considered as an evolutionary step towards cell formation through the formation of mineral–organic complexes. Their composition and organization into cell type structures (including a membrane mimicking the cell wall, [55]) could be consistent with the beginning of the compartmentalization process known as one of the critical steps in the genesis of earlier free or symbiotic cell forms.

Extracellular Vesicles

The progressive increase in complexity of bio-mineral complexes at cell emergence requires a critical step where a boundary occurs and separates the living cell system from its environment [38, 66, 67]. The compartmentalization of the primordial soup (*i.e.*, the process that allowed the isolation and creation of a physico-chemical and thermodynamic environment suitable for the synthesis of bio-macromolecules) into vesicles would have favored the emergence of primitive life forms [68]. These authors also suggested that membrane vesicles could have a role in early cell evolution and may have helped shape the nature of LUCA, our Last Universal Common Ancestor. Thus, lipid vesicles may have been the first protocells to concentrate RNA before the appearance of ribocells, ancestors of RNA-based cells, that preceded LUCA [68]. Beside this evolutionary theory, there is no doubt that extracellular vesicles (EVs) represent the smallest cell-like entities surrounded by a lipid structure.

The biology of EVs has been widely documented over the last decade, mainly in terms of their origin, composition, diversity and biological purposes (see references in [19, 69]). Scientists reported that EV production is a universal and conserved process that occurs in all branches of the tree of life: bacteria, archaea and eukaryotes [20, 25]. EVs are diverse in origin and

composition, and there is little consensus on their classification [70]. Bacterial vesicles are represented by extracellular vesicles (20–250 nm) or outer membrane vesicles (20–230 nm) while archaea produce membrane vesicles (50–230 nm). Eukaryotic EVs can be grouped into three main groups: microvesicles (50–1000 nm), exosomes (30–150 nm) and apoptotic bodies (500–2000 nm) [69, 71]. With the exception of apoptotic vesicles and large microvesicles, the other EVs are spherical nanoparticles [20, 21, 72–74]. These particles could therefore be found in plankton where they can be confused with other nanoparticles (**Figure 5 I–S**). Since all living cells on earth are probably capable of producing vesicles, we assume that their diversity could be as great as that of their parent cells.

Bacterial vesicles are formed by budding of the cytoplasmic, outer and outer-inner membrane. The composition of their membrane and lumen is therefore reminiscent of the membrane, periplasm and cytoplasm of their producer cells. For example, EVs may contain soluble proteins, membrane proteins, lipoproteins, phospholipids and glycolipids from the donor cells membrane. All of these molecules are involved in essential cell membrane functions, such as substances transfer, cell adhesion, ion conductivity, cell signaling, binding surface for several extracellular structure, *etc*. [19, 20, 68, 69]. They also carry elements of the cytoplasm of the producing cells, such as toxins, DNA, RNA, immunomodulatory compounds, communication factors, adhesins, adenosine triphosphate (ATP), enzymes involved in the degradation of peptidoglycans or antibiotics, virulence factors (anthrolysin, coagulases, lipase), *etc*. [19, 68] and references therein). The quality and quantity of molecular loads differ greatly from one EV to another. For example, in the marine environment, Biller *et al*. [75] demonstrated that the size and quantity of DNA varied between different bacterial taxa and that only a small proportion of EVs contain DNA.

Knowledge about the vesicles produced by archaea is less extensive and still in its infancy compared to bacteria. In aquatic environments, the models studied (mainly *Sulfolobus* and *Thermococcales*) show that archaea EVs are membrane vesicles produced by cytoplasmic membrane. The biology of these models, in terms of origin, composition, diversity and biological purpose, is detailed in [19]. As with bacteria, the composition of archaea vesicles is inherited from their producing cell. For example, membrane vesicles produced by *Sulfolobus* or *Thermococcus* species harbor S-layer proteins and the oligopeptide-binding protein OppA obtained from parental cells [76–79]. The EVs of three *Sulfolobus* species carry various proteins identified as having potential implications in cell division (ESCRT, Vps4),

adhesion, migration, homing, pattern formation and signal transduction (vWA), as well as in signaling, endocytosis (flotillin), cyanure detoxification (thiosulfate sulphur transferase) and antimicrobial processes (sulfolobicin) [19, 68]. EVs produced by *Thermococcus* species are often associated with genomic DNA or RNA [77, 78, 80]. Recently, Erdmann *et al.*[81] described a new type of EV containing plasmid in a psychrophilic halophilic archaea *Halorubrum lacusprofundi.*

The origin and composition of eukaryotic vesicles (*i.e.*, exosomes and microvesicles) are well documented (see reviews in [19, 69]). Gill *et al*. [19] mentioned that the release of EVs in the environment is characteristic, and probably conserved, in all eukaryotic cell types (*i.e.*, animals, plants, protists and fungi), including single and multicellular organisms. As such, they may be present in all types of environments, including aquatic systems. However, most studies to date have been conducted in animals, mainly in terrestrial mammalian models such as mice and humans [69]. Exosomes are formed through the endocytic pathway from the "outward" budding of the late endosomal membrane [82, 83]. They can accumulate in multivesicular bodies during the endosomal pathway and can be released into the environment after fusion with the plasma membrane [20, 84–87]. Microvesicle EVs are formed from direct outward budding or pinching of the cell's plasma membrane [88]. In some cases, they are released from tubular structures that are extensions of the plasma membrane [89, 90]. Exosomes and microvesicles are formed by packaging the cytoplasmic contents in membrane-bound vesicles and have been shown to carry all types of cellular components. Extensive reviews on cargo molecules and their functions have already been provided [19, 69, 91]. For example, microvesicles can contain proteins involved in cell adhesion, motility, activation and proliferation (tetraspanins and associated proteins). Other cargo proteins can also be present, such as those fundamental in pathogen recognition (immunoglobulins), cytoskeletal properties (tubulin and actin), vesicular trafficking (Rab GTPase proteins, annexins, stomatin, prohibitin, flotillin) or cell division (ESCRT-related proteins), *etc*. In addition, many lipids, including sphingomyelin, cholesterol, ganglioside GM3, desaturated lipids, phosphatidylserine and ceramide are also intravesicular components of eukaryotic EVs, as well as genetic materials [92–96]. These include a large amount of mRNA and sRNA, single-stranded DNA, mitochondrial DNA, plasmid DNA and double-stranded DNA [97–101].

Overall, EV composition varies greatly depending on the phylogenetic position, lifestyle and physiological state of the parental cells, as well as prevailing environmental conditions

(reviewed in [102]). They represent a huge reservoir of biomolecules and are essential vectors in the aquatic environment. Protein and nucleic acid contents mainly derived from parental cells but also from their viruses and other symbionts [19, 68, 103]. These authors suggested many potential interactions between viruses and EVs, in both evolutionary and physiological contexts. Gill and Forterre [68] proposed the existence of ribovirocells, derived from lipid vesicles, which evolved into virocells at the origin of viruses. EVs can be used as decoys against viral attack but virus-infected cells also produce EVs that enhance viral infection (reviewed in [19]). Improving our knowledge of the biology and ecology of EVs is essential for understanding the origin of viruses [104, 105].

Viruses and Gene Transfer Agents

Viruses

The genesis of EVs is an example of biological compartmentalization based on lipid arrangements and boundaries. Biological compartmentalization may also result from protein or protein–lipid arrangements and boundaries which are characteristics of encapsidated and enveloped viruses. The origin of viruses is widely debated. Three main hypotheses have been formulated, namely the progressive (or escape) hypothesis, the regressive (or reduction) hypothesis and the virus-first hypothesis. Krupovic and Koonin [106] defined these hypotheses as follows. The progressive hypothesis postulates that viruses evolved independently in different domains of life from cellular genes that embraced selfish replication and became infectious. The regression hypothesis submits that viruses are degenerated cells that have succumbed to obligatory intracellular parasitism and in the process, have shed many functional systems that are ubiquitous and essential in cellular life forms, particularly the translation apparatus. Finally, the virus-first hypothesis, also known as the primordial virus world hypothesis, views viruses (or virus-like genetic elements) as intermediaries between prebiotic chemical systems and cellular life and therefore postulates that virus-like entities are derived from the precellular world. These hypotheses are well discussed in [107]. In addition to the possible co-evolution between viruses and EVs [108], it is clear that the complexity of these particles increases from vesicles to viruses, to living cells. In the virus-first hypothesis, Koonin [109] suggested that capsid is a primitive form that may have paved the way for the formation

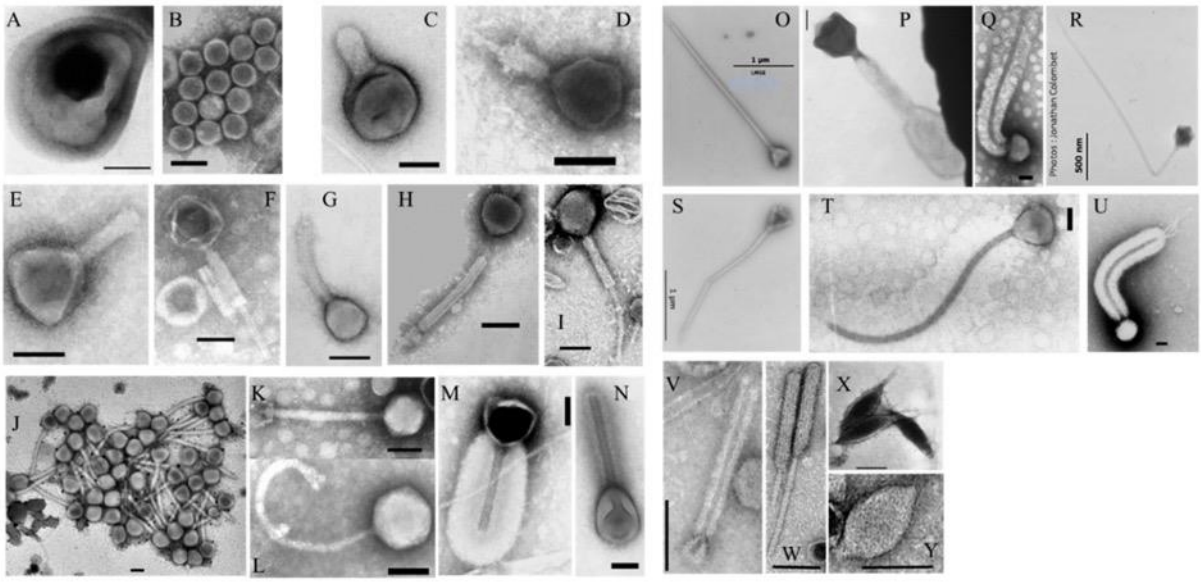

Figure 6: Transmission electron micrographs of different morphotypes of virus-like particles (VLPs).

(A) VLP embedded in a vesicle-like structure. (B) Tailless VLP. (C–N) Tailed VLPs representing phages like morphotypes. (O–U) Giant tailed VLPs. (V–Y) Archaea-like viruses. Scale bars = 100 nm, excepted notifications (O,S,R).

of the extant complex membranes of modern cells. This author mentioned that viral particles could have served as a "laboratory" to test molecular devices that were then incorporated into the membranes of emerging cells. Gill and Forterre [68] proposed that viruses may have existed prior to the appearance of the first cell and that they could be descendants of lipid vesicles through the formation of ribovirocells, prior to the emergence of RNA virions.

Viruses are acellular biological entities (**Figure 6**) unable to reproduce without their cell hosts. They have a genome consisting of DNA or RNA that could be double-stranded or single-stranded, linear or circular, segmented or unsegmented.

The genome is encapsulated in a protein coat called a capsid (with exception of Endornaviridae, Hypoviridae, Narnaviridae), which in specific cases can be enveloped by lipid membranes. All types of life forms, from prokaryotes (bacteria and archaea) to eukaryotes (animals and plants), can be infected by one or more viruses [110–113]. The diversity of viruses is therefore probably at least as great as that of their susceptible hosts [114]. Viruses have been classified according to a combination of different criteria: type (RNA or DNA) and form (single- or double-stranded; circular or linear) of the nucleic acids; the different ways in which they produce mRNA; morphology of viral particle; host type; and presence/absence of an envelope ([115, 116] and references herein). Thus, seven groups, organized into taxonomic levels, have been delineated: (i) positive-stranded RNA viruses, (ii) negative-stranded RNA viruses, (iii) double-stranded (ds) RNA viruses, (iv) reverse-transcribing viruses with positive-stranded RNA genomes, (v) reverse-transcribing viruses with ds DNA genomes, (vi) single-stranded (ss) DNA viruses, and (vii) dsDNA viruses [117, 118]. With the development of high-throughput sequencing technologies [119–122], the International Committee on Taxonomy of Viruses (ICTV) has considerably simplified the classification criteria by allowing all viruses to be classified on the basis of genome-sequence information [123]. The classification based on genome-sequence information opens up a new way in the classification of viruses that are known only from metagenomic data [114, 124]. Although no universally shared sequences are conserved across the entire genome of the viral world, the genomic approach also allows to target the phylogeny of specific viruses harboring common genetic markers [125]. The taxonomic classification of viruses is constantly evolving. In March 2020, the ICTV has identified 4 realms, 9 kingdoms, 16 phyla, 2 subphyla, 36 classes, 55 orders, 8 suborders, 168 families, 103 subfamilies, 1421

genera, 68 subgenera and 6590 species [123]. Note also the existence in femtoplankton of subviral agents which are not classified in the same way as viruses [123, 126–128]. These subviral agents are composed of three varieties: satellite viruses, viroids and prions (widely defined and described in [123, 126]). They mainly infect plants, fungi, and/or vertebrates. Satellite viruses are subviral agents morphologically indistinguishable from ordinary viral particles lacking genes capable of encoding functions necessary for replication. Thus, for their multiplication, they depend on the co-infection of a host cell with a helper virus. Viroids are small, circular, single-stranded, non-protein-coding RNAs that replicate autonomously when inoculated into higher plants. Prions are infectious protein particles devoid of nucleic acids.

To date, dsDNA and ssDNA viruses dominate the viral pool of the bacterial and archaeal communities. In contrast, positive-stranded RNA and dsRNA viruses are rare in these communities, while retroviruses are absent [129]. In eukaryote communities, RNA and retroviruses are dominant, with diversity and abundances far exceeding that of DNA viruses [129–131]. The size of the virus genome varies by about four orders of magnitude, with the smallest (0.859 kbp) recorded in ssDNA Circovirus SFBeef and the largest (2473 kbp) in dsDNA *Pandoravirus salinus* [132]. RNA viruses have the smallest genomes compared to other viruses [132, 133]. The capsid of viruses results from the arrangement of multiple copies of one or a few different proteins that determine their shape and size. Viruses harbor a remarkable variety of conformations (helical, polyhedral, spherical, ovoid, bacilliform, bullet-shape). Archaeal viruses have additional original forms (bottle-, lemon-, rod-shape). Some viruses are tailless (animal and plant viruses), while others present contractile or non-contractile tail (prokaryotic viruses = phages) characteristics of the families Ackermannviridae, Herelleviridae, Myoviridae, Siphoviridae and Podoviridae [123]. There are also viruses without a true capsid (Endornaviridae, Hypoviridae and Narnaviridae, for example); these are mostly parasites of eukaryote microorganisms or plants. The presence of an outer envelope in an "enveloped virus" combines virally encoded proteins with lipids and/or carbohydrates derived from the host cell membrane, depending on the viral family or genus [133]. Viruses vary in size and in diameter from 17 to over 400 nm for icosahedral forms, while filamentous forms vary in length from 650 to over 1950 nm [133, 134]. As non-motile entities, viruses meet their hosts by diffusive transport according to fluidic dynamic concepts (Brownian movement) or via biological or inanimate vehicles. The components of the capsid, tail or viral envelope, mainly proteins, play a crucial role in the recognition and in the specific binding of viruses to host cell receptors. Several stages can be distinguished in the life cycle of a virus: adsorption, penetration of nucleic

acids and uncoating, expression and replication of the nucleic acids, virion assembly and release [135]. Viral replication strategies range from obligatory host lysis (lytic cycle) to the persistence of viral genomes within hosts (lysogenic cycles), with strategies intermediate between these extremes (*e.g.*, chronic infections) [136]. In eukaryote viruses, a remarkable feature is the high diversity of genetic cycles, depending on nucleic acid content [111, 137].

Viruses are found wherever life is possible. The aquatic environment undoubtedly represents the largest reservoir of viral biodiversity on earth [110, 138–145] and associated references). In such an environment, metagenomic datasets have revealed the existence of numerous giant phages and their associated virophages [146, 147]. The genomes of some giant viruses are larger than those of many bacteria and archaea [148–152]. Genetic repertoires include various components of the viral world that have not previously been described (CRISPR–Cas systems, transfer RNAs (tRNAs), tRNA synthetases, tRNA-modification enzymes, translation-initiation and elongation factors and ribosomal proteins) [146]. These components are associated with functions that are characteristics of cellular organisms (translation machinery, DNA maintenance, and metabolic enzymes) [153]. Al-Shayeb *et al*. [146] argued that the characteristics of giant viruses, distinct from those of small phages and partially analogous to those of symbiotic bacteria, blur the distinctions between life and non-life. Finally, although there is no consensus on the scenario explaining the origin of viruses and their living or non-living nature, it is now accepted that they have been involved in the genesis and/or the evolution of cellular life forms.

Gene Transfer Agents (GTAs)

While viruses are implicated in cellular genesis and/or evolution, some of them have been suspected of drifting into gene transfer agents (GTAs), in a process that has been conceptualized as "prophage domestication" [154–156]. Briefly, GTAs arise though deletion and recombination processes that place the structural and DNA-packaging genes of prophage under the control of cellular regulators [157]. GTAs are suspected to be actively maintained by natural selection acting on benefits they confer [157]. GTAs are defined as tailed phage-like particles (with structural similarities to established phage morphotypes such as siphoviruses and podoviruses) that contain a random fragment of the genome of the producer cell genome [158, 159]. Their capsid sizes vary from 30 to 80 nm and they contain 4–14 kbp of DNA packaged in a protein capsid shell [160–166]. The stages of GTA production show similarities with those

of lysogenic infection from specific attachment to the release of GTAs into the extracellular environment via lysis of the producer cell [167–169]. However, unlike the prophage genes, the genes encoding GTAs are not excised from the genome of the host cell. GTAs are not replicative.

The amount of DNA it contains is insufficient to encode the protein components of the particle itself. Therefore, a GTA particle does not necessarily contain genes encoding GTA and cannot transfer a complete set of GTA structural genes to a recipient cell. This is distinct from a generalized transducer phage, for which usually only an occasional particle contains host genes, and the fragments of packaged DNA are the size of the phage genome [170]. GTAs have now been documented in a wide range of prokaryotes, including bacteria and archaea [161, 165, 166, 171–175]. The production of GTA particles depends on the physiology of the host, and the factors regulating GTA production differ from organism to organism [176]. It is possible that GTAs exist in abundance in all Earth environments in which they act primarily as mediators of horizontal gene transfer through a mechanism similar to transduction [176]. Identifying GTAs and distinguishing them from other femtoplankton particles, especially viruses, is a challenge. Many additional details concerning GTAs are provided in previous reviews [157–159, 170, 176–180].

CPR / DPANN

The tree of life gives a primordial role to prokaryotes in phylogenetic evolution. The recent discovery of CPR (Candidate Phyla Radiation) and DPANN (acronym of the first five phyla, "Candidatus Diapherotrites", "Candidatus Parvarchaeota", "Candidatus Aenigmarchaeota", Nanoarchaeota and "Candidatus Nanohaloarchaeota") has generated new knowledge concerning the place of prokaryotes in the evolutionary processes of life. These entities have the general characteristics of prokaryotes but present original peculiarities (volume close to the theoretical minimal cell volume, *i.e.*, 0.008 μm^3, genome and reduced metabolic capacities consistent with a symbiotic lifestyle, and cellular components, *e.g.*, ribosome, of unusual composition) which make them atypical prokaryotes and potentially the smallest known life form [23]. The evolutionary origins of the CPR and DPANN radiations in the two domains of bacteria and archaea, respectively, are still pending because the exact phylogenetic position of some of these entities in the tree of life is uncertain and controversial [23, 181, 182]. The hypothesis that some of these entities may have appeared during a dramatic but heterogeneous

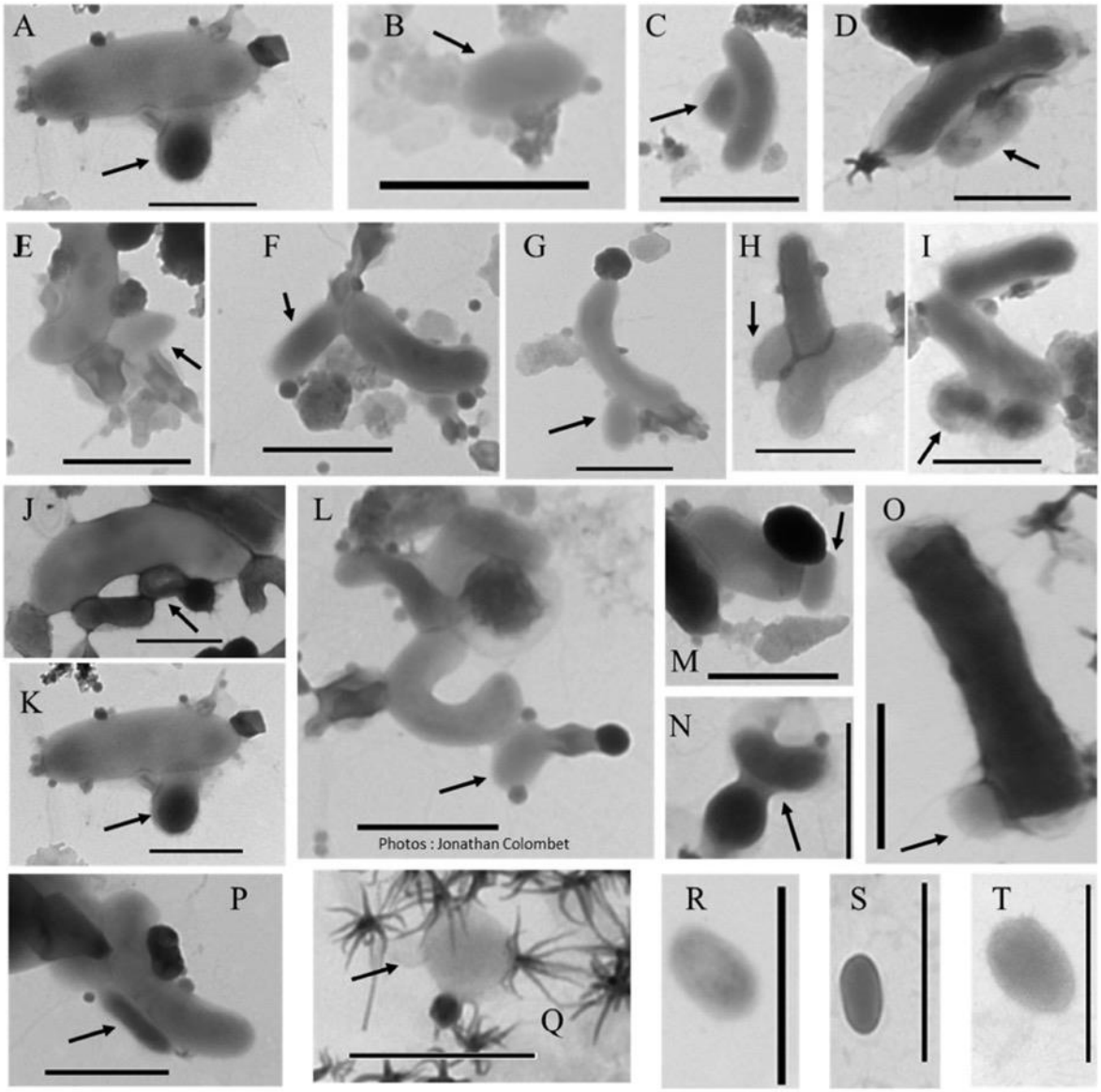

Figure 7: Transmission electron micrographs of attached (A–Q) or free (R–T) femtoplankton-like prokaryotes.

Arrows indicate the target particles when the samples are heterogeneous. Scale bar: 500 nm.

episode of genome reduction, or may have originated from a protogenote community and co-evolved with other prokaryotes, has recently emerged [182]. Considering the latter hypothesis and in a cell-centered view of life, CPR and DPANN could represent the smallest and simplest life form known from the last universal common ancestor (LUCA) and/or protogenotes [23, 183, 184]. These minimalist living entities could thus bridge the gap and establish the continuum between non-cellular but compartmentalized nano-entities (vesicles and viruses) and more complex cellular life forms.

Genome analyses and rare observations indicate that CPR and DPANN have the smallest genomes and cell size in the cellular world ([23] and references herein) (**Figure 7**). For example, the first member of Nanoarchaeota, *N. equitans*, is characterized by small cells, only 400 nm in diameter (volume = 0.0335 μm^3), and codes for one of the smallest known archaeal genomes (0.49 Mb) [185, 186].

Slightly larger genomes (0.64–1.08 Mb) of other ultra-small archaea (Parvarchaeota and Micrarchaeota) with cell volumes as low as 0.009 μm^3, have since been discovered [187–189], as well as some nanosized Nanohaloarchaea (0.1–0.8 µm) [190–193]. Reduced genome and cell size are also characteristics of many groups of CPR bacteria. For example, a reduced genome of less than 0.694 Mb has been recorded for the candidate population OD1 [194], with a few ultra-small bacteria of the shortest length (less than 179 nm) and an assumed minimal volume close to 0.004 μm^3 [195]. Most of the CPR is filterable onto 0.2 µm filter ([23] and references herein). Some CPR and DPANN species are characterized by sparse meta bolisms, with limited catabolic and anabolic capacities, consistent with a symbiotic lifestyle ([23, 181, 182] and references herein). These authors pointed out that CPR and DPANN entities are not monolithic in terms of metabolism but rather harbor a diversity of metabolic capacities, consistent with a range of lifestyles ranging from obligatory symbionts or putative parasites to free-living mode, depending on their degrees of dependence on other organisms (prokaryotes or eukaryotes).

The characteristics of CPR and DPANN call into question the fact that they are cellular life forms. Unlike vesicles and viruses, their ability to code genetic systems for cell division and to transform energy and carbon compounds, coupled with the existence of easily recognizable ribosomes (often of unusual composition), clearly distinguish them as cellular living organisms [23]. They therefore represent a substantial part of the diversity of bacteria and archaea domain.

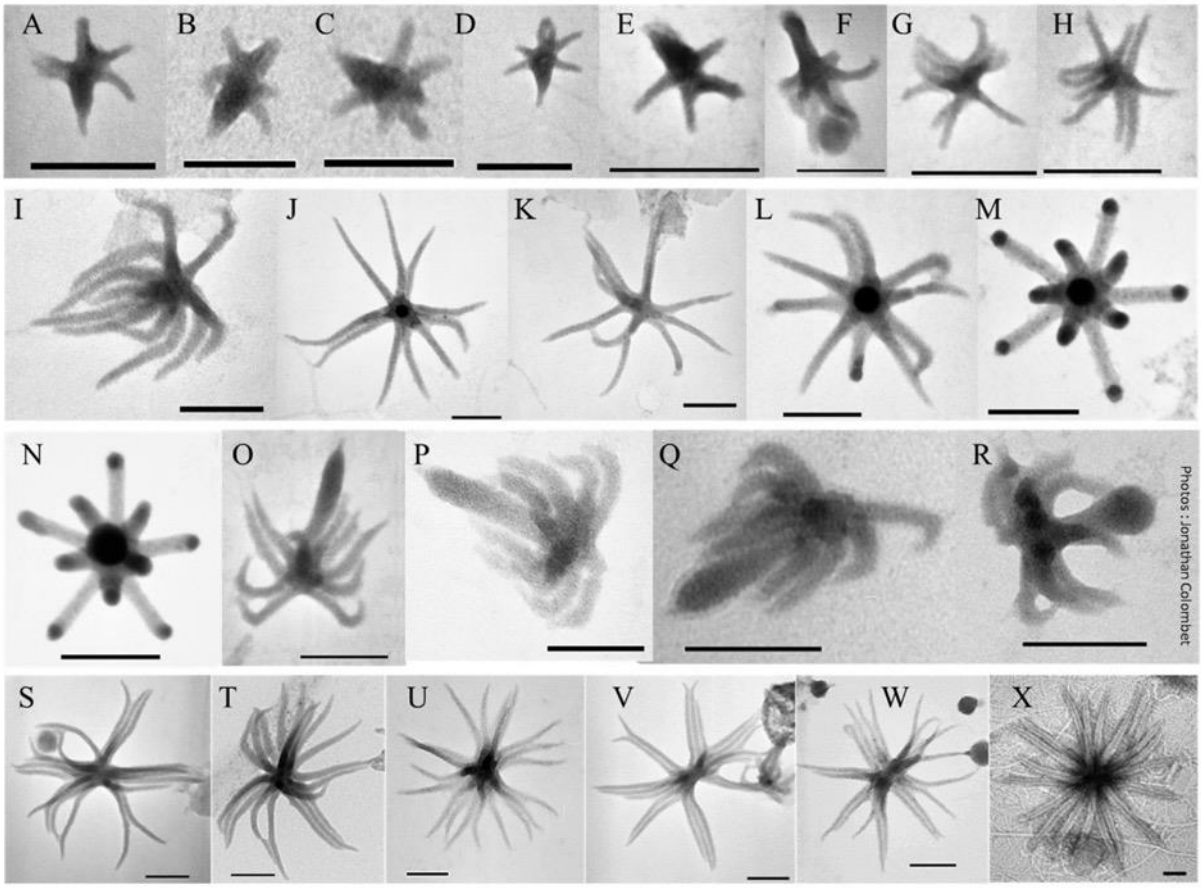

Figure 8: Transmission electron micrographs of different morphotypes of aster-like nanoparticles.
(A–H) 4–10-armed forms. (I–M) 11-armed forms and their budding 11-armed variants (N–R) with elongated and swollen bud-like excrescences. (S–X) 20-armed forms.
Scale bars = 100 nm.

The CPR seems to be a monophyletic radiation with at least 74 phylum-level lineages while DPANN encompasses at least 10 different lineages [23, 181]. In addition to terrestrial and animal microbiomes, these organisms were found in many aquatic environments, including acidic, alkaline, and hypersaline habitats, freshwater, and marine ecosystems ([23] and references herein).

Although these ubiquitous and diverse entities are recognized as the smallest known life form, the lack of an autonomous development in some of them opens a new path at the root of the tree of life to a group of organisms that are unable to reproduce by themselves. Finally, Lannes *et al*. [196] mentioned that CPR and DPANN superphyla may not be the only prokaryotes found in femtoplankton and they anticipated the discovery of new autotrophic aquatic nano-organisms with the development of single cell genomics.

Something New in the Femtoplankton

Over the past decade, the discovery of BMOPs, EVs and CPR/DPANN (see above) has significantly increased the complexity of the femtoplankton environmental fraction previously considered to be composed primarily of viruses [28]. This perception, discussed here, has been recently enriched by the discovery of mysterious aster-like nanoparticles (ALNs, **Figure 8**).

These new femtoplankton particles, whose origin is unknown, do not belong to any previously defined environmental entities (see [27]). Selected-area electron diffraction of ALNs revealed an amorphous structure, mainly composed of carbon, oxygen, calcium and nitrogen. Trace amounts of potassium were also identified in association with the particles.

ALNs are presumably formed of organic components [27]. ALNs are original pleomorphic nanoparticles (**Figure 8)** exhibiting puzzling aster-like shapes with arm-like outgrowths protruding from a central core. Three dominant morphotypes emerged based on the size and number of arms (4-, 11- and 20-armed forms). Some appeared endowed with a singular bud-like appendix that seemed to arise from the center of symmetry of the particle. The sagittal sections of the arms reveal a tubular appearance, with an area of electron light surrounded by a wall-like structure. Their average length ranges from 110 to over 439 nm, with volumetric estimates of less than 0.0014 μm^3.

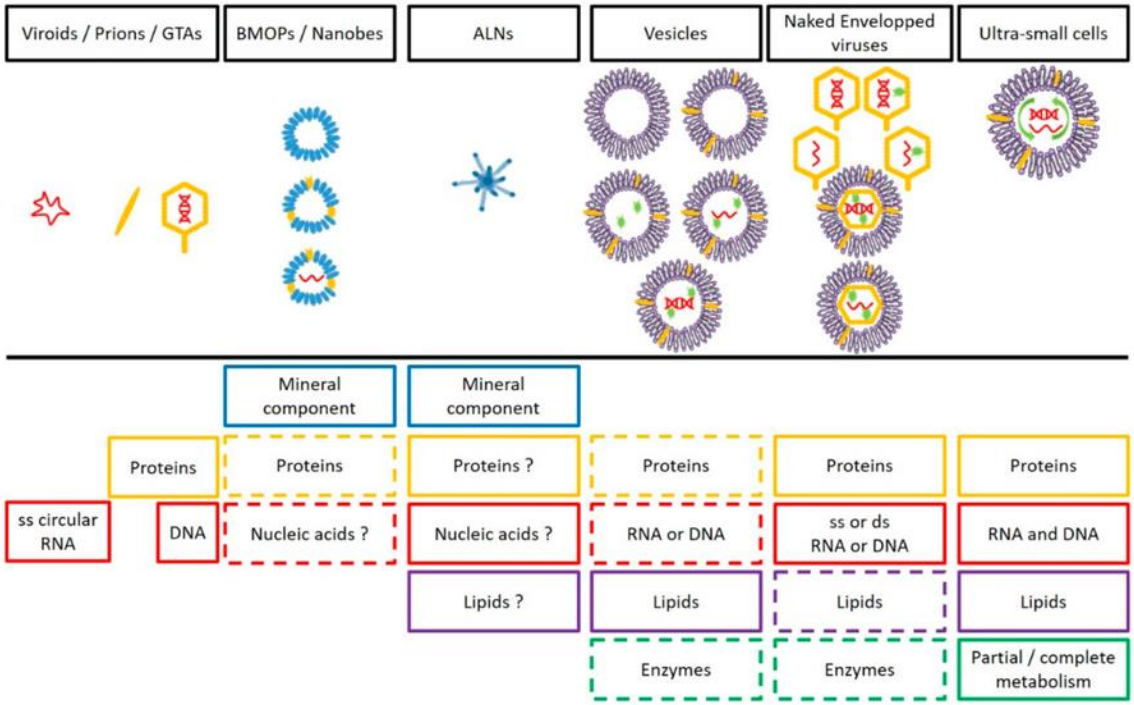

Figure 9: Schematic overview of the main components and of organizational complexity (increase in complexity from left to right) of the femtoplankton entities mentioned in this review.
The question mark (?) represent uncertainty about the presence/absence of this compound in the target entity. The dotted line (--) means "Optional". GTAs = gene transfer agents, BMOPs = Biomimetic mineral–organic particles, ALNs = aster-like nanoparticles. Note that the tail (mainly an attribute of bacteriophages) is not present in all naked viruses.

Table 1: Comparison of morphologies, some main constitutional elements and development strategies of femtoplankton entities.

		Gene Transfert Agents	BMOPs/Nanobes	ALNs	Vesicles	Viruses	CPR/DPANN
Shape		Tailed phage like-particle (polyhedral)	Coccoid, amoeboid, filamentous, ovoid…	Aster-like	Circular	Helicoidal, polyhedral, spherical, bacilliform…	Coccoid, ovoid…
Size (nm)		30–80 (capsid)	20–1000	110–439	20–2000	17–1950	ND–400
Main Composition	**Dominant Mineral Component**	/	$CaSO_4$, $CaCO_3$, Al_2O_3, …	Ca (and others?)	/	/	/
	Nucleic Acids	DNA	Controversial	ND	Optional: RNA or DNA	RNA or DNA	RNA and DNA
	Genome Size	(4 to 14 Kbp)	/	/	Dependent on the producer cell	(0.859 to 2473 Kbp)	(0.49 to 1.08 Mbp)
	Proteins	+	Optional	ND	Optional	+	+
	Lipids	/	ND	ND	+	Optional (envelopped viruses)	+
Surrounding Structure (Nature)		Capsid (proteic)	+ (ND)	+ (ND)	Membrane	Capsid (proteic) Envelop (mainly lipidic)	Membrane/Cell wall/Glycocalyx
Lifestyle		Symbiosis	ND	ND	/	From symbiosis to parasitism	Symbiont/free
Multiplication Strategy		Lysis	Symmetrical fission	ND	Budding	Spectrum from lytic to lysogenic	Cell division

Viroids and prions composed only of RNA molecule and proteins respectively are not shown in the table. BMOPs = Biomimetic mineral–organic particles, ALNs = aster-like nanoparticles, CPR/DPANN = Candidate Phyla Radiation/Diapherotrites Parvarchaeota Aenigmarchaeota Nanoarchaeota Nanohaloarchaeota. ND = not determined. / = absence. + = presence.

Despite positive nucleic acid labelling, the presence of nucleic acids in ALNs remains to be proven [27]. The hypothesis of a support of heredity is supported by the occurrence of the same ALN morphotypes regardless of the environmental context and the recurrent radial symmetry of the particles, which might reflect a developmental relationship between the morphotypes [27].

We supplemented these unusual and original descriptive characteristics with development studies of ALNs in vitro and in situ. These include sensitivity to biocidal treatments, changes in ALN abundance in the absence of potential host cells, marked seasonal dynamics and developmental processes of ALNs that confirm their originality and question their origin [27]. We have also shown that ALNs are ubiquitous entities capable of maintaining themselves in most continental and coastal aquatic environments (lakes, rivers, marshes, estuarine area) [197]. The positive correlation between prokaryotic abundance and ALN recorded between all environments considered in this study, and the close physical contact between ALNs and prokaryotes displayed in [27], suggest a potential link between prokaryotes and ALNs. Future work is required to elucidate the origin, composition and ecology of these entities, until now unclassified, and their place in the evolution of life.

Overall, the discovery of ALNs, following that of diverse and ubiquitous BMOPs/nanobes, EVs, and femtoplankton prokaryotes, suggests that femtoplankton could host novel types of other ultra-small particles that could provide new insights into biodiversity and the functioning of the aquatic environment. The main characteristics of the femtoplankton entities and their organizational complexity are summarized and schematized in **Table 1** and **Figure 9**.

This overlooked richness represents an unexpected windfall for understanding the evolutionary processes leading from minerals to the emergence of life on the earth (**Figure 10**). Indeed, femtoplankton entities can be placed in the context of prebiotic evolution by marking out the potential pathway to the cellular and viral world. In the early evolutionary stages, based on the hypothesis of a prebiotic peptide/RNA world developed in [198], BMOPs/nanobes, as potential supports (inside or fixed outside) of prebiotic organic chemistry, could have paved the way for the formation of primitive elements (organic molecules). The evolution of a procell towards the first protocell could have been achieved after encapsulation and compartmentalization of the primitive elements into fatty acids vesicles prior to evolution by unregulated and error-prone way division, depending on environmental conditions [68, 199]. The complexification of the

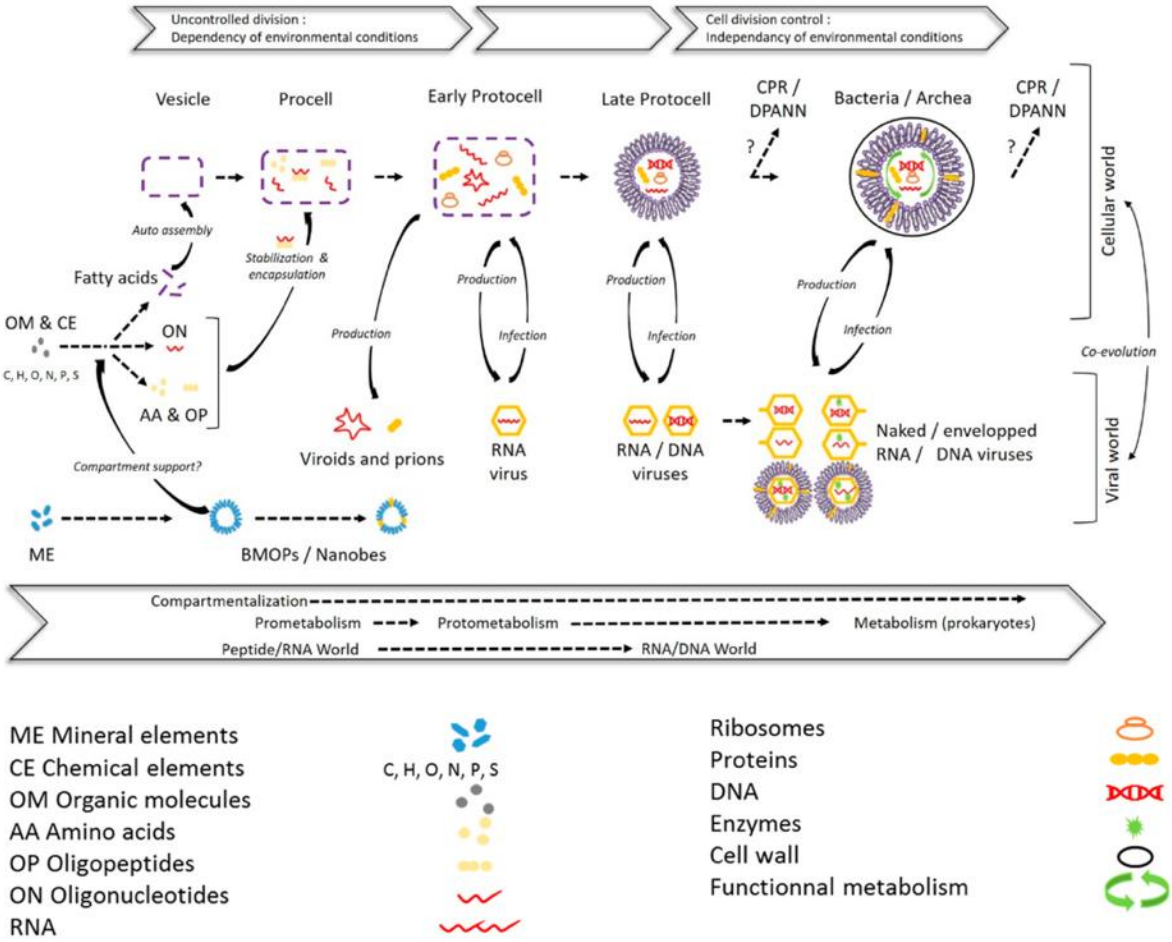

Figure 10: Significance of femtoplankton entities in prebiotic evolution: a potential pathway to the cellular and viral world.

Early stages of evolution leading to a procell are based on the hypothesis of a prebiotic peptide/RNA world developed in [198]. In these early stages biomimetic mineral–organic particles (BMOPs)/nanobes, as a potential support (inside or fixed outside) of prebiotic organic chemistry, could have paved the way for the formation of organic molecules. The evolution of a procell toward the first protocell can be achieved after encapsulation and compartmentalization of the primitive elements into fatty acid vesicles prior to evolution by unregulated and error-prone way division, depending on environmental conditions [68, 199]. Complexification of biochemical (metabolic) and replicative systems, as well as membrane/cell walls, during the protocell stages has led to divisions that are more independent of environmental conditions [199] and to the initiation of the cellular and viral world [111]. The emergence of Candidate Phyla Radiation/Diapherotrites Parvarchaeota Aenigmarchaeota Nanoarchaeota Nanohaloarchaeota (CPR/DPANN) from protocell or prokaryotic communities is adapted from [182].

biochemical (metabolic) and replicative systems, as well as of the membrane/cell walls, during the following protocell stages would have led to divisions more independent of environmental conditions and to the initiation of the cellular and viral world [111, 199]. CPR/DPANN emerged from late protocell stages or from prokaryotic communities as suggested in [182].

2.1.4 Quantitative and Functional Significances of Femtoplankton

One of the peculiarities of femtoplankton entities is their widespread distribution. The femtoplankton is present in all possible aquatic ecosystems. Viruses, vesicles and gene transfer agents as symbionts of prokaryotes are everywhere; they thrive from hot springs to polar glaciers, from acidic to alkaline environments, from freshwater to hypersaline systems [19, 20, 25, 110, 138–145, 176] and associated references). CPR/DPANN have also been listed in a wide variety of environments [23]. BMOPs/nanobes have been found in marine water and in some extreme environments [18, 52, 55, 63]. ALNs, although data are still sparse, appear to be salinity-tolerant and colonize a wide variety of freshwater ecosystems [197]. Each environment has its own unique diversity of femtoplankton entities. Some types or species are endemic or specific to a given ecosystem under given conditions, others are more tolerant of variations in the environment and are widely distributed. The endemicity and transbiome invasion (*e.g.*, marine-freshwater) of viruses and some femtoplankton prokaryotes are discussed in [200]. Movements or transfers from one ecosystem to another have been demonstrated for ALNs or viruses, for example, which can move along a watershed or through atmospheric systems [198, 201, 202]. Thus, femtoplankton entities are certainly the most diversified and widespread in the biological world. Capturing their diversity and specific abundance and comparisons between ecosystems is a challenge. By their diversity and composition, femtoplankton entities represent a huge reservoir of mineral and organic molecules. This reservoir makes them an essential player in the circulation, availability and transfer of elements affecting the biogeochemistry of their environment. The catabolic or anabolic metabolisms expressed in some of them or the potential symbiotic lifestyle in others, mean that these femtoplankton entities are not only an essential driving force in the diversification of aquatic organisms, but are also a significant driving force in the flow of matter and energy circulating in aquatic ecosystems. The following section reviews the quantitative and functional importance of the femtoplankton compartment according to their origin and composition as described above.

Quantitative Importance

Many efforts have been made to estimate the diversity of BMOPs/nanobes, EVs, GTAs and CPR/DPANN in the aquatic environment (see above). Nevertheless, estimates of their quantitative importance are still very rare. Although Wu *et al.* [18] mentioned that seawater contains a relatively high particle-seeding potential, to our knowledge, no data on the abundance of BMOPs or nanobes in the aquatic environment is available. Little more information is available for EVs. In a rare field study, Biller *et al.* [24] suggested that EV concentrations range from 10^5 to 10^6 vesicles per mL of sea water. To our knowledge, there are no data available about the abundance of GTAs in aquatic ecosystems. Genomic or proteomic studies of CPR and DPANN are increasingly documented, leading to a better consideration of their wide diversity [203–205]. However, to our knowledge there are no reports of their density in water neither as episymbionts (attached to a cell) nor as free-living elements. In a specific study, we reported significant amounts of ALNs in contrasted aquatic ecosystems [27]. These ubiquitous entities fluctuate spatially and temporally, with values ranging from undetectable to $9.0 \pm 0.5 \times 10^7$ particles·mL^{-1} [27]. As for other femtoplankton entities, the assessment of their quantitative importance requires a strong consideration in future work. Conversely, the quantitative importance of viruses has been widely documented and reviewed [110, 139, 140, 206–208]. More than 10^{30} viruses can exist in aquatic environments at any given time [139]. Their abundances vary spatially and temporally up to estimates exceeding 10^8viruses·mL^{-1} [110, 140, 208]. Their current biomass has been estimated to be equivalent to 75 million blue whales (approximately 200 million tons of carbon) [209]. The abundance of RNA viruses can match or exceed that of DNA viruses [210]. Viruses are perhaps the most abundant biological entities on earth. The high abundances of EVs, CPR/DPANN and ALNs raise the question of the real quantitative contribution of viruses. Indeed, most estimates of viral abundance are based on counting of "virus-like particles" through positive nucleic acids labeling. These estimates probably lead to an overestimation of true viruses by counting all potential nucleic acid carriers described above, *i.e.*, BMOPs/nanobes, EVs, GTAs, CPR/DPANN and ALNs [27, 211]. The extent of this overestimation could have a fundamental impact on the ecological roles of viruses. Soler *et al.* [212] suggested that EVs could outnumber true viral particles in some aquatic environments and Colombet *et al.* [27] reported that ALNs can account for up to 40% of virioplankton counted by transmission electron microscopy.

There is an evident lack of data on the relative quantification of the recently discovered and overlooked femtoplankton components, both temporally and spatially. A combination of

electronic microscopy and nucleic acid-based methods is needed to reveal the relative contribution of each of the femtoplankton categories [27]. In the future, such a consideration appears to be fundamental in deciphering the global importance of femtoplankton in the functioning of aquatic ecosystems and the related biogeochemical cycles.

Potential Ecological Importance

Estimating the overall functional importance of femtoplankton is a challenge for the future. This requires considering not only the diversity and quantity but also the biological/physiological state (composition, lifestyle, activity, *etc*.) of each of its representatives and the environmental contexts. A first approach is to speculate on the specific potential significance of each of the femtoplankton entities.

BMOPs/Nanobes

These entities are overlooked in aquatic systems and very little data are available on their putative ecological importance. Like all femtoplankton entities, BMOP/nanobe biomass may play a crucial role in the circulation, availability and transfer of matter in the environment [18]. The assumed ecological significance of these entities could be inferred from biomedical sciences. Yaghobee *et al*.[56] reported several roles for some of these entities in calcification-related human diseases. Breitschwerdt *et al*. [213] and Barr *et al*. [49] reported their occurrence in terrestrial mammals. It is therefore very likely that the BMOPs/nanobes can play an important role in the health of marine animals, which by inference suggests an ecological role in the environment. Çiftçioglu and Kajander [214] reported interactions (endocytosis) with cultured mammalian cells involving potential cytotoxicity. Such interactions with microbes in the environment could have a great implication for the receptor cell biology, although these are hypothetical and remain to be fully explored.

Extracellular Vesicles

A little more information about the ecological significance of vesicles in aquatic systems is available. Gill *et al*. [19] reported that EVs, as carriers of various molecular cargoes from cell to cell, can modify cellular physiology (stress response, intercellular competition, pathogenicity and detoxification) and can play important roles in all types of intercellular interactions. They can be involved in the quorum sensing, acclimatization to nutrient limitation, morphological plasticity and trapping of toxins and antibiotics [25]. Additionally, EVs as carriers of genetic

information between cells have been proposed as a novel vehicle for horizontal gene transfers (HGT), in addition to the well-known related mechanisms of transformation, transduction and conjugation[81, 215]. As a result, they can significantly modify the gene pool and associated metabolic capacities of their receptors. Interactions between EVs and viruses have also been documented [19, 216]. EVs have the potential to regulate host–virus dynamics [216]. Some EVs can propagate the viral genome or plasmids [108]. EVs can sometimes act as decoys to limit viral infection, while viruses can manipulate the production of EVs from infected cells to their own advantage [217, 218]. As consequence, several ecological roles can be inferred for EVs, including their influence on ecology and community structure, the trophic-level interactions and their impact on the carbon cycle [21, 24, 25, 70–202]. Nevertheless, as with BMOPs/nanobes, these potential roles are largely derived from biomedical sciences and remain to be extensively explored in natural environments.

Viruses and Gene Transfer Agents

Microbial ecologists have devoted more effort into understanding the functional importance of viruses in aquatic environments [22, 26, 110, 112, 121, 139, 140, 197, 210, 219–223]. These studies reported that viruses are major components of the aquatic food web, not only as parasites that can lead to cell death, but also as a powerful weapon able to manipulate the life histories, evolution and ecology of their hosts.

Suttle [139] reported that every second, approximately 10^{23} viral infections occur in the ocean. These infections are a major source of mortality, and cause disease in a wide range of organisms, from shrimp to whales. Through them, viruses contribute to both top-down and bottom-up control of the microbial community [26]. Viruses directly influence the abundance of aquatic communities. Lytic viruses may account for up to 50% of bacterial mortality in the pelagic ecosystems and can abruptly terminate eukaryote algae blooms [218, 224–227]. Bossart and Duignan [112] noted that viral infections also have major effects on the health of marine mammals, including neoplasia, epizootics and zoonoses. As a major source of mortality, lytic viral infections considerably affect biogeochemical cycles. The fate of matter produced by lysis can follow a different pathway, from direct remineralization/regeneration by the microbial loop, which can support a higher microbial biomass, to export by aggregation and sedimentation [110, 219, 228, 229]. Viral infection can alter cell stoichiometry and uptake rates [220, 230]. Zimmerman *et al*. [223] discussed how metabolic reprogramming of host cells during lytic viral infection alters the nutrient cycle and ocean exports of carbon. They reported that viral infection

transforms host metabolism through metabolic genes encoded by the virus, whose functions appear to alleviate energy and biosynthetic limitation in viral production. They emphasized the importance of the physiological state of the host cell and environmental conditions in the regulation of these processes.

Viruses are also important drivers of microbial diversity [110, 231, 232]. Two concepts can explain this power: the "antagonistic coevolution" (arms race) and "killing the winner". In the concept of "antagonistic coevolution", hosts and viruses coevolve in order to escape lethal infections for the hosts, a situation that can make surrounding hosts resistant to viruses [233]. In the "killing the winner" model, viral predation of temporarily abundant and specific hosts can weaken the between-host competition for resources and promote the coexistence of host diversity by allowing the growth of non-abundant or rare host species [231, 234–236]. Viruses affect also the diversification and physiology of aquatic hosts through horizontal transfers of genetic materials [237, 238]. One example is the transfer of photosynthesis genes between viruses and their hosts *Prochlorococcus* [239]. Ramisetty and Sudhakari [240] underlined that the temperate prophages are one of the most significant drivers of bacterial genome evolution and sites of biogenesis of genetic information. Nasir *et al*. [238] noted that phage conversion during transduction alters host physiology with respect to metabolism, pathogenicity, and niche adaptation. Although lacking metabolic activities, viruses can profoundly affect geochemical cycles by modelling the diversity and activity of their potential hosts.

GTAs are unusual vehicles for HGT, which appears to be an hybrid of bacteriophage transduction and natural transformation [170]. McDaniel, *et al*. [241] reported frequencies of antibiotic gene transfer by GTAs in in situ marine microcosms that were orders of magnitude greater than any other known mechanism. The transferred genes can enhance fitness or resilience and have the potential to drive bacterial evolution and genome plasticity, including the spread of virulence and antimicrobial resistance genes [242]. The ecological significance of GTAs is probably underestimated because they are difficult to distinguish from viral particles.

CPR/DPANN and Other Femtoplankton Prokaryotes

The main ecological implications of the femtoplankton entities described above are related to their composition (BMOPs/nanobes, vesicles, viruses), their ability to transport and transfer various molecules and genetic material (EVs, viruses, GTAs) and/or their "parasitic" lifestyles (viruses) which can modulate the physiology and ecology of receptor cells (prokaryotes or

eukaryotes). Until now, CPR/DPANN and other ultra-small prokaryotes are the only femtoplankton entities capable of metabolic activity. Although description of their potential metabolic activities is still in its infancy, this could profoundly impact biogeochemical cycles in the aquatic environment.

Castelle *et al*. [23, 243] and Anantharaman *et al*. [244] have demonstrated that members of CPR and DPANN superphyla have genetic supports able of encoding molecules involved in numerous autotrophic or heterotrophic reactions. For example, some CPR and DPANN have Rubisco type II/III genes, while others have gene-encoding enzymes involved in the carbon, nitrogen, sulfur and hydrogen cycles [244, 245]. Nevertheless, most CPR/DPANN lack parts of the central metabolic pathways, including nucleotides, amino acids and lipid biosynthesis and require a host to complete their life cycle [23, 169, 209, 246]. Achievement of the metabolic potential of episymbiotic CPR/DPANN is therefore dependent on the presence and availability of their hosts. The corollary of these interactions is the potential impact on the activities and metabolic capacities of the organisms on which they depend [23]. On a larger scale, Anantharam *et al*. [244] revealed evidence of extensive interconnection between the metabolisms of coexisting community members. These interrelationships are likely necessary to complete many biogeochemical pathways. This does not exclude the notion that some CPR/DPANN seem to have the genetic potential to be free-living, with aerobic and/or fermentative heterotrophic behavior [23, 246]. These discoveries are complemented by Lannes *et al*. [196] who have demonstrated that ultra-small marine prokaryotes, not necessarily CPR or DPANN, collectively harbor the genes required for the complex metabolism in carbon fixation, which could significantly increase their potential involvement in biogeochemical cycles. Lannes *et al*. [196] then anticipated that the discovery of new autotrophic marine nano-organisms with novel metabolic capacities is not impossible.

The potential ecological importance of CPR/DPANN, or other ultra-small prokaryotes is currently known through metagenomic and proteomic analyses or co-cultures of rare species. Therefore, their ability to express their genetic potential and to manipulate the metabolic potential of their hosts (symbiont, presumed new parasites) remains to be explored under contrasted environmental conditions, in order to estimate the overlooked ecological significance of these ultra-small prokaryotes.

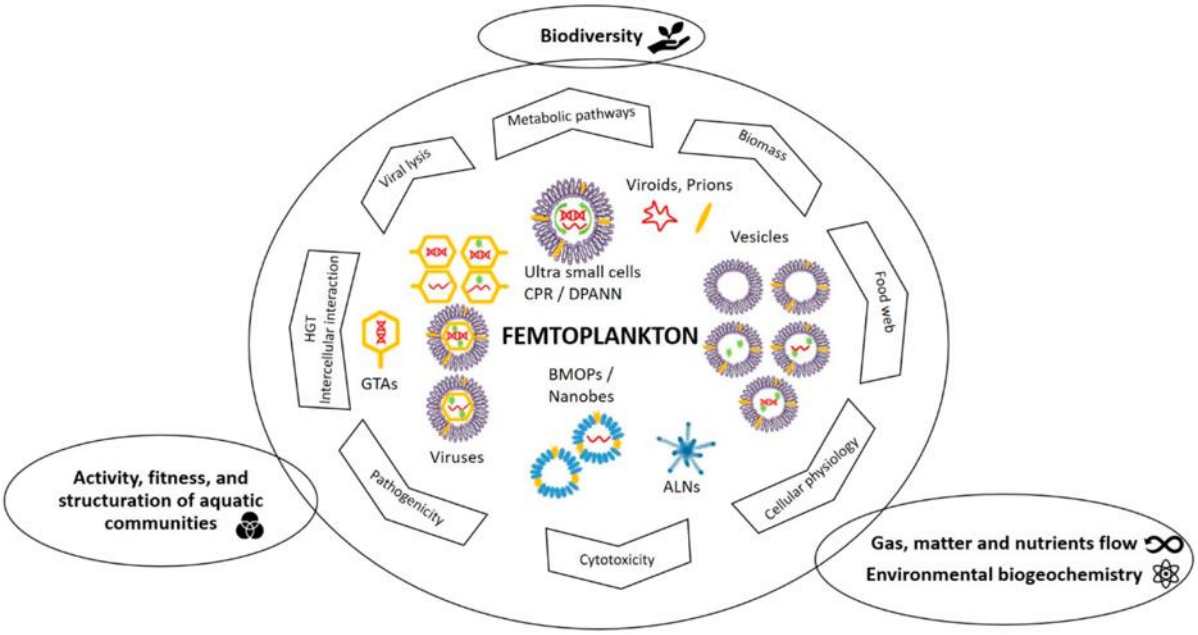

Figure 11: Schematic overview of the specific and major ecological roles of femtoplankton entities mentioned in this review.

BMOPs = Biomimetic mineral–organic particles, ALNs = aster-like nanoparticles, CPR/DPANN = Candidate Phyla Radiation/Diapherotrites Parvarchaeota Aenigmarchaeota Nanoarchaeota Nanohaloarchaeota, GTAs = gene transfer agents, HGT = horizontal gene transfers.

ALNs

The ecological role of the ALNs is currently unknown but could be potentially important. The total biomass of ALNs during bloom periods is likely to mobilize circulating mineral and organic nutrients to the detriment (competition?) of other microbial communities in aquatic ecosystems. For example, ALNs could be of great significance in the homeostasis of Ca in aquatic systems due to their high calcium composition. In addition, direct interplay with bacteria could significantly influence energy and matter flows mediated by prokaryote compartment [27]. The composition and activity of ALNs and interactions with the prokaryotic compartment remain to be confirmed and clarified to better understand the potential ecological role of ALNs. Clearly, these entities are new actors in the matter and energy flows circulating in aquatic systems which will have to be considered in future work.

Overall, recent evidence of numerous, diverse and ubiquitous, metabolically active (femtoplankton prokaryotes) or not (BMOPs/nanobes, EV), femtoentities as well as mysterious ALNs, implies a deep reconsideration of the diversity and ecological significance of femtoplankton. Historically considered through viral activity alone, this ecological significance may be greater than previously considered. **Figure 11** reviewed the ecological potentials of femtoplankton representatives in the environment.

The overlooked diversity and the associated biomass of all these entities necessarily have a deep impact on the circulation of conservative elements and the related biogeochemical cycling. Through the spectrum of their activities and potential hosts, femtoplankton entities have the ability to interact with all components of plankton. Femtoplankton maintains a privileged relationship with pico- and nanoplankton by not only being a parasite (*e.g.*, viral lysis [139]), but also a food source (*e.g.*, protozoan grazing [247]), a development factor (*e.g.*, symbiosis with CPR/DPANN [23, 244]) or evolution promotors (*e.g.*, HGT via virus [237, 238], EVs [81, 215], GTAs [242]). Femtoplankton models both the phenotype and genotype of their interacting hosts and thus could significantly impact the biodiversity and ecological functions of all the components of plankton.

The autonomous realization of metabolic pathways by free-living femtoplankton entities (*i.e.*, femtoplankton prokaryotes) could also significantly expand the ecological importance of femtoplankton in geochemical cycles.

Finally, taken together, femtoplankton entities represent a powerful engineering weapon able to deeply affect biodiversity and matter and energy flows circulating in aquatic environments. Nevertheless, most of the potential effects of femtoplankton remain to be explored. Their estimation needs to consider not only the diversity and biology of their representatives, but also their ability to interact with other biological elements and to express their activities in environmental contexts.

2.1.5 Conclusions

This review highlights that the femtoplankton compartment hosts a huge diversity of unidentified and overlooked entities at the frontiers of our knowledge. From an evolutionary point of view, this source of new diversity could be essential to a better understanding of the processes leading from the mineral–organic phase to a cell-like living entity. Femtoplankton could present all the stages presumably involved in the life initiation. Moreover, it could be crucial in many ecological processes. It represents a powerful engineering weapon capable of profoundly affecting biodiversity and matter and energy flows circulating in aquatic environments. Finally, this review highlights the need to deepen our knowledge of this still largely unknown compartment.

Funding
M.F. was supported by a PhD fellowship from the CPER 2015–2020 SYMBIOSE challenge program (French Ministry of Research, UCA, CNRS, INRA, Auvergne-Rhône-Alpes Region, FEDER). This review is a contribution to the "Nanopoulpes" project funded by the Interdisciplinary Mission of the French National Center of Scientific Research (CNRS) Program Origins, 2020 edition. This research was also financed by the French government IDEX-ISITE initiative 16-IDEX-0001 (CAP 20-25).

Acknowledgments
Thank you to the anonymous reviewers for their numerous helpful suggestions.

Conflicts of Interest
The authors declare no conflict of interest

2.2 Découverte de nouvelles entités femtoplanctoniques : les Aster-Like Nanoparticles

Discovery of High Abundances of Aster-Like Nanoparticles in Pelagic Environments: Characterization and Dynamics

Jonathan Colombet1*, Hermine Billard1*, Bernard Viguès1*, Stéphanie Balor[2], Christelle Boulé[3], Lucie Geay[3], Karim Benzerara[4], Nicolas Menguy[4], Guy Ilango[1], Maxime Fuster[1], François Enault[1], Corinne Bardot[1], Véronique Gautier[5], Angia Sriram Pradeep Ram[1] and Télesphore Sime-Ngando[1]
* These authors have contributed equally to this work

[1] Université Clermont Auvergne, CNRS, Laboratoire Microorganismes:Génome, Environnement, Clermont-Ferrand F-63000, France
[2] Université Paul Sabatier Toulouse III, CNRS, Plateforme de Microscopie électronique intégrative (METI), Centre de Biologie Intégrative (CBI), Toulouse F-31000, France
[3] Université Claude Bernard Lyon 1, Centre Technologique des Microstructures (Ctμ), Villeurbanne F-69100, France
[4] Sorbonne Universités, Université Pierre et Marie Curie Paris 06, Muséum National d'Histoire Naturelle, Institut de Recherche pour le Développement, CNRS, Institut de Minéralogie, de Physique des Matériaux, et de Cosmochimie, Paris F-75000, France
[5] Université Clermont Auvergne, INRAE, UMR GDEC, Plateforme GENTYANE, Clermont-Ferrand F-63000, France

Publié dans *Frontiers in Microbiology* - Octobre 2019
doi: 10.3389/fmicb.2019.02376

2.2.1 Abstract

This study reports the discovery of Aster-Like Nanoparticles (ALNs) in pelagic environments. ALNs are pleomorphic, with three dominant morphotypes which do not fit into any previously defined environmental entities [*i.e.*, ultramicro-prokaryotes, controversed nanobes, and non-living particles (biomimetic mineralo-organic particles, natural nanoparticles or viruses)] of similar size. Elemental composition and selected-area electron diffraction patterns suggested that the organic nature of ALNs may prevail over the possibility of crystal structures. Likewise, recorded changes in ALN numbers in the absence of cells are at odds with an affiliation to until now described viral particles. ALN abundances showed marked seasonal dynamics in the lakewater, with maximal values (up to 9.0 ± 0.5 × 107 particles·mL−1) reaching eight times those obtained for prokaryotes, and representing up to about 40% of the abundances of virus-like particles. We conclude that (i) aquatic ecosystems are reservoirs of novel, abundant, and dynamic aster-like nanoparticles, (ii) not all virus-like particles observed in aquatic systems are

necessarily viruses, and (iii) there may be several types of other ultra-small particles in natural waters that are currently unknown but potentially ecologically important.

2.2.2 Introduction

Recent advances in environmental and nanoparticle sciences have helped to reveal an unexpected diversity of living and non-living femto-entities (0.02–0.2 μm as defined for femtoplankton by [28]) in the environment. Previously considered to be mainly composed of viruses [28], the successive discovery in significant abundance, and in various environments, of mysterious nanobes [52, 55, 58, 59], extracellular vesicles (EVs) [75, 212], ultramicro-prokaryotes [23, 31, 32, 203, 204, 248, 249] and biomimetic mineralo-organic particles (BMOPs) [18], has significantly increased the complexity within the environmental fraction of femto-entities.

Contrary to viruses or EVs, controversed nanobes, some of which could be affiliable to BMOPs, and ultramicro-prokaryotes, including recently discovered CPR (*Candidate Phyla Radiation*) and DPANN (*Diapherotrites, Parvarchaeota, Aenigmarchaeota, Nanoarchaeota, Nanohaloarchaea*), have the ability to develop outside a host [18, 50, 54, 57, 250]. Nanobes exhibit diverse morphotypes: coccoid, amiboid, ovoid or filamentous shapes [52, 55, 58, 59]. Among them, only ultramicro-prokaryotes are clearly affiliated to living organisms according to the volumetric criteria advanced by the National Research Council (1999) [251], *i.e.*, the theoretical minimal cell volume (TMCV) sufficient to house nucleic acids and the associated biosynthetic machinery is at 0.008 μm3. Though these new entities were described in natural environments, relatively little is known about their ecological significance. Available data however suggests a significant impact on the biogeochemical cycles. EVs are potentially involved in cell communication, competition and survival of bacteria [252]. Interactions between ultramicro-prokaryotes and other micro-organisms communities may shape natural microbiome function [23]. Likewise, BMOPs incorporate trace elements and proteins suggesting that these entities may play a role in the circulation and availability of minerals and organic molecules in the environment [18]. Characterizing the femtoplankton biomass and the diversity of its representatives seems crucial to our understanding of the functioning of aquatic ecosystems.

Table 2: Physicochemical characteristics of the lakewater on February 2017.

Parameters	Values
Water temperature, °C	4
pH	7.4
Total carbon, $mg \cdot L^{-1}$	16
Total phosphorous, $mg \cdot L^{-1}$	0.28
Un-ionized ammonia, $mg \cdot L^{-1}$	<0.05
Alkali concentration, °F	0
Complete alkali concentration, °F	27.65
Kjeldahl nitrogen, $mg \cdot L^{-1}$	3.3
Overall nitrogen, $mg \cdot L^{-1}$	4
Ammonium, $mg \cdot L^{-1}$	0.12
Carbonate, $mg \cdot L^{-1}$	Below limit of detection
Chloride, $mg \cdot L^{-1}$	12.5
Nitrate, $mg \cdot L^{-1}$	3.1
Orthophosphate, $mg \cdot L^{-1}$	0.05
Nitrite, $mg \cdot L^{-1}$	0.05
Total potassium, $mg \cdot L^{-1}$	9.6
Total sodium, $mg \cdot L^{-1}$	3.1
Total calcium, $mg \cdot L^{-1}$	9.1
Total magnesium, $mg \cdot L^{-1}$	1.7

In this study, we report the discovery of abundant and seasonally-fluctuating populations of "Aster-Like Nanoparticles" (ALNs) in a freshwater lake of Massif Central (France), with volumes lower than TMCV. ALNs display typical and unique morphological features. Physical-chemical aspects, pleomorphism, flow cytometry and growth analyses of ALNs are presented and compared to distinctive features of living or not-living particles of similar size. Preliminary attempts to evidence DNA-based heredity support are reported.

2.2.3 Materials and Methods

Study sites and Sample Collection

Samples were collected at the surface of an artificial and highly eutrophic freshwater lake (surface area 1.2 ha, maximum depth 2.5 m) near Neuville in the French Massif Central (45°44'24"N; 3°27'39"E; 465 m altitude). Part of the samples were immediately fixed with 1% (v/v) formaldehyde and stored at 4°C until analysis (see below). Unfixed samples were transported at 4°C to the laboratory and treated within two h (see below). In situ dynamics of ALNs were monitored in 11 fixed samples collected between November 2016 and January 2018. **Table 2** lists the physical-chemical characteristics of the water analyzed once, in February 2017.

Detection of ALNs was also conducted on surface microlayer samples of 16 selected geographical stations (namely HL1 to HL16) from the Ha Long Bay (Vietnam). Details on these samples and their environment were provided in a previous work [253]. ALNs were quantified on electronic microscopy grids prepared as mentioned below.

ALN, Prokaryote, and Virus-Like Particle (VLP) Counts and Imaging

ALNs in fixed samples were collected by centrifugation at 15,000 g for 20 min at 14°C directly onto 400-mesh electron microscopy copper grids covered with carbon-coated Formvar film (Pelanne Instruments, Toulouse, France). Particles were over-contrasted using uranyl salts as described elsewhere [254]. ALNs were counted by transmission electron microscopy (TEM) using a Jeol 1200EX microscope (JEOL, Akishima, Tokyo, Japan) at 80 kV and x50,000 magnification. Grids were scanned before counting to check that ALNs were randomly

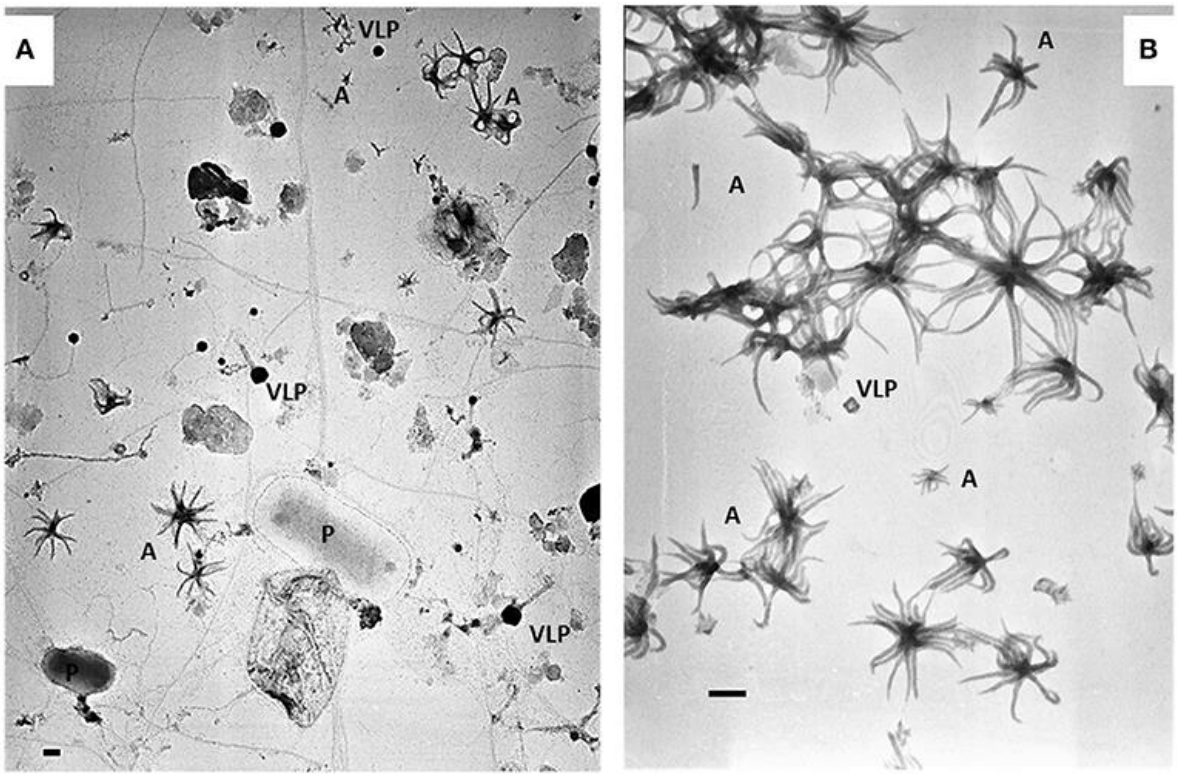

Figure 12: Electromicrographs showing heterogeneity of pelagic communities (A) in lakewater collected on March 15th 2017 and ALN-enriched culture (B) obtained from this sampling.

P, prokaryote; VLP, virus-like particle; A, ALNs. Scale bars = 100 nm.

distributed. A defined area of the grid was then randomly selected for counting ALNs. Counts of ALNs were converted into ALNs per milliliter using a conversion factor deduced from control grids prepared with pre-determined concentrations of viruses. Direct magnifications ranging from x50,000 to x150,000 were required for morphological characterization of the particles. Volume of the ALN particles was computed by considering the radial arms as cylinders (extrapolation validated by cryo-TEM and SEM imaging; see below) and the central core as a sphere. Ultra-thin (20-nm thickness) sections were obtained and imaged as previously described [255]. Counts of prokaryotes and VLPs from fixed samples were performed by flow cytometry as described elsewhere [256] using a BD FACS Calibur cytometer (BD Sciences, San Jose, CA) equipped with an air-cooled laser, delivering 15 mW at 488 nm with the standard filter set-up.

Experimental Design

Enrichment and Culture of ALNs

The sample with the highest density of ALNs collected on March 15th 2017 was used for enrichment and culture of ALNs. Within two h after sampling, 20 L of raw lake water was filtered through a 25-µm-pore-size nylon mesh and filtrates were immediately concentrated by tangential-flow ultrafiltration using a Kross-Flow system (Spectrum, Breda, The Netherlands) equipped with a 0.2-µm cut-off cartridge. Aliquots of this concentrated 0.2 µm−25 µm fraction were sequentially centrifuged at 8,000 g, 10,000 g (pellets discarded) then 12,000 g for 20 min each time at 14°C. ALNs contained in the supernatant of this last run were cultivated at 4°C in the dark with a regular supply of culture medium. To obtain this culture medium, ultra-filtrate <0.2 µm of the initial lake sample was filtered through a 30 KDa cut-off cartridge and autoclaved. **Figure 12** shows ALN cultures obtained through this procedure compared to the raw samples. The pellet obtained at 12,000 g was suspended in distilled/deionized sterile water (DDW), centrifuged at 10,000 g, and the supernatant was directly frozen to−20°C for microscopic and flow cytometry analyses of Enriched-ALNs (E-ALNs). Detailed procedure of experimental design and analyses is provided in supplementary materials (**Figure S1**).

Growth Monitoring

As state above, ALN cultures were enriched by sequential centrifugations at 8,000 *g*, 10,000 *g* (pellets discarded) then 12,000 *g* for 20 min each time at 14°C. For growth monitoring, this was followed by successive filtrations of the highest-speed supernatant through 0.45-µm and 0.2-µm filters (Sartorius, Göttingen, Germany) to obtain ALN-enriched but

prokaryote-free medium. This filtrate (<0.2-μm) was diluted 10-folds in the culture medium (see above) and incubated in triplicate over a 36-day period at 4°C in the dark, then 12 uneven subsamples were taken and formaldehyde-fixed before counts. Absence of prokaryotes at the start and end of the growth monitoring period was checked by flow cytometry, transmission electron microscopy and plate count agar spreading incubated at 4°C and 20°C during 4 weeks.

Susceptibility to Chemical or Physical Agents

To address the question of the living nature of the ALNs we examined their susceptibility to various chemical (lysozyme, antibiotics) or physical (heat) agents. Lysozyme is an antimicrobial enzyme that destructs Gram + bacteria cell wall by peptidoglycan hydrolysis [257] and which can also act against viruses [258, 259]. Antibiotics treatments used in this study are all known to block replication processes of bacteria DNA or protein synthesis [260, 261]. Novobiocin is principally active against Gram+ bacteria, gentamycin against Gram- bacteria and norfloxacin has a broad-spectrum bactericidal action. Heat shock above 85°C was used owing to the irreversible physiological damage caused by this treatment to biological entities [262].

Prokaryote-free ALN fractions prepared as described under the '*growth monitoring'* section were separately treated with 2 mg/mL lysosyme (1 h at room temperature), submitted to heat-shock (1 h at 90°C) or supplemented with antibiotics (50 μg/mL norfloxacin in sterile DDW; 10 μg/mL gentamycin in sterile DDW or 250 μg/mL novobiocin in sterile DDW) (all chemicals from Sigma-Aldrich, Saint-Quentin-Fallavier, France). Treated samples were incubated for 20 days in the dark at 4°C. To test the efficiencies of these biocide treatments, we used two treated "control fractions": ALN-free bacteria cultures isolated from lake Neuville and grown on the same culture medium as ALNs, and 0.2 μm filtered ALN-free but ultrafiltration-enriched VLP water lake. This second control fraction was obtained from Lake Pavin where ALNs are undetectable over the year. Biocide effects of treatments were determined by direct comparison of treated *vs*. untreated samples at day 20. ALN, prokaryote and femtoplanktonic communities were performed on formaldehyde-fixed samples at the end of the incubations as previously described. All tests were carried out in triplicates.

Cryo-Transmission Electron Microscopy (Cryo-TEM) Specimen Preparation and Imaging

For cryo-TEM, 3 µL of unfixed suspensions containing ALNs were deposited onto glow-discharged Lacey Carbon 200-mesh grids and loaded into the thermostatic chamber of a Leica EM-GP automatic plunge freezer, set at 20°C, and 95% humidity. Excess solution was blotted for 1" with a Whatman filter paper No. 1, and the grid was immediately flash-frozen in liquid ethane cooled at−185°C. Specimens were then transferred onto a Gatan 626 cryo-holder, and cryo-TEM was carried out on a Jeol 2100 microscope, equipped with a LaB_6 cathode and operating at 200 kV, under low-dose conditions. Images were acquired using SerialEM software [263], with defocus ranging of 1,000 nm, on a Gatan US4000 CCD camera. This device was placed at the end of a GIF Quantum energy filter (Gatan Inc., Pleasanton, CA), operated in zero-energy-loss mode, with a slit width of 25 eV. Images were recorded at a magnification corresponding to the calibrated pixel size of 1.80Å or 0.89Å.

Scanning Electron Microscopy (SEM) Specimen Preparation and Imaging

A fixed suspension (1% (v/v) formaldehyde) containing ALNs was deposited by filtration on 0.2-µm-pore-size filters (Whatman, Maidstone, UK), post-fixed with 1% osmium tetroxide, rinsed, and dehydrated through increasing concentrations of ethanol and then of hexamethyldisilasane. Following Cu sputter coating, dry filters were observed and imaged using a Zeiss Merlin Compact SEM operating at 2, 3 or 5 kV (Zeiss, Oberkochen, Germany).

Nucleic Acid Staining, Membrane Markers, and Flow Cytometry (FC) Analyses and Sorting of ALNs

Unfixed suspensions containing ALNs were thawed at 4°C and diluted in 0.02-µm-filtered Tris EDTA buffer prior to FC analyses. Analyses were performed using four nucleic acid dyes [SYBR Green I (Invitrogen S7563, Paisley, UK), SYBR Gold (Invitrogen S11494), propidium iodide (PI) (Sigma-Aldrich P4864) and DAPI (Sigma-Aldrich 32670)] and two lipophilic membrane markers [FM4-64 (Molecular Probes T13320, Eugene, OR) and PKH26 (Sigma-Aldrich P9691)]. ALNs were i) stained at 80°C for 10 min with SYBR Green I or SYBR Gold as described in [256]; ii) pre-heated at 80°C for 10 min then stained with 10 $\mu g \cdot mL^{-1}$ PI or 1 $\mu g \cdot mL^{-1}$DAPI for 10 min in the dark. Nucleic acids were also stained without heating. Staining with FM4-64 (5 $\mu g \cdot mL^{-1}$) and PKH26 (1/500 diluted from commercial solution) was carried

out in the dark for 10 min at room temperature. All experimental conditions were reproduced in triplicates. Triplicates of 0.2 µm ALN-free filtrated water lake (*i.e.*, enriched VLPs water from lake Pavin) and cultivated bacteria from lake Neuville were used for biological controls. Cytometric analysis was performed on a BD FACSAria Fusion SORP flow cytometer (BD Biosciences) equipped with a 70-µm nozzle. Laser and filter configuration was as follows: DAPI was excited by a 355-nm UV laser, fluorescence was collected with a 410 long pass (LP) and a 450/50 band pass (BP). SYBR Green I and SYBR Gold were excited at 488 nm and fluorescence was collected with a 502 LP and a 530/30 BP. PI and FM4-64 were excited at 561 nm and fluorescence was collected with a 600 LP and a 610/20 BP for PI, and with a 685 LP and a 710/50 BP for FM4-64. PKH26 was excited at 561 nm and fluorescence was collected with a 582/15 BP. Targeted particles were visualized on a "marker fluorescence *vs*. side scatter" dotplot. Data were acquired and processed using FACSDivA 8 software (BD Biosciences). Characterization of ALNs and VLPs from samples processed for cytometric analyses was carried out by TEM as previously described. Plots were compared with those of a similarly-processed VLPs community obtained from Lake Pavin (see site description in [254]) on October 24th 2017. FC sorting was performed on samples stained with SYBR Green I in un-heated conditions for optimal preservation of ALNs morphology and reliable morphotype diagnosis. Commonly described "viral fractions" [256] were gated on SYBR Green I fluorescence and sorted out using the continuous "Purity" mode. 0.5-µm fluorescent beads (Polysciences, Warrington, PA) served as control sorted fraction. Particles from sorted gates were re-analyzed by FC and identified and counted by TEM.

Genomic Analyses

Nucleic Acids Extraction and Amplification

Genomic DNA was extracted from unfixed suspensions containing ALNs obtained as described in the section "Growth monitoring". The sample was harvested by centrifugation at 12,000 g for 20 min at 14°C. The pellet was resuspended in 500 µl of sterile DDW and mixed with 600 mL of saturated phenol (pH 8.0). Then, two cycles of freezing in a liquid nitrogen bath (15 min) and thawing in a 100°C water bath (5 min) were conducted. The sample was mixed with 750 µL of chloroform and centrifuged at 14,000 g for 20 min at 4°C. Thereafter, the aqueous layer was transferred to another fresh 1.5 mL microtube and mixed with same volume of cold absolute ethanol and 3 M sodium acetate. The nucleic acid pellet obtained by centrifugation at 14,000 g for 20 min at 4°C was washed twice with ice-cold 70% ethanol and pelleted again.

The pellet was resuspended in 50 µL of deionized water. Total extracted DNA was randomly amplified by Whole Genome Amplification (WGA) with GenomiPhi V2 kit (GE Healthcare, Chicago, Illinois, USA).

Library Preparation and Sequencing

Single-molecule Real-time long reads sequencing was performed with a PacBio Sequel Sequencer (Pacific Biosciences, Menlo Park, CA, USA). The SMRTBell library was prepared using a DNA Template Prep Kit 1.0, following the "procedure and checklist for greater than 10 kb template using AMPure PB beads" protocol. Genomic DNA(1,7 ug) was slightly sheared using a Covaris g-Tube (Covaris, UK) generating DNA fragments of approximately 20 kb. A Fragment Analyzer (Agilent Technologies, Santa Clara, CA, USA) assay was used to assess the fragment size distribution. Sheared genomic DNA was carried into the first enzymatic reaction to remove single-stranded overhangs followed by treatment with repair enzymes to repair any damages that may be present on the DNA backbone. A blunt-end ligation reaction followed by exonuclease treatment was conducted to generate the SMRT Bell template. Two AMPure PB beads 0.45X purifications, and one at 0.4X were used to obtain the final library. The SMRTBell library was quality inspected and quantified on a Fragment Analyzer (Agilent Technologies) and a Qubit fluorimeter with Qubit dsDNA HS reagent Assay kit (Life Technologies). A ready-to-sequence SMRTBell Polymerase Complex was created using a Binding Kit 2.1 (PacBio) and the primer V4, the diffusion loading protocol was used, according to the manufacturer's instructions. The PacBio Sequel instrument was programmed to load and sequenced the sample on PacBio SMRT cells v2.0 (Pacific Biosciences), acquiring one movie of 600 min per SMRTcell and generate 8 Gb of bases and an insert N50 at 7.75Kb.

Sequence Assembly and Annotation

The 1,930,845 raw PacBio reads (4.1 Kb in average) were assembled using the SMRT Analysis software and the Hierarchical Genome Assembly Process (HGAP) workflow [264]. This procedure includes pre-assembly error correction, assembly and polishing. The circular nature of HGAP derived contigs was assessed via the dot-plotting tool Gepard [265] and circular genome sequences were derived through an alignment approach and manual curation. The 5,162 corrected long reads (12.6 Kb in average) produced after the pre-assembly error correction process were utilized to determine the coverage of each contig using BLASTn (threshold of 90% on the identity percent) [266]. These corrected reads and contigs were

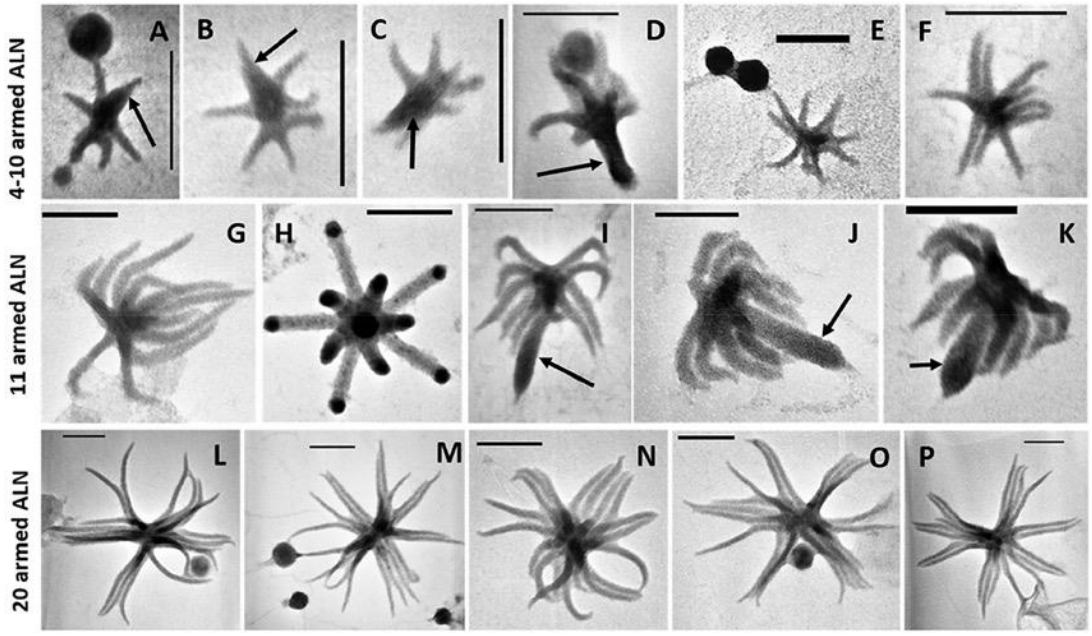

Figure 13: Transmission electron microscopy (TEM) micrographs of different morphotypes of aster-like nanoparticles.

(**A–F**) 4–10-armed forms with some (**A–D**) presenting a few arms articulated around a delta-shaped excrescence (arrows). (**G–K**) 11-armed forms and their budding 11-armed variants (**I–K**) with elongated and swollen bud-like excrescences (arrows). (**L–P**) 20-armed forms. Scale bars = 100 nm.

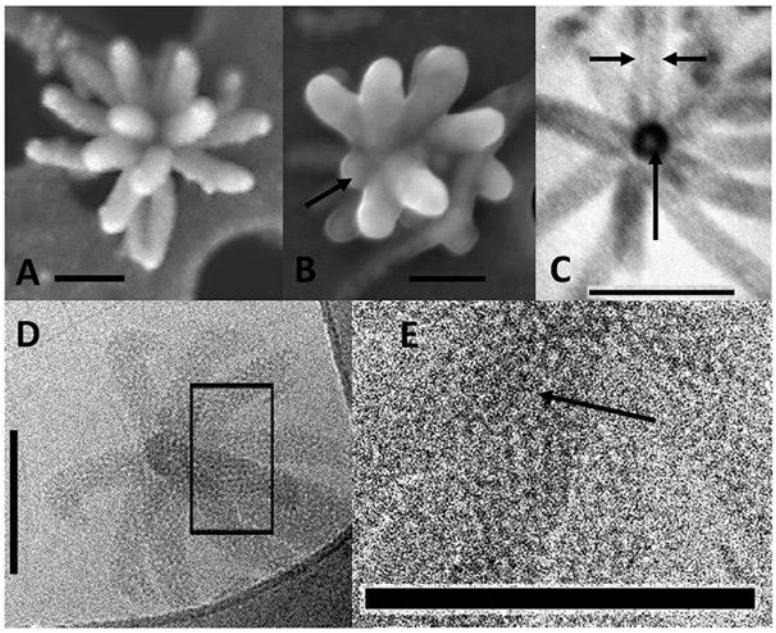

Figure 14: Electromicrographs of aster-like nanoparticles.

(**A,B**) Scanning electron microscopy (SEM) micrographs showing ALNs with multiple full-grown radial arms (A) or a mix of emerging (arrow) and full-grown arms (**B**). (**C**) TEM micrograph of an ultra-thin section of an ALN. Sagittal sections of arms reveal a tubular appearance with electron light area enclosed by a wall-like structure (arrows). (**D,E**) Cryo-TEM micrographs. (**D**) Radial arms display a similar mottled appearance. (**E**) Magnified view of the box selected from the previous image revealing circular substructures (arrow). Scale bars = 100 nm.

compared using BLASTn to the SILVA 16S rRNA gene reference database (version 132) [267]. The 233 contigs were also compared to the UniProt (February 2019) (UniProt Consortium, 2019) protein database using Diamond (sensitive mode) [268]. Gene-calling was performed on contigs through the Prodigal software [269] and proteins were also compared to Uniprot using Diamond. Genomic data are presented in Supplementary Data Sheet 1.

2.2.4 Results

Morphological Analyses

The ALN shape corresponds to arm-like segments which extend radially from a unique core structure. Three dominant morphotypes emerged on the basis of size and number of arms. The first morphotype displayed 4 to 10 arms connected to a delta-shaped tail with a mean length of 110 ± 18 nm and an average volume of 0.000055 μm3 (**Figures 13A–F).**

The second morphotype consisted of forms with 11-arms that were consistently observed within the ALN population (**Figures 13G–K**). They were clearly distinct from the first morphotype by their length (333 ± 28 nm) and volume (mean value: 0.00057 μm3). Some appeared endowed with a singular bud-like appendix that seemed to arise from the center of symmetry of the particle. This appendix is thicker and slightly longer than the radial arms (**Figures 13I–K**). Finally, the third ALN morphotype corresponds to a sub-population that was composed of 20 arms (**Figures 13L–P).** These 20-armed forms constituted the lengthiest (439 ± 39 nm) and the most voluminous (0.0014 μm3) ALNs identified in our samples. Their arms displayed characteristic tapered shapes, were frequently associated by pairs (**Figure 13P**), and there was no indication for supernumerary outgrowths as seen in other ALN morphotypes.

Standard, scanning, and cryo-transmission electron microscopy (cryo-TEM) indicated that the arms of ALN particles project from a central core (**Figures 14A–D**). This core displayed high and homogeneous electron density, while the arms showed differential contrasts depending on the plane of the section. Arms appeared as hollow structures when viewed in sagittal sections (**Figure 14C**). Cryo-TEM of whole specimens allowed direct comparison between the central core, the radial arms and the supernumerary appendix of the 11-armed morphotypes (**Figure 14 D,E**). All areas showed a similar dot-pattern, which was more conspicuous in the case of the

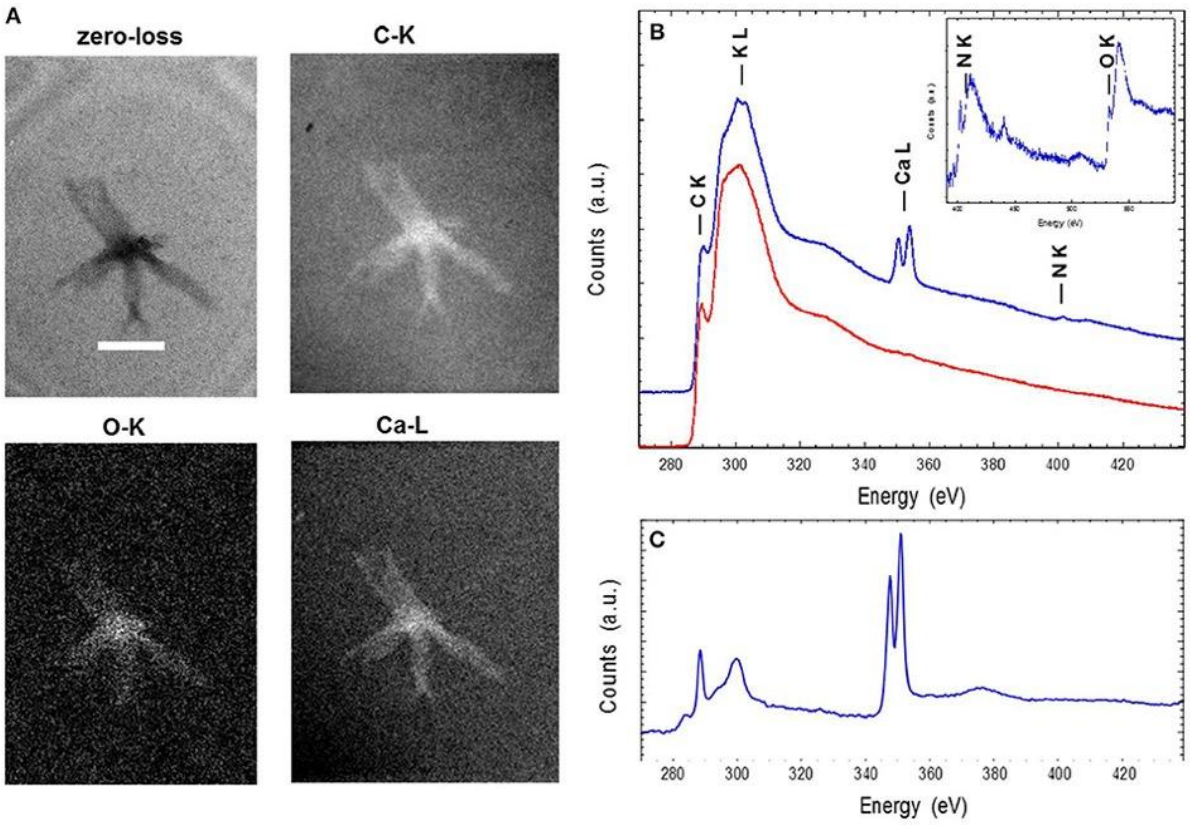

Figure 15: Energy-filtered transmission electron microscopy (EFTEM) (A) and electron energy loss spectroscopy (EELS) analyses (B,C) of aster-like nanoparticles.

(A) Zero-loss image and EFTEM C, O, and Ca maps of an ALN. Scale bar=200 nm. (B) EELS spectra of an ALN particle (blue) and formvar (red). Insert: close-up of the background-normalized spectrum of an ALN particle at the N and O K-edges. (C) EELS spectra of a reference calcite crystal at the C K-edge and the Ca L2,3-edges. The relative intensities at the C K-edge and Ca L2,3 edges correlate with C/Ca atomic ratio.

central-core/appendix complex. Branched chains formed by these elementary components might account for the higher electron contrast and apparent rigidity of the supernumerary appendix compared to the slacker aspect of radial arms. Descriptively, ALNs are pleomorphic nanoparticles with a reduced biovolume (<0.0014 μm3) exhibiting 4 to 20 radial arms organized around a unique central core.

Elementary Analysis

Energy-filtered transmission electron microscopy and electron energy loss spectroscopy (EELS) analyses performed on entire ALNs indicated that these nanoparticles were mostly composed of carbon, oxygen, calcium and nitrogen (**Figures 15 A,B**). Trace amounts of potassium were also identified in association with the particles. EELS spectra at the C K-edge and Ca L2,3-edges of ALNs were significantly different from those of Ca-carbonates used as reference (**Figure 15C**) as they did not show a peak at 290 eV indicative of 1s → π* electronic transitions in carbonates and a much lower Ca/C ratio. Likewise, selected-area electron diffraction of ALNs revealed an amorphous structure (K.B. personal communication). Elemental composition and selected-area electron diffraction patterns thus suggest that ALNs are presumably formed of organic components, indicating that their organic nature may prevail over the possibility of mineral structures.

Flow Cytometry Analysis

Flow cytometry (FC) analyses were performed on enriched-ALNs fraction (E-ALNs, *see Materials and methods*) composed of 96% ALNs and 4% of VLPs (**Figure 12B**) ascertained by TEM observation and counting.

No fluorescence signal was obtained using lipophilic markers FM4-64 or PKH26. Different nucleic acid dyes were tested, including DAPI, PI, SYBR Green I, SYBR Gold. While labeling with DAPI (a weakly permeant AT selective dye) and PI (impermeant nucleic acid intercalating dye) were unsuccessful, the SYBR dyes (permeant cyanine dyes), which are more sensitive compounds with high penetrating capacities, allowed to separate distinctive populations from E-ALN samples.

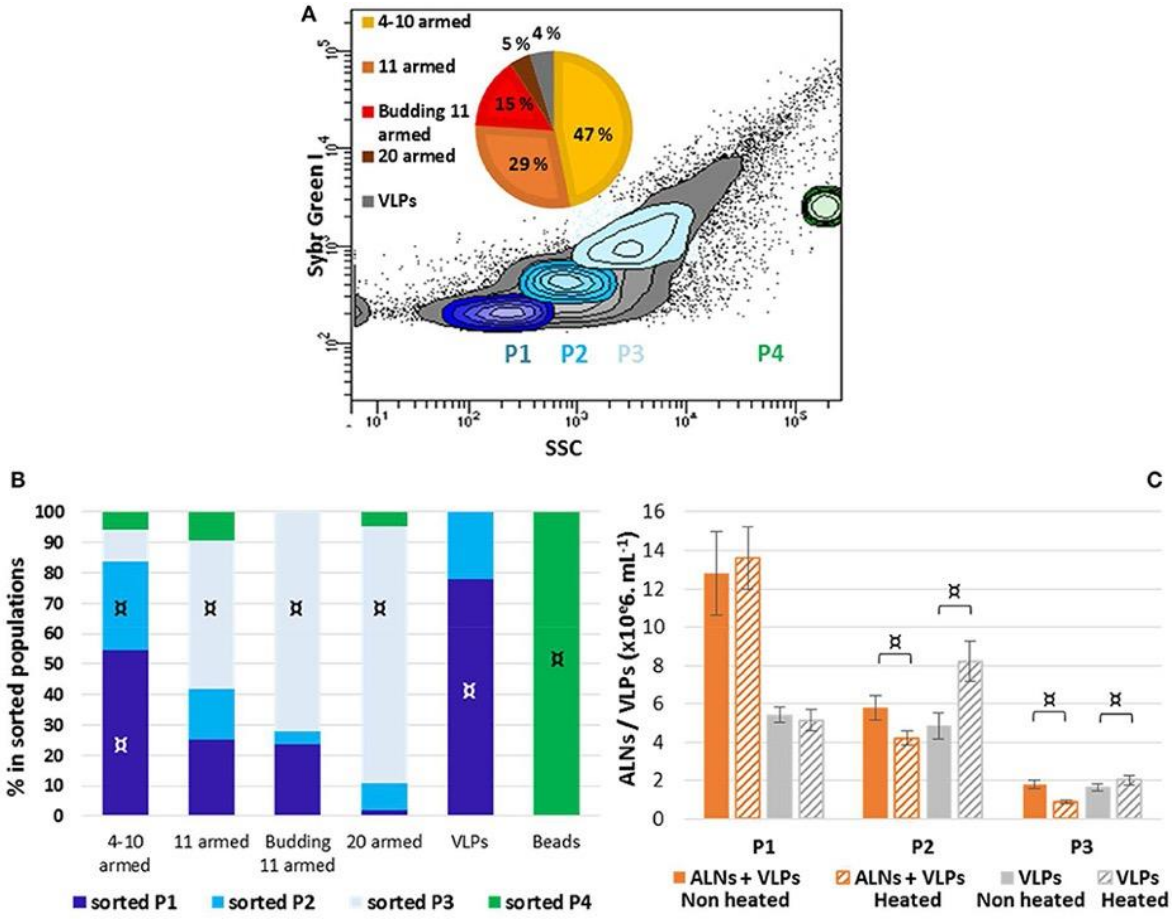

Figure 16: Flow cytometry analysis of aster-like nanoparticle-enriched preparations (E-ALNs).

(A) Gating of three distinctive populations (P1, P2, P3) of SYBR Green-stained E-ALNs. Heating was omitted during the staining procedure, and beads (0.5 µm) were used as control fraction (P4). The gray area in scatter plot including in P1, P2, and P3 commonly represents VLP fractions (see [256]). A pie chart shows the relative proportions of ALNs morphotypes attested by TEM. (**B**) Distribution of ALNs morphotypes and beads in the four FACS-sorted fractions counted by TEM. (**C**) Cytometry counts of P1, P2, and P3 gated fractions compared to counts obtained when heating was included in the SYBR Green staining procedure, and to counts of particles in ALNs-free viral community stained in heat-driven conditions. Mean values from triplicate and standard errors are plotted. Significant representativeness of morphotypes in sorted populations (**B**) is indicated by symbols: ¤ (Fisher's exact test on a contingency table, $p < 0.01$). Significant differences between "non-heated" and "heated" conditions (C) are indicated by an symbol ¤ (Student T-test, $p < 0.05$).

As shown in **Figure 16A,** three populations termed P1, P2, and P3 were reproducibly split on the basis of SYBR Green I signal intensity and side scatter. Because ALNs were shown to be thermo-sensitive, heating was omitted in the protocol used for SYBR labeling. TEM indicated ALNs with familiar shapes in all sorted gates excepted in P4 gate that exclusively contained beads used as a control for sorting quality control (**Figure 16B**). Absence of ALNs in P4 indicated a non-random but differential sorting of the nanoparticles using the selected sorting gates. This was confirmed by TEM analyses of ALNs from the three sorting gates (**Figure 16B**). The sub-population from P3 gate provided the strongest SYBR signal, and consisted of large ALN morphotypes, *i.e.*, 20-armed, budding 11-armed, and 11-armed morphotypes.

The smaller ALNs (4–10 armed forms) were mostly concentrated in gates P1 and P2 together with virus-like particles and similar-sized particles of undetermined nature (VLPs).

Interference between ALNs and VLPs in FC particle quantification was evaluated using thermo-sensitivity property of ALNs compared to VLPs. This was achieved through comparative analysis of E-ALNs and a VLP community used as an ALN-free control, submitted or not to heating (**Figure 16C**). Heat induced a significant increase of counted VLPs in P2 (from 4.8 ± 0.7 to 8.2 ± 1.1 × 106 mL−1) and P3 (from 1.7 ± 0.2 to 2.0 ± 0.3 × 106 mL−1) populations sorted from the ALN-free control. Heating of P2 and P3 sorted from E-ALNs resulted in the opposite effect, *i.e.*, a decrease in number of recorded events (P2: from 5.8 ± 0.6 to 4.2 ± 0.4 × 106 mL−1; P3: from 1.8 ± 0.2 to 0.9 ± 0.1 × 106 mL−1).
Overall, ALNs are positively labeled with SYBR nucleic acid dyes and interfere with VLPs quantification when using fluorescence based methods.

Nucleic Acid Detection

Detection of nucleic acid was performed on fraction composed of >99% ALNs and <1% of VLPs ascertained by TEM and obtained as described in section 'growth monitoring'.
No reads or contigs were similar to a prokaryotic 16S rRNA sequence. All the 233 contigs were shorter than 6 Kb except one contig of 11,258 bp. Almost all contigs could be unambigously affiliated to small single-stranded DNA viruses, 213 being affiliated to the Microviridae family and 16 to CRESS DNA viruses (circular Rep-encoding ssDNA viruses) (**Figure 17**).

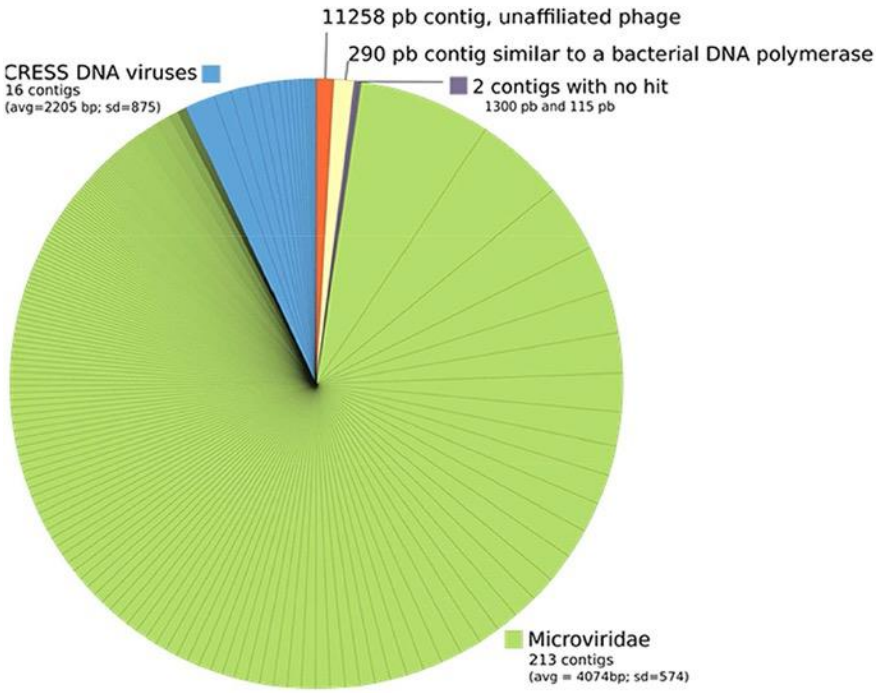

Figure 17: Taxonomic affiliation of the 233 contigs from ALN-enriched DNA templates.
Each piece of the pie corresponds to a contig and its size is proportional to the number of reads that were associated to this contig.

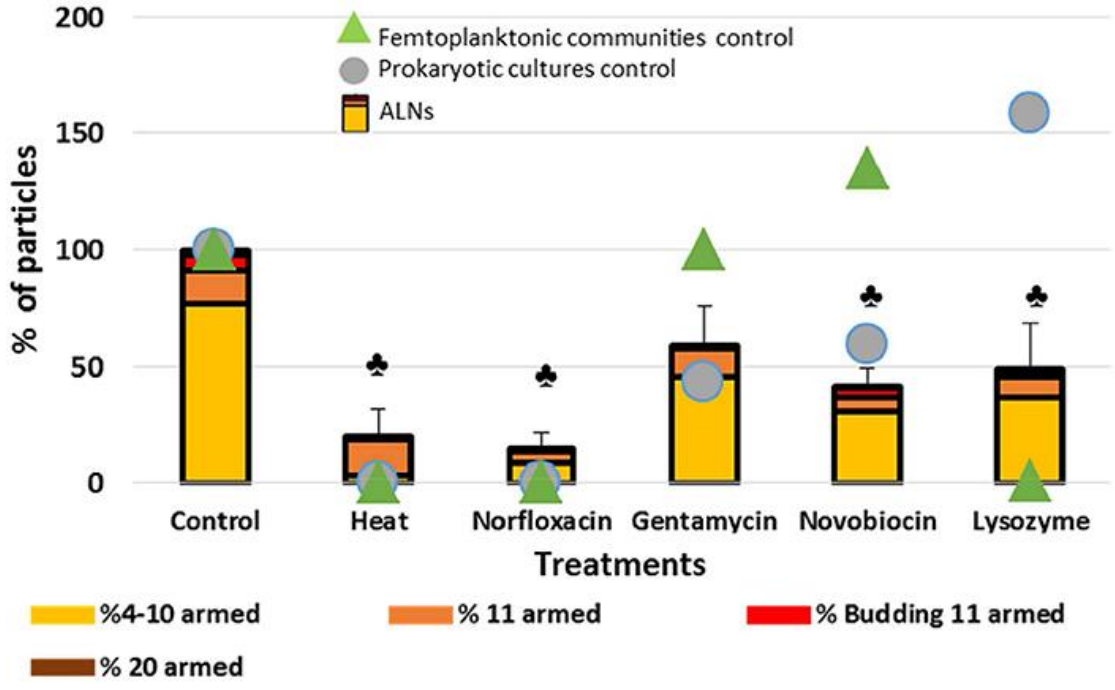

Figure 18: Sensitivity of the particles to heat, antibiotics or lysosyme treatments.
Effects of treatments by heat, antibiotics and lysosyme were assessed compared to untreated controls at day 20. Results are expressed as the percentage of ALNs which have resisted to treatments and continued to develop compared to control after a 20-day incubation. ALN-free prokaryotic cultures and femtoplanktonic communities (0.2 µm filtrated water from an eutrophic lake) were used as controls. Mean values from triplicate and standard errors are plotted. Significant differences with control are indicated by symbol ♣(T-test, $p < 0.05$).

Two contigs had no similarity to Uniprot proteins and one contig was similar to a bacterial DNA-directed DNA polymerase (49.5 amino acid identity on 94 residues), but these contigs were all very short (1,300, 115, and 290 bp, respectively). Although the largest contig of 11,258 bp had no obvious affiliation, its characteristics are similar to known viruses that infect prokaryotes: (i) short genes (23 protein coding genes, 442 bp long in average), (ii) no strand switching and (iii) only 4 proteins out of 23 being similar to a protein of Uniprot (3 similar to proteins from unaffiliated phages and one to an archaeal protein, all four proteins having an unknown function). Based on our genomic analyses and on the methodology used presence of nucleic acids in ALNs is not proved.

Susceptibility to Chemical or Physical Agents

Effects of various life-inhibiting treatments were tested on ALNs, and on ALN-free prokaryotes and femtoplanktonic communities used as control after 20-day incubations. Dramatic effects on total ALNs (T test, $p < 0.05$) were observed (**Figure 18**) after heating 1 h at 90°C or lysozyme (2 mg/mL) treatments (80 ± 12% and 51 ± 19% loss after 20 day incubation), and in the presence of the norfloxacin (50 µg/mL) and novobiocin (250 µg/mL) antibiotics (85 ± 7% and 58 ± 8%, respectively). Gentamycin antibiotic treatment had a smaller effect on the nanoparticles (41 ± 17% loss; p = 0.05). The losses were more pronounced following heating, lysozyme, norfloxacin, novobiocin and gentamycin treatments for the 4–10–armed form (96 ± 1, 53 ± 15, 89 ± 5, 61 ± 8, 41 ± 14%, respectively) compared to the 11–armed forms (0 ± 10, 37 ± 4, 66 ± 2, 53 ± 1, 12 ± 4%, respectively).

Lysozyme treatment leaded to a rise of prokaryotes (58%) suggesting that this ALN-free fraction was mostly composed of Gram – species. The complete loss of ALN-free femtoplanktonic communities (99%) showed the strong antiviral activity of this enzyme [258, 259]. As expected prokaryotic "control fraction" displayed drastic loss in response to heat, norfloxacin, gentamicin and novobiocin (100%, 100%, 57%, 41%, respectively) (**Figure 18**).

Clearly, ALNs are susceptible to the life-inhibiting treatments. It seems also worth noting that responses to the treatments differed depending on the morphotypes. For example, 11-armed morphotypes proved much more resilient than others, while the 4–10-armed appeared more sensitive to the treatments.

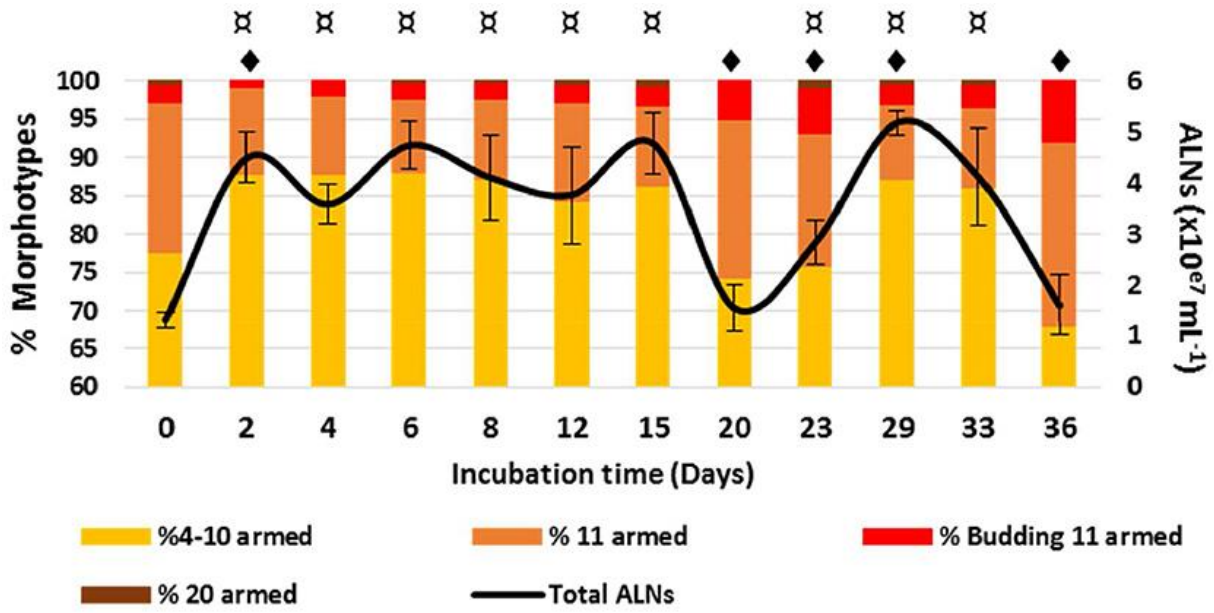

Figure 19: Development monitoring of aster-like nanoparticles in prokaryote-free medium.
Temporal variations of ALNs abundances and ratios (in %) of different morphotypes over a 36-day period. Mean values from triplicate and standard errors are plotted. Significant differences between ALNs abundance at t (n) and t (0) and between ALNs abundance at t (n) and t (n-1) are indicated by symbols ¤ and ✦, respectively (*T*-test, $p < 0.05$).

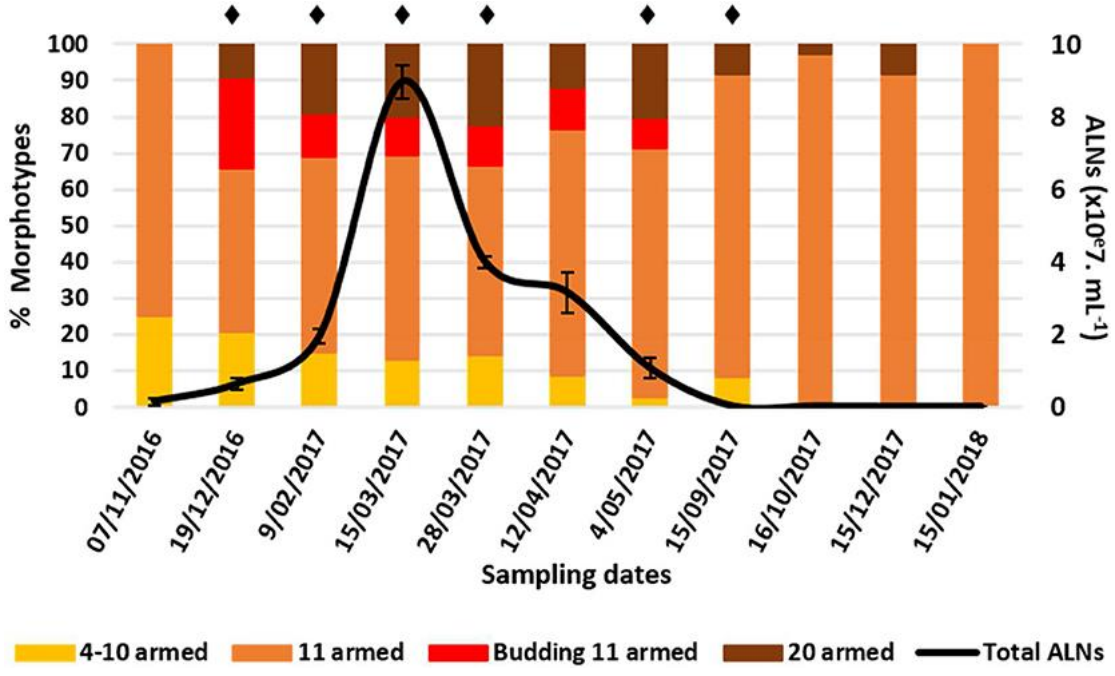

Figure 20: Abundance of aster-like nanoparticles in situ (Neuville-France) and ratios (in %) of different morphotypes over a 15-month period.
Note the peak of abundance between late December 2017 and mid-March 2017 and the return to low-density populations within a few months. Mean values from triplicate and standard errors are plotted. Significant differences between ALNs abundance and the previous time are indicated by asterisks ✦ (Student *T*-test, $p < 0.05$).

In vitro Monitoring

ALN population fluctuates over a 36-day period in prokaryote-free medium (PFM) at 4°C (**Figure 19**). A transient rise of abundance was evident from day 0 to day 1 (multiplication factor MF = 3.6). The population then appeared relatively stable from day 1 to day 15 before a marked decrease up to day 20, preceding a second rise period from day 20 to day 29 (MF = 3.3), then a second decline phase up to day 36. All these fluctuations with time were statistically significant (**Figure 19**). Quantification of ALN morphotypes in PFM revealed that 4–10-armed and 11-armed morphotypes fluctuate inversely over time (**Figure 19**, Spearman's $r = -0.86$, $p < 0.001$). These fluctuations were positively (4–10-armed forms) or negatively (11-armed forms) correlated to total ALN population (Spearman's $r = 0.66$ and $r = -0.82$, respectively, $p < 0.05$).

The proportion of the smallest ALN forms (predominant morphotype at day 0) increases concomitantly with total number of ALNs but decreases as the abundance of total ALNs returns to baseline (day 0, day 20, and day 36). Inversely, the proportion of 11-armed forms increases during phases of total ALN decline (days 20, day 36). Throughout the incubation period, we were not able to detect any prokaryotic cells using different approaches: flow cytometry, transmission electron microscopy, and plate count agar spreading.

The above incubation monitoring show that the abundance of ALNs can change significantly over time in the absence of cellular entities, with different patterns registered in contrasted morphotype categories. The mechanisms under these changes remain unclear in the absence of a detectable genomic support.

Ecosystemic Monitoring

Analysis of natural samples collected over a 13-month period in an eutrophic lake of the French Massif Central revealed high ALN abundances characterized by marked seasonal fluctuations (**Figure 20**).

The maximal density reached a value of $9.0 \pm 0.5 \times 10^7$ mL^{-1} (March 15th 2017). ALN abundances were up to 8-fold higher than those obtained for FC-counted prokaryotes and represented up to 39% of the total FC-counted VLPs in corresponding samples. ALN abundances increased with season from autumn to spring (MF = 60). Prokaryote abundances fluctuated slowly from 0.8 ± 0.1 to $2.1 \pm 0.4 \times 10^7$ mL^{-1}, while VLPs ranged from 2.0 ± 0.2 to

A

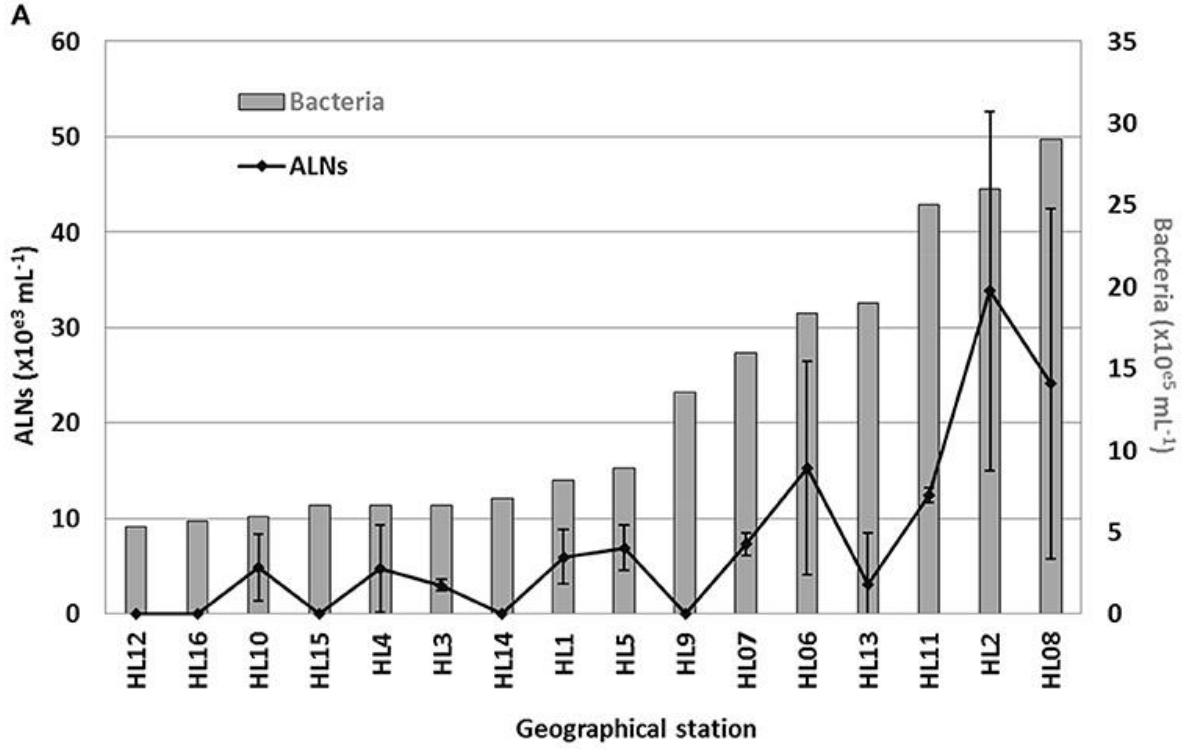

B

	Biological parameters				Physico-chemical parameters									
	VA	BA	BP	FIC	TEMP	SAL	Turb.	DOC	TPC	TPN	NO_3+NO_2-N	NH_4-N	PO_4-P	SiO_2
ALNs	**0.85 ***	**0.81 ***	0.59	0.62	-0.46	-0.33	-0.3	0.28	0.72	0.73	0.09	0.18	0.5	0.66

Figure 21:(A) Distribution of aster-like nanoparticles and bacteria abundances in 16 selected stations of a tropical coastal ecosystem (Ha Long Bay-Vietnam), and (B) analyses of correlations (Spearman's product-moment correlation coefficient) between ALNs and environmental parameters which compile all sampling points.

All details on Ha Long Bay (Vietnam) environment are available from [253]. Level of significance: *$p < 0.001$. VA, viral abundance; BA, bacterial abundance; BP, bacterial production; FIC, frequency of infected cells; TEMP, temperature; SAL, salinity; Turb, turbidity; DOC, dissolved organic carbon; TPC, total particulate carbon; TPN, total particulate nitrogen in the bulk sample.

48.4 ± 1.5 × 10^7particles mL^{-1}. For both communities, highest values were recorded in spring and in autumn, respectively (Figure S2). ALN abundance was not correlated to those of prokaryotes or VLPs.

At the morphotype level, we observed a high dominance of 11-armed forms which averaged 79 ± 16% of the total abundance over the 13-month sampling period (**Figure 20**). The 4–10 and 20-armed forms appeared in much smaller proportions (mean values = 10 ± 11% and 11 ± 11%, respectively). Proportions of these two forms were inversely correlated with those of 11-armed forms over time (Spearman's r = -0.77 and r = -0.73, respectively, $p < 0.05$). Proportions of budding 11-armed forms and 11-armed forms devoid of bud-like appendix were also negatively correlated to each other (Spearman's r = -0.91, $p < 0.01$). Budding forms accounted for the highest proportions at the onset and throughout the increasing phase of total ALNs, but then disappeared with the decline in the total ALN abundance. ALNs were exclusively composed of 11-armed morphotypes a few months after their population was stabilized at its lowest level.

Detection of ALNs conducted on surface microlayer of 16 selected geographical stations (namely HL1 to HL16) from Ha Long Bay (Vietnam) show a high spatial heterogeneity with values ranging from undetectable to 3.4 × 10^4 mL^{-1} (**Figure 21A**). The dynamics of ALNs and bacteria were significantly correlated (Spearman's r = 0.81, $p< 0.01$, **Figure 21B**). No reliable correlation could be established between ALNs and physico-chemical variables (**Figure 21B**).

ALNs show seasonal and ecosystemic fluctuations probably induced by environmental parameters. Proportions of each recorded morphotype shift according to seasonal dynamics.

2.2.5 Discussion

ALNs Are Original Pleomorphic Nanoparticles

Here we report the discovery of 'Aster-Like Nanoparticles' (ALNs) in lakewater. These pleomorphic entities, exhibit puzzling aster-like shapes with arm-like processes that project from a central core (**Figure 14**). All morphotypes exhibit shapes that distinguish ALNs from previously established groups of nanoparticles, including ultramicro-prokaryotes [23, 31, 32], controversed nanobes [52, 55, 56, 59, 270], biomimetic mineralo-organic particles (BMOPs) [18], viruses [271] or extracellular vesicles (EVs) [75, 212]. Their mean length ranges from 110 ± 18 nm (4–10-armed morphotype) to 439 ± 39 nm (20-armed morphotype). Volumetric

estimates of all ALN types indicated values (averaging 0.000055 μm3, 0.00057 μm3, and 0.0014 μm3 for 4–10, 11, and 20-armed morphotypes respectively) that were significantly lower compared to the smallest known prokaryotes [32] and to the Theoretical Minimal Cell Volume (TMCV). Nanobes, BMOPs, viruses (excepted giant viruses) and EVs are the sole examples of entities comparable to ALNs in terms of numerical volume. The composition (mostly carbon, oxygen, calcium and nitrogen with trace amounts of potassium) and the amorphous structure revealed by electronic microscopy (**Figure 15**) point out that ALN are possible organic particles [50, 55], or at least that their organic content may prevailed over their mineral composition known from mineral forming nanobes [272], BMOPs or "natural nanoparticles" [18, 273], partly or totally composed of minerals.

ALN volumes were largely under the theoretical minimal cell volume (TMCV) required to house nucleic acids and the associated biosynthetic machinery required for a self-sufficient form of life [251]. Use of the TMCV established there is 20 years ago to define compatibility with living nature must be however considered with caution. Indeed, recent advances in microbiology and virology have revealed existence of nanosized prokaryotes with biovolumes close to the TMCV. Giant viruses were reported as well. Genomic analysis of nanosized prokaryotes revealed a limited sub-cellular organization coupled with a significant reduction of biosynthetic and energy conservation pathways [23, 32]. Meanwhile, exceptionally large viruses were discovered that contain DNA encoding proteins involved in mRNA translation [274, 275]. These discoveries have reopened the debate on the origin and the definition of life. In the absence of scientific consensus on what the TMCV should be exactly, it would be perhaps premature to make the conclusion that ALNs cannot be living particles with the only criteria being their exceptionally small size. Various experimental approaches were developed to address this issue (see below).

The ability of ALNs to develop in the absence of cells (**Figure 19**) provides additional entry points to discuss the nature of these particles compared to viruses or extracellular vesicles (EVs). It seems worthwhile to underline, at this point, that host-independent morphogenesis is quite unusual in viral world or for EVs, although extracellular morphological plasticity has been reported for ATV viruses *(Acidianius Two-tailed Virus)* that infect archaeons living in particularly harsh aquatic environments [276, 277]. ALN morphotype fluctuations that happen in the absence of cells seem at odds with a viral nature of ALNs if viewed as gradual assembly/disassembly processes within a single particle having a pleomorphic lifestyle.

However, the alternative, *i.e.*, convergence of otherwise unrelated nanoparticles, toward an "aster-shaped" morphology must also be considered. In this case, morphotype fluctuations could merely reflect survival capabilities of unrelated particles in the absence of cells. Clearly, further studies are required to elucidate morphotype fluctuations related to the exact nature of ALNs.

Sensitivity to a wide range of antibiotics was used as a critical point to establish the non-living nature of biomimetic particles [54]. The abundance of ALNs was dramatically affected by biocide agents (norfloxacin, novobiocin, lysozyme or heat shock) (**Figure 18**). These results could suggest ALNs as self-sufficient forms of life. Differential responses of ALN morphotypes to the multiple damaging treatments should also be considered. 4–10-armed forms appeared more affected than the 11-armed forms, suggesting possibility of more resilient morphotypes within the population of nanoparticles. Comparisons of ALN responses to those of other populations used as controls did not however permit to draw more definite conclusions indicative of the living or non-living nature of these particles.

More basically, the ability of ALN populations to persist in the absence of cells and the sensibility of the particles to biocide agents both raise the question of the existence of endogenous nucleic acids. Hypothesis of an heredity support is also supported by the reoccurrence of different ALN morphotypes whatever was the environmental context or season (see below) and the recurrent radial symmetry of the particles which might reflect a developmental relationship between morphotypes. Flow cytometry (FC) plotting and subsequent TEM analysis of the sorted ALNs provided preliminary insights in this topic. The cytometry step was assessed using permeant cyanine SYBR dyes. These stains preferentially bind to double-stranded DNA, but can also stain single-stranded DNA and RNA with variable efficiency. TEM analyses of sorted fractions showed that SYBR Green I and side scatter signal intensities were morphotype-dependent and allowed to establish a positive correlation between the complexity of morphotypes and the intensity of fluorescence emitted by the particles (**Figure 16**). Assuming that FC-detected SYBR-staining is indicative for the presence of nucleic acids encased in the nanoparticle (core structure?), highly enriched ALN cultures (0.2 μm filtered) appeared as suitable material from which putative DNA could be directly extracted and characterized at the molecular level. Whole genome sequencing was then developed using the same DNA template. 16S rRNA genes have not been identified as part of the 233 contigs

assembled through this approach (**Figure 17**). Assuming that DNA extraction and amplification were efficient, our data suggests that ALNs lack a detectable genomic features and translation machinery of prokaryotes. The great majority of contigs delivered by whole genome analysis were affiliated to the microviridae, a family of bacteriophages with a single-stranded DNA genome. However, microviridae contigs must be viewed as assemblies of sequence fragments from remnants of viral populations initially comprised in the lake water sample. According to these results, we were not able to demonstrate the presence of nucleic acids in ALNs. Extraction and non-specific amplification efficiencies of nucleic acids are strongly linked to the nature of the particle. Development of a specific protocol to purified ALN enriched-cultures will be a critical point as soon as the exact nature of ALNs will be determined.

Overall, our data on the atypical morphology, the reduced biovolume, the suspected dominant organic nature, the sensibility to biocide treatments, and the ability to develop in the absence of cells indicate than ALNs are new femto-entities which, at the moment, cannot be classified in any known category of femto-entities previously described in environmental samples.

Ecological Significance of ALNs

Our discovery of ALNs and the existence of other ultra-small non-viral particles raise the ecological question of the accuracy of the "VLP" (*i.e.*, virus-like-particles) fraction in aquatic ecosystems. Commonly used to designate free-occurring viruses, the acronym VLP is also synonymous of "known and yet unknown viral aquatic particles" especially as standardized FC methodologies include heat-driven procedures particularly efficient for detection of viral particles that are, otherwise, refractory or weakly responsive to SYBR-staining [256]. Interference between ALNs and VLPs in FC particle quantification and successful sorting of largest morphotypes (**Figure 16**), indicate that ALNs must be viewed as atypical nanoparticles comprised in the VLP fraction. Events recorded from ALNs may lead to overestimate the viral load when analyzing viromes in aquatic ecosystems by counting SYBR-stained particles which is the methodology currently used for optimal detection of viruses by flow cytometry [110]. Experimental bias generated by overlapping of fluorescent signals produced by viruses and by other types of nanoparticles encompassed within the viral population was previously assessed in the case of EVs which constitute regular components of VLP fractions in natural environment [77, 211, 212]. Comparative studies between ecological groups comprising viral communities

should therefore be interpreted with caution when pleomorphic nanoparticles such as ALNs occur in samples, notably when seasonal variations favor temporary bloom or predominance of one ALN morphotype over others.

Ecological significance of ALNs was approached by *in situ* seasonal and ecosystemic analyses. Seasonal analyses in a French eutrophic lake revealed a marked seasonal dynamic in ALN abundances from $8.0 \pm 3.8 \times 10^4$ to $9.0 \pm 0.5 \times 10^7$ mL^{-1} (**Figure 20**) and suggest a tight control of the environmental parameters on ALNs. Relative proportions of each morphotype shifted concomitant to fluctuations in total ALN abundance. 11-armed form appeared the alone form in condition of the lowest density of ALNs, suggesting that this peculiar form could be more resistant to adverse environmental factors than others forms. Inverted correlation between 11-armed forms and the others forms, also noted when ALNs were maintained for 36 days in prokaryote-free lake water (in laboratory condition) suggests that these forms may be of importance in maintaining a permanent pool of ALNs in lake water and in promoting propagation of the nanoparticles when growth conditions become more favorable. This assumption is only possible assuming that pleomorphism arises from inter-conversion between morphotypes. The idea that morphotypes described in this study all develop from the same "stem entity" is not demonstrated and remains a fundamental question to be addressed in the future. The importance of ALN degeneration or starvation controlled by environmental factors, which can differently affect the abundances of ALN morphotypes in both controlled and *in situ* conditions, must also be addressed. Such a regulative function by environmental factors has been reported in the case of ultramicro-bacteria [31] and in the case of *Phaeodactylum tricornutum*, a 10 μm sized diatom [278].

Identification of ALNs in a tropical estuarine system and in Saloum river in Senegal (J.C. unpublished data) shows a pan-geographic distribution and adaptability of ALNs. This property prompted us to explore the environmental parameters potentially affecting ALN dynamics at the spatial scale. This was achieved on 16 selected geographical stations from Ha long bay estuary in Vietnam, a highly spatially contrasted environment previously characterized by [253]. This spatial survey indicated significant coupling between ALN and prokaryote abundances (**Figure 21**). No reliable correlation could be established with physico-chemical variables of the bay environment. In contrast, no closed relation between ALNs and prokaryote abundances was recorded at the seasonal scale in the French Lake. However, in this environment, ALNs displayed limited pleomorphism and abundance changes in cell-free

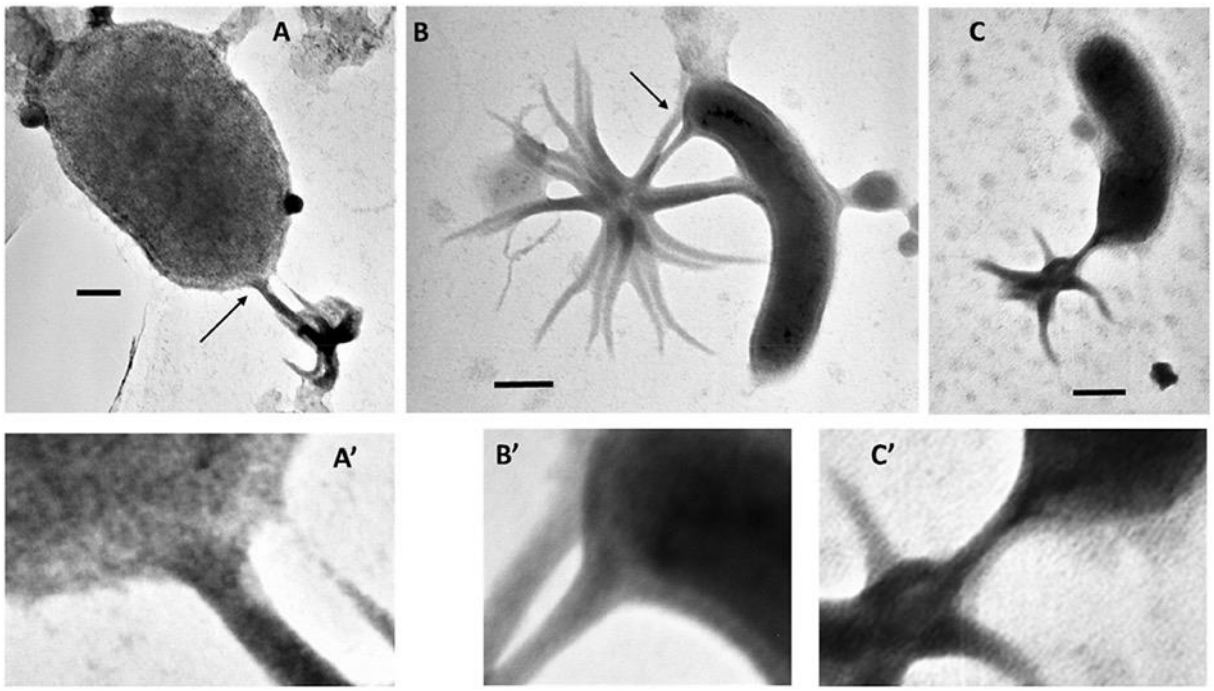

Figure 22: (A–C), Electromicrographs documenting a putative interaction between aster-like nanoparticles and microbial cells.

(A'–C') are magnified views of sections indicated by arrows in (A–C). Note the close contact between arms of the ALNs and the microbial cells. Scale bars = 100 nm.

medium compared to *in situ* analyses (multiplication factor of 3.6 in cell-free medium compared to 60 in French Lake). These data suggests that microbial communities may help promoting the nanoparticle dynamics. Interestingly, more detailed observations of microbial communities collected from eutrophic lakes revealed arm-mediated contacts between ALNs and bacteria (**Figure 22**). The role of microbial communities in the control of ALNs and the functional significance of the observed contacts between ALNs and bacteria are still unclear. Further ecological studies of these puzzling nanoparticles should be placed in the context of ecosystemic relationships between ALNs and prokaryotes as well as between ALNs and other biological or physic-chemical components.

Seasonal and spatial dynamics are a characteristic of aquatic microbial communities which regulate energy and matter flows in aquatic systems [110, 279]. To our knowledge, long-term ongoing researches on the ecology and population dynamics of nanobes or non-living particles are currently lacking. This precludes any comparison with our ALN studies. Nevertheless, our observations clearly raise the question of the ecological importance of ALNs in the functioning of aquatic ecosystems. Although reduced on a unit scale, the biomass of total ALNs during bloom periods is likely to mobilize circulating mineral and organic nutrients at the expense (competition?) of other microbial communities of aquatic ecosystems. In addition, direct interplay with bacteria (**Figure 22**) could significantly influence the energy and material flows mediated by the prokaryotic compartments.

2.2.6 Conclusion

This study shows, for the first time, that aquatic ecosystems may contain abundant and dynamic nanoparticles of a novel type with ecological potentialities, especially in meso- and eutrophic waters which are predilection sites for ALN detection. Tough the question of the living or non-living nature of ALNs remains unresolved at this time, their original features re-open the debate on the minimal cell volume for a self-sufficient form of life. Experiments are in progress to explore the exact nature of ALNs and identify biotic and abiotic factors involved in regulation of their dynamics in microcosm and environmental conditions. In this context, an upcoming challenge will be to obtain mass cultures of ALN particles grown in VLP-, EV- and prokaryote-free medium. Clearly, we have describe novel types of environmental nanoparticles that, as the most ecological outcome, emphasize that not all virus-like particles observed in aquatic systems

are necessarily viruses and that there may be several types of other ultra-small particles in natural waters that are currently unknown but potentially ecologically important.

Data Availability Statement

The datasets generated for this study are available on request to the corresponding author.

Author Contributions

JC and HB performed the experiments and the flow cytometric analyses. JC performed the transmission electron microscopy analyses. SB performed the cryo-transmission electron microscopy analysis. ChB and LG performed the scanning electron microscopy analysis. KB and NM performed the EFTEM and EELS analyses. JC, GI, MF, and AP analyzed samples from Ha Long Bay. FE, CoB, and VG realized genomic analyses. JC, HB, TS-N, and BV designed the research and wrote the manuscript. All authors have read, commented, and approved the final version of the manuscript.

Funding

FE was supported by the EUed Horizon 2020 Framework Programme for Research and Innovation (Virus-X, project no. 685778). This study is a contribution to the C NO LIMIT project funded by the Interdisciplinary Mission of the French National Center of Scientific Research (CNRS) Program X-life, 2018 edition. Funding for sampling at Halong Bay was obtained through the French-Vietnamese Hubert Curien Partnership (Contract No. 23971TK) and the Ministry of Science and Technology of Vietnam (Contract No. 46/2012/HD-NDT).

Conflict of Interest

The authors declare that the research was conducted in the absence of any commercial or financial relationships that could be construed as a potential conflict of interest.

Acknowledgments

This study was supported by the CYSTEM platform UCA-PARTNER (University of Clermont Auvergne UCA), Clermont-Ferrand, France) and the Microorganisms: Genome and Environment laboratory (LMGE, UMR6023 CNRS-UCA, Clermont-Ferrand, France). This work also benefitted from the assistance of the Multiscale Electron imaging platform (METi) at the CBI (Toulouse, France), from the Technological Center for Microstructures (CTμ) (Villeurbanne, France) and from the GENTYANE Sequencing Platform (Clermont-Ferrand, France). The authors thank the UCA Centre Imagerie Cellulaire Santé (UCA, Clermont-Ferrand) for help with microscopy intercalibration. We thank Anne Catherine Lehours (LMGE) and Guillaume Borrel (BECM, Institut Pasteur, Paris, France) for helpful comments and discussions on the manuscript and Matthieu Legendre (IGS, UMR7256 Aix Marseille Université-CNRS, Marseille, France) for his assistance with the assembly of the sequence data. We also thank the two reviewers for their comments and suggestions which greatly increased the quality of this manuscript.

2.2.7 Supplemental materials

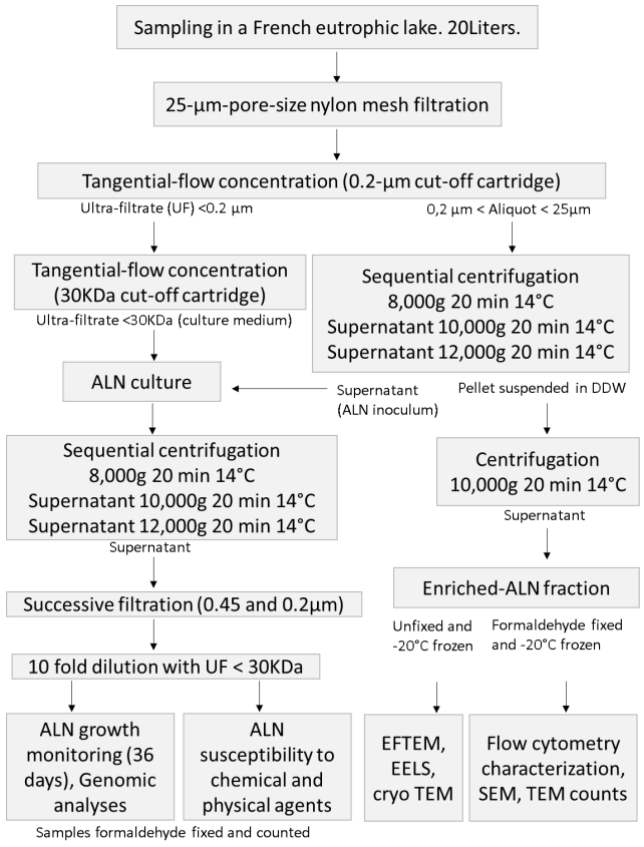

Supplementary figure 1. Detailed procedure of experimental design and analyses performed from a sample collected on March 15th 2017 in a eutrophic freshwater lake near Neuville in the French Massif Central.

EFTEM: Energy-Filtered Transmission Electron Microscopy; ALN: Aster Like Nanoparticles; EELS: Electron Energy Loss Spectroscopy; SEM: Scanning Electron Microscopy; TEM Transmission Electron Microscopy; DDW: Distilled Deionized Water.

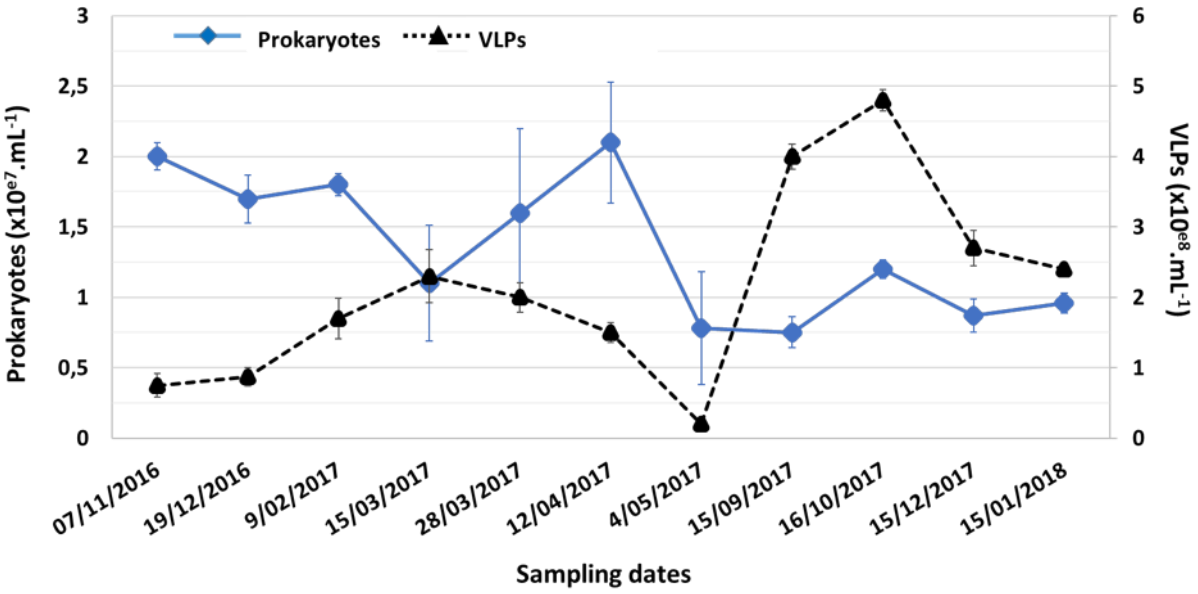

Supplementary figure 2. Abundance of prokaryotes and virus like particles (VLPs) during *in situ* (Neuville-France) seasonal survey from November 2016 to January 2018 in an eutrophic freshwater lake near Neuville in the French Massif Central. Mean values from triplicate and standard errors are plotted.

2.3 Conclusions

La découverte des ALNs, de nouvelles particules femtoplanctoniques aux caractéristiques inédites, suscite de nombreuses interrogations sur leur nature, leur écologie ainsi que leur rôle fonctionnel dans l'environnement.

Leur polymorphisme atypique, couplé à un volume réduit, une nature organique suspectée, une sensibilité aux traitements biocides et une capacité à se développer en l'absence de cellules indiquent en effet que les ALNs sont de nouvelles femtoparticules qui, pour le moment, ne peuvent être classées dans aucune catégorie connue de femtoparticules précédemment décrites dans les échantillons environnementaux. Leur place le long de l'échelle évolutive, du minéral à la cellule vivante reste également à être déterminée.

Au-delà des interrogations sur la nature exacte des ALNs, leur capacité de développement en conditions naturelles avec des densités pouvant atteindre 10^8 ALNs.mL^{-1} (ponctuellement 8 fois supérieur aux procaryotes), interroge sur leur écologie et leurs fonctions au sein des réseaux trophiques aquatiques.

La question fondamentale de leur écologie reste ouverte et inexplorée. C'est donc sur ce principal défi que réside les objectifs des travaux présentés dans ce mémoire. Comment les ALNs, jusqu'à présent jamais décrites, émergent, se développent et évoluent dans les écosystèmes aquatiques ? Dans quels systèmes sont-elles capables d'évoluer et selon quelle dynamique ? Quels sont les facteurs de forçage régissant leur développement ?

Les travaux présentés dans les chapitres suivants seront donc articulés autour de ces principaux axes de réflexion.

CHAPITRE 1 : ÉTUDE DE LA VARIABILITÉ SPATIALE DES ALNs

La détermination de l'écologie des ALNs représente un verrou fondamental à lever pour mieux comprendre leur importance quantitative et fonctionnelle dans les écosystèmes. Définir leur écologie passe avant tout par une prospective spatiale de leur distribution dans différents milieux ou habitats.

L'habitat se définit comme un environnement physique délimité dans lequel l'entité étudiée présente une dynamique en lien avec les facteurs abiotiques et biotiques. En écologie aquatique, les habitats sont définis à différentes échelles, du micro-habitat (*e.g.* zone délimitée d'un cours d'eau) au macro-habitat (*e.g.* l'ensemble du système fluvial étudié) [280]. L'habitat est donc une notion complexe dûe à de nombreux facteurs intrinsèques tels que [281] :

(i) L'échelle spatiale du milieu.
(ii) L'abondance et la densité des entités.
(iii) Les facteurs physico-chimiques du milieu.
(iv) Les composantes biotiques présentes.

Déterminer les différents habitats d'une entité va donc permettre de définir les facteurs de forçage pouvant influencer la présence ou l'absence de cette dernière [282].

Afin d'appréhender les conditions environnementales pouvant favoriser le développement des ALNs, une prospection à l'échelle géographique du bassin-versant de la Loire a été menée, intégrant des habitats aux conditions physico-chimiques et biologiques différentes. Cette étude a fait l'objet d'une publication parue.

Trophic Conditions Influence Widespread Distribution of Aster-Like Nanoparticles Within Aquatic Environments

Maxime Fuster[1], Hermine Billard[1], Marie Mandart[1], Johannes Steiger[2], Télesphore Sime-Ngando[1], Jonathan Colombet[1]

[1] Université Clermont Auvergne, CNRS, LMGE, Clermont-Ferrand F-63000, France

[2] Université Clermont Auvergne, CNRS, GEOLAB, Clermont-Ferrand F-63000, France

Publié dans *Microbial Ecology* – Juin 2020

doi: 10.1007/s00248-020-01541-6

3.1 Abstract

Aster-like nanoparticles (ALNs) are newly described femto-entities. Their ecology (*e.g.*, geographic distribution, spatial dynamic, preferences, forcing factors) is still unknown. Here, we report that these entities, which have largely been ignored until now, can develop or maintain themselves in most aquatic environments in the Loire River catchment, France. We observed a significant influence of the trophic state on ALN ecological distributions. A positive relationship between prokaryotic abundance and ALN (r2 = 0.72, $p < 0.01$) has been identified, but its exact nature remains to be clarified. Combined with their ubiquitous distribution and high abundances (up to 7.9 × 106 ALNs mL−1) recorded in our samples, this probably makes ALNs an overlooked functional component in aquatic ecosystems.

3.2 Note

The discovery of the importance of extracellular vesicles [212], bacteria CPR (Candidate Phyla Radiation), archaea DPANN (Diapherotrites, Parvarchaeota, Aenigmarchaeota, Nanoarchaeota, Nanohaloarchaea) [32, 246], and “biomimetic mineralo-organic particles” [18] permitted to reconsider the diver- sity and ecological role of the femtoplankton, hitherto confined to the sole viruses, some < 0.2 μm filterable prokaryotes [28]. The recent discovery of “aster like nanoparticles” (ALNs) in pelagic aquatic environments showed that the femtoplankton still hosts many unknown and undervalued entities [27]. In a previous, unprecedented study on these entities, the authors have shown that ALNs are amorphous starshaped entities suspected to be organic in nature (composed mainly of carbon, oxygen, calcium and nitrogen with traces of potassium). Pleomorphic, these entities present three main morphotypes, with 4, 11, and 20 arms, and a reduced biovolume, lower than of the smallest known prokaryote. These original characteristics, combined with their sensitivity to biocidal treatments and their ability to grow in the absence of cells, raise questions about their exact nature and origin [27]. Their high seasonal abundances (up to $9.0 \pm 0.5 \times 10^{7}$ entities·mL^{-1}), in the range of virus-like particles, may exceed those of prokaryotes by up to about one order of magnitude [27]. Added to obser- vations of phenotypic close contact with prokaryotes [27], such numerical abundance levels probably make ALNs a significant actor in the functioning of aquatic systems. For example, its calcium composition [27] could have a significant impact on calcium homeostasis of aquatic environments. Without yet knowing their full biological

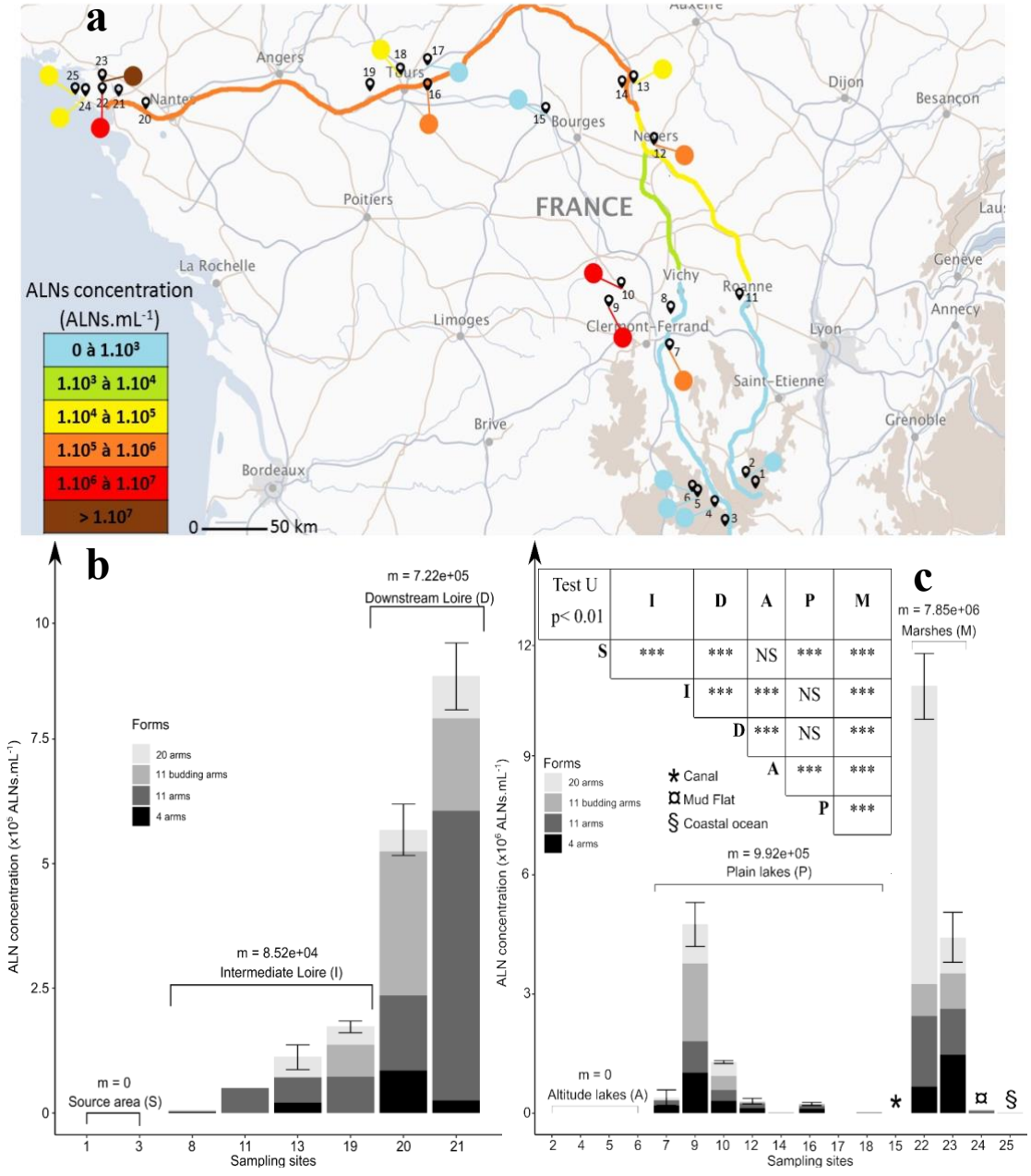

Figure 23: Sampling site locations (1–25) and distribution of ALNs in different aquatic environments along the watershed of Loire River (France).

a Site locations are plotted on the map of the Loire watershed. Each site or river continuum is characterized by ALN concentration range. **b** Distribution of the ALN concentrations and their different forms along the river continuum. **c** Comparisons of the ALN concentrations and their different forms between the different aquatic environments sampled. Statistical differences between aquatic environments (U test, ***p < 0.01) are provided in the inserted table (S Source area, I Intermediate Loire, D Downstream Loire, A Altitude lakes, P Plain lakes, M Marshes, NS Not significant). m mean

nature, we hypothesized that their distribution and dynamics in a wide range of aquatic environments will open a window on the understanding of their ecological significance.

Except for the first findings obtained from lake samples [27], we still lack information on the ecological distribution and spatiotemporal dynamics of ALNs, in relation to the potential environmental forcing factors.

Results acquired in this second study demonstrate that ALNs are overlooked femto-entities, widely distributed, and that their dynamics are controlled by trophic status, in particular by the biological environment. Identification and quantification of ALNs and of their morphological variants are described in Colombet and collaborators [27]. Twenty-five study sites distributed over the Loire River catchment (France) were selected to represent different aquatic systems (rivers, canal, marshes, lakes, mudflat, and coastal ocean) as well as longitudinal gradient from the source to the estuary (**Figure 23-A**).

Sampling sites were classified into three trophic states according to all abiotic and biotic parameters measured in situ. Further details on the methodology used are provided in the supplementary text and data. ALNs have the ability to colonize different aquatic environments: lakes, rivers, marshes, coastal oceanic waters, except source areas, and altitude lakes (**Figure 23**). They were found in environments with contrasting physicochemical (*e.g.*, conductivity, oxygen, nutrients) and biological (*e.g.*, virus, prokaryotes, algae) characteristics (Supplementary Table S1). This defines them as tolerant and ubiquitous entities capable of maintaining themselves in the majority of con- tinental and coastal aquatic environments. The abundances of ALNs recorded ($1.1 \times 10^7 \pm 0.17 \times 10^7$ ALNs mL^{-1}) indicate preferential development in plain lakes, marshes, Loire estu- ary, and in lesser extent within free-flowing river channels (**Figure 23-B,C**). Detection of ALNs has also been mentioned in the tropical estuarine system of Ha Long Bay (Vietnam) and in the Saloum River in Senegal, thus broadening the habitat preferences and potential distribution of these entities [27]. However, sampling of these studies was sporadic, and these conclusions must be weighted by the high seasonal or even daily fluctuations of ALNs recorded previously [27]. The sampling period, *i.e.*, spring, was based on the results obtained from the unique study on seasonal monitoring of ALNs in a eutrophic lake [27]. We recognize the need of additional data on the seasonal variability of ALNs in different aquatic envi- ronments in order to optimize sampling periods.

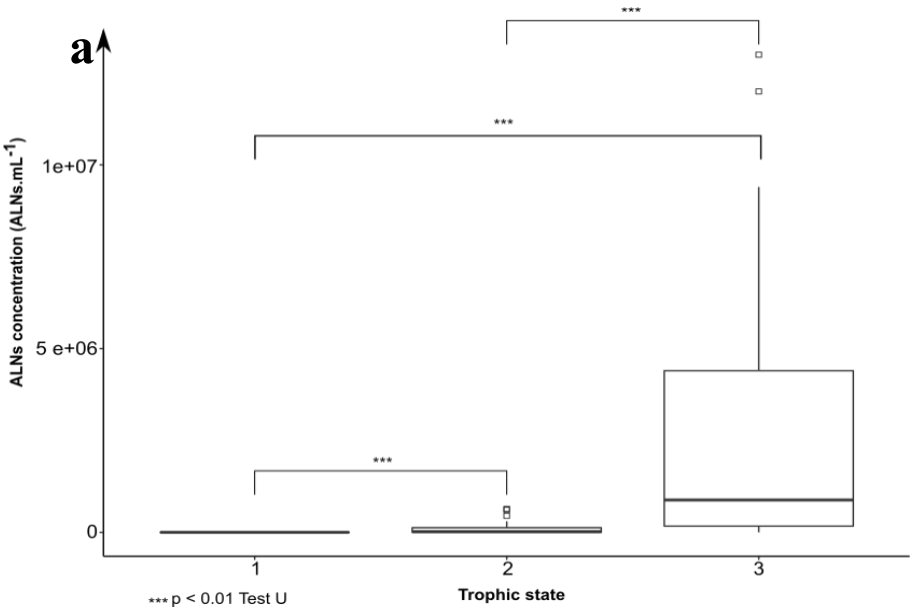

b

	Prokaryotes	Viruses	Microphytoplankton	Picocyanobacteria	Picophytoplankton	T°C	pH	O2	Conductivity	P	N	C
ALNs	0.72	0.55	0.53	0.66	0.5	0.47	0.46	-0.3	0.45	0.31	0.19	0.36
Prokaryotes		0.71	0.68	0.67	0.69	0.44	0.5	-0.18	0.45	0.32	0.14	0.61
Viruses			0.38	0.46	0.37	0.36	0.42	-0.02	0.28	0.12	-0.12	0.59
Microphytoplankton				0.5	0.57	0.1	0.16	-0.16	0.15	0.32	0.23	0.56
Picocyanobacteria					0.6	0.6	0.46	-0.12	0.6	0.15	0.3	0.23
Picophytoplankton						0.46	0.35	-0.19	0.36	0.2	0.15	0.44
T°C							0.51	-0.41	0.79	-0.09	0.13	0.08
pH								0.33	0.63	0.27	0.13	0.17
O2									-0.1	0.1	-0.08	-0.13
Conductivity										-0.04	0.17	0.09
P											0.38	0.4
N												-0.09

Spearman correlation coefficient
> 0.60 / < -0.60
p-value < 0.01

Figure 24: Relationships between ALNs and physical-chemical and biological environment.

a Comparison of the average (U test, $p < 0.01$) of ALNs according to the low (state 1 = sites 1, 2, 3, 4), medium (state 2 = sites 5, 6, 8, 11, 14, 15, 16, 18, 19, 20, 24, 25), and high (state 3 = sites 7, 9, 10, 12, 13, 17, 21, 22, 23) trophic levels of the different aquatic en- vironments. **b** Correlation analysis (Spearman's test, $p < 0.01$) between the different physical-chemical and biological parameters of the different sampling points. T°C temperature, O2 dissolved oxygen, P total organic phosphorus, N total organic nitrogen, C total organic carbon

The presence of ALNs in the coastal ocean samples raises questions about their potential for development in the marine environment and their possible transfer from continental waters to the oceans. We suggest that the gradual and significant increase of ALN abundance (undetectable to 8.8×10^5 ALNs.mL^{-1}) from the source to the estuary (**Figure 23-B**) can be explained through the ALN down- stream transfer along the river continuum, as observed for other entities or pollutants [283–285]. The occurrence of 11- budding-arm forms in the downstream area suggests that ALNs could be transported from the upstream catchment to more favorable conditions for their development down- stream. The occurrence of the different forms of ALN in- dicates dominance of 20-arm forms (69% of total ALNs) in marshes, while 11-arm forms dominate in lakes and rivers (38% and 47% of total ALNs, respectively; **Figure 23-C**). Environmental conditions probably select and/or favor the development of one type in respect to another, through a process that remains unexplained and which could either reflect the gradual development from one form to another or the occurrence and development of rather independent forms. In order to better understand spatial distributions of ALNs, future investigations will have to demonstrate if a form of resistance distinct from forms of propagation able to develop over time (*i.e.*, assuming distinct growth stages of the same organism) [27] exists.

These observations also point to the hypothesis that ALNs could be present in all aquatic environments but are selected by environmental factors (Baas Becking hypothesis) [286]. Such an assumption is supported by the capacity of ALNs to develop in unrelated biomes, from temperate regions separat- ed by hundreds of kilometers as in our study, to tropical regions [27].

According to the parameters recorded, we reported a significant influence of the trophic state on ecological distributions of ALNs (**Figure 24-A**) with a significant increase from undetectable ALNs.mL^{-1} in the environments classified in the first trophic state, to 2.2×10 ALNs.mL^{-1} in those classified in the third trophic state [287]. In this study, the trophic state was estimated according to the Trophic State Index, a reference method for the classification of aquatic environments [288].

Therefore, we suggest that ALNs, in addition to certain microbial components such as phytoplankton communities [289] may serve as a putative indicator of trophic conditions of aquatic environments. Whatever the aquatic system consid- ered, it seems that biological features prevail over physico- chemical ones in the regulation of the distribution and abun-

dances of ALNs (**Figure 24-B**). The major correlative factor identified is the abundance of prokaryotes ($r^2 = 0.72$, $p < 0.01$; **Figure 24-B**). A significant statistical correlation and the observation of direct physical contact between prokaryotes and ALNs [27] suggest an interaction between these two components. Previous study showed that ALNs can grow without a potential host [27]; however, the presence of prokaryotes could promote their development through mechanisms that remain un- known [27]. Therefore, future investigations are needed to elucidate the nature of this mutual relationship which, perhaps, could be related to either bottom-up resource-driven or to top- down host-symbiont interactions.

Our findings reinforced the hypothesis of the biological origin of ALNs [27] and the hypothesis that ALNs are ubiquitous and widespread within continental freshwaters and coastal brackish waters. The estimation of the ecological importance of femtoplanktonic entities depends closely on their abundance and functions. This is demonstrated for viruses [140, 290], extracellular vesicles, ultramicro-prokaryotes [32, 246], and suspected for non-biological entities such as "biomimetic mineralo-organic particles" [18]. The average abundances of 9.9×10^5 and 7.9×10^6 we recorded respectively in plain lakes and marshes area (see **Figure 23-A**) are in the range of those of prokaryotes or viruses. The strong empirical relationship with prokaryotes and the regulation by their environment implies that ALNs are additional and so far ignored actors in aquatic ecosystems. Furthermore, to fully understand the ecological significance of ALNs in plankton dynamics, it is crucial to validate their biological nature.

Author's Contribution
MF, HB, MM, JC designed the study and analyzed data. All authors wrote the manuscript, contributed critically and gave final approval for publication.

Funding Information
This study was supported by the CYSTEM platform UCA-PARTNER (University of Clermont Auvergne UCA), Clermont-Ferrand, France) and the Laboratory Microorganisms: Genome and Environment (LMGE, UMR6023 CNRS-UCA, Clermont- Ferrand, France). MF was supported by a PhD fellowship from the CPER 2015-2020 SYMBIOSE challenge program (French Ministry of Research, UCA, CNRS, INRA, Auvergne-Rhône-Alpes Region, FEDER). This study is a contribution to the "C NO LIMIT" project funded by the Interdisciplinary Mission of the French National Center of Scientific Research (CNRS) Program X-life, 2018 edition. This research was also financed by the French government IDEX-ISITE initiative 16-IDEX- 0001 (CAP 20-25).

Conflict of Interest
The authors declare that they have no conflict of interest.

Table S1: Biological and physical-chemical features of the studied aquatic environments sampled from February to April 2019.

Sampling points	ALNs* (10^5)	Prokaryotes* (10^7)	Viruses* (10^7)	Micro - phytoplankton ¥	Nanocyanobacteria* (10^5)	Nanophytoplankton* (10^5)	T°C	pH	O_2 ¤	Conductivity Ɣ	P ¤	N ¤	C ¤	Ca ¤	Cl ¤
1	ND	0.06 (0.00)	0.47 (0.01)	2.34	1.4	0.50	5.0	6.74	10.9	37.9	0.07	0.303	1.90	ND	ND
2	ND	0.30 (0.01)	1.71 (0.04)	6.72	2.4	0.60	7.6	6.81	10.96	47.1	0.01	0.435	13.00	ND	ND
3	ND	0.03 (0.002)	0.15 (0.01)	7.2	2.9	1.66	5.1	6.62	11.24	18.4	0.03	0.113	5.20	ND	ND
4	ND	0.40 (0.04)	0.95 (0.09)	4.4	4.00	30.85	8.6	6.71	10.13	16.7	0.01	0.143	5.90	ND	ND
5	ND	0.11 (0.01)	2.17 (0.22)	9.94	1.5	0.41	3.4	6.09	10.56	25.0	0.04	0.113	20.00	ND	ND
6	ND	0.12 (0.01)	1.01 (0.07)	14.69	2.9	1.93	1.6	6.32	10.11	26.8	ND	0.325	2.40	ND	ND
7	3.9 (2.75)	3.51 (0.35)	14.14 (1.04)	103.33	150.00	71.73	8.5	7.7	10.25	100.0	0.09	2.508	21.00	ND	ND
8	0.05 (0.04)	0.14 (0.01)	2.00 (0.17)	5.74	5.6	14.29	7.5	7.52	11.32	149.2	0.06	1.21	26.00	ND	ND
9	57 (11.00)	1.51 (0.15)	4.60 (0.70)	30.79	19.00	15.82	8.4	8.01	11.48	188.5	0.06	1.37	8.00	ND	ND
10	13 (0.77)	1.20 (0.11)	7.58 (0.86)	17.04	29.00	23.09	8.5	7.83	11.21	226.0	0.06	1.25	9.80	ND	ND
11	0.5 (0.29)	0.50 (0.02)	7.97 (0.17)	6.17	5.9	9.13	15.5	7.5	8.81	190.5	0.06	1.346	7.00	ND	ND
12	3.1 (1.40)	0.83 (0.06)	1.64 (0.03)	18.36	3.7	11.33	8.7	7.23	9.56	326.0	0.04	9.214	10.20	1.8	ND
13	1.1 (0.49)	0.56 (0.04)	1.55 (0.07)	12.07	10.00	9.49	9.6	8.3	10.86	197.7	0.18	5.972	16.60	1.1	ND
14	0.27 (0.19)	0.48 (0.03)	4.04 (0.26)	17.57	63.00	5.82	10.1	8.09	12.66	281.0	0.03	0.975	5.80	1.9	ND
15	ND	0.37 (0.03)	1.62 (0.08)	4.05	20.00	2.42	11.7	7.43	10.17	443.0	0.01	7.892	4.20	3.3	ND
16	2.3 (0.75)	0.89 (0.12)	12.78 (0.36)	5.11	5.00	2.43	9.0	8.4	10.16	226.0	0.04	0.113	16.80	1.5	ND
17	ND	1.29 (0.01)	7.04 (0.48)	81.29	13.00	37.60	9.6	8.33	12.82	431.0	0.08	2.24	31.00	2.6	1.38
18	0.23 (0.40)	1.24 (0.10)	1.09 (0.00)	17.2	15.00	188.79	13.2	7.88	10.13	370.0	0.04	0.511	10.00	2.5	ND
19	1.7 (0.24)	0.24 (0.02)	1.63 (0.13)	10.58	4.5	7.27	11.5	8.11	10.5	227.0	0.04	2.743	5.00	1.8	ND
20	5.7 (1.03)	0.58 (0.02)	4.25 (0.11)	8.28	63.00	7.64	13.5	7.74	9.97	344.0	0.03	3.626	5.70	2.6	ND
21	8.8 (1.30)	0.63 (0.02)	0.50 (0.09)	15.69	46.00	5.01	12.8	7.71	9.21	12730.0	0.08	2.428	10.60	4.5	144.00
22	110 (16.59)	1.57 (0.09)	21.05 (1.13)	47.63	26.00	93.82	14.4	7.86	9.07	679.0	0.03	0.113	48.00	1.3	6.45
23	44 (12.62)	2.84 (0.12)	19.42 (0.39)	82.24	99.00	263.84	13.6	7.73	9.25	1266.0	0.03	0.113	34.00	1.2	4.45
24	0.79 (0.34)	1.06 (0.07)	17.66 (0.37)	2.43	7.00	1.93	13.1	8.49	13.41	45400.0	0.03	0.113	6.50	3.6	150.00
25	0.12 (0.06)	0.11 (0.02)	0.66 (0.07)	2.73	18.00	17.26	13.2	8.04	11.24	47800.0	0.02	0.425	0.60	6.6	311.00

	trophic state 1	ND = Not detectable	C = total carbon	0_2 = dissolved oxygen
	trophic state 2	P= total phosphorus	Ca = total calcium	(...) = Standard deviation
	trophic state 3	N = total nitrogen		Cl = total chlorides

* = $X.mL^{-1}$ ¥ = $\mu g.\mu L^{-1}$ ¤ = $X .mg.L^{-1}$ Ɣ = $\mu S.cm^{-1}$

3.3 Supplemental materials

Materials and methods

Study sites and sample collection

Samples were collected at the surface (0-40cm) of 25 aquatic environments from February to May 2019, distributed along the Loire River watershed (France, see locations and characteristics in **Figure 1** and supplementary **Tables S1 and S2**): 8 rivers samples (Loire and Allier: sites 1, 3, 8, 11, 13, 19, 20 and 21), 12 lakes samples (sites 2, 4, 5, 6, 7, 9, 10, 12, 14, 16, 17 and 18), 1 canal sample (site 15), 2 marshes samples (sites 22, 23), 1 estuary sample (site 21), 1 mudflat sample (site 24) and 1 coastal ocean sample (Atlantic Ocean, site 25). The Loire is the longest French river with 1012 kilometers long, from its source in the Ardeche department, up to the Loire-Atlantique department, at the estuary of Saint-Nazaire where it reaches the Atlantic Ocean. The watershed covers 117,800 km², or 20% of France's total area. Data on the flows of pollutant matters are available for the Loire catchment (http://www.eau-loire-bretagne.fr/informations_et_donnees/donnees_brutes). Part of the samples were immediately fixed with 1% (v/v final concentration) formaldehyde and stored at 4°C until virus-like particles and prokaryotes counts. Unfixed samples for phytoplanktonic communities, Aster Like Nanoparticles counts and measurement of nutrients concentration were transported at 4°C in the sampling day and immediately treated to the laboratory (see below).

Abiotic parameters measurements

Temperature (°Celsius), conductivity (µSiemens.cm^{-1}) and dissolved oxygen content (mg.L^{-1}) were measured *in situ* with a submersible probe (ProOdo YSI, Yellow Springs, Ohio, USA). pH was measured on an unfixed sample in the laboratory (Thermo Scientific, Orion Star A111, Waltham, MA). Total organic nitrogen, chlorides and organic phosphorus (mg.L^{-1}) were analyzed by UV-VIS spectrophotometry whereas total organic calcium was determined by ion chromatography and total organic carbon was determined by IR spectrophotometry after persulfate oxidation, on unfixed samples.

Biotic parameters measurements

Planktonic communities measurement: Chlorophyceae, cyanobacteria, Cryptophyceae and diatoms biomass was inferred from *in situ* measurement of chlorophyll a, phycoerythrin and phycocyanin (µg.L^{-1}) using a submersible spectrofluorometric probe (BBE FluoroProbe) (Moldaenke GmbH, DE). The description of phytoplankton content was supplemented with the

Table S2. Typology, geographical characteristics and sampling dates of the studied aquatic environments sampled from February to April 2019.

Sampling points	Aquatic environment	Altitude (m.a.s.l)	Sampling date	Latitudes / Longitudes*
1	fluvial (S)	1396	05/09/2019	44°51'53.04"N / 4°11'39.49"E
2	lake (A)	1004	05/09/2019	44°49'01.14"N / 4°03'52.87"E
3	fluvial (S)	1115	02/26/2019	44°33'48.98"N / 3°51'00.98"E
4	lake (A)	1208	05/09/2019	44°38'31.40"N / 3°51'26.34"E
5	lake (A)	1372	02/26/2019	44°48'30.53"N / 3°29'27.86"E
6	lake (A)	1369	02/26/2019	44°54'01.14"N / 3°25'21.76"E
7	lake (P)	462	03/04/2019	45°44'36.01"N / 3°27'23.94"E
8	fluvial (I)	283	03/04/2019	45°54'58.50"N / 3°21'49.76"E
9	lake (P)	679	03/04/2019	46°02'15.56"N / 2°48'46.52"E
10	lake (P)	489	03/04/2019	46°13'19.63"N / 2°53'10.56"E
11	fluvial (I)	252	05/27/2019	46°08'48.29"N 4°05'54.90"E
12	lake (P)	193	03/18/2019	46°54'37.87"N / 3°12'41.59"E
13	fluvial (I)	148	03/19/2019	47°16'41.97"N / 2°57'34.42"E
14	lake (P)	148	03/19/2019	47°16'28.37"N / 2°57'19.57"E
15	canal	121	03/19/2019	47°05'04.15"N / 2°20'36.07"E
16	lake (P)	46	03/26/2019	47°22'32.12"N / 0°44'09.46"E
17	lake (P)	99	03/26/2019	47°26'45.67"N / 0°43'04.23"E
18	lake (P)	38	03/27/2019	47°19'44.06"N / 0°25'07.08"E
19	fluvial (I)	36	03/27/2019	47°19'15.23"N / 0°24'16.17"E
20	fluvial (D)	4.5	04/16/2019	47°12'29.42"N / 1°42'55.27"O
21	fluvial (D)	1.7	04/16/2019	47°18'19.32"N / 2°04'28.97"O
22	marsh	0.82	04/16/2019	47°23'31.52"N / 2°12'40.10"O
23	marsh	0.85	04/16/2019	47°19'23.19"N / 2°11'52.26"O
24	mud flat	2.21	04/15/2019	47°17'35.40"N / 2°26'15.64"O
25	costal ocean	0	04/162019	47°17'41.99"N / 2°32'50.08"O

counts of nanophytoplankton and nanocyanobacteria populations, from unfixed samples, by flow cytometry as described elsewhere [291] using a BD FACS Calibur cytometer (BD Sciences, San Jose, CA) equipped with an air-cooled laser, delivering 15 mW at 488 nm with the standard filter set-up.

Prokaryotes, virus-like particles (VLPs) and ALN counts: Counts of prokaryotes and VLPs from fixed samples were performed by flow cytometry as described elsewhere [291] using a BD FACS Calibur flow cytometer (BD Sciences, San Jose, CA) equipped with an air-cooled laser, delivering 15 mW at 488 nm with the standard filter set-up. Since the source area showed low microbial load for robust TEM (Transmission Electronic Count) counting (Table 1), ALNs detection and quantification of all sites were realized from 60 fold concentrated water. This was obtained by tangential-flow ultrafiltration of 40 L of raw water, previously filtered through a 25-µm-pore-size nylon mesh, using a Kross-Flow system (Spectrum, Breda, The Netherlands) equipped with a 0.2-µm cut-off cartridge. Aliquot of the concentrated 0.2 µm–25 µm fraction was immediately fixed with 1% (v/v) formaldehyde and stored at 4°C for ALNs counts. The microbial concentration of the concentrated fraction was determined by flow cytometry as described above. Most loaded samples were then diluted after concentration to prepare the microscopy grids. This dilution factor was calculated for each sample to obtain an equal load of prokaryotes on each grid. The sample with the lowest prokaryotic concentration after concentration was considered standard. The concentration factor and dilution were experimentally tested and chosen to promote clear discrimination between the ALNs and all entities present on the grid. Fixed-concentrated sample were centrifuged at 18,000 *g* for 20 min at 14°C directly onto 400-mesh electron microscopy copper grids covered with carbon-coated Formvar film (Pelanne Instruments, Toulouse, France). Collected particles were over-contrasted using uranyl salts as described here [254]. Ratio of ALNs/prokaryotes was determined by transmission electron microscopy (TEM) using a Jeol 1200EX microscope (JEOL, Akishima, Tokyo, Japan) at 80 kV and x50,000 magnifications [27]. For all samples, 300 prokaryotes were counted (*i.e.* a minimum of 6 transects randomly distributed on the grid), in triplicate to ensure robust statistical processing of the data. At the same time, we also counted the number of ALNs present on these transects to determine this ratio. Entities with membrane folds and non-homogeneous shapes, characteristic of large extracellular vesicles (*i.e.* microvesicles and some apoptotic vesicles), were excluded from the prokaryotic count.
Concentration of ALNs per millilitre was obtained by multiplying ALNs/prokaryotes ratio by prokaryotes abundance (see schematic view of the used procedure in **Fig S1**)

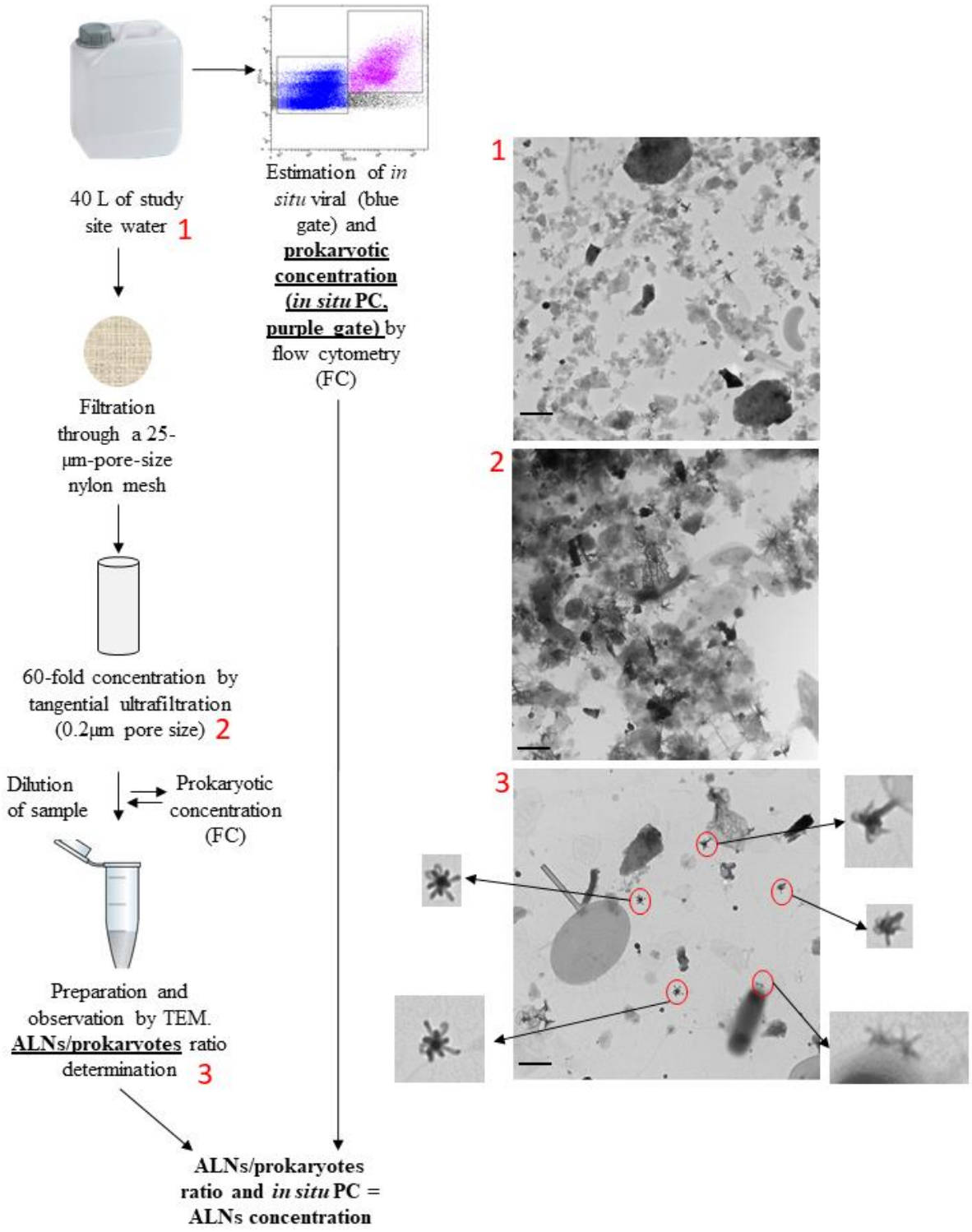

Fig S1: Schematic view of the experimental strategy used to determine the abundances and the different ALNs morphotypes.

Images of TEMs associated with the critical steps of sample preparation, showing a clear purification of the sample.

Scale bars = 500 nm. TEM: Transmission Electron Microscopy. Additional technical details are available in supplementary materials.

Determination of trophic status of sampled aquatic environments

The classification in 3 different trophic states is done using the TSI (Trophic State Index) defined by Carlson in 1977 [288] and recommended by the OECD [292]. As the Secchi value was not applicable on all samples (river sample), we used an average TSI inferred from phosphorus and chlorophyll concentrations ([P] and [Chla] respectively):

TSI - P = 14.42*Ln[P] + 4.15 (in µg.L-1)

TSI - Chla = 30.6 + 9.81 Ln [Chla] (in µg.L-1)

Average TSI = (TSI-P + TSI-Chla)/2

Our samples were then categorized as follow : sites 1, 2, 3, 4 in trophic state 1 (low), sites 5, 6, 8, 11, 14, 15, 16, 18, 19, 20 ,24, 25 in trophic state 2 (moderate) and sites 7, 9, 10, 12, 13 ,17, 21, 22, 23 in trophic state 3 (high) (see **Table S1**).

Correlation analyzes

Differences between the trophic states were assessed using a U test. Potential relationships between variables were tested with a Spearman test then visualized through a correlogram using the "Hmisc" package. All tests were performed under RStudio (R Core Team version 3.2.2, 2015).

3.4 Conclusions

Les travaux menés dans cette étude montrent que les ALNs ont un large spectre d'habitats : rivières, lac, marais, vasière, eaux côtières. Leur présence est également rapportée en milieux marins (mer de chine [293] et mer d'Arabie -données non montrées-), ce qui en fait des particules ubiquistes dont le développement, avec des concentrations atteignant celles des procaryotes ou des virus selon le milieu, pourrait impacter le fonctionnement de grandes masses d'eaux. Leur distribution est étroitement associée au statut trophique du milieu considéré. D'un point de vue empirique, les conditions biologiques prévalent sur les paramètres physico-chimiques dans le contrôle de leur importance quantitative. Leur forte concentration, du même ordre que celles des procaryotes ou des virus selon les milieux, ainsi que leur présence dans des environnements aquatiques très variés, suggèrent une grande importance des ALNs dans le fonctionnement de ces écosystèmes.

Les conclusions de cette étude ouvrent de nouvelles perspectives et hypothèses de travail. Les prélèvements ponctuels ayant permis de mettre en évidence des facteurs de contrôle putatifs des ALNs, étudier la présence des ALNs dans un même milieu au cours du temps semble indispensable, afin de préciser et valider les facteurs de forçage de leur dynamique.

CHAPITRE 2 : ÉTUDE *IN-SITU* DE LA VARIABILITÉ TEMPORELLE DES ALNs

L'étude exploratoire précédente a permis de mettre en évidence un lien étroit entre ALNs et statut trophique du milieu, avec des plus fortes abondances dans les milieux eutrophes. Cela indique que la présence des ALNs serait dépendante de la productivité de l'écosystème.

Cependant, cette étude spatiale menée dans des milieux dispersés, intégrant une variabilité géographique, ne tient pas compte de la dynamique temporelle des ALNs.
Intégrer cette dimension temporelle permettra de mieux appréhender l'écologie des ALNs et une exploration des facteurs biologiques pouvant contrôler non seulement leur présence mais aussi leur développement. L'étude de la dynamique temporelle des ALNs dans un même milieu permettra également de mettre en lumière les interactions potentielles avec les différents facteurs biologiques et physico-chimiques du milieu. C'est pour atteindre cet objectif spécifique de la thèse que la présente étude, qui a fait l'objet d'une publication parue, a été conduite.

La dynamique temporelle des organismes est un élément clé dans la structuration saisonnière des communautés, et plus largement dans le bon fonctionnement des écosystèmes. Les premières études, portant sur la succession de plantes et d'animaux dans des environnements variés ont démontré l'importance de cette saisonnalité dans l'équilibre et le bon fonctionnement des écosystèmes [294, 295]. Par la suite, les progrès technologiques et notamment en microscopie, cytométrie en flux ainsi que le séquençage haut-débit ont permis de mettre en évidence une telle importance chez les organismes planctoniques [296], et notamment les organismes procaryotes [297, 298] et les phages [110]. La variabilité de ces organismes, à différentes échelles de temps, impacte donc la structuration des communautés et plus largement les réseaux trophiques aquatiques [299].

Ainsi, la phénologie et les successions écologiques des communautés microbiennes dans le temps régissent le fonctionnement des écosystèmes aquatiques. Cette étude menée dans 3 écosystèmes lacustres vise à identifier un « pattern » temporel dans la dynamique des ALNs, en relation avec les communautés microbiennes pouvant potentiellement réguler cette dynamique.

Occurrence and seasonal dynamics of ALNs in freshwater lakes are influenced by their biological environment

Maxime Fuster[1], Hermine Billard[1], Gisèle Bronner[1],Télesphore Sime-Ngando[1], Jonathan Colombet[1]

[1] Université Clermont Auvergne, CNRS, LMGE, Clermont-Ferrand F-63000, France

Publié dans *Microbial Ecology* – Mars 2022
doi : 10.1007/s00248-022-01974-1

4.1 Abstract

Aster Like Nanoparticles (ALNs) are femtoentities, recently discovered in different aquatic environments, whose intrinsic nature and ecological features remain to be determined. In this study, we investigate the *in-situ* temporal dynamics of ALNs during one year in 3 different lakes, in relation with the physico-chemical and biological environment. ALN abundances in investigated lakes showed a marked seasonal dynamic (from no detectable to $4.28 \pm 0.75 \times 10^6$ ALNs.mL^{-1}), with characteristic peaks in spring. We recorded correlation between ALNs and some prokaryotic phyla suggesting a broad and non-specific relationship. From their seasonal dynamics and potential link with prokaryotes, we conclude that ALNs represent an important ecological actor in the functioning of aquatic ecosystems

4.2 Introduction

The ecological importance of planktonic communities closely depends on their diversity and the associated spatio-temporal dynamics, in response to environmental changes. In the past, the ecological importance of picoplankton (0.2-2 µm) [15, 300] and nanoplankton (2-20 µm) [301, 302] making up the bulk of the so-called microbial loop has been studied extensively. Their roles in the flow of energy and matter on a global scale has become evident [12]. Highlighting the importance of viruses resulted in the inclusion of femtoplankton (< 0.2 µm) in ecological models [219, 225, 303]. Viruses have long been considered as the main, if not the only, compartment of femtoplankton, mainly because of their interactions within the microbial loop where they shunt microbial particles into dissolved matter, *i.e.* the 'viral shunt' [28, 230]. However, in the recent years, the discovery of an unsuspected diversity of femtoplankton

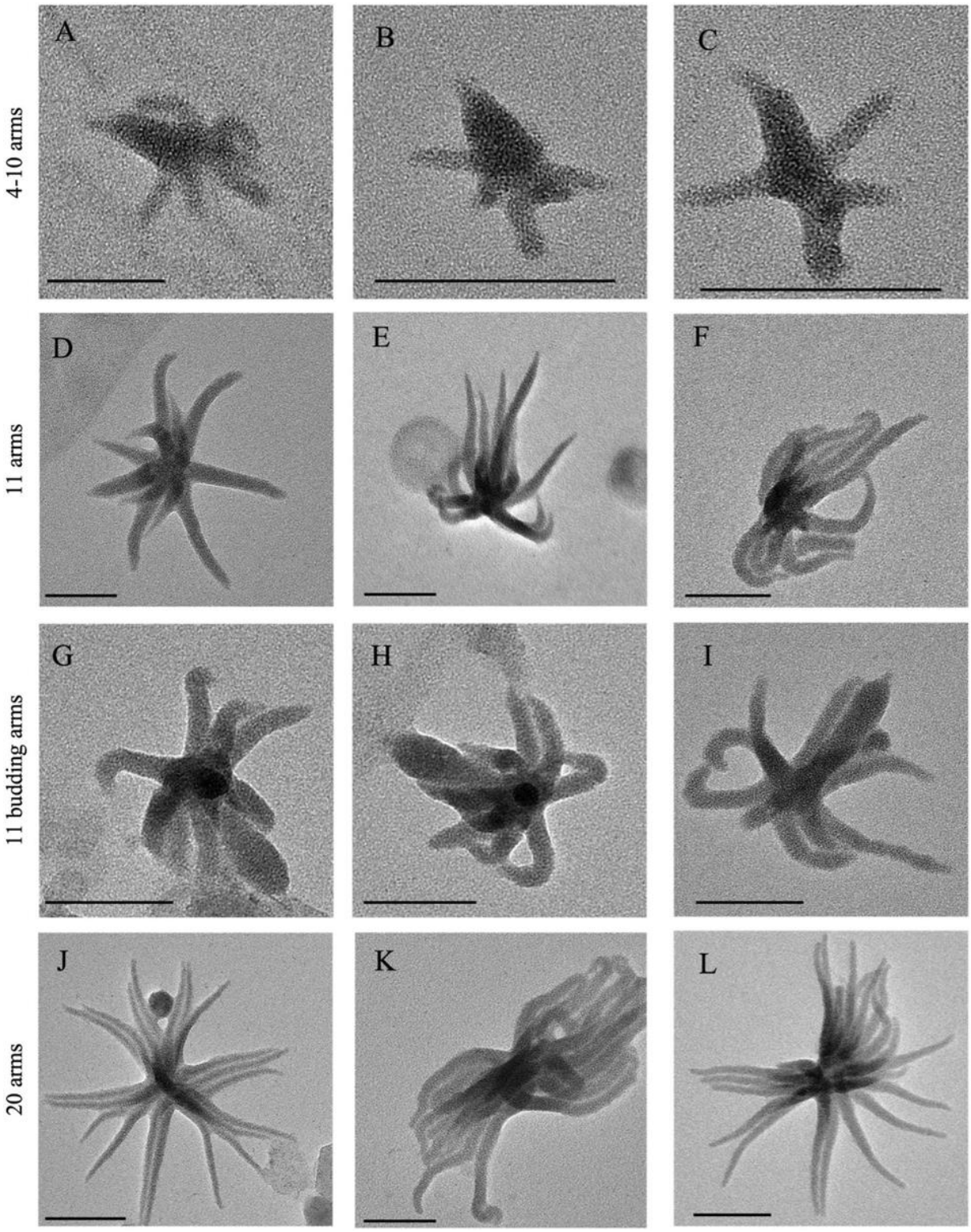

Figure 25: Transmission electron microscopy (TEM) micrographs of different morphotypes of aster-like nanoparticles (ALNs).

A-C, 4-10 arms forms. **D-F**, 11 arms forms and their budding variants **G-I**. **J-L** 20 arms forms. Scale Bars = 100 nm

entities as Candidate Phyla Radiation (CPR), Diapherotrites-Parvarchaeota-Aenigmarchaeota-Nanoarchaeota-Nanohaloarchaeota (DPANN), Bio-Mineral Organic Particles (BMOPs), Extracellular Vesicles (EVs), and Aster Like Nanoparticles (ALNs), leads to a necessary reconsideration of the ecological role of femtoplankton compartment, at least through the study of the diversity and dynamics of their representatives (Colombet et al.,[16]). Attempts to evaluate the quantitative and qualitative importance of CPR / DPANN [203, 204], BMOPs [18], EVs [24] underscores this necessity. Likewise, pioneering reports on ALNs also showed that these entities might have important ecological functions [27, 197]. ALNs are original aster-like entities composed of C, O, Ca, N, K with distinct morphotypes depending on the number of arms (4, 11 and 20 arms) present and their budding (**Figure 25**). Their size (on average from 110 to 430 nm) and volume (less than $1.4x10^{-3}$ μm^3) lower than the minimum required for life expression (Theoretical Minimal Cell Volume, *i.e.* 0.008 μm^3) [251], together with their organic nature, their sensitivity to different biocidal treatments, and their capacity to change their numbers in the absence of potential hosts [27], question their exact nature. The presence of nucleic acids remains to be proven [16, 27].

However, (i) their ability to colonize different continental and coastal aquatic environments according to their trophic status [197], (ii) their capabilities to produce bloom situations, with abundance peaks reaching up to $9.0 \pm 0.5 \times 10^7$ ALNs.mL^{-}1 [27], and (iii) their putative functional interactions with prokaryotes [27, 197] strongly suggest that they are potentially significant actors in the flow of energy and matter transiting in aquatic systems. To understand the quantitative and functional importance of ALNs in the environment and their exact nature, it seems to be crucial to realize ecological studies integrating temporal variations of ALNs in various ecosystems considering possible environmental forcing parameters.

For this purpose, we monitored the *in-situ* dynamic of ALNs as well as the physico-chemical and biological parameters in three lakes of the Massif Central, France, during a one-year period. Our results indicate that ALNs are new dynamic players in the ecology of aquatic systems, with potential links with microbial phyla.

4.3 Materials and methods

Study sites and sample collections

Samples were collected every month during one year (10-2018 to 09-2019) in three artificial freshwater lakes: Fargettes (45°44’39’’N ; 3°27’21’’E ; 465 m altitude ; surface area 1.2 ha ; maximum depth 2.5 m), Lapeyrouse (46°13’20’’N ; 2°53’15’’E ; 490 m altitude ; surface area 12 ha ; maximum depth 6 m) and Saint-Gervais-d’Auvergne (St. Gervais) (46°02’15’’N ; 2°48’43’’E ; 680 m altitude ; surface area 10.5 ha ; maximum depth 4.5 m). These lakes are in the French Massif Central (within a 120 km area). Fargettes is a hyper eutrophic lake while St. Gervais and Lapeyrouse are eutrophic lakes with a significant human presence. Five liters of water was collected at the surface (0-40cm) of the deepest point of the lake, using a sampling bottle (5L-Niskin-type, Bionef, Fr). St. Gervais has the particularity of having been emptied during November, December 2018 and January 2019 and returned to its maximum depth in December 2019. During the empty period, samples were taken from a permanent puddle at the center of the lake supplied by the upstream source flowing into the lake. Monitoring of the number of Aster Like Nanoparticles (ALNs) in this upstream source was performed during all the survey, in addition to the lake. Samples of virus-like particles (VLPs), prokaryotes and Aster Like Nanoparticles (ALNs) were fixed with 1% (v/v) formaldehyde and stored at 4°C until counts within 4 hours following sampling. Samples of heterotrophic eukaryotes (HE) were fixed with 1% (v/v) formaldehyde and stored at -20°C until counts.

Unfixed samples for analyses of phytoplanktonic communities, microbial diversity, nutrients concentrations and pH measurements were transported at 4°C and treated in the 4 hours following sampling.

Abiotic parameters measurements

Dissolved oxygen content (mg.L-1), temperature (°Celsius) and conductivity (µSiemens.cm-1) were measured in-situ with a submersible probe (ProDSS YSI, Yellow Springs, Ohio, USA), while pH was measured in the laboratory (probe Thermo Scientific, Orion Star A111, Waltham, MA). Organic phosphorus, chlorides and total organic nitrogen were analyzed by UV-VIS spectrophotometry (NF ISO 15923-1). Total organic carbon was determined by IR spectrophotometry after persulfate oxidation (NF EN 1484) and total organic calcium, potassium, magnesium and sodium were determined by ion chromatography (NF EN ISO 14911). These standardized and normed measurements were carried out by an accredited institute (Eurofins, Saint-Etienne, France NF EN ISO/IEC 17025:2005 COFRAC 1-2091)

Biotic parameters measurements

Phytoplanktonic communities

The biomasses of different groups of the Nanophytoplankton (*i.e.* Chlorophyceae, cyanobacteria, Cryptophyceae and diatoms) were inferred from in situ measurements of chlorophyll a, phycoerythrin and phycocyanin (µg.L-1) using a submersible spectrofluorometric probe (BBE FluoroProbe, Moldaenke GmbH, DE). Counts of picophytoplankton populations were determined by flow cytometry as described elsewhere [19] using a BD FACSCalibur (BD Sciences, San Jose, CA) equipped with an air-cooled laser, delivering 15 mW at 488 nm with the standard filter set-up.

VLP, Prokaryote, Heterotrophic eukaryote and ALN counts

Counts of VLPs, prokaryotes and heterotrophic eukaryotes (HE) were performed in triplicates by flow cytometry according to Brussaard [256] and Christaki *et al.,* [304] respectively using a BD FACSAria Fusion SORP (BD Sciences, San Jose, CA) equipped with an air-cooled laser, delivering 50 mW at 488 nm with 502 longpass, and 530/30 bandpass filter set-up. ALN (and their different forms) detection and quantification were realized by transmission electron microscopy (TEM) using a Jeol JEM 2100-Plus microscope (JEOL, Akishima, Tokyo, Japan) operating at 80 kV and x50,000 magnifications as described in Colombet *et al.,[27]*.

ALN/prokaryote ratios were determined in triplicate following uranyl salt contrasting of particles centrifuged at 18,000xg; 20 min; 14°C directly onto 400-mesh electron microscopy copper grids covered with carbon-coated Formvar film (Pelanne Instruments, Toulouse, France). The number of ALN results from the multiplication of this ratio-fold by prokaryote concentration obtained by cytometry.

Diversity of microbial communities

Nucleic acid extractions and amplifications : For each unfixed sample, microbial communities were collected on a 0.2 µm (Millipore) polycarbonate filter (until saturation, pressure < 25 kPa) and stored at -20°C until DNA extraction. The filters were covered with a lysing buffer (lysozyme 2 mg.mL^{-1}, SDS 0.5%, Proteinase K 100 µg.mL^{-1} and RNase A 8.33 µg.mL^{-1} in TE buffer pH 8) at 37°C for 90 minutes. A CTAB 10% / NaCl 5M solution was added, and the samples were incubated at 65°C for 30 minutes. The nucleic acids were extracted with phenol-chloroform-isoamyl alcohol (25:24:1) ; the aqueous phase containing the nucleic acids was recovered and purified by adding chloroform-isoamyl alcohol (24:1).

The nucleic acids were then precipitated with a mixture of glycogen 5mg.mL^{-1}, sodium acetate 3M and ethanol 100% overnight at -20°C. The DNA pellet was rinsed with ethanol (70%), dried

and dissolved in the TE buffer. DNA was then purified using a commercial kit (NucleoSpin® gDNA Clean-up, Macherey-Nagel).

For archae, amplification of the V4-V6 region of the small subunit rDNA was amplified using the universal archae 519F and 1017R primers [305] (**Tab s1**). For bacteria, the V4-V5 region of the bacterial small subunit rDNA was amplified using the universal bacteria 515F and 928R primers [306] (**Tab s1**). In addition, the ITS region of fungi was amplified using common fungi primers ITS7f and ITS4r [307] (**Tab s1**). Each PCR was performed in a total volume of 50µL containing 1x final reaction buffer, 2 mM $MgCl_2$, 0.2mM dNTP, 100 µg.mL^{-1} BSA, 0.2 µM of each primer, 0.025 U.µL^{-1} PROMEGA GoTaq HotsStart G2 and 5 µL of DNA. The different PCR programs are detailed in the supplemental (**Tab s1**).

Amplicon analysis and taxonomic affiliation : Bacterial sequencing data were processed with the PANAM2 pipeline [308]. Briefly, sequence reads were assembled with Vsearch [309], excluding reads <200pb, with ambiguous calls (N) or having mismatch in the forward/reverse primer. Demultiplexed amplicons were clustered into OTUs using Vsearch at a 95% id threshold. Representative sequence of OTUs were compared against the SILVA SSURef 115 database restricted to sequences with length > 1,200 pb, quality score > 75% and a pintail value > 50. Archaea and Fungi sequencing data were analysed through the FROGs pipeline [310]. Sequence reads were assembled with Vsearch [309], excluding reads < 200pb, with ambiguous calls (N) or having mismatch in the forward/reverse primer. Demultiplexed amplicons were clustered into OTUs using Swarm [311] with distance (d) = 1. OTUs sequences were compared against the SILVA_132_16s database for archaea and Unite_Fungi_8,0 database for fungi.

Data analysis

Differences in physico-chemical and biological variables between seasons (Spring: March-May, Summer: June-August, Autumn: September-November, Winter: December-February) and lakes were tested by Kruskal-Wallis and Dunn tests. To investigate the potential proximity between our sampling points, function of lakes or seasons, principal component analysis (PCA) was used with the FactoMineR package. Potential relationships among all variables were tested

Table 3: Mean ± SD of physico-chemical and biological characteristics according to the lakes (A) or the seasons (B).

(A)	**Fargettes**	**St. Gervais**	**Lapeyrouse**
O_2 ^{ns} (mg.L $^{-1}$)	8.46 ± 3.45	9.36 ± 3.02	9.86 ± 2.07
Temperature ^{ns} (°C)	12.63 ± 7.13	12.79 ± 8.04	13.32 ± 7.72
pH ^{ns}	7.54 ± 0.67	7.88 ± 0.83	7.53 ± 0.56
K (mg.L^{-1})	31.15 ± 5.53 ^{a}	2.78 ± 0.51 ^{b}	5.11 ± 0.49 ^{c}
Mg (mg.L^{-1})	4.84 ± 0.52 ^{a}	3.22 ± 1.13 ^{b}	4.23 ± 0.48 ^{c}
Na (mg.L^{-1})	8.98 ± 2.27 ^{a}	12.52 ± 1.29 ^{b}	13.04 ± 1.41 ^{b}
Ca (mg.L^{-1})	22.94 ± 2.44 ^{a}	17.61 ± 6.08 ^{b}	24.06 ± 2.75 ^{a}
P (mg.L^{-1})	0.23 ± 0.06 ^{a}	0.14 ± 0.12 ^{ab}	0.06 ± 0.02 ^{b}
T.O.C. (mg.L^{-1})	23.92 ± 4.34 ^{a}	10.78 ± 3.70 ^{b}	10.67 ± 1.05 ^{b}
T.N. (mg.L^{-1})	4.73 ± 2.65 ^{a}	3.13 ± 1.89 ^{ab}	1.75 ± 0.67 ^{b}
VLP ^{ns} (VLPs.mL^{-1})	1.31 ± 0.70 x10^{8}	1.08 ± 0.88 x 10^{8}	0.78 ± 0.66 x 10^{8}
Prokaryotes (cells.mL^{-1})	2.73 ± 1.77 x10^{7} ^{a}	1.59 ± 0.92 x 10^{7} ^{a}	0.39 ± 0.36 x 10^{7} ^{b}
Nanophytoplankton (µg.L^{-1})	178.20 ± 98.80 ^{a}	106.27 ± 70.84 ^{a}	222.44 ± 13.13 ^{b}
Picophytoplankton (cells.mL^{-1})	4.62 ± 2.01 x 10^{5} ^{a}	4.97 ± 6.43 x 10^{5} ^{a}	0.76 ± 0.93 x 10^{5} ^{b}
Heterotrophic eukaryotes (cells.mL^{-1})	2.34 ± 1.46 x10^{4} ^{a}	2.08 ± 1.56 x10^{4} ^{ab}	1.23 ± 0.77 x10^{4} ^{b}
ALN (ALNs.mL^{-1})	6.12 ± 11.7 x10^{5} ^{a}	2.32 ± 2.60 x10^{5} ^{ab}	0.83 ± 1.99 x10^{5} ^{b}

by linear pair-wise correlations (Pearson correlation analyses). Potential relationships between the presence/absence of ALNs and OTUs were tested by pairwise correlations (Spearman correlation analyses). Link between the log-transformed abundance of ALNs and prokaryotes was tested by linear regression using data obtained in the 3 lakes and those obtained from a previous study in Colombet *et al.,*[27]. Cross effects of measured parameters were tested by the omega-square method ω2 [312].

4.4 Results

Environmental parameters

Physico-chemical environment of the studied sites

Absolute values and seasonal variations in oxygen content, temperature and pH were characteristics of freshwater lakes in temperate regions. The three lakes showed similar average values ($p > 0.05$, **Table 3-A**) with marked statistical differences ($p < 0.01$) between seasons (**Table 3-B**). As expected, temperature was inversely correlated to oxygen ($r^2=-0.77, p < 0.01$). The summer and autumn warming periods of the lakes corresponded to oxygen depletion while the cold spring and winter periods corresponded to a rise in oxygenation of lake waters (**Table 3-B**). pH was stable during spring, summer and autumn and decreased significantly in winter ($p < 0.01$) (**Table 3-B**).

The availability of mineral elements (K, Mg, Na, Ca) showed different distributions between lakes (**Table 3-A**). K and Mg had similar distributions with significant differences ($p < 0.01$) between the three lakes, with highest and lowest values recorded respectively in Fargettes and St. Gervais (**Table3-A**). Na concentration was significantly lower in Fargettes compared to St. Gervais and Lapeyrouse ($p < 0.01$). Ca was significantly lower in St. Gervais compared to Fargettes and Lapeyrouse ($p < 0.01$) (**Table 3-A**).

The main chemical factors that discriminated the three lakes appeared to be productivity indicators such as Phosphorus (P), Total Organic Carbon (TOC) or Total Nitrogen (TN). P, TOC and TN were significantly higher in Fargettes compared to Lapeyrouse while St. Gervais

(B)	**Spring**	**Summer**	**Autumn**	**Winter**
O_2 (mg.L $^{-1}$)	10.22 ± 2.80 ^{bc}	6.29 ± 1.31 ^{a}	8.46 ± 1.82 ^{ac}	11.94 ± 1.93 ^{b}
Temperature (°C)	12.70 ± 3.18 ^{a}	22.39 ± 2.54 ^{b}	11.87 ± 6.68 ^{a}	4.70 ± 1.36 ^{c}
pH	8.31 ± 0.44 ^{a}	7.69 ± 0.44 ^{a}	7.60 ± 0.83 ^{ab}	7.01 ± 0.29 ^{b}
K ^{ns} (mg.L^{-1})	11.75 ± 12.18	14.94 ± 16.23	13.97 ± 15.02	11.40 ± 11.84
Mg ^{ns} (mg.L^{-1})	3.97 ± 0.95	4.45 ± 0.87	4.37 ± 1.15	3.59 ± 0.96
Na ^{ns} (mg.L^{-1})	11.95 ± 2.75	12.54 ± 2.15	11.40 ± 2.43	10.16 ± 2.27
Ca ^{ns} (mg.L^{-1})	21.33 ± 4.08	23.78 ± 3.64	21.86 ± 5.42	19.18 ± 5.80
P ^{ns} (mg.L^{-1})	0.14 ± 0.12	0.16 ± 0.08	0.17 ± 0.13	0.11 ± 0.09
T.O.C. ^{ns} (mg.L^{-1})	14.34 ± 7.78	16.10 ± 6.56	17.44 ± 7.95	12.60 ± 6.21
T.N. ^{ns} (mg.L^{-1})	3.46 ± 3.28	2.61 ± 1.34	3.14 ± 1.95	3.59 ± 2.20
VLP ^{ns} (VLPs.mL^{-1})	0.88 ± 0.51 x 10^{8}	1.32 ± 0.87 x 10^{8}	1.07 ± 1.09 x10^{8}	0.95 ± 0.44 x 10^{8}
Prokaryotes ^{ns} (cells.mL^{-1})	2.09 ± 2.33 x 10^{7}	1.46 ± 1.10 x 10^{7}	1.33 ± 1.25 x10^{7}	1.39 ± 1.05 x 10^{7}
Nanophytoplankton ^{ns} (µg.L^{-1})	137.84 ± 138.11	103.03 ± 88.35	111.31 ± 78.03	56.79 ± 45.02
Picophytoplankton ^{ns} (cells.mL^{-1})	2.69 ± 2.77 x 10^{5}	5.32 ± 6.32 x 10^{5}	4.27 ± 4.58 x 10^{5}	1.54 ± 1.38 x 10^{5}
Heterotrophic eukaryotes (cells.mL^{-1})	1.80 ± 1.75 x 10^{4} ^{ab}	2.35 ± 0.91 x 10^{4} ^{ac}	2.69 ± 1.20 x 10^{4} ^{c}	0.69 ± 0.39 x 10^{4} ^{b}
ALN (ALNs.mL^{-1})	7.14 ± 13.30 x10^{5} ^{a}	2.11 ± 2.16 x10^{5} ^{ab}	1.72 ± 2.50 x10^{5} ^{ab}	1.39 ± 2.55 x10^{5} ^{b}

O_2 : Oxygen; K: Potassium; Mg: Magnesium; Na: Sodium; Ca: Calcium; P: Phosphorus; T.O.C.: Total Organic Carbon; T.N.: Total Nitrogen; VLP: Viral Like Particles; ALN: Aster Like Nanoparticles

^{a,b,c} indicate significant differences between lakes or seasons (*Dunn test, $p < 0.01$*)

^{ns} indicate no effect of lakes or seasons on this parameter. * = data are obtained from mean of the 3 lakes

displayed intermediate values ($p < 0.01$) (**Table 3-A**). At the seasonal scale, no significant variation ($p > 0.05$) was recorded for the three lakes in the availability of mineral elements, P, TOC and TN (**Table 3-B**)

Standing stocks of Viruses like particles, prokaryotes, phytoplankton and heterotrophic eukaryotes

The variations of biological environment (Viruses Like Particles (VLPs), prokaryotes, phytoplankton and heterotrophic eukaryotes (HE)) between lakes and seasons are listed in **Table 3** and **Figs s1-s2**. The average numbers of VLPs were similar for the three lakes ($p > 0.05$) (**Table 3-A**). Prokaryote and HE numbers followed the spatio-temporal dynamic of the productivity indicators (P, TOC and TN) with highest average recorded in Lake Fargettes compared to Lapeyrouse ($p < 0.01$) and no significant difference with lake St. Gervais ($p > 0.05$). Lapeyrouse had higher content in nanophytoplankton and lower content in picophytoplankton compared to Fargettes and St. Gervais ($p < 0.01$).

At the seasonal scale, no significant variations ($p > 0.05$) were recorded for the three lakes (**Table 3-B**), excepted for HE. HE dynamic was significantly affected by seasons ($p < 0.01$) with a maximum number in autumns and minimal number in winter. Detailed lake-specific monthly variations for each biological parameter are presented in **Figs s1-s2**.

Composition of communities

Metabarcoding of bacterial, archaeal, and fungal communities revealed the predominance of the same phyla, whatever the lake and the season (**Fig s3**). Bacterial communities in the three lakes were dominated by Proteobacteria (30%), *Bacteroïdetes* (15%) and unclassified bacteria (13%) (**Fig s3**). Euryarchaeota (43%), Nanoarchaeota (40%) and Crenarchaeota (11%) were the major phyla for Archaea (**Fig s3**). While the fungus community is dominated by unclassified fungi (40%), major known phyla correspond to Chytridiomycota (27%) and Basidiomycota (17%) (**Fig s3**). The mean percentage of the relative abundance of these major phyla presents important temporal variations specific to each lake. For Lake Fargettes, we can notice a peak of Proteobacteria in March and April (More than 60% of total abundance), Bacteroidetes in May (50%) and the dominance of unclassified fungi in April (98%) (**Fig s3**). In St. Gervais, Bacteroidetes (40%) increase in March, Euryarchaeota in February and April (50%), and Basidiomycota in December (90%) (**Fig s3**). For Lapeyrouse lake, Bacteroidetes increase in

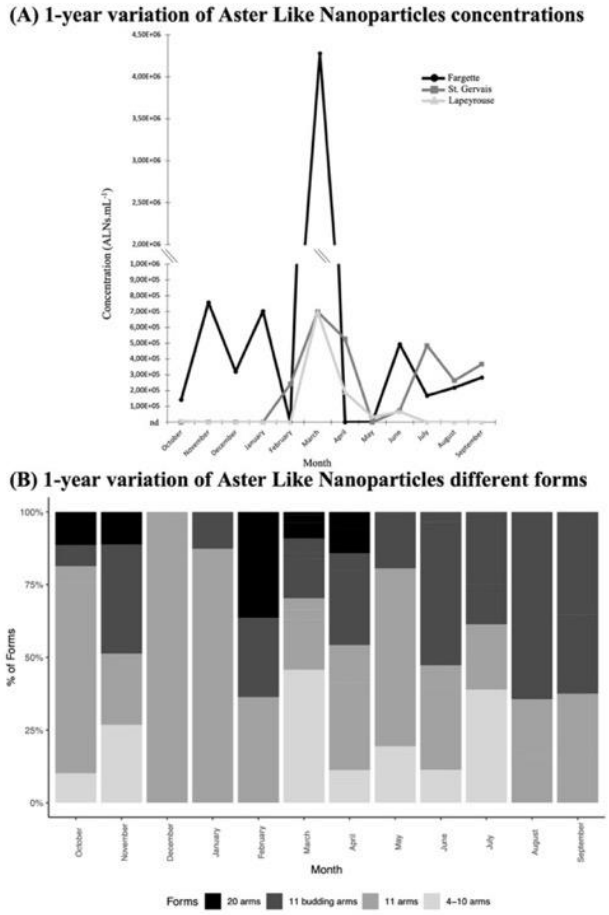

Figure 26: Dynamics of Aster Like Nanoparticles concentrations (A) and their different forms (B).
Total ALNs concentration in the 3 lakes during the 12 months of sampling (A). Dynamics of the different forms during this period (B)*. ND = No Detectable. * = data are obtained from mean of the 3 lakes

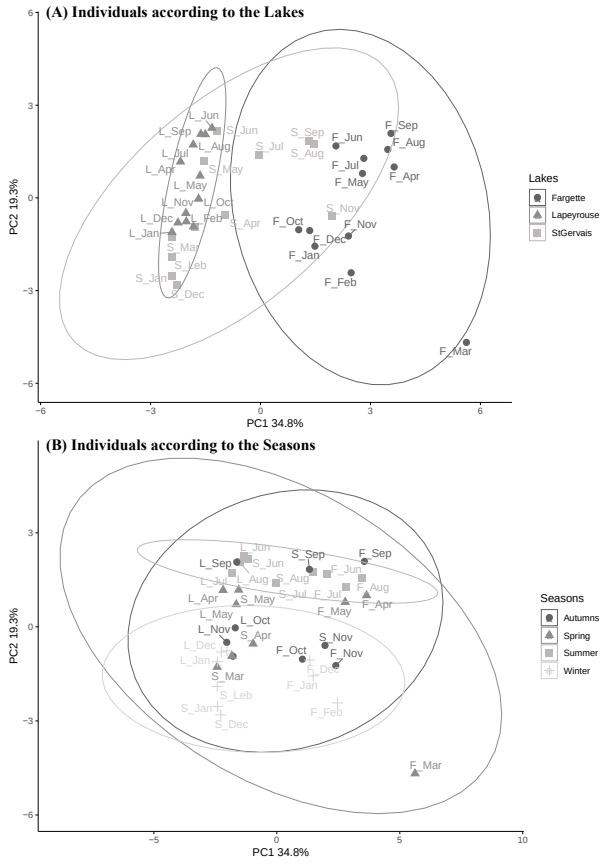

Figure 27: Principal Component Analysis of individuals (sampling points) in function of lakes (A) or seasons (B).
F: Fargettes ; S: St. Gervais ; L: Lapeyrouse ; Oct: October ; Nov: November ; Dec: December ; Jan: January ; Feb: February ; Mar: March ; Apr: April ; May: May ; Jun: June ; Jul: July ; Aug: August ; sep: September

October and May (35 and 40 % respectively) (**Fig s3**).

Aster-Like Nanoparticles distribution

As for productivity indicators (P, TOC, TN) and prokaryotes concentrations, significant differences between ALN anbundances ($p < 0.01$) were recorded between lakes (**Table 3-A**). As the above-mentioned parameters, the highest and lowest annual mean abundance of Aster Like Nanoparticles (ALNs) were recorded in lake Fargettes ($6.12 \pm 11.7 \times 10^5$ ALNs.mL^{-1}) and Lapeyrouse ($0.83 \pm 1.99 \times 10^5$ ALNs.mL^{-1}). St. Gervais had an inteχrmediate average value ($2.32 \pm 2.60 \times 10^5$ ALNs.mL^{-1}) (**Table 3-A**). ALN dynamic was significantly affected by seasons ($p < 0.01$) with remarkable spring peaks in the three lakes, recorded in March 2019 (**Table 3-B**). In these lakes, ALN abundances fluctuated from undetectable to a low range from October 2018 to February 2019 before a strong increase towards the main peaks recorded in March 2019 (from no detectable to 10^6 for Fargettes, 2.4×10^5 to 7.0×10^5 for St. Gervais and from no detectable to 10^5 ALNs.mL^{-1} for Lapeyrouse) (**Figure 26-A**), immediately followed by a decline in April in the three lakes. A second increasing phase was recorded from May until July, especially in St. Gervais.

The mean distribution combined from the three lakes of different forms (**Figure 25)** varied with time (**Figure 26-B**). The 4-10 arms forms were recorded preferentially from October (15%) to November (27%) and showed highest values from March (45%) to July (35%) during and following the spring peaks of ALNs (**Figure 26-B**). The 11 arms forms dominated the ALNs communities in October (71%), December (100%), January (87%), April (43%) and May (61%) mainly when the lowest concentrations of ALNs were recorded, whereas the 11 budding arms form dominated from June (53%) to September (63%) (**Figure 26-B**). The 20 arms were detected from October (13%) to November (13%) and had highest values from February (35%) to April (15%) concomitantly with the spring peaks of ALNs (**Figure 26-B**). During the ALN peaks of (March 2019), the contributions of the 4 different forms (4-10, 11, 11 budding and 20 arms) were at 45, 25, 21 and 9%, respectively (**Fig 26-B**). When the abundances of ALNs were particularly low, *i.e.,* in December and January (**Fig 26-A**), only the 11-arm form was represented, with absence or very low proportion of the budding form.

Table 4: Pearson correlation between Aster Like Nanoparticles and the environmental variables in the 3 lakes.

	O_2	T°c	pH	K	Mg	Na	Ca	P	TOC	TN	VLP	Prok	NPP	PPP	HE
ALN	- 0.26	0.28	0.24	0.22	-0.01	-0.21	0	0.23	0.25	0.17	0.47*	0.32*	0.31	0.26	-0.01

Prok: prokaryotes; VLP: Viral Like Particles; N.P.P:Nanophytoplankton; P.P.P: Picophytoplankton; HE:Heterotrophic Eukaryotes; T°c: Temperature; O_2 : Oxygen; T.O.C: Total organic Carbon; T.N: Total Nitrogen; Mg: Magnesium; K: Potassium; Ca: Calcium; Na: Sodium; P: Phosphorus
*Pearson test, *p ≤ 0.05*

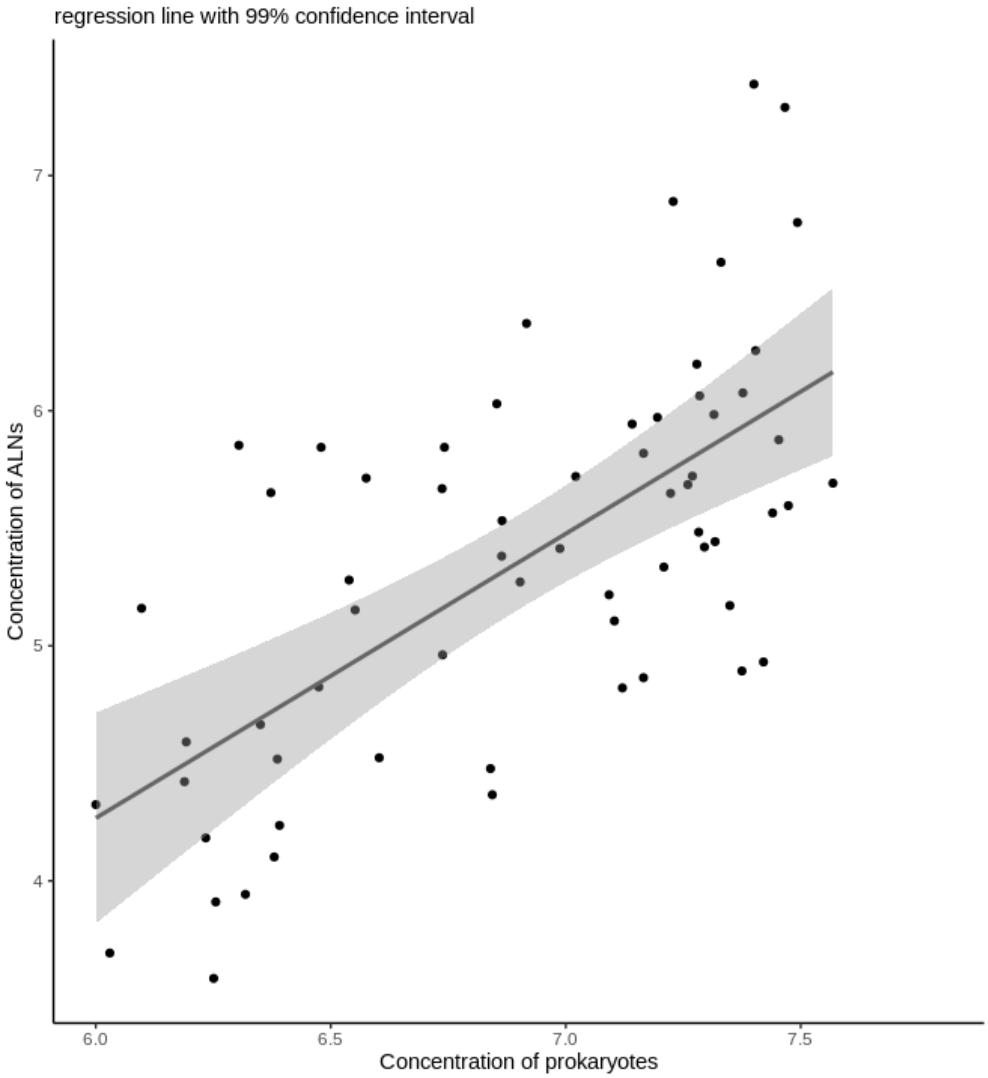

Figure 28: Linear regression between ALNs concentration and concentration of prokaryotes.
Linear regression (y = -3 + 1,2*x) was performed with data from the 3 lakes during the 12 months of sampling and data from Colombet *et al.*, [13].

All parameters and ALNs were integrated in a principal component analysis (**Figure 27**). 54.1% of the variance is explained by the first 2 axes. This analysis showed a pronounced inter-lake variability, mainly due to the biological variables. Like the patterns of ALN abundance, Fargettes Lake was clearly distinguished from Lake Lapeyrouse with St. Gervais in intermediary (**Figure 27-A**). The summer/winter seasonal discrimination with spring and autumn in between is classic for temperate zone lake systems (**Figure 27-B**). The remarkable point of Fargettes in March stands out clearly from this analysis which coincides with the bloom of ALNs.

Interaction between Aster-like Nanoparticles and their environment

There was no significant correlation between ALNs and any of the measured physico-chemical parameters (**Table 4**). In contrast, significant correlations ($p \leq 0.05$) were recorded between ALNs and their biotic environment, primarily with VLPs ($r^2 = 0.47$) and prokaryotes ($r^2 = 0.32$) (**Table 4**)

Linear regression of data including data obtained from a former study in lake Fargettes (Colombet *et al*.,[27]), revealed a significant relation between ALNs and prokaryotes (**Figure 28**). The regression line linking number of ALNs as a function of number of prokaryotes appears highly significant (ALN concentration = -3 + 1.2 x prokaryotes concentration, $R^2 = 0.43$, $\omega^2 = 0.43$, one way ANOVA (*$F(1,62) = 49.14, p < 0.001$*)) (**Figure 28**). As revealed by $\omega^2 = 0.43$, one of the two parameters can explain 43 % of the distribution of the other (**Figure 28**).

No significant correlations were observed between ALNs and archaeal OTUs during the sampling period in the three lakes (**Table 5**). On the other hand, ALNs were significantly correlated (*$p < 0.01$*) with 5 bacterial phyla (Acidobacteria, Cyanobacteria, Firmicutes, Planctomycetes.

Table 5: Significant Spearman correlation coefficients between the presence of ALNs and the presence of microbial OTUs.

Kingdom	Phylum	Lake	R^2
Bacteria	Acidobacteria	St. Gervais	0.85
	Cyanobacteria	St. Gervais	0.71
		Lapeyrouse	0.71
	Firmicutes	Fargettes	0.82
	Planctomycetes	Fargettes	0.77
	Proteobacteria	Fargettes_1	0.77
		Fargettes _2	1
		St. Gervais	0.84
Fungi	Ascomycota	Fargettes_1	0.77
		Fargettes _2	0.77
		St. Gervais _1	0.85
		St. Gervais_2	0.85
	Chytridiomycota	Lapeyrouse	0.84

Positive correlation analyses (Spearman's test, $p < 0.01$) between the presence of different OTUs (and their affiliations) and the presence of ALNs.
_(x) = different OTU

4.5 Discussion

Here we report the seasonal fluctuations of Aster Like Nanoparticles (ALNs) concentrations in 3 different lakes. These entities were first described in 2019 [27] and colonize different continental and coastal environments, reaching important concentrations in the order of 10^7 ALNs.mL^{-1} [197]. We recently demonstrated that their distribution could be influenced by the trophic state of the environment [197]. These pioneering works result in a partial understanding of the ecology of ALNs. Information on their spatial and seasonal dynamics in relation to their environment are crucial and could allow us to (i) reveal their environmental forcing factors, (ii) understand their contribution to the flow of matter and energy and (iii) perhaps open a window on their exact nature. The seasonal variations of ALN abundances were similar in the three lakes which were in a restricted geographical area (French Massif Central) and were apparently driven more by differences in biological parameters. This is in agreement with our previous study [197] were ALNs increased in environments with high microbial density and nutrients content, such as Lake Fargettes. The study of the temporal dynamics of ALNs revealed a marked seasonality. The seasonal patterns of ALNs in the three lakes was relatively similar, with characteristic peaks in spring. The ALNs communities exhibited a rapid growth capacity with a high amplitude of abundance variations (from undetectable to 4.28 ± 0.74 x 10^6 ALNs.mL^{-1} between two consecutive time point in lake Fargettes for example). ALNs are therefore a rapid mobilization and sequestration factor of their constituent elements. Colombet and colleagues [27] showed that Ca is a preponderant constitutive element of ALNs. It is therefore very likely that ALNs have a key role in the aquatic Ca cycle. Considering the biomass dynamics of ALNs can therefore be fundamental in understanding the flow of elements through aquatic ecosystems, as has been demonstrated for viruses for example [303].

Seasonal variations in the form of bloom are a recurring pattern in aquatic microbial and viral communities [110, 279, 303, 313]. All the models showing this kind of dynamics (free or symbiotic), have a prominent role in the functioning of the ecosystem. It is therefore undoubtedly that ALNs are intrinsic actors in the ecology of aquatic systems. However, the understanding of their ecology is intimately linked to the understanding of their control factors. Different factors can explain temporal variations of microbial entities, including geographic and environmental factors [314], abiotic and biotic factors, bottom-up and top-down factors [315], or the presence/absence of hosts for the life cycle such as for viruses [316]. The case of

lake Saint Gervais, which was emptied for several weeks, makes it possible to specify here that

the ALNs are aboriginal to the lake. Indeed, during the drying phase and until the peak of ALNs, we carried out regular sampling in the tributaries feeding the lake without ever detecting the presence of ALNs. The controlling factors of ALNs are thus intrinsic to the lake. No abiotic factors seem to have an impact on the variations of ALNs abundance in lake ecosystems.

It's interesting to note that with equal temperature between spring and fall, we recorded a significant development of ALNs in spring. The development of ALNs could therefore be more associated with the seasonal succession of biological communities forced by the interaction of physico-chemical environmental variables rather than with a single physico-chemical variable. Among biotic factors measured, correlations with prokaryotes and VLPs were identified. We further explored these putative links to the microbial environment by integrating data previously acquired in Fargettes Lake [27]. The linear regression model used allows us to highlight a strong link between ALNs and prokaryotes. The ω2 allowed us to estimate that 47 % of the variation in number of ALNs could be explained by the prokaryotes. These results support the observations described in Colombet *et al.,* [27] where one can clearly distinguish a close physical interaction between ALNs and prokaryotes. These data raise the hypothesis that ALNs could have strong interactions with prokaryotes. One of the particularities of ALNs is their pleomorphism. Each form (see description in Colombet *et al*., [27]) has a particular seasonal dynamic (**Fig 26-B**). In the hypothesis that they are dependent on each other within a developmental cycle, it is likely that a partner, possibly prokaryotic, may intervene at certain stages and regulate the dynamics of the different forms. 11-arms forms could be a resistant form.

To identify more precisely which microbial communities may be involved in these interactions with ALNs, we analyzed the covariation of the presence of ALNs with those of the different bacterial, archaeal, and fungal phyla identified in the three lakes. ALNs appeared strongly positively correlated ($r^2 > 0,7, p < 0.05$) with some fungal (Ascomycota and Chytridiomycota) and bacterial (Acidobacteria, Cyanobacteria, Firmicutes, Planctomycetes, Proteobacteria) OTUs in lakes. Ascomycota is the most common fungal phylum in aquatic environments [317] and Chytridiomycota is a phylum with a huge implication in the regulation of aquatic organisms, especially influencing directly or indirectly the microbial loop [318, 319]. Although we cannot rule out a direct relationship, it is more likely that fungi interact indirectly with ALNs via a third-party microbe. The positive correlations between ALNs and prokaryotes seem to

target a large heterogeneity of bacterial phyla. Acidobacteria, Cyanobacteria, Firmicutes,

Planctomycetes, and Proteobacteria represent most lake bacteria [320]. Thus, although we cannot formally infer a direct relationship, these data suggest that the spectrum of possible prokaryotic partners for ALNs may be broad and non-specific.

The data acquired here allow a better understanding of the ecology of ALNs, namely, a pronounced seasonal dynamic in the form of spring "bloom" that can be controlled by the microbial and probably prokaryotic environment. The hypothesis that ALNs have strong interactions with prokaryotes is emerging but will have to be verified in the future as well as the possibility of a development cycle linking the different morphotypes. The functionality of ALNs is certain for the transfer of their constitutive elements within the microbial network but their role on other microbial components (neutrality, mutualism, parasitism...) remains to be determined. Through their dynamics, ALNs are undoubtedly new actors to consider in the functioning of aquatic ecosystems. More generally, our data highlight the seasonal importance of overlooked femtoplankton in aquatic ecosystems and their potential roles in the ecosystem functioning.

Author's contribution
MF, HB and JC designed and performed the experiments. MF and GB analyze genomic datas. MF, HB, GB, TSN and JC wrote the manuscript. All authors have read, commented, and approved the final version of the manuscript.

Funding Information
MF was supported by a PhD fellowship from the CPER 2015-2020 SYMBIOSE challenge program (French Ministry of Research, UCA, CNRS, INRA, Auvergne-Rhône-Alpes Region, FEDER). This study is a contribution to the "C NO LIMIT" project funded by the Interdisciplinary Mission of the French National Center of Scientific Research (CNRS) Program X-life, 2018 edition. This study is a contribution to the "NANOPOULPE" project funded by the Interdisciplinary Mission of the French National Center of Scientific Research (CNRS) Program Origines, 2020. This research was also financed by the French government IDEX-ISITE initiative 16-IDEX-0001 (CAP 20-25).

Acknowledgments
This study benefited from equipment and technical assistance of CYSTEM platform UCA-PARTNER (University of Clermont Auvergne UCA), Clermont-Ferrand, France) and the Laboratoire Microorganismes: Genome et Environment (LMGE, UMR6023 CNRS-UCA, Clermont-Ferrand, France). The authors thanks Thomas Ruiz (LMGE) for helpful comments and discussions on the manuscript.

Conflicts of interest:
The authors declare that they have no conflict of interest.

4.6 Supplemental materials

Table S1: Primers used for the amplification and their PCR programs.

	Bacteria	Archae	Fungi
Forward primer	515f- GTGYCAGCMGCCGCGGTA	519f- CAGCMGCCGCGGTAA	its7f- GTGARTCATCGAATCTTTG
Reverse Primer	928r- CCCCGYCAATTCMTTTRAGT	1017r- GGCCATGCACCWCCTCTC	its4r- TCCTCCGCTTATTGATATGC
Program	95°c 3mn ------x32------ 98°c 20s 65°c 40s 72°c 30s ---------- 72°c. 10mn	95°c 3mn ------x32------ 98°c 20s 68°c 30s 72°c 30s ---------- 72°c. 5mn	95°c 3mn ------x32------ 98°c 20s 57°c 30s 72°c 30s ---------- 72°c. 5mn

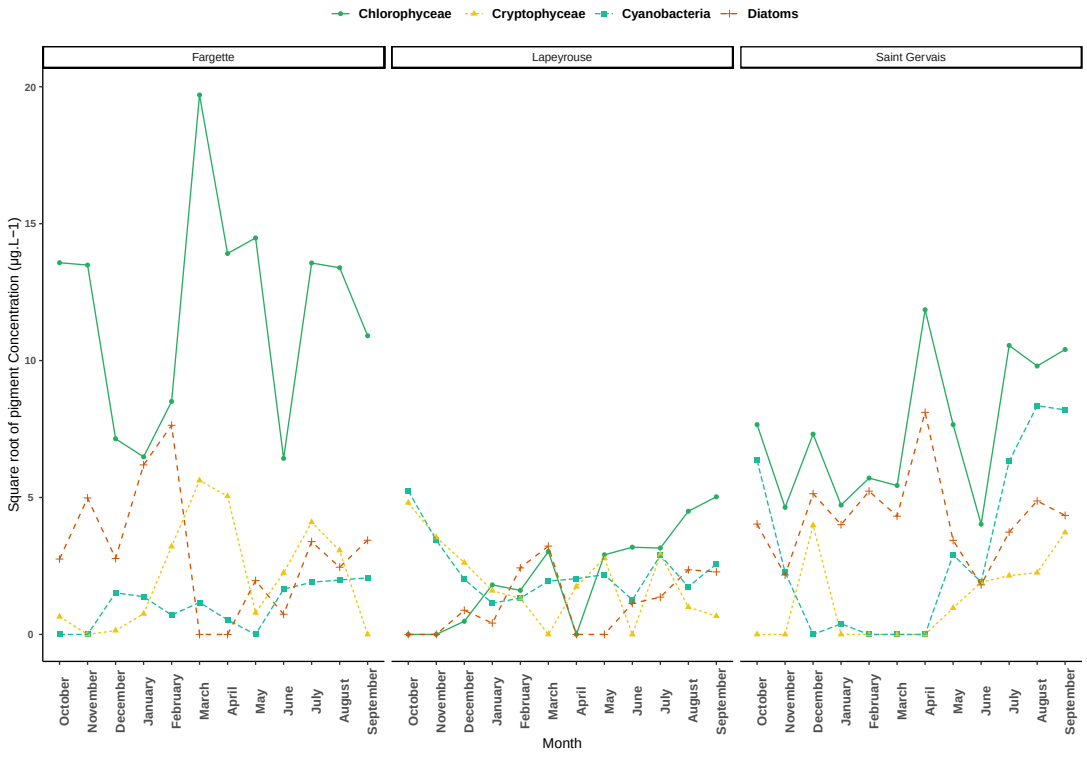

Figure S1. Variation of prokaryotic (A), Viral Like Particles (B), heterotrophic eukaryotes (C), nanophytoplanktonic (D) and picophytoplanctonic (E) concentrations over the 12-months sampling period.

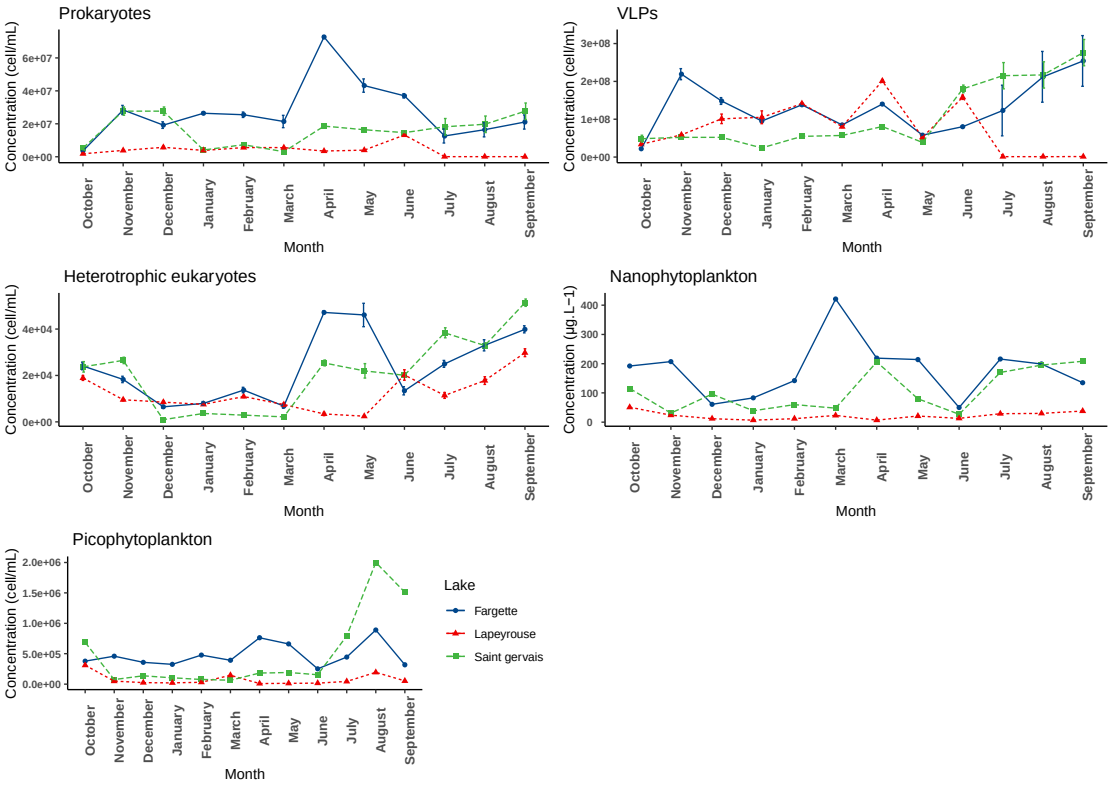

Figure S2. Variation of different groups of nanophytoplanktonic communities (Chlorophyceae, Cryptophyceae, Cyanobacteria and Diatoms) in our 3 lakes over the 12-months sampling period.

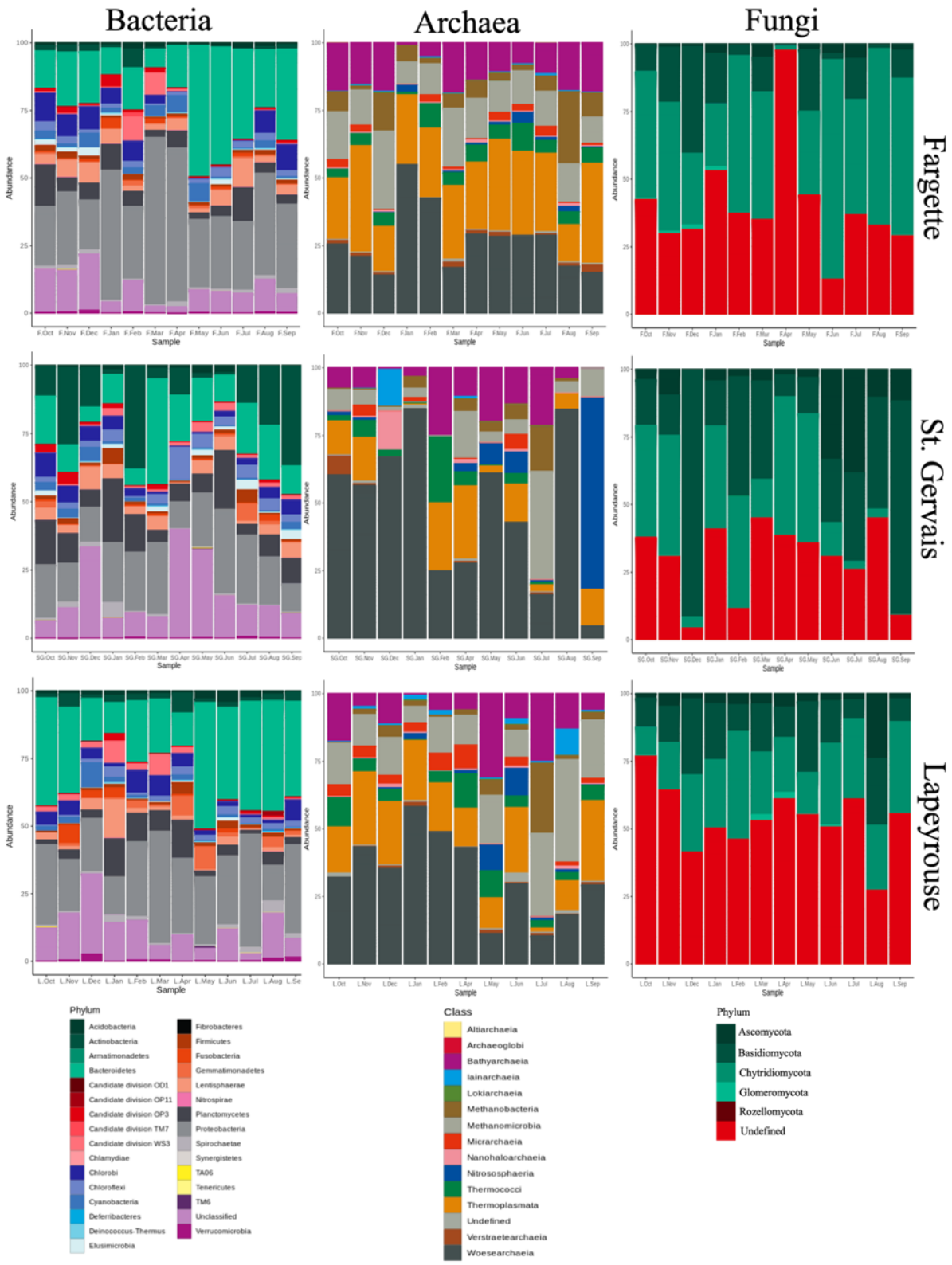

Figure S3. Variation of the different bacterial, archaeal and fungal phyla in the 3 lakes during the 12-months of sampling period.

4.7 Conclusions

Les travaux associés à cette étude ont mis en évidence l'existence d'un pattern de développement basé sur une dynamique saisonnière des ALNs marquée dans les systèmes étudiés. Cette dynamique se manifeste par l'apparition de « blooms » printaniers, avec une grande amplitude de variation de concentrations (*i.e.* de non détectable à 4.28 x 10^6 ALNs.mL^{-1} pour la saison 2018-2019).

Leur dynamique spatiale ainsi que temporelle en font donc un acteur qui pourrait avoir un impact sur le fonctionnement des écosystèmes aquatiques, notamment sur la mobilisation des éléments consitutifs majoritaires (*i.e.* C, O, Ca). Ces résultats viennent appuyer les hypothèses formulées précédemment quant aux conditions biologiques semblant prévaloir sur les paramètres physico-chimiques pour expliquer la présence et la quantité des ALNs. L'intégration des différentes communautés microbiennes a permis de mettre en évidence l'importance des successions écologiques saisonnières dans le développement des ALNs. Un lien plus particulier avec les procaryotes a pu être mis en évidence, sans montrer de lien direct avec un phylum spécifique.

Ces résultats ouvrent de nouvelles perspectives d'étude, notamment sur la nature des interactions potentielles entre les ALNs, leurs différentes formes et les procaryotes. Des expériences *ex-situ* en microcosmes pourraient confirmer ces liens et permettraient de mieux appréhender la nature de ces interactions.

CHAPITRE 3 : INTERACTIONS ENTRE ALNs ET PROCARYOTES EN CONDITIONS CONTROLÉES

Les études précédentes de ce manuscrit ont permis de mieux appréhender la dynamique des ALNs dans les écosystèmes naturels. En effet, nous avons mis en évidence que leur présence dans un large spectre d'habitats ou que leur dynamique saisonnière, marquée par de fortes variations d'abondances, serait étroitement liée à celle des procaryotes.

Les procaryotes qui comprennent les bactéries et les archées, sont des acteurs essentiels des réseaux trophiques aquatiques. Retrouvés également dans la littérature sous le terme de bactérioplancton, ces derniers interviennent dans différents processus cruciaux des écosystèmes :

- Les bactéries autotrophes (*i.e.* cyanobactéries) jouent un rôle dans la production primaire [300, 321].
- Les bactéries hétérotrophes sont impliquées dans la circulation de la matière minérale et organique dans les milieux aquatiques, notamment comme décomposeurs ou comme proies pour le zooplancton [9].
- Les archées, qui peuvent représenter jusqu'à 30% des procaryotes dans les zones euphotiques des écosystèmes lacustres [322], sont elles aussi impliquées dans différents processus biogéochimiques [323].

Les études écosystèmiques (c'est-à-dire à l'échelle des communautés naturelles) ayant suggéré des interactions potentielles entre les ALNs et les procaryotes, il nous a paru nécessaire d'aborder l'étude de ces interactions d'un point de vue expérimental, afin de mieux comprendre leur importance pour les communautés de procaryotes (*e.g.* impact sur la concentration, la diversité, le métabolisme…). Une partie des résultat de ce chapitre a fait l'objet d'une publication parue.

5.1 Interactions between concentration of prokaryotes and concentration of ALNs in *in-vitro* conditions

Maxime Fuster[1], Hermine Billard[1],Télesphore Sime-Ngando[1], Jonathan Colombet[1]

[1] Université Clermont Auvergne, CNRS, LMGE, Clermont-Ferrand F-63000, France

In preparation.

5.1.1 Introduction

In the past years, the discovery of extracellular vesicles, CPR (Candidate Phylum Radia) bacteria, DPANN (*Diapherotrites, Parvarchaeota, Aenigmarchaeota, Nanoarchaeota, Nanohaloarchaea*), a,d biomimetic mineralo-organic particles, have highlighted the necessity of deepen our knowledge on femtoplanktonic compartment, considered for years to be composed only of viruses and few prokaryotic entities < 0.2 µm [16]. The discovery of the above entities has thus led to a reconsideration of the ecological importance of this compartment in the functioning of aquatic systems.

Moreover, the recent discovery of ALNs, *i.e.* the last of the discovered femtoplankton entities [27], reinforces the hypothesis that femtoplankton remains today a reservoir of unknown entities with potential roles in aquatic ecosystems. ALNs are entities with a characteristic aster-shaped morphology. They are composed mainly of C, O, Ca, and present distinct morphotypes based on the number of arms of the entity (4, 11, 20). These original characteristics, combined with their organic nature as well as their reduced bio-volume and their sensitivity to biocide treatments, raise many questions about their nature and origin. The few data accumulated on the ecology of these new particles have shown that they are distributed worldwide [27, 197] and closely associated with eutrophic environments [197]. Biological parameters seem to be the main forcing factor of their dynamics [324]. Correlative data obtained from these environmental studies have led to the hypothesis that prokaryotes may be a potential interactor involved in the regulation of their development. However, this speculation is purely empirical and needs to be verified and specified under controlled conditions.

In this work, we performed the first monitoring of ALNs under controlled prokaryotic conditions to evaluate the possible interactions between them. The results obtained indicate that

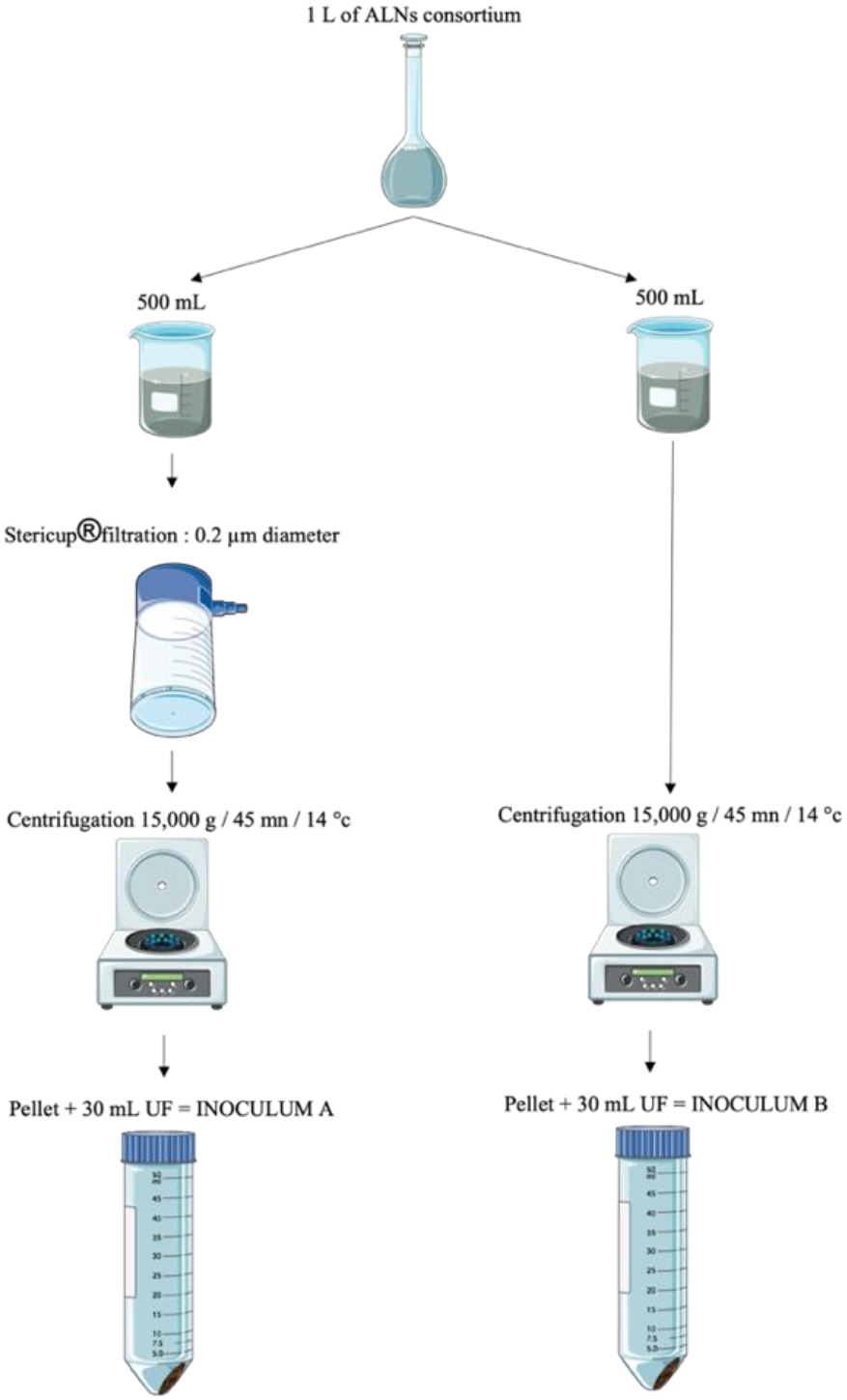

Figure 29: Experimental design for the preparation of inocula.

the development of ALNs could be, at least partly, controlled by the development of a prokaryotic interactant. Our results support the hypotheses formulated in natural environmental studies, as for an interaction between ALNs and prokaryotic communities, that is stronger in nutrient-rich environments.

5.1.2 Materials and methods

Preparation of inocula

Consortia of different morphotypes of ALNs and prokaryotes derived from Lake Fargettes (a hyper eutrophic lake located in the French Massif Central; 45°44'24"N; 3°27'39"E; 465 m altitude; surface area 1.2 ha; maximum depth 2.5 m) were used for incubations. These *consortia* (ALNs length between 40 and 450nm) were selected, enriched and cultivated for a long-term (> 2 years at 4°C in dark condition) through tangential-flow ultrafiltration and differential centrifugation as described in Colombet *et al.* [27].

ALNs contained in a 500 mL consortium aliquot that was filtered on 0.2 µm at low pressure (< 25 kPa) to remove prokaryotes (stericup, Millipore), were pelleted at 15,000 g for 45 min at 14°C and re-suspended in 30 mL of ultra-filtrate medium (UF – see supplementals for the preparation of the medium) leading to an inoculum A (*i.e.* containing ALNs and VLPs). (**Figure 29**). Other 500 mL aliquot, namely inoculum B (*i.e.* containing ALNs, VLPs and prokaryotes), were directly concentrated and resuspended in the same way without prior filtration (**Figure 29**).

Incubation and growth monitoring

Incubations

0.5 mL of each inoculum was amended with 19.5 mL of 4 different culture medium (with an increasing degree of nutrient enrichment, respectively UF, Minimum Medium (MM), Synura and BG-11 (see composition in **supplemental Table S1**)) in 50 mL sterile culture flask (Falcon® tissue culture flask) and incubated in triplicate at 6°C or 12°C in the dark.

3 different sampling points were realized (T0 / T1 = 7 months incubation / T2 = 13 months incubation). Each experimental sample (1.5 mL) was then immediately fixed with 2% final

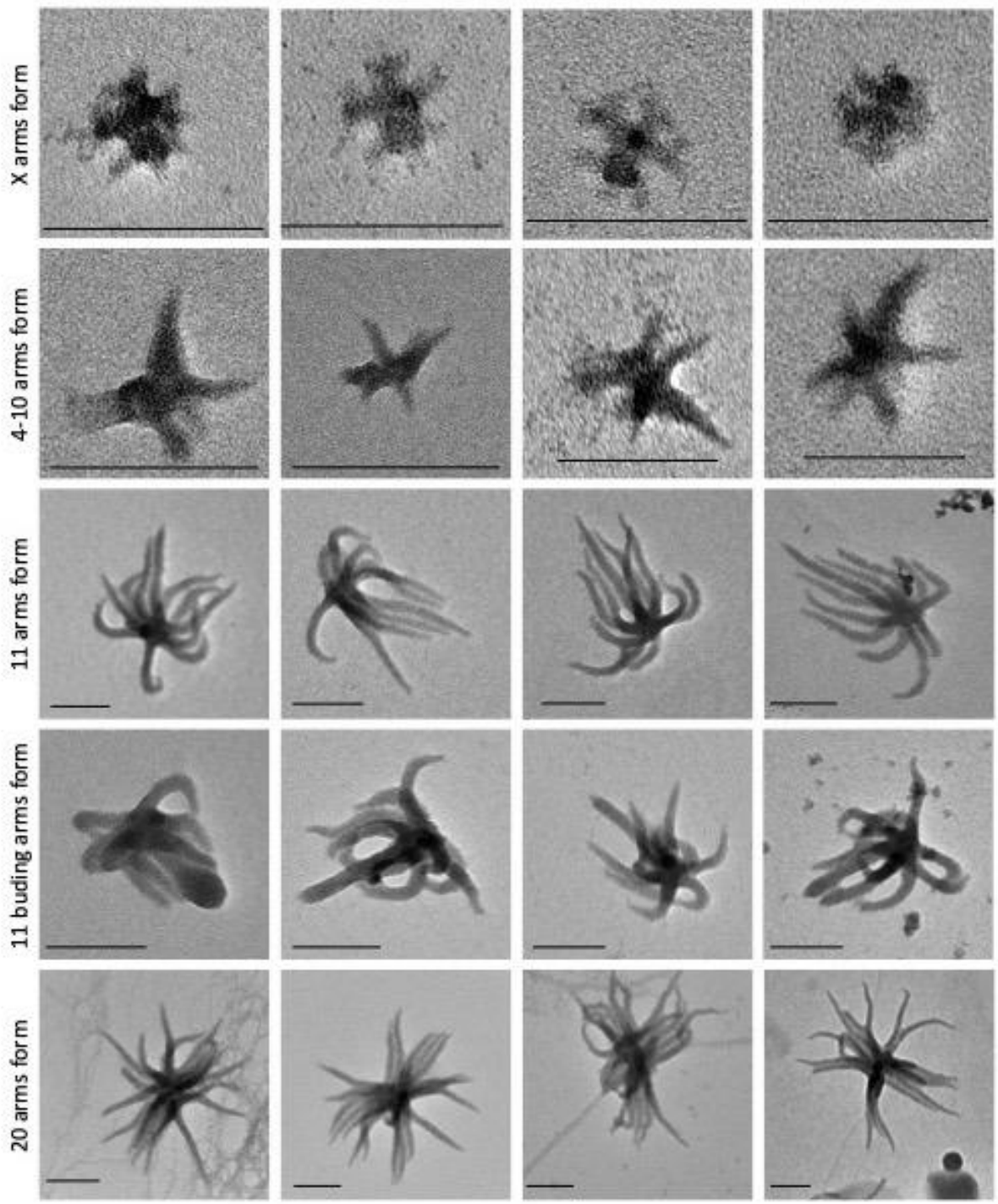

Figure 30: Transmission electron micrographs of different morphotypes of aster-like nanoparticles (ALNs).
Scale bars = 100 nm. *Crédits photos: J.colombet – plateform CYSTEM*

concentration of formaldehyde. Before each sampling, the volumetric loss due to evaporation during the incubation period was compensated by adding an equivalent volume of medium.

ALNs, prokaryotes and VLPs counts

ALNs detection and quantification were realized by transmission electron microscopy (TEM) using a Jeol JEM 2100-Plus microscope (JEOL, Akishima, Tokyo, Japan) operating at 80 kV and x50,000 magnification as described in Colombet *et al. [27]*. 5 different shapes were detected and counted. The 4 shapes described in Colombet *et al*. [27] (4-10 arms, 11 arms, 11 budding arms and 20 arms) and a new shape called X-shape (**Figure 30**).

Counts of ALNs were converted into ALNs per milliliter using a conversion factor deduced from control grids prepared with pre-determined concentrations of bacteria. Volume of the ALN particles was computed by considering the radial arms as cylinders and the central core as a sphere [27]. Counts of prokaryotes and Virus Like Particles were performed in triplicates by flow cytometry according to Brussaard [256] using a BD FACSAria Fusion SORP (BD Sciences, San Jose, CA) equipped with an air-cooled laser, delivering 50 mW at 488 nm with 502 longpass, and 530/30 bandpass filter set-up.

Diversity of bacterial communities

Nucleic acid extractions and amplifications

At the end of incubations, for each condition with the inoculum containing prokaryotes (*i.e.* inoculum B), triplicates were pooled, and bacterial microbial communities were collected on a 0.2 µm (Millipore) polycarbonate filter (until saturation, pressure < 25 kPa) and stored at -20°C until DNA extraction. The filters were covered with a lysing buffer (lysozyme 2 $mg.mL^{-1}$, SDS 0.5%, Proteinase K 100 $\mu g.\ mL^{-1}$ and RNase A 8.33 $\mu g.\ mL^{-1}$ in TE buffer pH 8) at 37°C for 90 minutes. A CTAB 10% / NaCl 5M solution was added, and the samples were incubated at 65°C for 30 minutes. The nucleic acids were extracted with phenol-chloroform-isoamyl alcohol (25:24:1) ; the aqueous phase containing the nucleic acids was recovered and purified by adding chloroform-isoamyl alcohol (24:1). The nucleic acids were then precipitated with a mixture of glycogen $5mg.mL^{-1}$, sodium acetate 3M and ethanol 100% overnight at -20°C. The DNA pellet was rinsed with ethanol (70%), dried and dissolved in the TE buffer. DNA was then purified using a commercial kit (NucleoSpin® gDNA Clean-up, Macherey-Nagel). The V4-V5 region of the bacterial small subunit rDNA was amplified using the universal bacteria 515F and 928R

primers [306] (**Table S2**). PCR was performed in a total volume of 50µL containing 1x final reaction buffer, 2 mM $MgCl_2$, 0.2mM dNTP, 100 µg.mL^{-1} BSA, 0.2 µM of each primer, 0.025 U.µL^{-1} PROMEGA GoTaq HotsStart G2 and 5 µL of DNA. PCR programs is detailed in the supplemental (**Table S2**).

Amplicon analysis and taxonomic affiliation

Bacterial sequencing data were processed with the PANAM2 pipeline [308]. Briefly, sequence reads were assembled with Vsearch [309], excluding reads < 200pb, with ambiguous bases (N) or having mismatch in the forward/reverse primer. Demultiplexed amplicons were clustered into OTUs using Vsearch at a 95% id threshold. Representative sequence of OTUs were compared against the SILVA SSURef 115 database restricted to sequences with length > 1,200 pb, quality score > 75% and a pintail value > 50.

Data Analysis

The differences in ALNs concentrations depending on the culture media and the inocula were tested with the Kruskal-Wallis test. Concentration variations within the same condition were tested with Dunn test. The evolution of prokaryotic concentrations within the same condition were tested by a Wilcoxon test. The changes in the different ALNs forms in culture media were tested using a Chi 2 test.

5.1.3 Results

Starting conditions of growing media

At the starting incubation time (T0), no significant effect of inoculum ($p > 0.05$) or medium ($p > 0.05$) were observed on ALNs concentration (mean ALNs in inoculum A = 2.3 x 10^4 mL^{-1}, inoculum B = 2.6 x 10^4 mL^{-1}). The proportions of the different forms of ALNs were distributed in a similar way whatever the culture medium or the starting inoculum (mean 70% of 4-10 arms, 15% of 11 arms, 10% of 11 budding arms and 5% of 20 arms). Conversely, we observed a statistical difference between prokaryotes concentration ($p < 0.01$) in inoculum A (mean = 3.6E+03) and inoculum B (mean = 5.7E+04). Inocula A and B were characterized by ratio of ALNs / Prokaryotes / VLPs of 10/2/1 and 10/16/2 respectively.

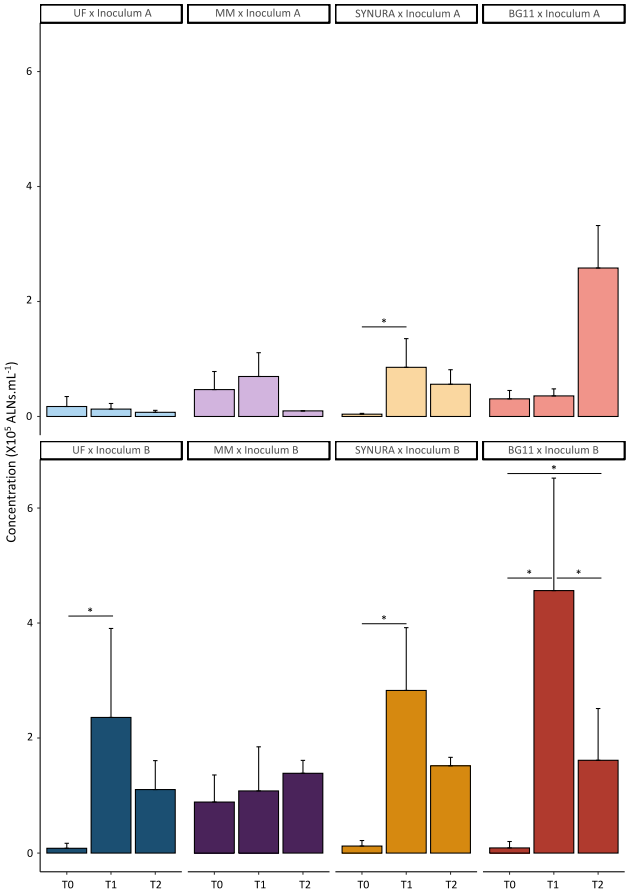

Figure 31: Monitoring of the concentration of ALNs over time, function of medium culture and inoculum.

* indicate significant temporal difference between ALN concentration in a same condition (Dunn test, $p < .05$).

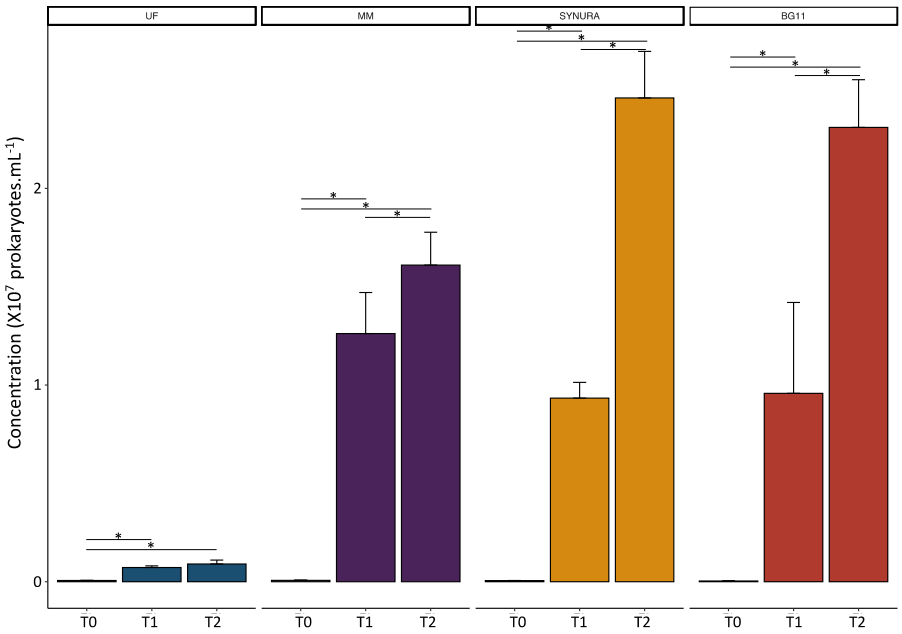

Figure 32: Monitoring of the concentration of prokaryotes (A) in inoculum B over time, function medium culture.

* indicate significant temporal differences between prokaryotes concentration in a same condition (Wilcoxon test, $p < .05$).

Dynamic of Aster-Like Nanoparticles, prokaryotes and VLPs-Bacteria Ratio in the different experimental conditions

The temporal dynamic of Aster Like Nanoparticles and prokaryotes corresponding to the different culture inocula and media are presented in **Figure 31** and **Figure 32** respectively.
We recorded statistically significant effects of the inoculum (Kruskal-Wallis, $\chi^2(2) = 15.8$, $p < .001$, n = 96) and a significant effect of the culture medium (Kruskal-Wallis, $\chi^2(2) = 28.9$, $p < .001$, n = 96) on the increase in the concentration of ALNs (**Figure 31**).

The number of ALNs in culture media supplemented with inoculum A was statistically stable over time ($p > 0.05$), except in Synura medium at T1 in which we can record a 20x augmentation, from 4.03 x 10^3 ALNs.mL^{-1} to 8.55 x 10^4 ALNs.mL^{-1} ($p < 0.05$) (**Figure 31**). Conversely, we observed significant increase in the concentration of ALNs over time in all the media with ALNs and prokaryotes (inoculum B) ($p < 0.05$), except in the minimum medium (**Figure 31)**. The maximum rise of concentration was observed in BG11 medium and inoculum B with a multiplication factor between T1/T0 = 51 from 8.92 x 10^3 ALNs.mL^{-1} to 4.56 x 10^5 ALNs.mL^{-1}. Multiplication factor between T0 and T1 in UF and synura media are respectively equal to 29 (from 8.26 x 10^3 ALNs.mL^{-1} to 2.36 x 10^5 ALNs.mL^{-1}) and 23 (from 1.21E x 10^4 ALNs.mL^{-1} to 2.8 x 10^5 ALNs.mL^{-1} ALNs.mL^{-1}) .

The variation of the prokaryote concentration obviously depended on the starting inoculum, whether filtered or not (**Figure 32**). The concentration of prokaryotes in inoculum A remained below 9.56 x 10^4 cell.mL^{-1} (low level of concentration, at detection limits). On the opposite, the prokaryotic concentration in inoculum B increased significantly throughout the incubation period (**Figure 32**), to reach a maximum of 2.71 x 10^7 cell.mL^{-1}. In the BG11 (highly nutrient enriched medium) at T2, we noticed a high difference in prokaryote abundances between the inoculum A and B, respectively at 7.29 x 10^3 cells.mL^{-1} and 2.31 x 10^7 cells.mL^{-1}.

The VBR, used as a proxy for viral infection, remained below 0.5 under conditions where the development of prokaryotes was observed. This demonstrates the tiny influence of VLPs on the growth of prokaryotes.

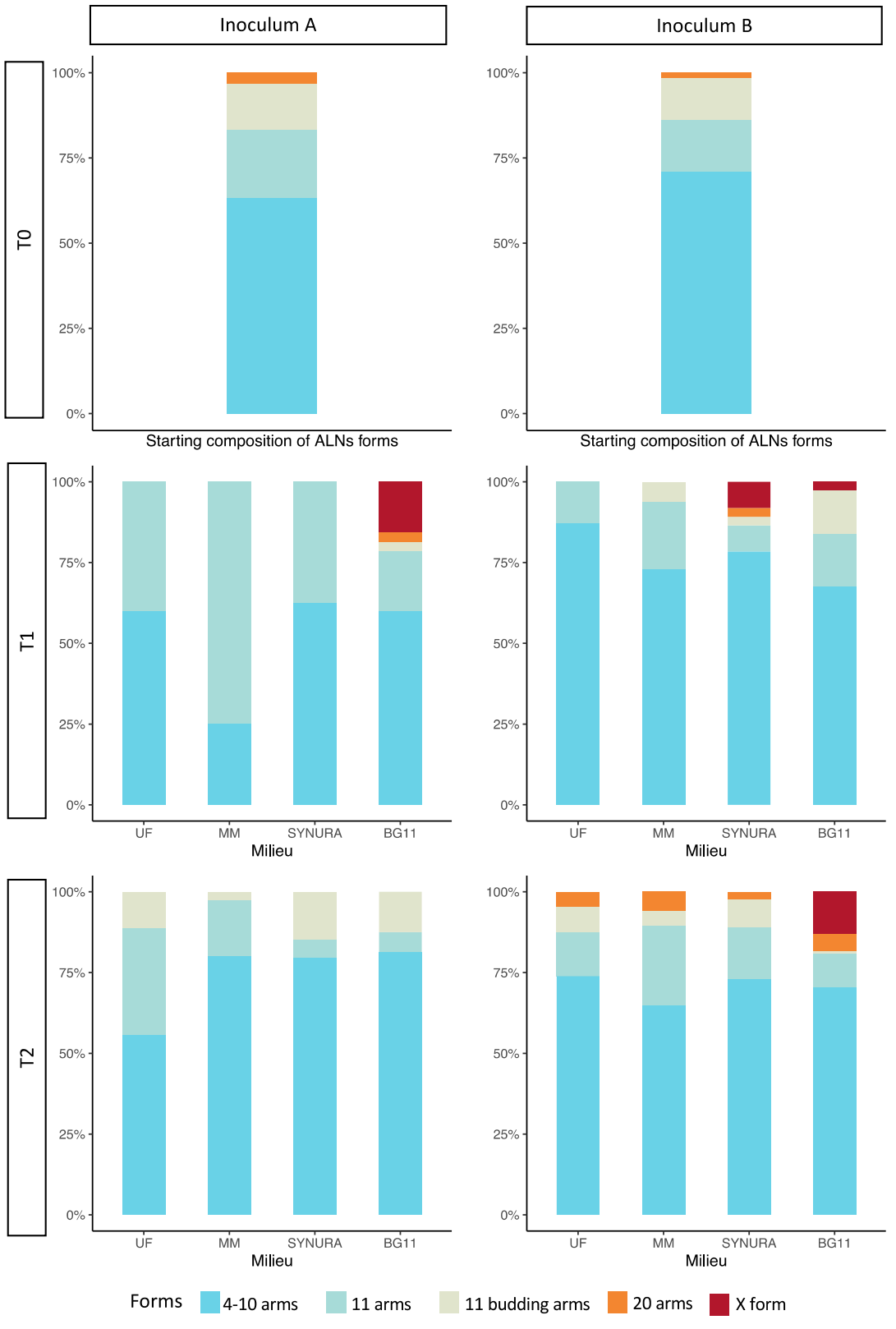

Figure 33: Dynamic of ALNs different forms function of culture medium.
This dynamic was followed through time by differentiating the 2 starting inocula. UF=Ultra Filtrate. MM= Minimal Medium.

Variation of different ALNs morphotypes over time

The dynamics of different ALNs morphotypes in each monitored condition are shown in **Figure 33**. We report, for the first time, the appearance of an undescribed form of ALNs. This one presents a X-shape with 4 main arms symmetrically distributed from the central core. The mean diameter of this form is 47.6 ± 9 µm for an average volume of 1.12E-04 μm^3 which is inferior in diameter to the smallest form of ALNs (110 ± 18 µm) reported until now (**Figure 30).**

A significant change in the distribution of forms according to the inoculum was observed at T2=1 ($\chi^2 = 15$, df = 4, $p < .01$) and T3 ($\chi^2 = 11$, df = 4, $p < .05$) (**Figure 33**). We also observed a significant effect of the culture medium, whatever the inoculum or incubation time ($\chi^2 = 53$, df = 12, $p < .01$) (**Figure 33**).

We recorded changes in the communities of ALNs at T1. The forms 11 budding and 20 arms disappeared in the media incubated with inoculum A, except for the highly enriched BG11. In this, we noticed the remarkable appearance of new forms X-shape (60% 4-10 arms, 19% 11 arms, 3% of 11 budding and 20 arms, 15% of the X form) (**Figure 33**). Forms at T1 in the inoculum B was significantly different. 11 budding and 20 arms forms disappeared only in UF medium (87% 4-10 arms, 13% 11 arms) (**Figure 33**). We recorded a development of new x-shape form in the synura (8%) and BG11 (2%) media.

At T2, the 20-arm and X forms were no longer detected in inoculum A (**Figure 33**). In contrast to T1, we detected the presence of 11 budding arms form in UF, MM, synura and BG11 (respectively 8, 4, 9 and 1%) (**Figure 33**). With inoculum B at T2, and contrary to T1, the 4 initially described forms of ALNs (4-10 arms, 11 arms, 11 budding arms and 20 arms) were present in all culture media. The X-form remained detectable only in the BG11 medium (14%) (**Figure 33**).

For inoculum A, a significant diminution of the volume of ALNs was observed between T0 (mean = 1.4 x 10^{-4} μm^3) and T2 (mean = 0.82 x 10^{-4} μm^3) ($p < 0.05$). For inoculum B, although no significant differences ($p > 0.05$) were observed, the mean volume of ALNs in T0 (mean = 0.87 x 10^{-4} μm^3) was inferior to that recorded in T2 (mean = 1.1 x 10^{-4} μm^3). No significant differences were observed between inoculum A and inoculum B at T0 and T2 ($p > 0.05$).

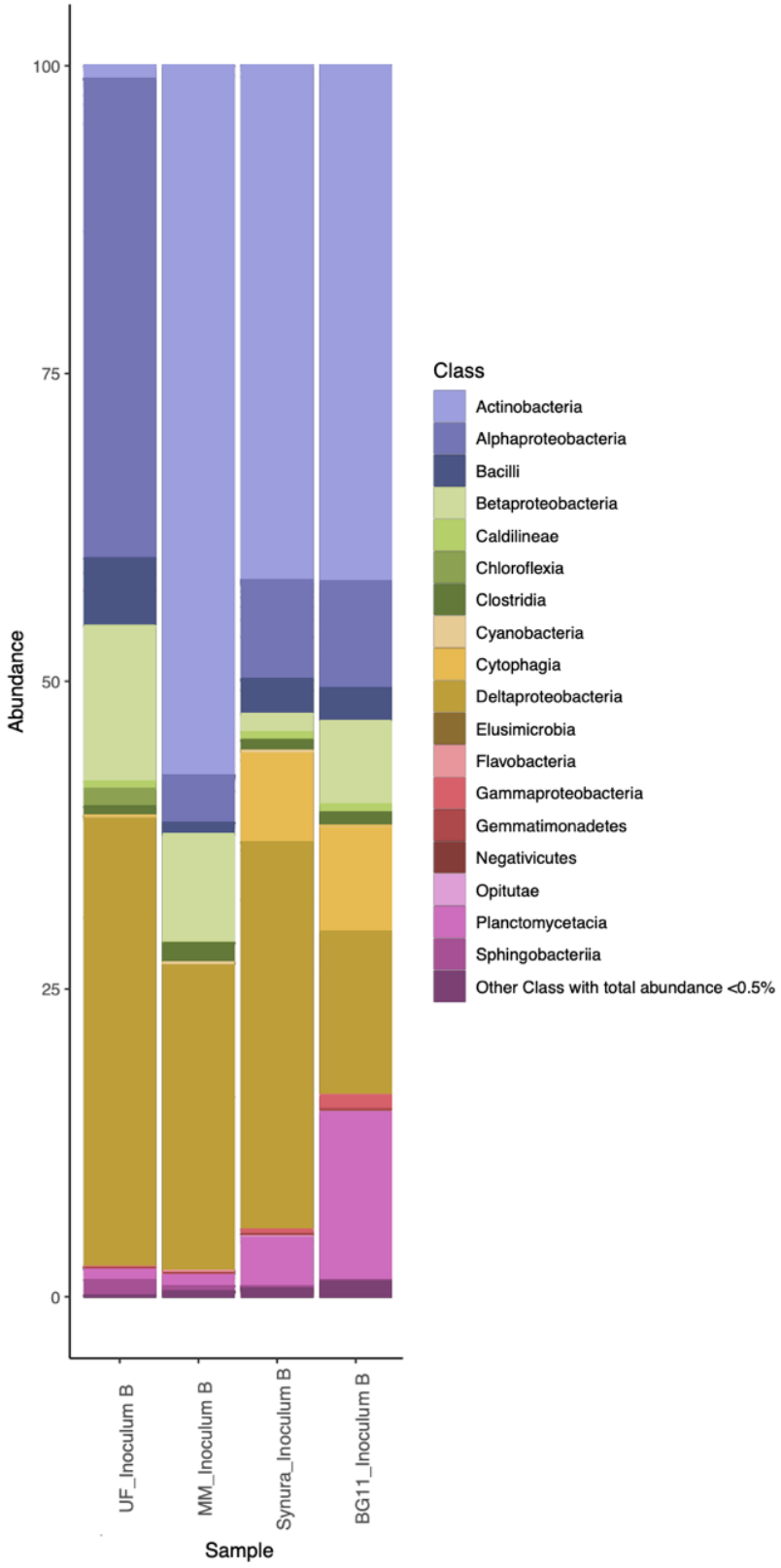

Figure 34: Bacterial composition of the incubations of inoculum B, according to the culture medium.

Other class with total abundance < 0.5% = Erysipelotrichi, Coriobacteriia, Acidimicrobiia, Lentisphaeria, Spirochaetes, Chlorobia, Fusobacteriia, Rubrobacteria, Thermomicrobia, Deinococci, Anaerolineae, Acidobacteria, Phycisphaerae, Thermoleophilia, Bacteroidia.

Composition of prokaryotes communities

The final compositions of the bacterial communities of prokaryote enriched-inoculum B, in the different culture media are presented in **Figure 34.** We observe an increase in the observed richness index with an increase in the richness of the medium (UF index = 62, MM = 73, Synura = 76), except for BG11 (index = 66) (**Figure 32-A, 34).**

In UF medium (lowest nutrient environment, **supp Table 1**), bacteria were mainly distributed among the 3 following classes of proteobacteria: Alphaproteobacteria (35%), Betaproteobacteria (15%) and Deltaproteobacteria (35%) (**Figure 34)**. In the other media the Alphaproteobacteria shown a strong decrease in their proportion to the benefit of Actinobacteria (60, 40 and 40% respectively). The increasing enrichment in nutrients (from MM to BG11, with synura as intermediate) benefits to the development of Cytophaga, Planctomycetes and Other classes (mean 7%, 8% and 5% respectively) at the expense of Proteobacteria.

5.1.4. Discussion and conclusion

In this study, we monitored the temporal changes in ALNs abundances under prokaryotic controlled *in-vitro* conditions. We used inocula from a culture originating from Fargettes Lake, in which the diversity and dynamic of ALNs and of their environment were previously documented [27, 197, 324]. The conditions of preparation and incubation of the culture and inocula (see materials and methods) allowed a selection/enrichment of the different morphotypes of ALNs (**Figure 33**) simultaneously with the depletion of viruses (VBR = 2.07 and 0.08 for inoculum A and B respectively at t0) and the elimination of the accompanying eukaryotic microbial communities. This strategy allows a direct linkage of ALNs and accompanying prokaryotes. A VBR (proxy of viral infection) lower than 1 during the whole incubation period in prokaryotes enriched incubations confirms that the only dynamic entities in our incubations are ALNs and prokaryotes.

The strong multiplication of ALNs recorded in the conditions enriched in prokaryotes (inoculum B: factors of the multiplication of ALNs of 29, 23 and 41 respectively in UF, Synura and nutrient enriched BG11 media) compared to prokaryotes depleted conditions (inoculum A:

no significant factors of the multiplication of ALNs in UF and BG11 media, factor of 20 in Synura) indicates a close interaction between them. These experimental observations confirm those previously suggested in environmental surveys [27, 197, 324] and reinforces the presumption that ALNs are a new player in aquatic ecosystems. This has already been demonstrated for other femto-planktonic communities, such as viruses or CPRs and DPANNs (discussed in Colombet *et al*. [16]).

One of the peculiarities of ALNs is their pleomorphism. Described in Colombet *et al*. [27], 4 majority forms were previously identified, based on the number of arms and the presence of a bud. Experiments led in this study revealed the apparition of a new form during incubation period. This X shape is smaller in terms of size (47.58 ± 9 µm) and volume (mean 1.12 $x10^{-4}$ μm^3) than those previously described. Add to the significant modification of the relative abundance of the different forms according to the culture medium and initial inoculum, these observations support the hypothesis of an interconversion of form during a putative development cycle. Occurrence of new X shape form, 20 arms and 11 budding arms in the richest culture medium or when we have a high concentration of prokaryotes also postulates for the intervention of prokaryotes in the realization of this cycle.

To understand the ALNs-prokaryotes interaction, we analyzed the bacterial composition of the media at the end of incubation. We have highlighted an overall increase in the observed richness with the increase in the availability of nutrients in the culture media. Like previous study, we can't infer a direct relationship between a specific phylum of prokaryotes and ALNs. On the opposite, ALNs seems to have a broad and non-specific spectrum of prokaryotic partners. However, an interaction with prokaryotes could have a direct impact on matter and energy fluxes, particularly in the degradation of organic matter.

The data acquired here confirm the hypothesis of an interaction between ALNs and prokaryotic communities. The exact nature of this interaction (neutralism, parasitism, mutualism...) remains to be determined. Further studies on the impact of ALNs on prokaryotic communities in natural environments would allow us to:

(i) Better understand the forcing factors governing their distribution and therefore to better understand their presence in ecosystems.

(ii) Formulate hypotheses as to their contribution to the flow of materials and energies of food webs.

(iii) Establish hypotheses about their exact nature

ALNs are therefore new players to be considered in the functioning of aquatic ecosystems, which should henceforth be taken into account in studies on femtoplankton and its impact in aquatic environments.

5.1.5 Supplemental materials

Table S1: Composition of culture medium used for incubations

Ultra-Filtrat (UF) medium

1/ Water from the lake filtered frontally on a filtration tissue with a porosity of 20 µm

2/ Successive tangential filtration with a porosity of 0.65 µm, 0.20 µm and 20 kd.

3/ Ultrat filtrate autoclaved and stored in the dark at 4°C until use

Minimum medium (MM)

Stocks

1/ K_2HPO_4	160 g per L
2/ KH_2PO_4	40 g per L
3/ $MgSO_4$	20 g per L
4/ NaCl	10 g per L
5/$CaCl_2$	20 g per L
6/ Trisodium citrate $2H_2O$	100 g per L
7/$FeSO_4$	0.5 g per L
8/ Oligoelements trace	9 g per L
9/ Vitamines	0.101 g per L

Medium

- Mix 10 mL of 1, 2, 3, 4, 5 and 0.5 mL of 8
- 929 mL distilled water
- Autoclaved
- Add 10 mL of 6, 7 and 0.5 mL of 9 filtered on 0.2 µm filter

Synura medium

Stocks

$CaCl_2$ 2 H_2O	36.8 g per L
$MgSO_4$ 7H_2O	37 g per L
$NaHCO_3$	12.6 g per L
K_2HPO_4 3H_2O	5.7 g per L
$NaNO_3$	85 g per L
Na_2SiO_3 5H_2O	28.42 g per L
Oligoelements trace	9 g per L
Vitamines	0.101 g per L
Soil extract	400 g per L

Medium

- Mix 1 mL of 1, 2, 3, 4, 5, 6, / 0.5 mL of 7 / 10 mL of 9 filtered on 0.2 µm filter
- Add distilled water
- Autoclaved
- Add 0.5 mL 8 filtered on 0.2 µm filter

BG-11 medium

Commercial medium

Components	Molecular Weight	Concentration (mg/L)	mM
Inorganic Salts			
Boric Acid (H_3BO_3)	61.83	28.7	0.464175107
Calcium Chloride ($CaCl_2 \cdot 2H_2O$)	147.0	27.0	0.183673347
Cupric sulfate ($CuSO_4 \cdot 5H_2O$)	249.69	0.8	0.003203973
Ferric ammonium citrate	261.96	12.0	0.045805022
Magnesium Sulfate ($MgSO_4 \cdot 7H_2O$)	246.47	75.0	0.304279667
Manganese chloride ($MnCl_2 \cdot 4H_2O$)	197.9	18.1	0.091446034
Potassium phosphate dibasic (K_2HPO_4)	174.2	39.0	0.2238806
Sodium Molybdate ($Na_2MoO_4 \cdot 2H_2O$)	205.92	3.9	0.018935556
Sodium Nitrate ($NaNO_3$)	84.99	1500.0	17.649136
Sodium carbonate (Na_2CO_3 H2O)	105.99	20.0	0.188685706
Zinc sulfate ($ZnSO_4 \cdot 7H_2O$)	287.55	2.2	0.007650944
Other Components			
EDTA	292.24	1.0	0.003421945

Table S2: Primers used for the amplification and their PCR programs.

	Bacteria	Archae	Fungi
Forward primer	515f-GTGYCAGCMGCCGCGGTA	519f- CAGCMGCCGCGGTAA	its7f-GTGARTCATCGAATCTTTG
Reverse Primer	928r-CCCCGYCAATTCMTTTRAGT	1017r-GGCCATGCACCWCCTCTC	its4r-TCCTCCGCTTATTGATATGC
Program	95°c 3mn ------x32------ 98°c 20s 65°c 40s 72°c 30s ---------- 72°c. 10mn	95°c 3mn ------x32------ 98°c 20s 68°c 30s 72°c 30s ---------- 72°c. 5mn	95°c 3mn ------x32------ 98°c 20s 57°c 30s 72°c 30s ---------- 72°c. 5mn

5.2 Long-term incubation of ALNs in lake water: Development of specific communities

Long-Term Incubation of Lake Water Enables Genomic Sampling of Consortia Involving Planctomycetes and Candidate Phyla Radiation Bacteria

Alexander L. Jaffe[a*], Maxime Fuster[b*], Marie C. Schoelmerich[c], Lin-Xing Chen[d], Jonathan Colombet[b], Hermine Billard[b], Télesphore Sime-Ngando[b], Jillian F. Banfield[c,d,e,f]

*These authors contributed equally to this work.

[a]Department of Plant and Microbial Biology, University of California, Berkeley, California, USA

[b]Laboratoire Microorganismes: Génome et Environnement (LMGE), UMR CNRS 6023, Université Clermont-Auvergne, Clermont-Ferrand, France

[c]Innovative Genomics Institute, University of California, Berkeley, California, USA

[d]Department of Earth and Planetary Science, University of California, Berkeley, California, USA

[e]Department of Environmental Science, Policy, and Management, University of California, Berkeley, California, USA

[f]Chan Zuckerberg Biohub, San Francisco, California, USA

Publié dans *mSystems* – Mars 2022
doi : 10.1128/msystems.00223-22

5.2.1 Abstract

Microbial communities in lakes can profoundly impact biogeochemical processes through their individual activities and collective interactions. However, the complexity of these communities poses challenges, particularly for studying rare organisms such as Candidate Phyla Radiation bacteria (CPR) and enigmatic entities such as aster-like nanoparticles (ALNs). Here, a reactor was inoculated with water from Lake Fargettes, France, and maintained under dark conditions at 4°C for 31 months and enriched for ALNs, diverse Planctomycetes, and CPR bacteria. We reconstructed draft genomes and predicted metabolic traits for 12 diverse Planctomycetes and 9 CPR bacteria, some of which are likely representatives of undescribed families or genera. One CPR genome representing the little-studied lineage "Candidatus Peribacter" was curated to completion (1.239 Mbp) and unexpectedly encodes the full gluconeogenesis pathway. Metatranscriptomic data indicate that some planctomycetes and CPR bacteria were active under the culture conditions, accounting for ~30% and ~1% of RNA reads mapping to the genome

set, respectively. We also reconstructed genomes and obtained transmission electron microscope images for numerous viruses, including one with a >300-kbp genome and several predicted to infect Planctomycetes. Together, our analyses suggest that freshwater Planctomycetes are central players in a subsystem that includes ALNs, symbiotic CPR bacteria, and viruses.

5.2.2 Note

Laboratory incubations of natural microbial communities can aid in the study of member organisms and their networks of interaction. This is particularly important for understudied lineages for which key elements of basic biology are still emerging. Using genomics and microscopy, we found that members of the bacterial lineage Planctomycetes may be central players in a subset of a freshwater lake microbiome that includes other bacteria, archaea, viruses, and mysterious entities, called aster-like nanoparticles (ALNs), whose origin is unknown. Our results help constrain the possible origins of ALNs and provide insight into possible interactions within a complex lake ecosystem.

Freshwater lakes host diverse microbial communities that likely control ecosystem biogeochemistry [325, 326]. Here, we established a laboratory culture based on an inoculum from Lake Fargettes, France, a site chosen as part of a parallel study of enigmatic aster-like nanoparticles (ALNs) [27, 197]. ALNs are enigmatic, organic, femtoplankton entities that exhibit bloom-like behavior in various freshwater and coastal environments [27, 197]. In this experiment, microscopy showed that the proportion of ALNs increased substantially during incubation, from 26% to 36% of imaged objects (see Table S1). To seek clues to the origins of ALNs and the organisms that they might associate with, and to better understand the lake ecosystem overall, we studied the culture using a combination of metagenomics, metatranscriptomics, and microscopy. In doing so, we recovered draft genomes for abundant and transcriptionally active *Planctomycetes* as well as CPR bacteria, phages, and eukaryotic viruses. Overall, we provide clues to associations and potential interactions among microbial groups in a lake ecosystem.

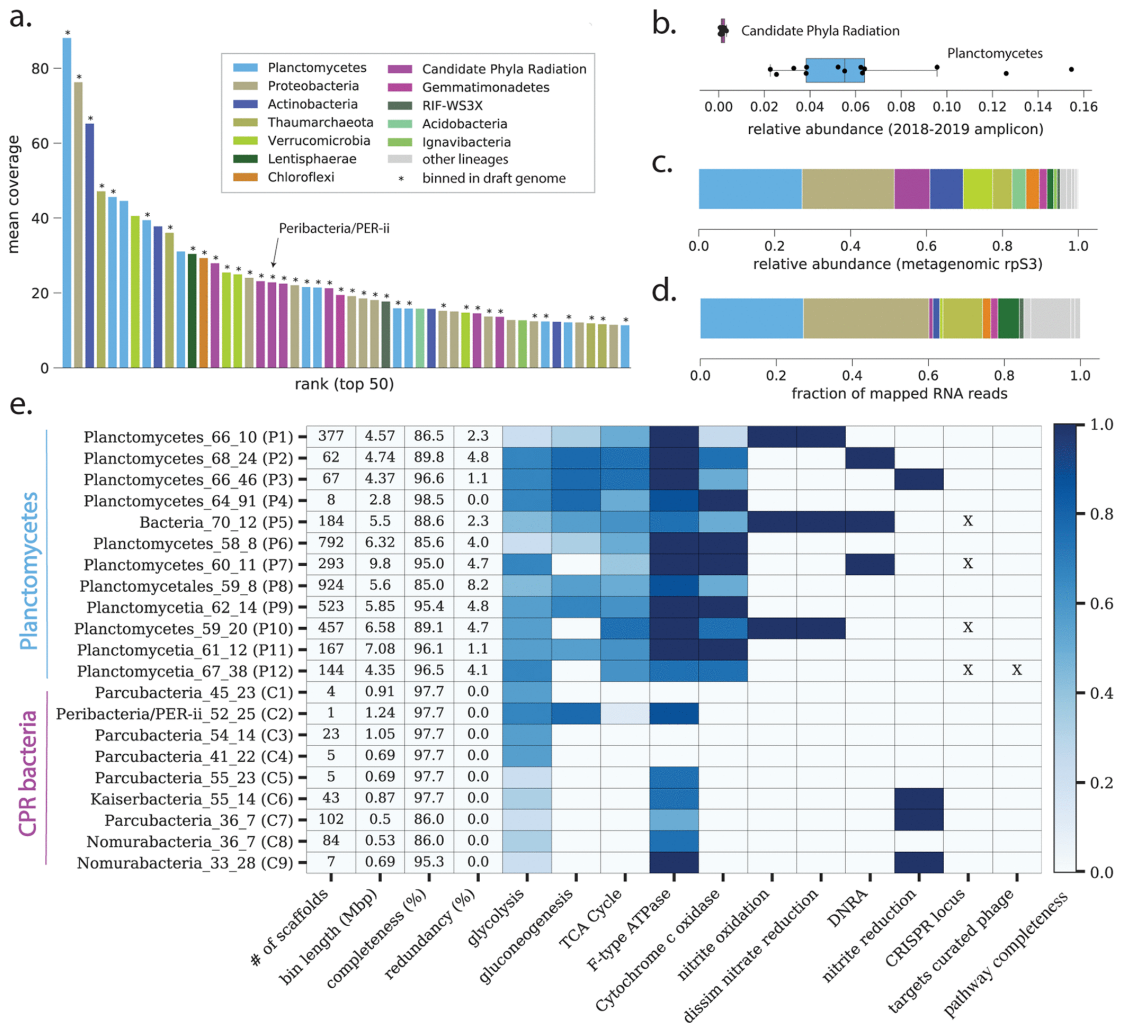

Figure 35: Long-term incubation enriched for members of the Planctomycetes and CPR bacteria.

(a) Rank abundance curve based on ribosomal protein S3 (rps3) coverage for organisms recovered at the end of incubation. Asterisks indicate marker genes that were binned into genomes. (b) Relative abundance of CPR bacteria and *Planctomycetes* during monthly sampling of Lake Fargettes based on 16S rRNA amplicon sequencing. Each point represents the relative abundance of CPR bacteria or *Planctomycetes* in a given month. (c) Overall community composition at the end of incubation, based on cumulative coverage of rpS3. Panel d displays the fraction of RNA reads from the end of incubation that could be mapped to genomes. (e) Sequence characteristics, metabolic predictions, and CRISPR-Cas loci information for genomes affiliated with the *Planctomycetes* and CPR bacteria. Cells with color fill indicate the fraction of key genes for each pathway (as defined by KEGGDecoder) that are present. X indicates genomes with CRISPR loci and if those loci contained spacers targeting at least one curated phage genome from the sampl

Community composition and genome reconstruction.

Concentrate from the 0.2-µm to 25-µm size fraction of the highly eutrophic Lake Fargettes, France, was incubated at 4°C in the dark with filtered and sterilized lake water (<20 kDa). The incubation was performed under dark conditions to favor heterotrophic organisms associated with ALNs instead of phototrophic eukaryotes. After 31 months, DNA and RNA were extracted for metagenomic and transcriptomic analyses. DNA reads were assembled and the scaffolds profiled to identify ribosomal protein S3 (rpS3). Profiling using the predicted rpS3 protein sequences revealed that the enrichment was bacterially dominated, although several members of the *Thaumarchaeota* were present (**Figure 35-A**; see also Table S2). The most abundant organisms overall were *Planctomycetes* (~27% of overall rpS3 coverage), including the most abundant singular organism (**Figure 35** and Table S2). CPR bacteria were 5 of the top 25 most abundant organism groups (~9% overall rpS3 coverage; **Figure 35** and Table S2). Compared to baseline abundances in Lake Fargettes, these results indicated enrichment of these groups, particularly CPR bacteria, which were barely detectable in the lake (<1% relative abundance; **Figure 35-B** and Table S3).

Where possible, scaffolds were assigned to genome bins that ranged in quality from draft to nearly complete. The 48 genomes captured most of the phylogenetic diversity (76% of the most abundant rpS3 genes; **Figure 35-A** and Tables S2 and S4); 12 genomes represent phylogenetically diverse *Planctomycetes*, including several from the *Planctomycetes* and *Phycisphaerae*classes (see Fig. S1 and Table S4). Metabolic reconstructions suggested that the *Planctomycetes* are primarily heterotrophs with the potential to oxidize nitrite or reduce nitrate in three cases (**Figure 35-E**). We also recovered 9 genomes of CPR bacteria, 8 of which were classified as "*Candidatus* Parcubacteria" (Figure S1). The "*Candidatus* Parcubacteria" genomes encoded minimal metabolic capacities, consistent with symbiotic lifestyles [23]. However, several had a phylogenetically distinct *nirK* gene that may play a role in denitrification or energy conservation [327] (**Figure 35-E)**. Read mapping from a metatranscriptome collected contemporaneously with the metagenome suggested that some *Planctomycetes* and, to a lesser extent, CPR bacteria were actively transcribing under the culture conditions, with *Planctomycetes* and CPR accounting for about 27% and 1%, respectively, of RNA reads stringently mapping to the nonredundant set of genomes (**Figure 35-D** and Table S4). However, only a small proportion of total RNA reads (201,809 reads, or ~0.2% of the total) mapped stringently to the genome set and passed filtering for non-mRNAs.

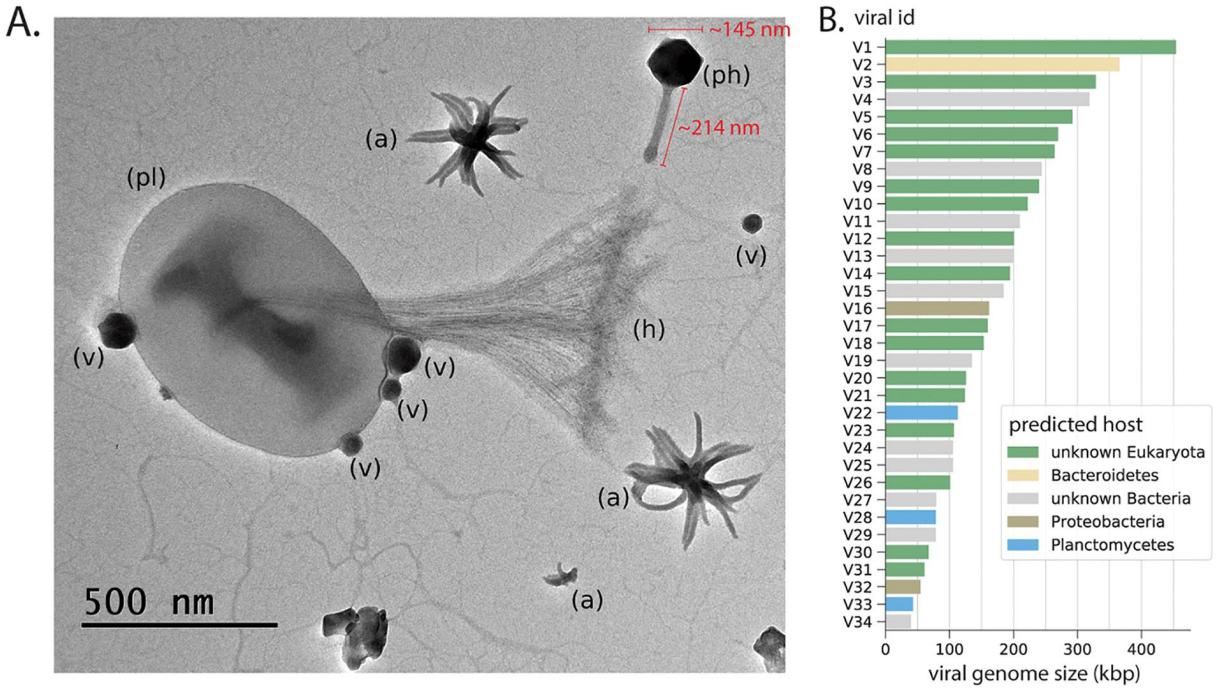

Figure 36: TEM imaging and viral genomics in the enrichment culture.
(A) Featured in this image is a cell inferred to be a *Planctomycetes* (pl) with a characteristic stalk and holdfast (h). Attached to the cell are four phage particles (v) (two different sizes; thus, likely different phages). Also visible is one large tailed jumbo phage (ph) that is 145 nm in diameter with a 214-nm tail as well as several aster-like nanoparticles (ALNs) (a). (B) Genome sizes and predicted hosts for phages and eukaryotic viruses.

The ninth draft CPR genome was for a member of the undersampled CPR lineage "*Candidatus* Peribacteria." We manually curated the original bin of 6 fragments into a single fragment that was circularized by a small, unbinned contig, and all scaffolding errors and local misassemblies were fixed (see **Figure S2**). The newly reported, fully curated 1,239,242-bp genome shares ~89% similarity in its 16S rRNA gene and is largely syntenous with a closely related "*Candidatus* Peribacteria" genome from Rifle, Colorado [328], supporting the accuracy of both assemblies (see **Figure S3**). Unlike the Rifle genomes, this peribacter likely cannot synthesize purines *de novo*. Other notable differences include the presence of vacuolar-type H^+/Na^+-transporting ATPase complex and the lack of genes for biosynthesis of mevalonate. Based on biosynthetic deficiencies, we conclude that this bacterium probably relies on other organisms for many building block but to a lesser extent than the "*Candidatus* Parcubacteria." Supporting this idea, we observed that the peribacter genome encodes all gluconeogenesis enzymes, including fructose-1,6-bisphosphatase I, which was not found in the "*Candidatus* Parcubacteria" genomes (**Figure 35-E**)

We reconstructed 12 phage sequences and 5 phage-like sequences, including 3 circularized genomes exceeding 100 kbp and 2 incomplete phage/phage-like fragments of >300 kbp (see **Table S5**). Phylogenetic analyses of encoded terminase and capsid proteins suggested that the phages likely fall within the *Caudovirales*, which are known to include numerous tailed phages with large capsids [329]. Additionally, we used phage gene content and analyses of bacterial CRISPR loci to infer that phages infect *Planctomycetes*, *Proteobacteria*, and *Bacteroidetes* (**Figure 36** and **Table S5**).

We also reconstructed large fragments of 17 eukaryotic viruses. Based on the phylogenetic placement of the major capsid protein and homologs of the poxvirus late transcription factor VLTF3, some viruses belonged to Iridoviridae (Betairidoviridae), extended Mimiviridae, Phycodnaviridae, and Pitho-like viruses (see **Figure S4 and S5** and **Table S5**). Other viruses could only be classified at the superclade level, including those within a potentially novel Phycodnaviridae, Asfarviridae, Megavirales (PAM) clade, or did not contain either marker protein (see **Figure S4 and S5**). Interestingly, we detected very little transcription of genes from phage or eukaryotic viruses (mean coverage, $\ll 1\times$), suggesting that they were not actively replicating in the incubated community (see **Table S5**). The lack of eukaryotes in the enrichment suggests that some of these particles have derived from the inoculum and persisted for over 2 years.

Imaging of incubation community

We imaged a diversity of cellular, cellular-like, and noncellular particles, as well as many ALNs, using transmission electron microscopy (TEM) (**Figure 36** and **Figure S6**). Based on the presence of the extracellular holdfast [330, 331], we infer that the cell imaged in **Figure 36** is likely a member of the *Planctomycetes*, with at least two attached distinct types of virus-like particles (VLPs). This finding is consistent with the high abundance of *Planctomycetes* in the enrichment as well as multiple phages predicted to infect them (~18 to 100× coverage). We also imaged numerous tailed phages (see Fig. S6), including one with a 145-nm-diameter capsid and 214-nm tail (**Figure 36**, ph). This large capsid size is consistent with those of jumbo phages with genomes in the 300-kbp range [329], two of which were reconstructed here (see **Table S5**). Despite these observations, TEM image counts suggested that the overall proportion of tailed phages decreased from 26% to less than 1% of imaged objects over the course of the incubation (see **Table S1**).

5.2.4 Discussion and conclusion

Planctomycetes are globally distributed across freshwater ecosystems, where they are thought to play important roles in nitrogen and carbon cycling [332, 333]. Our analyses expand genomic sampling for these organisms, and coenrichment suggests that they interact with CPR bacteria. Although we cannot establish a direct association between *Planctomycetes* and CPR bacteria from the current data, reported lifestyles for other CPR suggest that they are host cell-attached, at least at sometimes [334]. Furthermore, the enrichment contains a similar level of diversity of both *Planctomycetes* and CPR, raising the possibility of species-specific associations (see **Figure S1**). As episymbionts, CPR would almost certainly influence the physiology of *Planctomycetes* cells, either via mutualistic interactions or parasitism, and, thus, the biogeochemical cycles that *Planctomycetes* mediate. The approach used in the current study could guide future coisolation of CPR bacteria of the "*Candidatus* Parcubacteria" and "*Candidatus* Peribacteria" lineages to test this hypothesis.

Like CPR bacteria, phages clearly impact their hosts and, thus, ecosystem structure and performance. It is intriguing that phages were maintained over the long incubation period, as they are often lost from laboratory cultures [335]. A subset of the phages clearly infect *Planctomycetes*, the diversity of which may have enabled their sustained replication

Table S1. Taxonomic affiliation and coverage of ribosomal protein S3 marker genes used to survey microbial community composition in the enrichment sample.

scaffold	bin	lineage	in_draft_genome	coverage
LakeFargette_0920_ALND_scaffold_281956	LakeFargette_0920_ALND_Planctomycetes_64_91	Planctomycetes	VRAI	88,14
LakeFargette_0920_ALND_scaffold_603991	LakeFargette_0920_ALND_Burkholderiales_70_71	Proteobacteria	VRAI	76,37
LakeFargette_0920_ALND_scaffold_544059	LakeFargette_0920_ALND_Actinobacteria_63_63	Actinobacteria	VRAI	65,3
LakeFargette_0920_ALND_scaffold_273213	LakeFargette_0920_ALND_Nitrosoarchaeum_limnia_33_41	Thaumarchaeota	VRAI	47,21
LakeFargette_0920_ALND_scaffold_208593	LakeFargette_0920_ALND_Planctomycetes_66_46	Planctomycetes	VRAI	45,7
LakeFargette_0920_ALND_scaffold_63232	LakeFargette_0920_ALND_Planctomycetia_59_40	Planctomycetes	FAUX	44,66
LakeFargette_0920_ALND_scaffold_616036	LakeFargette_0920_ALND_UNK	Verrucomicrobia	FAUX	40,64
LakeFargette_0920_ALND_scaffold_58038	LakeFargette_0920_ALND_Planctomycetia_67_38	Planctomycetes	VRAI	39,53
LakeFargette_0920_ALND_scaffold_24295	LakeFargette_0920_ALND_Actinobacteria_52_33	Actinobacteria	FAUX	37,85
LakeFargette_0920_ALND_scaffold_721642	LakeFargette_0920_ALND_Nitrosoarchaeum_limnia_33_41	Thaumarchaeota	VRAI	36,13
LakeFargette_0920_ALND_scaffold_8147	LakeFargette_0920_ALND_Planctomycetes_63_28	Planctomycetes	FAUX	31,14
LakeFargette_0920_ALND_scaffold_401388	LakeFargette_0920_ALND_Bacteria_66_32	Lentisphaerae	VRAI	30,5
LakeFargette_0920_ALND_scaffold_625734	LakeFargette_0920_ALND_Chloroflexi_53_29	Chloroflexi	VRAI	29,39
LakeFargette_0920_ALND_scaffold_493788	LakeFargette_0920_ALND_Nomurabacteria_33_28	Candidate Phyla Radiation	VRAI	28,01
LakeFargette_0920_ALND_scaffold_423256	LakeFargette_0920_ALND_Chthoniobacter_flavus_63_25	Verrucomicrobia	VRAI	25,54
LakeFargette_0920_ALND_scaffold_768437	LakeFargette_0920_ALND_Verrucomicrobia_56_25	Verrucomicrobia	VRAI	25,05
LakeFargette_0920_ALND_scaffold_51390	LakeFargette_0920_ALND_Betaproteobacteria_62_19	Proteobacteria	VRAI	24,1
LakeFargette_0920_ALND_scaffold_894461	LakeFargette_0920_ALND_Parcubacteria_55_23	Candidate Phyla Radiation	VRAI	23,2
LakeFargette_0920_ALND_scaffold_695414	LakeFargette_0920_ALND_PER-li_52_24	Candidate Phyla Radiation	VRAI	22,9
LakeFargette_0920_ALND_scaffold_272472	LakeFargette_0920_ALND_Parcubacteria_45_23	Candidate Phyla Radiation	VRAI	22,57
LakeFargette_0920_ALND_scaffold_76017	LakeFargette_0920_ALND_Rhodocyclales_64_19	Proteobacteria	VRAI	22,14
LakeFargette_0920_ALND_scaffold_13249	LakeFargette_0920_ALND_Planctomycetes_59_20	Planctomycetes	VRAI	21,64
LakeFargette_0920_ALND_scaffold_186177	LakeFargette_0920_ALND_Planctomycetes_68_24	Planctomycetes	VRAI	21,52
LakeFargette_0920_ALND_scaffold_491135	LakeFargette_0920_ALND_Parcubacteria_41_22	Candidate Phyla Radiation	VRAI	21,32
LakeFargette_0920_ALND_scaffold_497873	LakeFargette_0920_ALND_Gemmatimonadetes_70_15	Gemmatimonadetes	VRAI	19,55
LakeFargette_0920_ALND_scaffold_129779	LakeFargette_0920_ALND_Parvibaculum_lavamentivorans_63_19	Proteobacteria	VRAI	19,25
LakeFargette_0920_ALND_scaffold_214369	LakeFargette_0920_ALND_Parvibaculum_lavamentivorans_63_19	Proteobacteria	VRAI	18,62
LakeFargette_0920_ALND_scaffold_440048	LakeFargette_0920_ALND_Alphaproteobacteria_61_16	Proteobacteria	VRAI	18,2
LakeFargette_0920_ALND_scaffold_123941	LakeFargette_0920_ALND_RBG_16_RIF_WS3X_69_13	RIF-WS3X	VRAI	17,81
LakeFargette_0920_ALND_scaffold_596440	LakeFargette_0920_ALND_Planctomycetia_62_14	Planctomycetes	VRAI	15,99
LakeFargette_0920_ALND_scaffold_89631	LakeFargette_0920_ALND_Planctomycetia_62_14	Planctomycetes	VRAI	15,89
LakeFargette_0920_ALND_scaffold_8116	LakeFargette_0920_ALND_Acidobacteria_64_15	Acidobacteria	FAUX	15,88
LakeFargette_0920_ALND_scaffold_265761	LakeFargette_0920_ALND_UNK	Actinobacteria	FAUX	15,84
LakeFargette_0920_ALND_scaffold_274210	LakeFargette_0920_ALND_Betaproteobacteria_49_15	Proteobacteria	VRAI	15,27
LakeFargette_0920_ALND_scaffold_897265	LakeFargette_0920_ALND_Parvibaculum_lavamentivorans_58_9	Proteobacteria	FAUX	15,12
LakeFargette_0920_ALND_scaffold_184246	LakeFargette_0920_ALND_Verrucomicrobia_58_12	Verrucomicrobia	VRAI	14,82
LakeFargette_0920_ALND_scaffold_312775	LakeFargette_0920_ALND_Kaiserbacteria_55_14	Candidate Phyla Radiation	VRAI	14,64
LakeFargette_0920_ALND_scaffold_1093151	LakeFargette_0920_ALND_Methylophilales_50_13	Proteobacteria	VRAI	13,76
LakeFargette_0920_ALND_scaffold_118019	LakeFargette_0920_ALND_Parcubacteria_54_14	Candidate Phyla Radiation	VRAI	13,7
LakeFargette_0920_ALND_scaffold_406568	LakeFargette_0920_ALND_UNK	Proteobacteria	FAUX	12,83
LakeFargette_0920_ALND_scaffold_372729	LakeFargette_0920_ALND_UNK	Ignavibacteria	FAUX	12,75
LakeFargette_0920_ALND_scaffold_136658	LakeFargette_0920_ALND_Deltaproteobacteria_72_12	Proteobacteria	VRAI	12,51
LakeFargette_0920_ALND_scaffold_231019	LakeFargette_0920_ALND_Bacteria_70_12	Planctomycetes	VRAI	12,46
LakeFargette_0920_ALND_scaffold_1067166	LakeFargette_0920_ALND_UNK	Actinobacteria	FAUX	12,39
LakeFargette_0920_ALND_scaffold_680977	LakeFargette_0920_ALND_Planctomycetia_61_12	Planctomycetes	VRAI	12,22
LakeFargette_0920_ALND_scaffold_132528	LakeFargette_0920_ALND_Parvibaculum_62_11	Proteobacteria	FAUX	12,18
LakeFargette_0920_ALND_scaffold_143954	LakeFargette_0920_ALND_Nitrosoarchaeum_33_12	Thaumarchaeota	VRAI	11,97
LakeFargette_0920_ALND_scaffold_744926	LakeFargette_0920_ALND_Nitrosoarchaeum_33_12	Thaumarchaeota	VRAI	11,74
LakeFargette_0920_ALND_scaffold_461457	LakeFargette_0920_ALND_Alphaproteobacteria_62_11	Proteobacteria	FAUX	11,57
LakeFargette_0920_ALND_scaffold_299947	LakeFargette_0920_ALND_Planctomycetes_60_11	Planctomycetes	VRAI	11,45
LakeFargette_0920_ALND_scaffold_720996	LakeFargette_0920_ALND_UNK	Acidobacteria	FAUX	10,97
LakeFargette_0920_ALND_scaffold_515556	LakeFargette_0920_ALND_Planctomycetes_66_10	Planctomycetes	VRAI	10,6
LakeFargette_0920_ALND_scaffold_848823	LakeFargette_0920_ALND_UNK	Acidobacteria	FAUX	10,52
LakeFargette_0920_ALND_scaffold_857978	LakeFargette_0920_ALND_UNK	Acidobacteria	FAUX	10,45
LakeFargette_0920_ALND_scaffold_331752	LakeFargette_0920_ALND_UNK	Proteobacteria	FAUX	10,32
LakeFargette_0920_ALND_scaffold_829436	LakeFargette_0920_ALND_UNK	Planctomycetes	FAUX	10,32
LakeFargette_0920_ALND_scaffold_186100	LakeFargette_0920_ALND_UNK	Planctomycetes	FAUX	10,29
LakeFargette_0920_ALND_scaffold_518171	LakeFargette_0920_ALND_UNK	Proteobacteria	FAUX	10,27
LakeFargette_0920_ALND_scaffold_621702	LakeFargette_0920_ALND_UNK	Acidobacteria	FAUX	10,24
LakeFargette_0920_ALND_scaffold_847323	LakeFargette_0920_ALND_UNK	Proteobacteria	FAUX	10,17
LakeFargette_0920_ALND_scaffold_1067717	LakeFargette_0920_ALND_UNK	Proteobacteria	FAUX	9,98
LakeFargette_0920_ALND_scaffold_980850	LakeFargette_0920_ALND_UNK	Actinobacteria	FAUX	9,85
LakeFargette_0920_ALND_scaffold_863729	LakeFargette_0920_ALND_UNK	Planctomycetes	FAUX	9,78
LakeFargette_0920_ALND_scaffold_57619	LakeFargette_0920_ALND_UNK	Proteobacteria	FAUX	9,7
LakeFargette_0920_ALND_scaffold_537840	LakeFargette_0920_ALND_UNK	Verrucomicrobia	FAUX	9,57
LakeFargette_0920_ALND_scaffold_75275	LakeFargette_0920_ALND_Haliangium_ochraceum_69_9	Proteobacteria	FAUX	9,56
LakeFargette_0920_ALND_scaffold_867308	LakeFargette_0920_ALND_UNK	Acidobacteria	FAUX	9,43
LakeFargette_0920_ALND_scaffold_915891	LakeFargette_0920_ALND_UNK	Acidobacteria	FAUX	9,42
LakeFargette_0920_ALND_scaffold_112286	LakeFargette_0920_ALND_UNK	Planctomycetes	FAUX	9,27
LakeFargette_0920_ALND_scaffold_515120	LakeFargette_0920_ALND_Spirochaetia_49_9	Spirochaetes	VRAI	9,25
LakeFargette_0920_ALND_scaffold_366703	LakeFargette_0920_ALND_UNK	Verrucomicrobia	FAUX	8,92
LakeFargette_0920_ALND_scaffold_340692	LakeFargette_0920_ALND_UNK	Proteobacteria	FAUX	8,86
LakeFargette_0920_ALND_scaffold_785936	LakeFargette_0920_ALND_UNK	Planctomycetes	FAUX	8,79
LakeFargette_0920_ALND_scaffold_500109	LakeFargette_0920_ALND_UNK	Proteobacteria	FAUX	8,68
LakeFargette_0920_ALND_scaffold_984081	LakeFargette_0920_ALND_UNK	Gemmatimonadetes	FAUX	8,65
LakeFargette_0920_ALND_scaffold_698987	LakeFargette_0920_ALND_UNK	Proteobacteria	FAUX	8,52
LakeFargette_0920_ALND_scaffold_82079	LakeFargette_0920_ALND_Chloroflexi_57_8	Chloroflexi	FAUX	8,47
LakeFargette_0920_ALND_scaffold_792610	LakeFargette_0920_ALND_UNK	Proteobacteria	FAUX	8,45
LakeFargette_0920_ALND_scaffold_966786	LakeFargette_0920_ALND_UNK	Planctomycetes	FAUX	8,28
LakeFargette_0920_ALND_scaffold_861196	LakeFargette_0920_ALND_Actinobacteria_42_5	Actinobacteria	FAUX	8,26
LakeFargette_0920_ALND_scaffold_1061080	LakeFargette_0920_ALND_Planctomycetales_59_8	Planctomycetes	VRAI	8,22
LakeFargette_0920_ALND_scaffold_1108551	LakeFargette_0920_ALND_UNK	Proteobacteria	FAUX	8,22
LakeFargette_0920_ALND_scaffold_1097660	LakeFargette_0920_ALND_UNK	Planctomycetes	FAUX	8,17
LakeFargette_0920_ALND_scaffold_79971	LakeFargette_0920_ALND_Verrucomicrobia_57_8	Verrucomicrobia	VRAI	8,1
LakeFargette_0920_ALND_scaffold_441425	LakeFargette_0920_ALND_Planctomycetes_58_8	Planctomycetes	VRAI	8,08
LakeFargette_0920_ALND_scaffold_95241	LakeFargette_0920_ALND_Armatimonadetes_54_8	Armatimonadetes	VRAI	8,01
LakeFargette_0920_ALND_scaffold_27400	LakeFargette_0920_ALND_UNK	Proteobacteria	FAUX	7,98
LakeFargette_0920_ALND_scaffold_217289	LakeFargette_0920_ALND_Parcubacteria_36_7	Candidate Phyla Radiation	VRAI	7,97
LakeFargette_0920_ALND_scaffold_358504	LakeFargette_0920_ALND_UNK	Proteobacteria	FAUX	7,92
LakeFargette_0920_ALND_scaffold_1025004	LakeFargette_0920_ALND_UNK	Actinobacteria	FAUX	7,86
LakeFargette_0920_ALND_scaffold_147053	LakeFargette_0920_ALND_Bacteria_57_7	Proteobacteria	VRAI	7,85
LakeFargette_0920_ALND_scaffold_618165	LakeFargette_0920_ALND_UNK	Proteobacteria	FAUX	7,73
LakeFargette_0920_ALND_scaffold_34747	LakeFargette_0920_ALND_UNK	Planctomycetes	FAUX	7,72
LakeFargette_0920_ALND_scaffold_23073	LakeFargette_0920_ALND_UNK	Planctomycetes	FAUX	7,71
LakeFargette_0920_ALND_scaffold_191264	LakeFargette_0920_ALND_UNK	Planctomycetes	FAUX	7,71
LakeFargette_0920_ALND_scaffold_878114	LakeFargette_0920_ALND_Elusimicrobia_65_5	Elusimicrobia	FAUX	7,67
LakeFargette_0920_ALND_scaffold_821632	LakeFargette_0920_ALND_Parcubacteria_52_6	Candidate Phyla Radiation	FAUX	7,54
LakeFargette_0920_ALND_scaffold_610682	LakeFargette_0920_ALND_UNK	Proteobacteria	FAUX	7,47
LakeFargette_0920_ALND_scaffold_131892	LakeFargette_0920_ALND_UNK	Planctomycetes	FAUX	7,42
LakeFargette_0920_ALND_scaffold_237264	LakeFargette_0920_ALND_UNK	Actinobacteria	FAUX	7,41
LakeFargette_0920_ALND_scaffold_236654	LakeFargette_0920_ALND_UNK	Candidate Phyla Radiation	FAUX	7,4
LakeFargette_0920_ALND_scaffold_1028751	LakeFargette_0920_ALND_UNK	Planctomycetes	FAUX	7,39
LakeFargette_0920_ALND_scaffold_225644	LakeFargette_0920_ALND_Bacteroidetes_35_6	Bacteroidetes	VRAI	7,35
LakeFargette_0920_ALND_scaffold_778924	LakeFargette_0920_ALND_UNK	Proteobacteria	FAUX	7,3
LakeFargette_0920_ALND_scaffold_222078	LakeFargette_0920_ALND_Nomurabacteria_36_7	Candidate Phyla Radiation	VRAI	7,29
LakeFargette_0920_ALND_scaffold_223589	LakeFargette_0920_ALND_UNK	Planctomycetes	FAUX	7,25
LakeFargette_0920_ALND_scaffold_836706	LakeFargette_0920_ALND_UNK	Planctomycetes	FAUX	7,24
LakeFargette_0920_ALND_scaffold_797512	LakeFargette_0920_ALND_UNK	Planctomycetes	FAUX	7,2
LakeFargette_0920_ALND_scaffold_1058136	LakeFargette_0920_ALND_UNK	Chloroflexi	FAUX	7,17
LakeFargette_0920_ALND_scaffold_309233	LakeFargette_0920_ALND_UNK	Proteobacteria	FAUX	7,17
LakeFargette_0920_ALND_scaffold_408613	LakeFargette_0920_ALND_UNK	Gemmatimonadetes	FAUX	7,15
LakeFargette_0920_ALND_scaffold_679117	LakeFargette_0920_ALND_UNK	Chloroflexi	FAUX	7,09
LakeFargette_0920_ALND_scaffold_435731	LakeFargette_0920_ALND_UNK	Gemmatimonadetes	FAUX	7,03
LakeFargette_0920_ALND_scaffold_313467	LakeFargette_0920_ALND_UNK	Planctomycetes	FAUX	7,03
LakeFargette_0920_ALND_scaffold_174291	LakeFargette_0920_ALND_UNK	unknown	FAUX	7,02
LakeFargette_0920_ALND_scaffold_559607	LakeFargette_0920_ALND_Leptospira_40_6	Spirochaetes	VRAI	6,97
LakeFargette_0920_ALND_scaffold_344979	LakeFargette_0920_ALND_UNK	unknown	FAUX	6,7
LakeFargette_0920_ALND_scaffold_861210	LakeFargette_0920_ALND_Actinobacteria_42_5	Actinobacteria	FAUX	6,68
LakeFargette_0920_ALND_scaffold_1102982	LakeFargette_0920_ALND_UNK	Proteobacteria	FAUX	6,64
LakeFargette_0920_ALND_scaffold_92228	LakeFargette_0920_ALND_UNK	Proteobacteria	FAUX	6,64
LakeFargette_0920_ALND_scaffold_429158	LakeFargette_0920_ALND_UNK	Proteobacteria	FAUX	6,41
LakeFargette_0920_ALND_scaffold_1055040	LakeFargette_0920_ALND_UNK	Proteobacteria	FAUX	6,34
LakeFargette_0920_ALND_scaffold_712356	LakeFargette_0920_ALND_UNK	Planctomycetes	FAUX	6,34
LakeFargette_0920_ALND_scaffold_1052743	LakeFargette_0920_ALND_UNK	Proteobacteria	FAUX	6,31
LakeFargette_0920_ALND_scaffold_916344	LakeFargette_0920_ALND_UNK	Planctomycetes	FAUX	6,21
LakeFargette_0920_ALND_scaffold_924620	LakeFargette_0920_ALND_UNK	unknown	FAUX	6,17
LakeFargette_0920_ALND_scaffold_28878	LakeFargette_0920_ALND_UNK	Actinobacteria	FAUX	6,1
LakeFargette_0920_ALND_scaffold_872568	LakeFargette_0920_ALND_UNK	Verrucomicrobia	FAUX	6,1
LakeFargette_0920_ALND_scaffold_344650	LakeFargette_0920_ALND_UNK	Proteobacteria	FAUX	6,08
LakeFargette_0920_ALND_scaffold_356858	LakeFargette_0920_ALND_Chloroflexi_68_6	Chloroflexi	FAUX	6,07
LakeFargette_0920_ALND_scaffold_603014	LakeFargette_0920_ALND_UNK	Proteobacteria	FAUX	6,04
LakeFargette_0920_ALND_scaffold_1021972	LakeFargette_0920_ALND_UNK	Bacteroidetes	FAUX	5,91
LakeFargette_0920_ALND_scaffold_122183	LakeFargette_0920_ALND_UNK	Candidate Phyla Radiation	FAUX	5,86
LakeFargette_0920_ALND_scaffold_624629	LakeFargette_0920_ALND_Ignavibacteriales_43_5	Ignavibacteria	FAUX	5,85
LakeFargette_0920_ALND_scaffold_458886	LakeFargette_0920_ALND_UNK	Bacteroidetes	FAUX	5,83
LakeFargette_0920_ALND_scaffold_524793	LakeFargette_0920_ALND_Gammaproteobacteria_39_5	Proteobacteria	FAUX	5,83
LakeFargette_0920_ALND_scaffold_458193	LakeFargette_0920_ALND_UNK	Actinobacteria	FAUX	5,82
LakeFargette_0920_ALND_scaffold_204951	LakeFargette_0920_ALND_UNK	Verrucomicrobia	FAUX	5,74
LakeFargette_0920_ALND_scaffold_634250	LakeFargette_0920_ALND_UNK	Verrucomicrobia	FAUX	5,71
LakeFargette_0920_ALND_scaffold_606014	LakeFargette_0920_ALND_UNK	Planctomycetes	FAUX	5,68
LakeFargette_0920_ALND_scaffold_898784	LakeFargette_0920_ALND_UNK	Lentisphaerae	FAUX	5,66
LakeFargette_0920_ALND_scaffold_1078232	LakeFargette_0920_ALND_UNK	Bacteroidetes	FAUX	5,62
LakeFargette_0920_ALND_scaffold_777089	LakeFargette_0920_ALND_UNK	Proteobacteria	FAUX	5,51
LakeFargette_0920_ALND_scaffold_387256	LakeFargette_0920_ALND_UNK	Planctomycetes	FAUX	5,5
LakeFargette_0920_ALND_scaffold_1035013	LakeFargette_0920_ALND_UNK	Planctomycetes	FAUX	5,5
LakeFargette_0920_ALND_scaffold_653084	LakeFargette_0920_ALND_UNK	unknown	FAUX	5,47
LakeFargette_0920_ALND_scaffold_1008936	LakeFargette_0920_ALND_UNK	Proteobacteria	FAUX	5,39
LakeFargette_0920_ALND_scaffold_199395	LakeFargette_0920_ALND_UNK	Chloroflexi	FAUX	5,36
LakeFargette_0920_ALND_scaffold_993087	LakeFargette_0920_ALND_UNK	Planctomycetes	FAUX	5,32
LakeFargette_0920_ALND_scaffold_437057	LakeFargette_0920_ALND_UNK	Chloroflexi	FAUX	5,29
LakeFargette_0920_ALND_scaffold_23882	LakeFargette_0920_ALND_UNK	Bdellovibrio	FAUX	5,24
LakeFargette_0920_ALND_scaffold_941758	LakeFargette_0920_ALND_UNK	Proteobacteria	FAUX	5,18
LakeFargette_0920_ALND_scaffold_703634	LakeFargette_0920_ALND_UNK	Planctomycetes	FAUX	5,17
LakeFargette_0920_ALND_scaffold_84111	LakeFargette_0920_ALND_UNK	Candidate Phyla Radiation	FAUX	5,1
LakeFargette_0920_ALND_scaffold_314964	LakeFargette_0920_ALND_UNK	Proteobacteria	FAUX	5,05
LakeFargette_0920_ALND_scaffold_4142	LakeFargette_0920_ALND_UNK	Planctomycetes	FAUX	4,99
LakeFargette_0920_ALND_scaffold_905352	LakeFargette_0920_ALND_UNK	unknown	FAUX	4,88
LakeFargette_0920_ALND_scaffold_667746	LakeFargette_0920_ALND_UNK	Proteobacteria	FAUX	4,76
LakeFargette_0920_ALND_scaffold_466018	LakeFargette_0920_ALND_UNK	Planctomycetes	FAUX	4,71
LakeFargette_0920_ALND_scaffold_688680	LakeFargette_0920_ALND_UNK	Chloroflexi	FAUX	4,52
LakeFargette_0920_ALND_scaffold_610251	LakeFargette_0920_ALND_UNK	Verrucomicrobia	FAUX	4,38
LakeFargette_0920_ALND_scaffold_760013	LakeFargette_0920_ALND_UNK	unknown	FAUX	4,29
LakeFargette_0920_ALND_scaffold_164266	LakeFargette_0920_ALND_Parcubacteria_34_5	Candidate Phyla Radiation	FAUX	4,22
LakeFargette_0920_ALND_scaffold_449776	LakeFargette_0920_ALND_UNK	Candidate Phyla Radiation	FAUX	4,02
LakeFargette_0920_ALND_scaffold_19460	LakeFargette_0920_ALND_UNK	Verrucomicrobia	FAUX	3,69
LakeFargette_0920_ALND_scaffold_455567	LakeFargette_0920_ALND_UNK	Verrucomicrobia	FAUX	3,45
LakeFargette_0920_ALND_scaffold_87228	LakeFargette_0920_ALND_UNK	Proteobacteria	FAUX	3,29
LakeFargette_0920_ALND_scaffold_538712	LakeFargette_0920_ALND_UNK	Bacteroidetes	FAUX	3,2

One motivation of our study was to seek clues to the origin of ALNs, and it is also intriguing to find them coenriched with *Planctomycetes* and CPR bacteria. Their defined morphologies suggest that they develop under genetic control; however, the genetic system responsible for producing ALNs remains unknown. We found no evidence for nucleic acid sequences from completely unknown organisms or mobile genetic elements or were not able to extract them with the methods used here. Thus, one possible interpretation is that ALNs originate from cooccurring bacteria and that *Planctomycetes* and CPR should be among candidates for further study.

Materials and methods can be found in the supplemental material.

Data availability

Read data and draft genomes from this study are available through NCBI at PRJNA757735. Genome accession information for the 48 bacterial and archaeal genomes is also listed in Table S3 at https://zenodo.org/record/5362898#.YiuiRBPML5Y. Custom codes for the described analyses are also available on GitHub (github.com/alexanderjaffe/aln-enrichment). All supplementary figures, tables, extended data files, and genomes (including phage/viral genomes) are also available through Zenodo (https://doi.org/10.5281/zenodo.5362897).

ACKNOWLEDGMENTS

We thank Alex Crits-Christoph, Adair Borges, Rohan Sachdeva, and Yue Clare Lou for informatics support and helpful discussions. We also thank Plateforme CYSTEM-UCA PARTNER (Clermont-Ferrand, France) for their technical support and expertise, the Innovative Genomics Institute, and the Vincent J. Coates Genomics Sequencing Laboratory at UC Berkeley.

M.F., H.B., J.C., and T.S.-N. performed sample collection, incubation experiments, and microscopy. A.L.J., L.-X.C., M.C.S., and J.F.B. performed metagenomics and sequence analysis, and J.F.B carried out the manual genome curation. All authors contributed to project design and manuscript writing.

J.F.B. is a founder of Metagenomi. The other authors declare no competing interests.

Funding was provided by the Innovative Genomics Institute at UC Berkeley, the Chan Zuckerberg Biohub, and a Moore Foundation grant 71785. M.F. was supported by a Ph.D. fellowship from the CPER 2015-2020 SYMBIOSE challenge program (French Ministry of Research, UCA, CNRS, INRA, Auvergne-Rhône-Alpes Region, FEDER). M.C.S. was supported by a DFG fellowship. This study is a contribution to the "C NO LIMIT" project funded by the Interdisciplinary Mission of the French National Center of Scientific Research (CNRS) Program X-life, 2018 edition. This research was also financed by the French government IDEX-ISITE initiative 16-IDEX-0001 (CAP 20-25).

5.2.5 Supplemental materials

In vitro incubation, selection, and sequencing of microbial communities associated with ALNs

Lake Fargettes is an artificial and highly eutrophic freshwater lake (surface area 1.2 ha, maximum depth 2.5 m) near Neuville in the French Massif Central (45°44'24"N; 3°27'39"E;

Table S2. Relative abundance data during monthly sampling of Lake Fargettes ("prelim", based on amplicon sequencing) and at incubation end point ("end", based on metagenomic sequencing of ribosomal protein S3). Percent change between end point and preliminary average is also shown. Only lineages detected by both sequencing efforts are shown here.

lineage	prelim_relative_abundance	end_relative_abundance	percent_change
Planctomycetes	0,063892308	0,272084772	3,258490288
Proteobacteria	0,340461538	0,243024664	-0,286190547
Candidate Phyla Radiation	0,001776923	0,093725909	51,74618252
Actinobacteria	0,016492308	0,087798011	4,323573425
Verrucomicrobia	0,002846154	0,077431372	26,20561715
Acidobacteria	0,011692308	0,036826707	2,149652585
Chloroflexi	0,021438462	0,035126866	0,6384975
Gemmatimonadetes	0,005346154	0,020292756	2,795767272
Lentisphaerae	0,045869231	0,017314442	-0,622526001
Bacteroidetes	0,235038462	0,013364106	-0,94314077
Spirochaetes	0,010530769	0,0077666	-0,262485045
Armatimonadetes	9,23E-05	0,003835417	40,55035122
Elusimicrobia	0,010492308	0,003672615	-0,649970681

Table S3. Characteristics of bacterial and archaeal genomes reconstructed in this study.

bioproject	biosample	genome_name	genome_id	lineage	gtdbtk_classification	bin_length_bp	num_scaffolds	checkm_completene	checkm_redundancy	rna_read_count
PRINA757735	SAMN20994847	LakeFargette_0920_ALND_Actinobacteria_63_63	None	Actinobacteria	d__Bacteria;p__Actin	3206627	18	93,59	2,14	2734
PRINA757735	SAMN20994881	LakeFargette_0920_ALND_Mycobacterium_68_14	None	Actinobacteria	d__Bacteria;p__Actin	2909805	462	90,26	5,05	854
PRINA757735	SAMN20994879	LakeFargette_0920_ALND_Alphaproteobacteria_58_11	None	Alphaproteobacteria	d__Bacteria;p__Prote	2110177	87	96,16	2,2	1181
PRINA757735	SAMN20994877	LakeFargette_0920_ALND_Alphaproteobacteria_61_16	None	Alphaproteobacteria	d__Bacteria;p__Prote	3485382	417	76,93	2,33	3993
PRINA757735	SAMN20994837	LakeFargette_0920_ALND_Parvibaculum_lavamentivorans_63_19	None	Alphaproteobacteria	d__Bacteria;p__Prote	3624273	53	95,16	9,28	10245
PRINA757735	SAMN20994865	LakeFargette_0920_ALND_Armatimonadetes_54_8	None	Armatimonadetes	d__Bacteria;p__Arma	3129870	282	93,98	2,78	2147
PRINA757735	SAMN20994874	LakeFargette_0920_ALND_Bacteroidetes_35_6	None	Bacteroidetes	d__Bacteria;p__Bacte	3640609	793	82,7	1,92	3650
PRINA757735	SAMN20994864	LakeFargette_0920_ALND_Betaproteobacteria_49_15	None	Betaproteobacteria	d__Bacteria;p__Prote	2525574	172	89,87	2,2	89
PRINA757735	SAMN20994844	LakeFargette_0920_ALND_Betaproteobacteria_62_19	None	Betaproteobacteria	d__Bacteria;p__Prote	3967837	704	85,33	4,7	5537
PRINA757735	SAMN20994843	LakeFargette_0920_ALND_Methylophilales_50_13	None	Betaproteobacteria	d__Bacteria;p__Prote	1454965	104	78,34	0,36	2656
PRINA757735	SAMN20994867	LakeFargette_0920_ALND_Rhodocyclales_64_19	None	Betaproteobacteria	d__Bacteria;p__Prote	2912685	567	86,6	4,23	1891
PRINA757735	SAMN20994836	LakeFargette_0920_ALND_Burkholderiales_70_71	None	Burkholderiales	d__Bacteria;p__Prote	5281630	30	97,2	3,42	27443
PRINA757735	SAMN20994838	LakeFargette_0920_ALND_Chloroflexi_53_29	None	Chloroflexi	d__Bacteria;p__Chlor	3869740	17	97,27	2	4273
PRINA757735	SAMN20994863	LakeFargette_0920_ALND_Kaiserbacteria_55_14	C6	CPR (Kaiserbacteria)	d__Bacteria;p__Pates	867436	43	97,6744186	0	349
PRINA757735	SAMN20994859	LakeFargette_0920_ALND_Nomurabacteria_33_28	C9	CPR (Nomurabacteria	d__Bacteria;p__Pates	691430	7	95,34883721	0	68
PRINA757735	SAMN20994869	LakeFargette_0920_ALND_Nomurabacteria_36_7	C8	CPR (Nomurabacteria	d__Bacteria;p__Pates	527439	84	86,04651163	0	411
PRINA757735	SAMN20994842	LakeFargette_0920_ALND_PER-li_52_24	C2	CPR (Peribacteria)	d__Bacteria;p__Pates	1239242	1	97,6744186	0	648
PRINA757735	SAMN20994873	LakeFargette_0920_ALND_Parcubacteria_36_7	C7	CPR (Nomurabacteria	d__Bacteria;p__Pates	500334	102	86,04651163	0	32
PRINA757735	SAMN20994841	LakeFargette_0920_ALND_Parcubacteria_41_22	C4	CPR (Vogelbacteria)	d__Bacteria;p__Pates	689206	5	97,6744186	0	277
PRINA757735	SAMN20994840	LakeFargette_0920_ALND_Parcubacteria_45_23	C1	CPR (Andersenbacteri	d__Bacteria;p__Pates	913537	4	97,6744186	0	91
PRINA757735	SAMN20994855	LakeFargette_0920_ALND_Parcubacteria_54_14	C3	CPR (Uhrbacteria)	d__Bacteria;p__Pates	1050475	23	97,6744186	0	30
PRINA757735	SAMN20994839	LakeFargette_0920_ALND_Parcubacteria_55_23	C5	CPR (Parcubacteria)	d__Bacteria;p__Pates	694997	5	97,6744186	0	168
PRINA757735	SAMN20994850	LakeFargette_0920_ALND_Bacteria_57_7	None	Deltaproteobacteria	d__Bacteria;p__UBA2	2607638	385	73,03	1,78	939
PRINA757735	SAMN20994871	LakeFargette_0920_ALND_Deltaproteobacteria_72_12	None	Deltaproteobacteria	d__Bacteria;p__Myxo	10778332	564	93,87	5,05	12702
PRINA757735	SAMN20994854	LakeFargette_0920_ALND_Gemmatimonadetes_70_15	None	Gemmatimonadetes	d__Bacteria;p__Gem	3081198	56	94,82	1,2	3775
PRINA757735	SAMN20994853	LakeFargette_0920_ALND_Bacteria_66_32	None	Lentisphaerae	d__Bacteria;p__Verr	5430970	42	91,39	4,05	11418
PRINA757735	SAMN20994878	LakeFargette_0920_ALND_Nitrospirae_57_8	None	Nitrospirae	d__Bacteria;p__Nitro	2366434	1019	82,56	7,07	2954
PRINA757735	SAMN20994849	LakeFargette_0920_ALND_Bacteria_70_12	P5	Planctomycetes	d__Bacteria;p__Plan	5498985	184	88,57	2,27	5658
PRINA757735	SAMN20994875	LakeFargette_0920_ALND_Planctomycetales_59_8	P8	Planctomycetes	d__Bacteria;p__Plan	5600513	924	85,02	8,22	963
PRINA757735	SAMN20994880	LakeFargette_0920_ALND_Planctomycetes_58_8	P6	Planctomycetes	d__Bacteria;p__Plan	6322228	792	85,57	3,95	4253
PRINA757735	SAMN20994868	LakeFargette_0920_ALND_Planctomycetes_59_20	P10	Planctomycetes	d__Bacteria;p__Plan	6576304	457	89,08	4,67	1652
PRINA757735	SAMN20994866	LakeFargette_0920_ALND_Planctomycetes_60_11	P7	Planctomycetes	d__Bacteria;p__Plan	9797810	293	95,05	4,65	9728
PRINA757735	SAMN20994851	LakeFargette_0920_ALND_Planctomycetes_64_91	P4	Planctomycetes	d__Bacteria;p__Plan	2801258	8	98,48	0	5670
PRINA757735	SAMN20994862	LakeFargette_0920_ALND_Planctomycetes_66_10	P1	Planctomycetes	d__Bacteria;p__Plan	4573548	377	86,55	2,34	5812
PRINA757735	SAMN20994858	LakeFargette_0920_ALND_Planctomycetes_66_46	P3	Planctomycetes	d__Bacteria;p__Plan	4373169	67	96,59	1,14	9384
PRINA757735	SAMN20994857	LakeFargette_0920_ALND_Planctomycetes_68_24	P2	Planctomycetes	d__Bacteria;p__Plan	4738582	62	89,78	4,84	10152
PRINA757735	SAMN20994860	LakeFargette_0920_ALND_Planctomycetia_61_12	P11	Planctomycetes	d__Bacteria;p__Plan	7079622	167	96,13	1,15	805
PRINA757735	SAMN20994872	LakeFargette_0920_ALND_Planctomycetia_62_14	P9	Planctomycetes	d__Bacteria;p__Plan	5853981	523	95,4	4,77	377
PRINA757735	SAMN20994848	LakeFargette_0920_ALND_Planctomycetia_67_38	P12	Planctomycetes	d__Bacteria;p__Plan	4346575	144	96,55	4,13	295
PRINA757735	SAMN20994882	LakeFargette_0920_ALND_Leptospira_40_6	None	Spirochaetes	d__Bacteria;p__Spiro	2990272	730	88,54	0,11	13285
PRINA757735	SAMN20994861	LakeFargette_0920_ALND_Spirochaetia_49_9	None	Spirochaetes	d__Bacteria;p__Spiro	4488021	134	95,29	0,59	7955
PRINA757735	SAMN20994846	LakeFargette_0920_ALND_Nitrosoarchaeum_33_12	None	Thaumarchaeota	d__Archaea;p__Ther	1288093	65	91,42	1,05	658
PRINA757735	SAMN20994835	LakeFargette_0920_ALND_Nitrosoarchaeum_limnia_33_41	None	Thaumarchaeota	d__Archaea;p__Ther	1875056	26	99,03	1,46	20465
PRINA757735	SAMN20994852	LakeFargette_0920_ALND_Chthoniobacter_flavus_63_25	None	Verrucomicrobia	d__Bacteria;p__Verr	5004242	37	97,86	1,38	1440
PRINA757735	SAMN20994856	LakeFargette_0920_ALND_Verrucomicrobia_56_25	None	Verrucomicrobia	d__Bacteria;p__Verr	2395852	32	97,3	1,35	26
PRINA757735	SAMN20994876	LakeFargette_0920_ALND_Verrucomicrobia_57_8	None	Verrucomicrobia	d__Bacteria;p__Verr	3049454	387	86,62	1,36	142
PRINA757735	SAMN20994870	LakeFargette_0920_ALND_Verrucomicrobia_58_12	None	Verrucomicrobia	d__Bacteria;p__Verr	1904895	392	85,66	9,29	110
PRINA757735	SAMN20994845	LakeFargette_0920_ALND_RBG_16_RIF_WS3X_69_13	None	WS3X	d__Bacteria;p__Eiser	2095941	513	82,77	3,4	2424

Table S4. Characteristics of viral (phage and eukaryotic viruses) sequences reconstructed in this study. Abbreviations: mcp - major capsid protein, vltf3 - Poxvirus Late Transcription Factor.

virus_name	virus_id	bin_length_kbp	scaffold_number	checkv_quality	checkv_completene	viral_lineage	marker_gene	predicted_host	prediction_method	rna_coverage_mean	rna_coverage_breadth
LakeFargette_0920_ALND_Phaeocystis_Virus_25_19	V1	453,941	1	High-quality	97,1	Extended Mimiviridae	vltf3	unknown Eukaryota	None	0,002428431	0,001152132
LakeFargette_0920_ALND-Phage-like-45-26	V2	365,116	1	Medium-quality	88,82	probable Caudovirales	mcp	Bacteroidetes	gene content	0,009258397	0,004483507
LakeFargette_0920_ALND_Euk_Virus_uncertain_35_24	V3	328,689	3	None	None	Iridoviridae (Betairidoviridae)	mcp	unknown Eukaryota	None	0,004624679	0,002360894
LakeFargette_0920_ALND_Phage_41_43	V4	318,533	1	Medium-quality	89,55	probable Caudovirales	mcp, terminase	unknown Bacteria	None	0,061799783	0,02814779
LakeFargette_0920_ALND_Euk-Virus-like_43_13	V5	292,118	1	Low-quality	39,18	Phycodnaviridae	mcp	unknown Eukaryota	None	0,005281401	0,001749293
LakeFargette_0920_ALND_Euk_Virus_23_53	V6	269,488	3	None	None	Iridoviridae (Betairidoviridae)	mcp	unknown Eukaryota	None	0,006493507	0,003083625
LakeFargette_0920_ALND_Euk_Virus_60_22	V7	264,161	3	None	None	Pitho-like virus	vltf3	unknown Eukaryota	None	0,003723773	0,0014953
LakeFargette_0920_Bacteroidetes_Phage_31_13	V8	244,156	1	Medium-quality	83,71	probable Caudovirales	mcp, terminase	unknown Bacteria	None	0,003549093	0,002953303
LakeFargette_0920_ALND_Euk_Virus_30_90	V9	239,893	2	None	None	None	None	unknown Eukaryota	None	0,005534385	0,003155574
LakeFargette_0920_ALND_Euk_virus_57_23	V10	222,082	1	Low-quality	40,78	PAM superclade	mcp	unknown Eukaryota	None	0,003703837	0,001864176
LakeFargette_0920_ALND_Bacteroidetes_Phage_34_48	V11	210,042	2	None	None	None	None	unknown Bacteria	None	0,003642571	0,001318784
LakeFargette_0920_ALND_Virus_51_31	V12	200,528	5	None	None	None	None	unknown Eukaryota	None	0,006532251	0,003296298
LakeFargette_0920_ALND_Bacteroidetes_Phage_34_33	V13	199,985	1	Medium-quality	66,26	probable Caudovirales	mcp, terminase	unknown Bacteria	None	0,007621287	0,003885291
LakeFargette_0920_ALND_Euk_Virus_28_48	V14	194,208	2	None	None	None	None	unknown Eukaryota	None	0,001670896	0,000978333
LakeFargette_0920_ALND_Potentially_Complete_Phage_38_44	V15	184,249	1	Medium-quality	70,86	probable Caudovirales	terminase	unknown Bacteria	None	0,008647521	0,004526483
LakeFargette_0920_Potentially_Complete_Phage-like-59_217	V16	161,51	1	Complete	100	None	None	Proteobacteria	gene content	0,24485002	0,07829236
LakeFargette_0920_Euk_virus_35_23	V17	159,398	2	None	None	None	None	unknown Eukaryota	None	0,006976832	0,002691376
LakeFargette_0920_ALND_Virus_31_91	V18	153,302	1	Low-quality	32,65	Iridoviridae (Betairidoviridae)	mcp	unknown Eukaryota	None	0,021109747	0,008786578
LakeFargette_0920_ALND_Phage-like_42_13	V19	134,911	1	Low-quality	26,47	None	None	unknown Bacteria	None	0,001899659	0,00161588
LakeFargette_0920_ALND_Virus_50_31	V20	125,625	1	Low-quality	26,89	novel clade in PAM superclade	mcp	unknown Eukaryota	None	0,004399283	0,002332338
LakeFargette_0920_ALND_Virus_30_12	V21	124,125	2	None	None	None	None	unknown Eukaryota	None	0,028645266	0,00248137
LakeFargette_0920_ALND_Phage-like_AC_TGA_55_18	V22	113,056	1	Not-determined	None	None	None	Planctomycetes	gene content	0,028909003	0,006518893
LakeFargette_0920_ALND_Virus_28_14	V23	106,566	1	Low-quality	32,63	MAPI superclade	mcp, vltf3	unknown Eukaryota	None	0,002086153	0,00090085
LakeFargette_0920_ALND_Putative_Phage_57_26	V24	105,432	1	Complete	100	None	None	unknown Bacteria	None	0,008538972	0,004363002
LakeFargette_0920_ALND_Potentially_Complete_Phage_67_101	V25	105,294	1	Complete	100	probable Caudovirales (Siphoviridae)	mcp, terminase	unknown Bacteria	None	0,0626379	0,035889983
LakeFargette_0920_ALND_Virus_28_46	V26	100,712	1	Low-quality	21,58	Extended Mimiviridae	mcp, vltf3	unknown Eukaryota	None	0,000626479	0,000625546
LakeFargette_0920_ALND_Phage-like_60_19	V27	79,26	1	Low-quality	35,25	None	None	unknown Bacteria	None	0,010163064	0,006156952
LakeFargette_0920_ALND_Phage_44_31	V28	78,461	1	High-quality	100	probable Caudovirales (Siphoviridae)	terminase	Planctomycetes	crispr targeting	0,19995914	0,07282599
LakeFargette_0920_ALND_Phage_34_28	V29	78,261	1	None	None	probable Caudovirales	mcp, terminase	unknown Bacteria	None	0,004096734	0,004088882
LakeFargette_0920_ALND_Virus_42_12	V30	67,091	1	Low-quality	14,36	novel clade in PAM superclade	mcp	unknown Eukaryota	None	0,00061248	0,00061111
LakeFargette_0920_ALND_Virus_49_30	V31	60,882	1	Low-quality	13,03	Extended Mimiviridae	mcp, vltf3	unknown Eukaryota	None	0,001745373	0,001084064
LakeFargette_0920_ALND_Phage-like_59_11	V32	54,736	1	Complete	100	probable Caudovirales (Podoviridae)	terminase	Proteobacteria	gene content	0,005349357	0,002667349
LakeFargette_0920_ALND_Likely_Planctomycete_Phage_53_37	V33	42,71	1	Medium-quality	51,4	None	None	Planctomycetes	gene content	0,004605263	0,002317958
LakeFargette_0920_ALND_Phage_50_35	V34	39,638	1	Medium-quality	62,59	None	None	unknown Bacteria	None	0	0

465 m altitude). Lake water was collected on March 15, 2017 when the highest density of ALNs was recorded in 2017 ($9.0 \pm 0.5 \times 10^7$ ALNs·mL^{-1}). Information about this sample is provided in Colombet *et al*. 2019 [1]. Within two hours after sampling, 100 L of raw lake water was filtered through a 25-µm-pore-size nylon mesh. Microbial communities were enriched by tangential-flow ultrafiltration using a Kross-Flow system (Spectrum, Breda, The Netherlands) equipped with a 0.2-µm cut-off cartridge. Aliquots (600 mL) of this concentrated 0.2 µm−25µm fraction were sequentially centrifuged at 8,000 g, 10,000 g (pellets discarded) then 12,000 g for 20 minutes each time at 14°C. Microbial communities contained in the final supernatant were cultivated for an initial period of 6 months at 4°C in the dark (to favor the development of prokaryotic communities associated with ALNs, instead of phototrophic eukaryotic communities) . The physico-chemical parameters of the starting sample are listed in Table S6.

After 6 months, the selected microbial community was enriched by centrifugation at 6000 g for 20 minutes at 14°C and the pellet (in liquid phase) incubated 25 more months at 4°C in the dark. At the end of the incubation, the medium was sonicated using Elmasonic S30 (Elma, Germany) and microbial communities were pelleted by centrifugation at 6000 g for 20 minutes at 14°C. The pellet suspended in distilled deionized water was used for nucleic acid extraction and amplification.

DNA and RNA extractions were performed using the RNA x DNA from soil kit (740143, Macherey-Nagel, Germany). The RNA sample was treated with Turbo DNA-free Kit (Invitrogen, Massachusetts, USA). The concentration of the samples was checked using a Qubit fluorometer (Invitrogen, Massachusetts, USA).

TEM imaging of enrichment communities

Microbial communities were imaged at T0 and T31 to visualize their evolution, using a JEOL JEM 2100-Plus microscope (JEOL, Akishima, Tokyo, Japan) operating at 80 kV and 40,000x magnification. For each sample, 10 images were randomly captured in order to have a significant representation of microbial communities. We then defined the percentage of different observed phenotypes as a proportion of the total observed communities (Table S1).

Monthly microbial community profiling at Lake Fargettes

Samples were collected every month for 1 year (10/2018 to 09/2019) from the depth interval of 0-40 cm of lake Fargettes. For each sample, microbial communities were collected on a 0.2 µm (Millipore) polycarbonate filter (until saturation, pressure < 25 kPa) and stored at -20°C until DNA extraction. The filters were covered with a lysing buffer (lysozyme 2 mg.mL-1 SDS 0.5%, Proteinase K 100 µg.mL-1 and RNase A 8.33 µg.mL-1 in TE buffer pH 8 at 37°C for 90 minutes. A CTAB 10% / NaCl 5M solution was added, and the samples were incubated at 65°C for 30 minutes. The nucleic acids were extracted with phenol-chloroform-isoamyl alcohol (25:24:1) the aqueous phase containing the nucleic acids was recovered and purified by adding chloroform-isoamyl alcohol (24:1). The nucleic acids were then precipitated with a mixture of glycogen 5mg/mL-1, sodium acetate 3M and ethanol 100% overnight at -20°C. The DNA pellet was rinsed with ethanol (70%), dried and dissolved in TE buffer. The DNA was purified with NucleoSpin® gDNA Clean-up (Macherey-Nagel).

Table S5. Particle composition in the starting and final incubation samples as determined by cell counts.

	ALNs				Virus				Cellular Like Particles			
					Huge (> 100 nm)		Small (< 100 nm)			> 200 nm		
	4-10 arms	11 arms	11 budding arms	20 arms	Tailed	Untailed	Tailed	Untailed	< 200nm (CPR like / vesicles)	Rod-shaped	Spherical	Spiral- shaped
start	9,95	8,25	2,67	5,34	3,88	3,88	14,08	37,62	6,55	4,85	2,18	0,73
end	11,45	16,01	4,15	4,66	0,00	1,93	0,81	55,02	2,13	2,23	1,22	0,41

Table S6. Physico-chemical parameters associated with the starting sample.

pH	TAC	C	P	N	K	Na	Ca	Mg	NH3	NH4+	CO32-	Cl-	NO3-	PO43-	NO2-
7,45	27,65	16	0,28	4	9,6	3,1	9,1	1,7	< 0.05	0,12	0	12,5	3,1	0,05	0,05

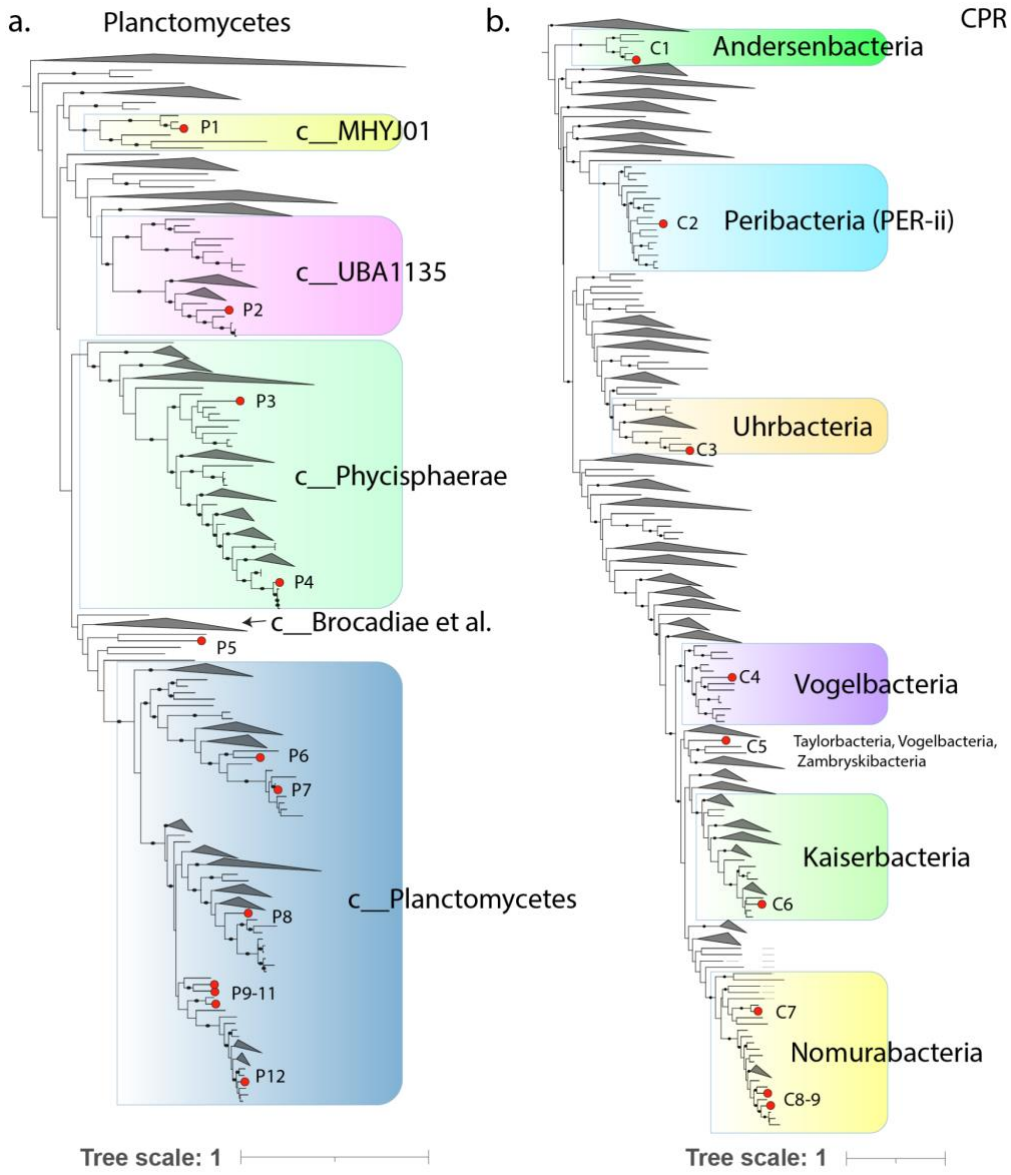

Figure S1. Phylogenetic placement of Planctomycetes (left panel) and CPR bacteria (right panel) genomes reconstructed in this study (indicated by red dots at branch tips).
Scale bar represents the average number of substitutions per site. Black dots at interior nodes indicate ultrafast bootstrap support >=95%.

The amplification of the V4-V5 region of the bacterial small subunit rDNA was performed using the universal bacteria 515F (GTGYCAGCMGCCGCGGTA) and 928R (CCCCGCYAATTCMTTTRAGT) primers modified with barcodes. PCR was performed in a total volume of 50 µL containing 1x final green reaction buffer, 2 mM final $MgCl_2$, 0.2mM final dNTP, 100 $\mu g.mL^{-1}$ final BSA,0.2 µM final of primers, 0.025 $U.\mu L^{-1}$ final PROMEGA GoTaq HotsStart G2 and 5 µL of sample DNA.

To process the bacterial sequencing data (Illumina Miseq©, 2*250 bp), we used the FROGS pipeline [2]. After the clean-up procedure, sequences were assembled and clustered into OTUs with a similarity threshold of 95%. The representative sequences of each OTU were affiliated by similarity using the SILVA_132_16s database.

Metagenomic/metatranscriptomic sequencing, binning, and marker gene analysis

Library preparation and sequencing of extracted DNA and RNA was performed at the Vincent J. Coates Genomics Sequencing Laboratory and Functional Genomics Laboratory at U.C. Berkeley. Extracted RNA was treated with the QiaSeq FastSelect kit to deplete rRNA. Samples were sequenced on a NovaSeq 6000 with 150 bp, paired-end reads. DNA and RNA were sequenced to a depth of ~10 Gbp and 25 million read pairs, respectively. Quality filtering and assembly of DNA reads, as well as binning of assembled scaffolds and genome annotation followed the workflow outlined in [3]. Briefly, metagenomic reads were trimmed using Sickle [4] and subsequently assembled using MEGAHIT (v. 1.2.9) [5]. Gene calls were made with Prodigal ('meta' mode) [6] and genes were annotated with USEARCH [7] against several protein databases. Finally, scaffolds were binned both manually, using GC content, coverage, and phylogenetic profile, as well as in an automated fashion using MetaBAT2 [8]. The highest quality bins were chosen from the set of manual and automated bins using DASTool [9]. Genomes were classified at the phylum or class level based on the majority taxonomic affiliation of member contigs, and supplemented with BLAST searches of ribosomal proteins where necessary. Additionally, genome classification according to the GTDB scheme was assigned by running GTDB-tk with default parameters [10].

For the marker gene analysis (Fig. 1ac), we computed the mean coverage of scaffolds encoding a ribosomal protein S3 (rpS3) gene using bowtie2. Phylum-level taxonomic affiliation of these scaffolds was manually curated based on consensus gene-level taxonomy, binning information, and BLAST searches of protein sequence, where necessary.

Quality filtering and genome curation for bacteria and archaea

Genomic bins were profiled for single copy genes using CheckM. For CPR bacteria, a custom workflow was used with a set of 43 marker genes sensitive to lineage-specific losses of ribosomal proteins in this group. We filtered all bins to those ≥ 70% completeness and ≤10% contamination and removed redundancy in the set at the species level using dRep (95% ANI) [11]. Retained genomic bins were manually 'polished' by removing contigs that were outliers in terms of GC content and coverage. Contigs with aberrant or ambiguous consensus taxonomy were manually expected if ≥ 5 kbp or automatically removed if <5 kbp.

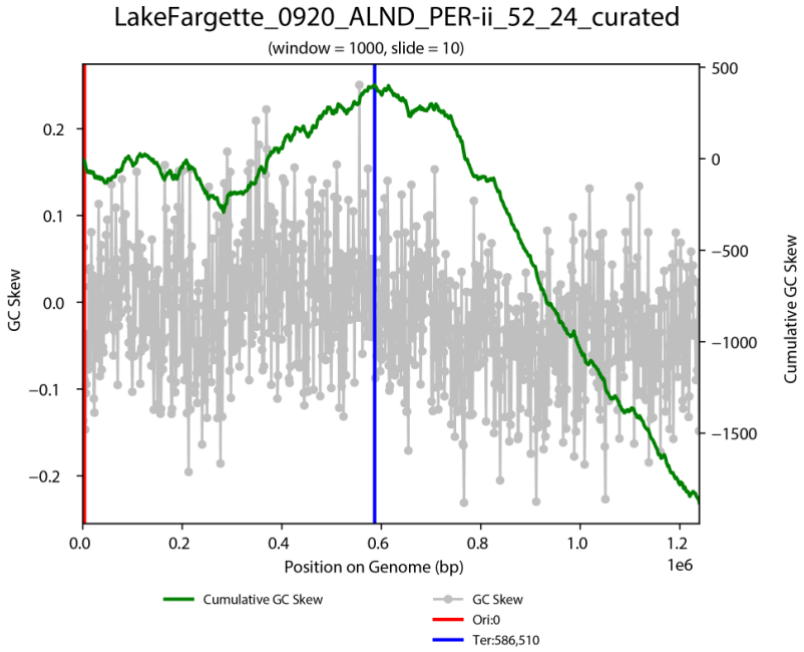

Figure S2. Windowed and cumulative GC skew plot for the Peribacteria/PER-ii genome that was curated to completion.
The peaked nature of cumulative GC skew, beginning at the origin and proceeding through the terminus, suggests that the genome assembly is accurate (see Chen *et al*., 2020 doi:10.1101/gr.258640.119).

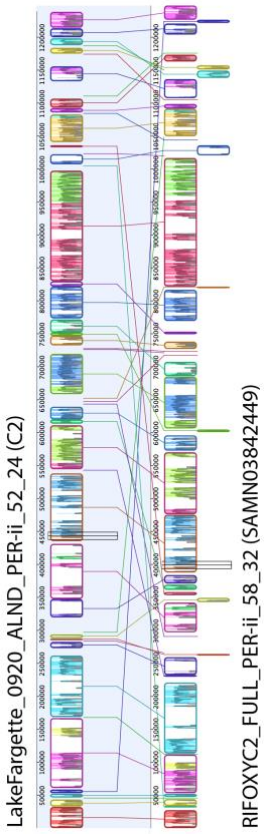

Figure S3. The newly reconstructed, curated Peribacteria genome (top sequence) is largely syntenous with a reference Peribacteria genome from Rifle, CO.
Colored blocks indicate Locally Collinear Blocks as determined by the genome aligner Mauve.

For the Peribacteria genome (LakeFargettes_0920_ALND_PER-ii_52_24), additional manual genome curation was performed. This involved fixing local scaffolding errors and extending the six original contigs using unplaced paired reads. The extended contigs were then joined based on end overlaps and paired read support. This resulted in two contigs, the larger of which was circularized and the other contained the 16S rRNA gene. Based on identification of a sequence within the larger contig that was also present at the end of the smaller contig, the larger contig was broken and joined to the smaller contig. This produced a single linear fragment. We used BLAST against the metagenome of the sample to identify a 4 kbp fragment that perfectly aligned to the ends of the linear fragment, circularizing the genome. The circularization overlap was trimmed and paired read support was verified by visualization throughout the entire final genome. Finally, the start position was adjusted based on the cumulative GC skew (Fig. S2). Genes/proteins were then re-predicted for the curated genome using Prodigal (single) [6].

We selected one of a set of near-identical complete Peribacteria genomes (SAMN03842449) from a previous publication [12] for comparison to the newly curated genome. Full genomes and 16S rRNA sequences were aligned in Geneious (Mauve plugin and MAFFT aligner, respectively).

Phylogenomic and gene content analyses for CPR bacteria and Planctomycetes

For analyses of gene content, we focused on a subset of 21 genomes from the CPR bacteria and Planctomycetes. Gene/protein predictions were re-computed for this subset using Prodigal (single mode). Predicted protein sequences were annotated using kofamscan and resulting HMM hits were preliminarily filtered to those with $e < 1x10^{-6}$ for use in downstream phylogenetic and metabolic analyses.

First, proteins annotated as rpS3 (K02982) were extracted and combined with reference sequences drawn either from NCBI (Planctomycetes) or a previous publication [13] on CPR phylogeny as well as a balanced sampling of other bacterial phyla as an outgroup. Each sequence set was aligned using mafft (*auto) [14]* and the resulting alignment was trimmed using trimal (*gt 0.1*) [15]. Maximum-likelihood trees were inferred using iqtree (*-m TEST -safe -st AA -bb 1500 -nt AUTO -ntmax 20*) [16] and subsequently visualized/annotated using iTOL [17].

For analyses of metabolism, we stringently filtered the kofamscan results, requiring that protein hits attain a score equal to or greater than the model specific thresholds for each KO. Results were then passed to KEGGDecoder [18] for visualization. For CRISPR-Cas analyses, we employed a custom script that first identifies repeat regions on scaffolds using PILER-CR [19] with default parameters, then detects Cas protein using the TIGRFAM HMM database [20] using hmmsearch [21] within 10 kbp (both upstream and downstream) of each identified repeat region. If at least one Cas protein was detected for a given repeat region, the spacer sequences from the adjacent CRISPR locus and also the paired reads and unplaced paired reads were extracted to identify spacer targets. Target identification was performed by blastn-short with an

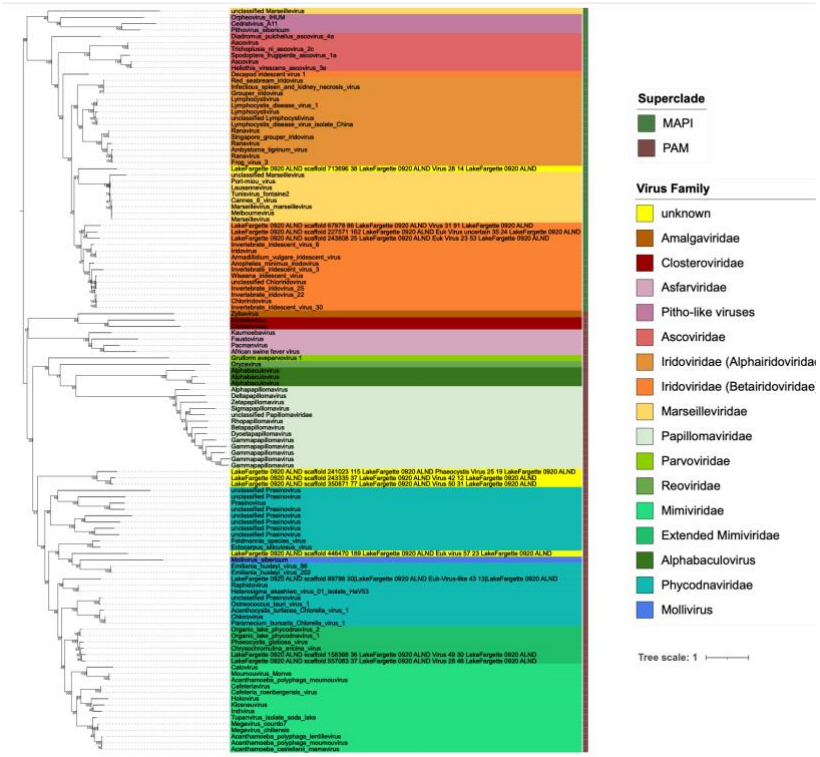

Figure S4. Maximum likelihood (ML) single-protein tree of major capsid protein from putative eukaryotic virus genomes. The tree is rooted between the PAM and the MAPI putative superclades (see: doi.org/10.1073/pnas.1912006116).

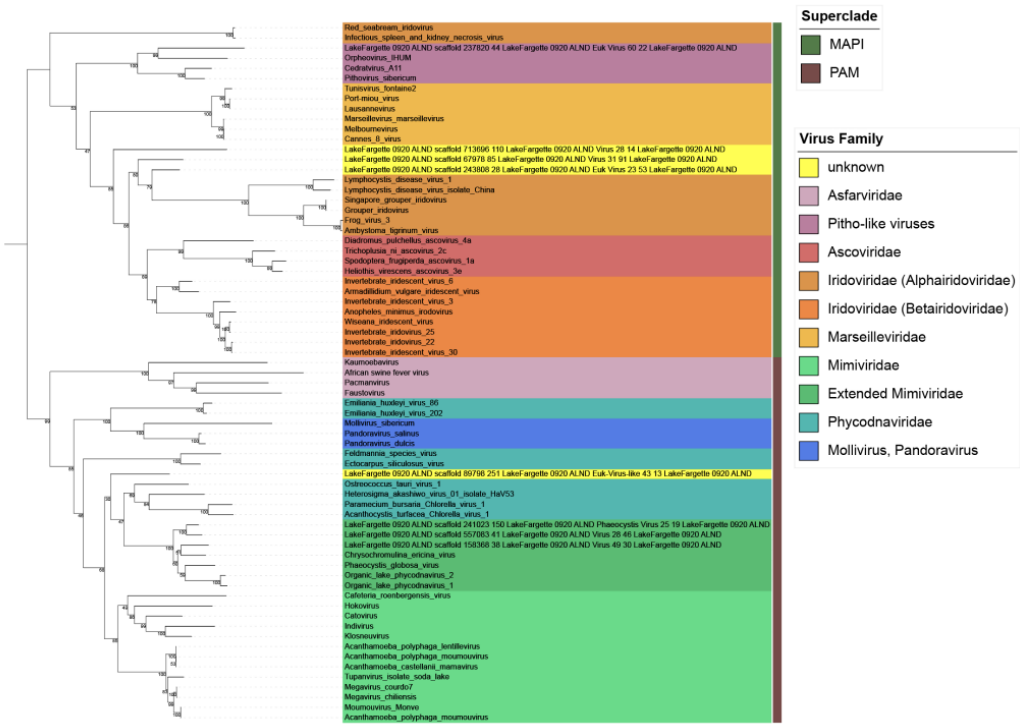

Figure S5. Maximum likelihood (ML) single-protein tree of VLTF3-like protein from putative eukaryotic virus genomes.

The tree is rooted between the PAM and the MAPI putative superclades (see: doi.org/10.1073/pnas.1912006116).

e-value threshold of $1x10^{-3}$. Hits were further filtered to those in which the spacer and targeted sequence were aligned over ≥90% of the spacer length and with no more than 2 mismatches.

Viral genome identification and analysis

Viral genomes were identified through taxonomic profiling and identification of key viral structural proteins. While most recovered viral genomes were single-contig, in some cases multiple contigs of putative viral origin were binned together on the basis of GC content, coverage, and scaffold overlap. Viral genomes were tentatively classified as bacteriophage or eukaryotic viruses based on taxonomic profiling. Completeness and quality information for single-contig viruses was estimated using CheckV [22].

To establish phylogenetic affiliation of bacteriophages, we gathered curated sets of reference sequences for viral terminase and major capsid protein (MCP) from RefSeq. Reference sets were filtered to those sequences with sequence lengths 1±0.5 times the median and subsequently de-replicated at 95% identity using usearch (*-cluster_fast, -id 0.95*) [7]. Proteins for the newly identified phage genomes were predicted using Prodigal (meta mode). Terminase and MCP sequences were identified using BLAST (*-evalue 1e-20*) against a database built from the reference set. Sequences were concatenated with those of the reference set and aligned using MAFFT (*--reorder --auto*). Alignments were trimmed using trimal (*-gt 0.2*) and maximum likelihood trees were inferred using IQtree (*-m TEST -st AA*, version 1.6.12). Trees were decorated using taxonomic information for RefSeq sequences and putative lineages were assigned to newly identified phage genomes based on tree placement.

Host prediction for phages was performed using a combination of CRISPR-Cas targeting (described above) and taxonomic profiling. Briefly, for phylogenetic profiling, phage proteins were compared against UniRef100 using a custom DIAMOND database (*diamond blastp)* [23]. Hits were filtered to those with 70% or greater coverage of the query sequence and an e-value less than or equal to $1x10^{-10}$. We retrieved taxonomic affiliation for above-threshold hits and computed the percentage of genes on each phage with highest similarity to various bacterial lineages. If the bacterial lineage with the most hits among phage genes reached a percentage ≥ 3x that of the next highest lineage, it was assigned as the putative phage host. This method was previously shown to be consistent with host prediction via CRISPR-Cas targeting [24].

To infer the taxonomy of the 17 putative viruses of eukaryotes, all proteins were profiled against the Pfam database. 17 major capsid proteins (PF16903|PF04451) from 11 eukaryotic virus bins and 8 VLTF3-like proteins (PF04947) from 8 bins served as markers. If there were multiple major capsid proteins per bin, the protein with the highest PFAM score was selected. The marker proteins were aligned with a reference dataset of capsid or VLTF3-like proteins from Nucleo-Cytoplasmic Large DNA Viruses [25] and 48 additional capsid proteins retrieved from NCBI (Extended Data File 1-2). The sequences were aligned, trimmed and the phylogenetic tree was constructed as described above. Finally, viruses were taxonomically classified based on phylogenetic placement.

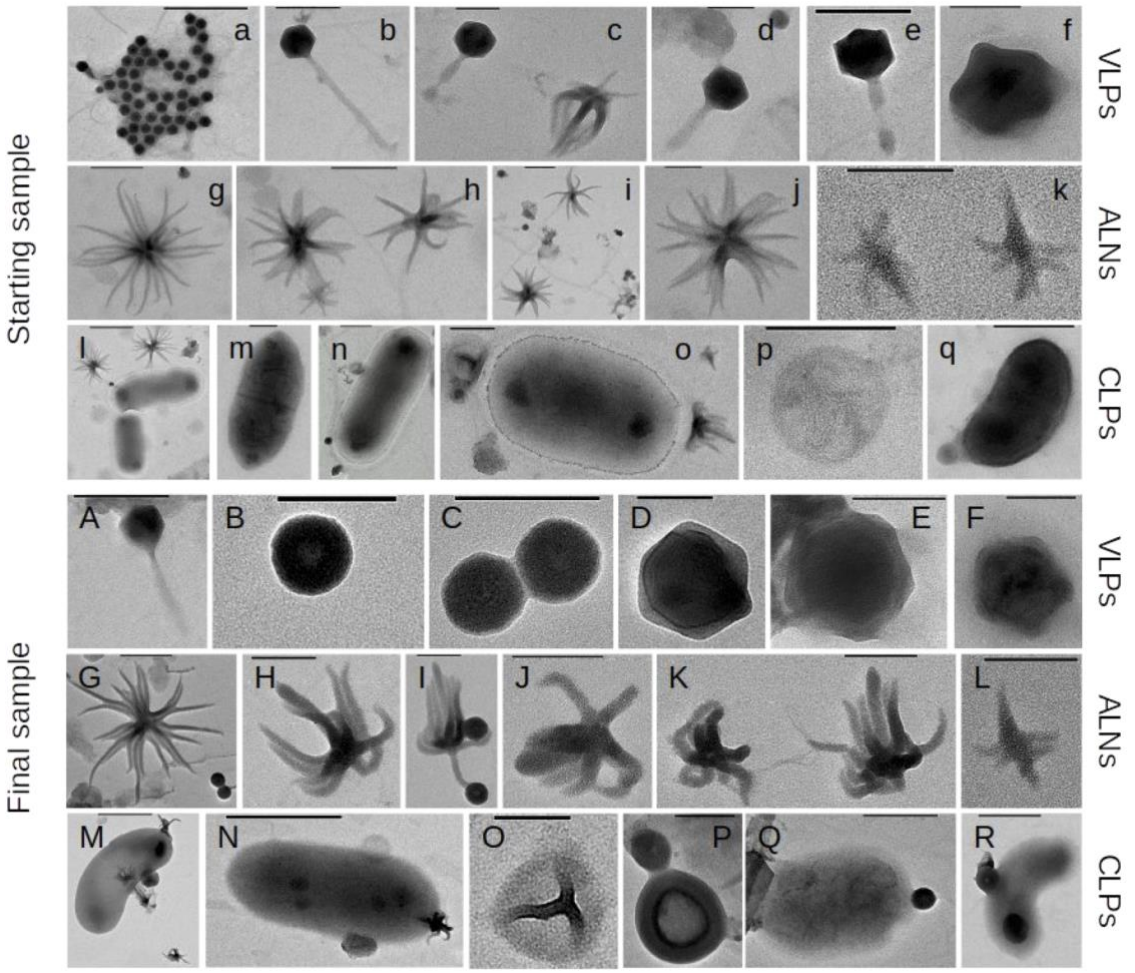

Figure S6. Transmission electron micrographs of different phenotypes present in starting and final sample after 31 months of incubation.

(a-q): starting sample / (A-R): final sample. VLPs: Virus Like Particles. CLPs: Cellular Like Particles. Scale bar: 500 nm (a, l, M, N, R), 200 nm (b, c, e, g-i, m-q, A, G, Q), 100 nm (d, f, j, k, B-F, H-L, O, P).

Transcriptome analysis

RNA reads were subjected to the same quality filtering pipeline referenced for DNA reads above and were subsequently mapped to the quality-filtered, de-replicated set of bacterial and archaeal genomes using bowtie2. To remove remnant rRNA and other non-mRNAs, we computed per-gene mapped read counts using pysam and removed those > 100 times the median non-zero per-gene read count for each genome. This process filtered about ~60 anomalously high-coverage ORFs, many of which corresponded to 16S rRNA or tRNA regions on scaffolds. Read counts were then aggregated by phylum-level lineage. RNA reads were also mapped against the set of curated viral genomes described above. Mean coverage and coverage breadth were computed using CoverM (*genome mode, --min-read-percent-identity 0.95 --min-covered-fraction 0*).

REFERENCES:

1. Colombet J, Billard H, Viguès B, Balor S, Boulé C, Geay L, et al. Discovery of High Abundances of Aster-Like Nanoparticles in Pelagic Environments: Characterization and Dynamics. *Front Microbiol* 2019; **10**: 2376.
2. Escudié F, Auer L, Bernard M, Mariadassou M, Cauquil L, Vidal K, et al. FROGS: Find, Rapidly, OTUs with Galaxy Solution. *Bioinformatics* 2018; **34**: 1287–1294.
3. He C, Keren R, Whittaker ML, Farag IF, Doudna JA, Cate JHD, et al. Genome-resolved metagenomics reveals site-specific diversity of episymbiotic CPR bacteria and DPANN archaea in groundwater ecosystems. *Nat Microbiol* 2021.
4. Joshi NA, Fass J, Others. Sickle: A sliding-window, adaptive, quality-based trimming tool for FastQ files (Version 1.33)[Software]. 2011.
5. Li D, Liu C-M, Luo R, Sadakane K, Lam T-W. MEGAHIT: an ultra-fast single-node solution for large and complex metagenomics assembly via succinct de Bruijn graph. *Bioinformatics* 2015; **31**: 1674–1676.
6. Hyatt D, Chen G-L, Locascio PF, Land ML, Larimer FW, Hauser LJ. Prodigal: prokaryotic gene recognition and translation initiation site identification. *BMC Bioinformatics* 2010; **11**: 119.
7. Edgar RC. Search and clustering orders of magnitude faster than BLAST. *Bioinformatics* 2010; **26**: 2460–2461.
8. Kang D, Li F, Kirton ES, Thomas A, Egan RS, An H, et al. MetaBAT 2: an adaptive binning algorithm for robust and efficient genome reconstruction from metagenome assemblies.
9. Sieber CMK, Probst AJ, Sharrar A, Thomas BC, Hess M, Tringe SG, et al. Recovery of genomes from metagenomes via a dereplication, aggregation and scoring strategy. *Nat Microbiol* 2018; **3**: 836–843.
10. Chaumeil P-A, Mussig AJ, Hugenholtz P, Parks DH. GTDB-Tk: a toolkit to classify genomes with the Genome Taxonomy Database. *Bioinformatics* 2019.
11. Olm MR, Brown CT, Brooks B, Banfield JF. dRep: a tool for fast and accurate genomic comparisons that enables improved genome recovery from metagenomes through de-replication. *ISME J* 2017; **11**: 2864–2868.
12. Anantharaman K, Brown CT, Burstein D, Castelle CJ, Probst AJ, Thomas BC, et al. Analysis of five complete genome sequences for members of the class Peribacteria in the recently recognized Peregrinibacteria bacterial phylum. *PeerJ* 2016; **4**: e1607.
13. Jaffe AL, Castelle CJ, Matheus Carnevali PB, Gribaldo S, Banfield JF. The rise of diversity in metabolic platforms across the Candidate Phyla Radiation. *BMC Biology* . 2020. , **18**
14. Katoh K, Standley DM. MAFFT multiple sequence alignment software version 7: improvements in performance and usability. *Mol Biol Evol* 2013; **30**: 772–780.
15. Capella-Gutiérrez S, Silla-Martínez JM, Gabaldón T. trimAl: a tool for automated alignment trimming in large-scale phylogenetic analyses. *Bioinformatics* 2009; **25**: 1972–1973.
16. Nguyen L-T, Schmidt HA, von Haeseler A, Minh BQ. IQ-TREE: a fast and effective stochastic algorithm for estimating maximum-likelihood phylogenies. *Mol Biol Evol* 2015; **32**: 268–274.
17. Letunic I, Bork P. Interactive tree of life (iTOL) v3: an online tool for the display and annotation of phylogenetic and other trees. *Nucleic Acids Res* 2016; **44**: W242–5.
18. Graham ED, Heidelberg JF, Tully BJ. Potential for primary productivity in a globally-distributed bacterial phototroph. *The ISME Journal* . 2018. , **12**: 1861–1866
19. Edgar RC. PILER-CR: fast and accurate identification of CRISPR repeats. *BMC Bioinformatics* 2007; **8**: 18.
20. Haft DH, Selengut JD, White O. The TIGRFAMs database of protein families. *Nucleic Acids Res* 2003; **31**: 371–373.
21. Johnson LS, Eddy SR, Portugaly E. Hidden Markov model speed heuristic and iterative HMM search procedure. *BMC Bioinformatics* 2010; **11**: 431.
22. Nayfach S, Camargo AP, Schulz F, Eloe-Fadrosh E, Roux S, Kyrpides NC. CheckV assesses the quality and completeness of metagenome-assembled viral genomes. *Nat Biotechnol* 2021; **39**: 578–585.
23. Buchfink B, Reuter K, Drost H-G. Sensitive protein alignments at tree-of-life scale using DIAMOND. *Nat Methods* 2021; **18**: 366–368.
24. Al-Shayeb B, Sachdeva R, Chen L-X, Ward F, Munk P, Devoto A, et al. Clades of huge phages from across Earth's ecosystems. *Nature* 2020; **578**: 425–431.
25. Guglielmini J, Woo AC, Krupovic M, Forterre P, Gaia M. Diversification of giant and large eukaryotic dsDNA viruses predated the origin of modern eukaryotes. *Proc Natl Acad Sci U S A* 2019; **116**: 19585–19592.

DISCUSSION ET CONCLUSIONS GÉNÉRALES, PERSPECTIVES

6.1 Les ALNs : un nouvel acteur du femtoplancton

Dans un contexte de changement global, et notamment du réchauffement des eaux de surfaces, il est plus que jamais nécessaire de comprendre le fonctionnement des réseaux trophiques aquatiques dans leur globalité, afin de mieux anticiper l'impact de ces changements [1]. Cela passe par la compréhension des flux biogéochimiques et de leurs équilibres, étroitement associés à l'activité d'entités biologiques de tailles variées. Les progrès scientifiques de ces dernières décennies ont permis la mise en évidence d'une importante diversité de microorganismes et de leur rôles fonctionnels dans les flux de matière et d'énergie, avec notamment l'intégration du concept de boucle microbienne dans les réseaux trophiques [6, 7]. Si les fractions de tailles supérieures (macro et microplancton) sont aujourd'hui largement étudiées, les fractions les plus petites (nano et femtoplancton) ont longtemps été délaissées, dû notamment aux limitations technologiques. La mise en évidence d'une importante diversité dans ces dernières fractions, grâce notamment aux progrès technologiques, remet en question la compréhension des flux de matière et d'énergie qui passent par les écosystèmes aquatiques [18, 24–26].

La compréhension de l'évolution des écosystèmes aquatiques passe nécessairement par une meilleure appréhension du fonctionnement des entités femtoplanctoniques, qui sont à la base de l'organisation trophique de ces écosystèmes. Comme discuté dans Colombet *et al.* [16], les organismes femtoplanctoniques peuvent être classés le long d'un gradient de complexification, allant d'entités minéral-organiques jusqu'aux entités entièrement organiques. Les entités femtoplanctoniques sont aux frontières de la définition actuelle du vivant. L'étude de ce compartiment, au-delà de son rôle dans les écosystèmes aquatiques, pourrait permettre de comprendre les processus qui ont mené à la compartimentalisation cellulaire et ceux qui ont mené à l'apparition de métabolismes cellulaires.

Les écosystèmes aquatiques sont des réservoirs de nouvelles entités nanométriques, sources de nouvelles connaissances écologiques. L'étude du femtoplancton pourrait aussi être un point clé dans la compréhension des limites du vivant et de l'apparition de la vie. La découverte récente de nouvelles femtoparticules, et notamment les ALNs [27] dans les écosystèmes aquatiques soulève la question de leur importance dans ces écosystèmes. Historiquement considérée à travers la seule activité virale, l'importance écologique de toutes les entités nanométriques, y

compris les ALNs nouvellement découverts, est sans doute plus grande qu'on ne l'avait pensée auparavant. La diversité méconnue et l'abondance de toutes ces entités ont nécessairement un impact sur la circulation des éléments conservés qui sont à la base des cycles biogéochimiques. La plupart des effets potentiels du femtoplancton reste donc à explorer, en tenant compte de la diversité des différentes entités qui la composent, mais aussi de leur capacité à interagir avec d'autres entités à l'échelle de l'écosystème.

Cette thèse s'est effectuée dans le cadre de cette découverte, en prenant en compte les apects écologiques, notamment l'importance quantitative, la dynamique et le rôle fonctionnel des ALNs dans les écosystèmes.

La découverte des ALNs soulève de nombreuses questions sur leur nature et leurs potentiels rôles dans l'environnement. Dans un premier temps, il était important de caractériser ces entités, afin de définir leur nature. Les travaux préliminaires à cette thèse ont permis une caractérisation partielle de ces entités. Colombet et collaborateurs [27] ont montré que les ALNs par leur morphologie, leur composition chimique (*i.e.* C, O, Ca, N et K), leur structure amorphe et leur susceptibilté à des traitements physico-chimiques étaient de nouvelles particules bio-compatibles.

La nature des ALNs, couplée à l'observation de contacts étroits avec des cellules (**Figure 22**) [27] suggère une interaction forte avec d'autres organismes dans les écosystèmes [27]. Les études portant sur l'interaction entre certaines entités femtoplanctoniques comme les CPR et DPANN ou les virus et leurs hôtes ont démontré un rôle important de ces interactions dans la structure et le fonctionnement des écosystèmes [22, 23, 219, 223]. Au même titre que ces entités, les ALNs pourraient donc jouer un rôle dans les écosystèmes. Leur capacité à se maintenir *in-vitro* en absence d'hôtes, réduite en comparaison des valeurs retrouvées *in-situ* [27] laisse suggérer différents rôles pour ces différentes formes. Dans tous les cas, négliger l'existence des ALNs et leurs impacts potentiels dans l'environnement, conduira nécessairement à une compréhension partielle des flux de matière et d'énergie dans les écosystèmes.

La découverte des ALNs souligne donc la nécessité d'étudier non seulement les ALNs mais aussi plus en détail l'ensemble du compartiment femtoplanctonique.

6.2 Écologie des ALNs et importance putative

Comprendre l'importance quantitative et fonctionnelle d'entités aquatiques telles que les ALNs passe nécessairement par une appréhension de leur écologie. Cela sous-entend d'étudier leur habitat, leur distribution ainsi que leur trophodynamique dans les milieux naturels, afin de comprendre les facteurs de forçage qui régissent leur importance écologique.

L'étude géographique menée dans Fuster *et al.* [197] à l'échelle du bassin-versant de la Loire a permis de mettre en évidence la présence des ALNs dans un large spectre d'habitats aux caractéristiques hydrologiques différentes (*i.e.* lacs, rivières, vasières, marais, eaux côtières, canaux). Ces résultats ont permis de prouver l'ubiquité des ALNs, capable de se développer dans des environnements physico-chimiques variés. L'étude menée dans Fuster *et al.* [324] complète les résultats ponctuels obtenus précédemment [27, 197], puisqu'elle dresse la dynamique temporelle des ALNs dans différents écosystèmes aquatiques. Cette étude dynamique menée dans 3 lacs du Puy-de-Dôme a permis de confirmer l'importance des paramètres biologiques dans la distribution des ALNs et, notamment, l'importance potentielle des procaryotes. Cette étude a également permis de mettre en évidence une dynamique saisonnière marquée des ALNs, avec une grande amplitude de variation des abondances d'une saison à l'autre, suggérant que les ALNs sont un acteur majeur à intégrer dans les modèles de successions écologiques.

Ces résultats ont permis d'acquérir des informations sur l'écologie des ALNs et de soulever de nouvelles questions sur le rôle de ces entités dans les milieux aquatiques et notamment leur impact sur les autres communautés microbiennes. Leur forte concentration, pouvant être du même ordre que celle des procaryotes ou des VLPs, en font des entités pouvant impacter la biodiversité, l'activité et la structuration des communautés aquatiques. Les fortes variations de leurs abondances naturelles au cours du temps, sous forme de « blooms », en font également des entités pouvant jouer un rôle dans les flux de matière et d'énergie, notamment en mobilisant et en séquestrant des éléments constitutifs (*e.g.* rôle dans l'homéostasie du calcium dans les environnements aquatiques), comme cela a été suggéré pour d'autres entités comme les PMOBs par exemple [18]. La présence des mêmes formes d'ALNs quelque soit la nature du milieu ou sa localisation géographique suggère l'existence, dans la communauté naturelle des ALNs, d'un support d'hérédité constitutionnel ou associé à un symbionte qui permet d'aboutir aux mêmes

conformations phénotypiques. Ces caractéristiques, décrites pour de nombreuses autres entités femtoplanctoniques [19, 110, 139, 243], font des ALNs des acteurs pouvant avoir un impact sur les autres communautés microbiennes. Nos résultats ont donc démontré l'importance des ALNs en tant que nouveaux acteurs dans les écosystèmes aquatiques, qu'il faudra désormais prendre en compte dans l'étude de ces écosystèmes.

Les études en milieu naturel nous ont permis de mettre en avant les facteurs potentiels de forçage pouvant expliquer la distribution des ALNs, notamment un lien étroit avec les communautés de procaryotes. Les études en conditions controlées ont permis de confirmer l'importance de ce lien corrélatif, avec des résultats montrant un développement jusqu'à 20 fois plus important des ALNs en présence d'une forte concentration de procaryotes. En outre, la mise en évidence d'une nouvelle forme d'ALNs dans nos cultures, forme par la suite observée occasionnellement dans l'environnement (données non montrées), soulève également de nombreuses questions sur les relations ontologiques entre les différentes formes d'ALNs et le rôle des procaryotes dans leur développement. La modification du ratio des différentes formes au cours du temps pourrait suggérer une interconnexion des formes, avec un lien entre procaryotes et ALNs plus poussé pour certaines formes que pour d'autres.

Dans tous les cas, déterminer la nature exacte des ALNs et de leurs interactions avec les procaryotes représente un véritable défi pour les recherches futures sur les ALNs.

6.3 Perspectives d'études

Utilisation de la modélisation comme outil d'étude de la dynamique des ALNs dans les environnements

Les expériences *in-situ* et en microcosmes ont permis de mettre en évidence l'importance des communautés procaryotes dans le développement des ALNs. L'utilisation de la modélisation pourrait donc permettre de prévoir la variation des concentrations en ALNs dans l'environnement. A titre d'exemple, la modélisation est utilisée dans la prédiction de blooms

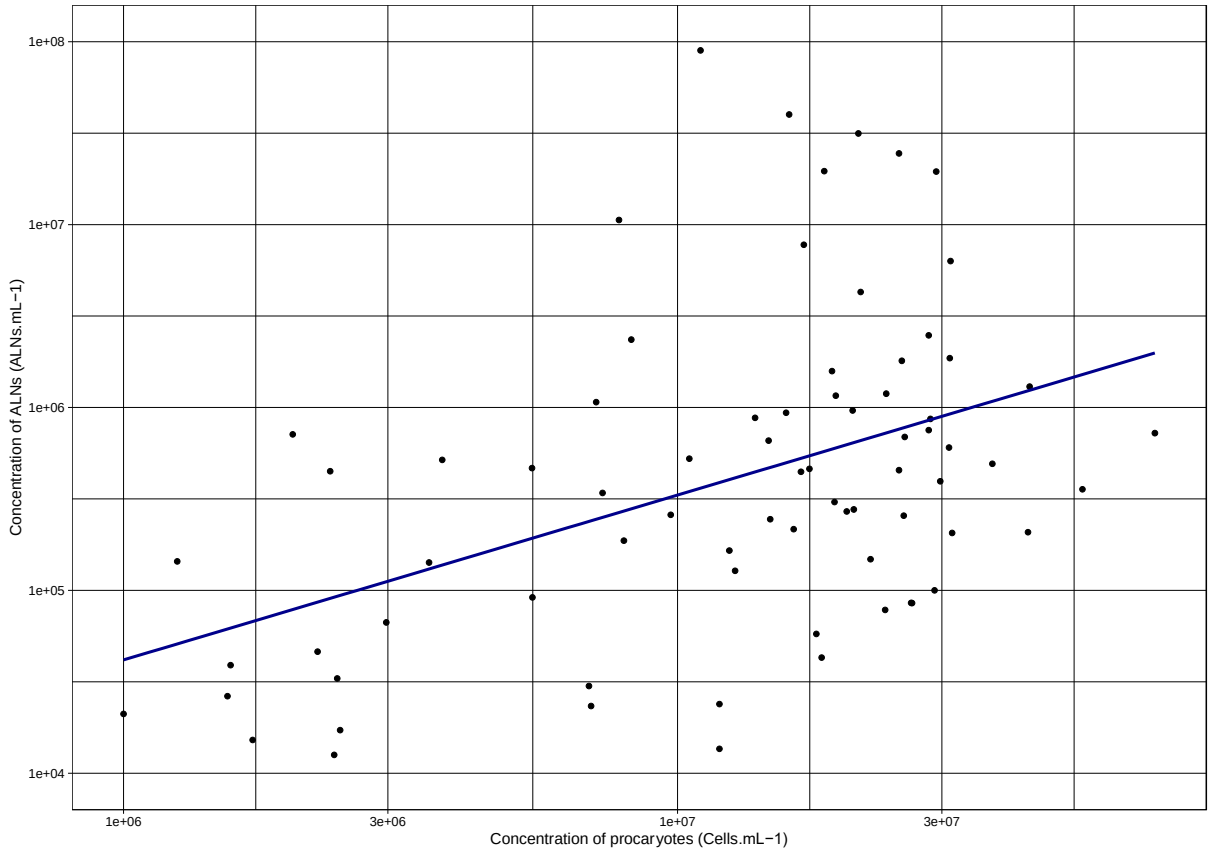

Figure 37 : Evolution de la concentration en ALNs et en procaryotes entre 2017 et 2021 dans le lac Fargettes.

notamment cyanobactériens [336]. La modélisation pourrait donc être un outil puissant pour prédire les variations de la quantité d'ALNs dans l'environnement.

Des résultats annexes de ma thèse, sur le suivi sur le long-terme des ALNs (suivi *in-situ* depuis maintenant plus de 5 ans) semblent indiquer que la concentration en procaryotes pourrait être utilisée comme un éventuel proxy (R^2=0,36, $p < 0.01$) (**Figure 37**), même si ces derniers ne sont pas la seule variable à prendre en compte.

Les résultats du chapitre 3 quant à eux indiquent que la disponibilité en nutriments dans le milieu pourrait aussi jouer un rôle important. Le développement d'un modèle prédictif nécessite donc de suivre la variation de nombreux paramètres *in-situ,* sur plusieurs années, pour pouvoir obtenir un modèle robuste et fiable.

Etude de l'écologie fonctionnelle des ALNs

Les différentes expériences réalisées durant la thèse ont également permis de mettre en évidence des caractéristiques écologiques importantes des ALNs. La prochaine étape sera de déterminer la nature de leurs impacts sur les écosystèmes, et notamment sur les communautés procaryotes. La microcalorimétrie, une technologie disponible au laboratoire, pourrait être envisagée pour :

(i) déterminer l'impact des ALNs sur le métabolisme des procaryotes et
(ii) déterminer si les ALNs ont leur propre métabolisme.

La microcalorimétrie est une approche déjà utilisée en écologie aquatique pour déterminer des modifications de métabolismes dans différentes classes de tailles planctoniques [337–341]. Un développement de méthode pour appliquer cette technique aux ALNs semble donc un moyen pertinent pour quantifier l'impact de ces entités sur les communautés procaryotes.

Des approches par le marquage et le suivi d'incorporation d'éléments constitutifs des ALNs (*i.e.* C, Ca, N, O) pourraient être envisagées. Ce genre de méthode est utilisé classiquement en écologie aquatique pour estimer le rôle d'entités sur les flux énergétiques [342–344], et pourrait permettre d'estimer les flux potentiels transitant directement ou indirectement par les ALNs.
L'utilisation de ces deux approches dans un premier temps pourrait donc nous permettre d'explorer les fonctions et les impacts potentiels des ALNs dans les environnements aquatiques.

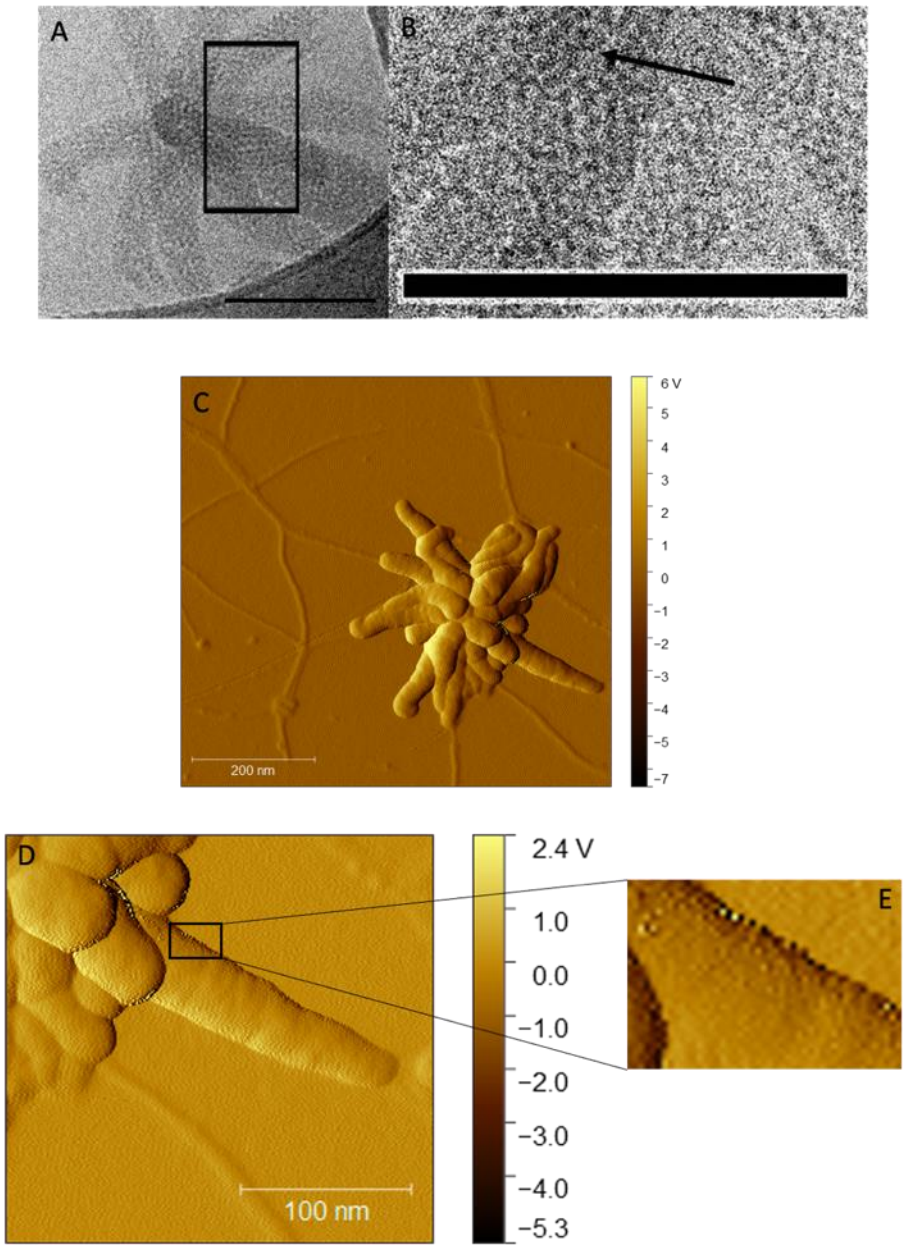

Figure 38 : Images d'ALNs en microscopie électronique à transmission (A,B) ou en microscopie à force atomique (C,D) détaillant la structure des ALNs.

Les images A et B sont issues de Colombet *et al*. [27] et montrent la présence d'une sous-structure circulaire sur les bras des ALNs. La microscopie à force atomique d'ALNs (C-E) avec zoom (E) confirme l'existence d'éléments répartis de façon ordonée à la surface des ALNs. Barre d'échelle (A-B) = 100 nm. *Images AFM David Albertini*

Utilisations d'approches moléculaires

L'étude de l'écologie des ALNs est essentielle dans la compréhension du rôle de ces entités dans les écosystèmes. L'utilisation d'outils moléculaires semble donc nécessaire et complémentaire pour appréhender l'origine des ALNs. L'identification de molécules constitutives et/ou spécifiques des ALNs pourrait permettre non seulement d'étudier l'origine des ALNs (notamment l'origine et le rôle des différentes formes), mais également d'ouvrir de nouvelles perspectives de travail. Cette identification pourrait permettre la mise au point d'outils de marquage, pouvant déboucher sur une identification plus rapide en milieu naturel des ALNs et faciliter leur mise en culture et leur purification, enjeu majeur pour les recherches futures sur les ALNs.

La première étape dans ce travail (déjà mis en place en parallèle de ma thèse) est le développement d'une méthode de purification des ALNs issus du milieu naturel. Des résultats d'approches moléculaires ont déjà été abordés dans Colombet *et al., [27]*. La microscopie électronique à transmission (**Figure 38-A et B)** et la microscopie à force atomique couplée à de la spectrométrie (**Figure 38 C-E)** ont permis de mettre en évidence une structure organisée et des molécules à la surface des ALNs. Ces résultats confirment que l'identification de ces molécules semble une étape complémentaire et importante dans l'appréhension de l'origine des ALNs et de leur rôle dans les environnements aquatiques.

En se basant sur les résultats obtenus durant cette thèse, les perspectives du point de vue écologique sont celles qui pourraient permettre d'améliorer la compréhension du rôle des ALNs dans l'environnement. Ces perspectives et un travail sur la nature exacte des ALNs seront nécessaires pour, à terme, anticiper leurs dynamique et et leur impact dans des environnements en constante évolution.

Références Bibliographiques

1. WHITEHEAD PG, WILBY RL, BATTARBEE RW, et al (2009) A review of the potential impacts of climate change on surface water quality. Hydrological Sciences Journal 54:101–123. https://doi.org/10.1623/hysj.54.1.101

2. Wetzel RG, Rich PH, Miller MC, Allen HL (1972) METABOLISM OF DISSOLVED AND PARTICULATE DETRITAL CARBON IN A TEMPERATE HARD- WATER LAKE. Michigan State Univ., Hickory Corners. W. K. Kellogg Biological Station

3. Li WK, Rao DV, Harrison WG, et al (1983) Autotrophic picoplankton in the tropical ocean. Science 219:292–295. https://doi.org/10.1126/science.219.4582.292

4. Pomeroy LR (1974) The Ocean's Food Web, A Changing Paradigm. BioScience 24:499–504

5. Sorokin JuI (1971) On the Role of Bacteria in the Productivity of Tropical Oceanic Waters. Internationale Revue der gesamten Hydrobiologie und Hydrographie 56:1–48. https://doi.org/10.1002/iroh.19710560102

6. Azam F, Fenchel T, Field J, et al (1983) The Ecological Role of Water-Column Microbes in the Sea. Mar Ecol Prog Ser 10:257–263. https://doi.org/10.3354/meps010257

7. Lalli C, Parsons T (1997) Biological Oceanography: An Introduction. Elsevier

8. Bratbak G, Thingstad F, Heldal M (1994) Viruses and the microbial loop. Microb Ecol 28:209–221. https://doi.org/10.1007/BF00166811

9. Mostajir B, Amblard C, Buffan-Dubau E, et al (2012) LES RÉSEAUX TROPHIQUES MICROBIENS DES MILIEUX AQUATIQUES ET TERRESTRES. Presses Universitaires de Pau et des Pays de l'Adour

10. Sime-Ngando T (1997) Importance des virus dans la structure des réseaux trophiques microbiens aquatiques. Annee Biologique, Elsevier 36:181–210

11. Buchan A, LeCleir GR, Gulvik CA, González JM (2014) Master recyclers: features and functions of bacteria associated with phytoplankton blooms. Nat Rev Microbiol 12:686–698. https://doi.org/10.1038/nrmicro3326

12. Pomeroy L, leB. Williams P, Azam F, Hobbie J (2007) The Microbial Loop. Oceanog 20:28–33. https://doi.org/10.5670/oceanog.2007.45

13. Grami B, Rasconi S, Niquil N, et al (2011) Functional Effects of Parasites on Food Web Properties during the Spring Diatom Bloom in Lake Pavin: A Linear Inverse Modeling Analysis. PLOS ONE 6:e23273. https://doi.org/10.1371/journal.pone.0023273

14. Haraldsson M, Gerphagnon M, Bazin P, et al (2018) Microbial parasites make cyanobacteria blooms less of a trophic dead end than commonly assumed. ISME J 12:1008–1020. https://doi.org/10.1038/s41396-018-0045-9

15. Callieri C, Stockner JG (2002) Freshwater autotrophic picoplankton: a review. J Limnol 61:1. https://doi.org/10.4081/jlimnol.2002.1

16. Colombet J, Fuster M, Billard H, Sime-Ngando T (2020) Femtoplankton: What's New? Viruses 12:881. https://doi.org/10.3390/v12080881

17. Lindeman RL (1942) The Trophic-Dynamic Aspect of Ecology. Ecology 23:399–417. https://doi.org/10.2307/1930126

18. Wu C-Y, Martel J, Wong T-Y, et al (2016) Formation and characteristics of biomimetic mineralo-organic particles in natural surface water. Sci Rep 6:28817. https://doi.org/10.1038/srep28817

19. Gill S, Catchpole R, Forterre P (2019) Extracellular membrane vesicles in the three domains of life and beyond. FEMS Microbiology Reviews 43:273–303. https://doi.org/10.1093/femsre/fuy042

20. Raposo G, Stoorvogel W (2013) Extracellular vesicles: exosomes, microvesicles, and friends. J Cell Biol 200:373–383. https://doi.org/10.1083/jcb.201211138

21. Gorlas A, Marguet E, Gill S, et al (2015) Sulfur vesicles from Thermococcales: A possible role in sulfur detoxifying mechanisms. Biochimie 118:356–364. https://doi.org/10.1016/j.biochi.2015.07.026

22. Sime-Ngando T (2014) Environmental bacteriophages: viruses of microbes in aquatic ecosystems. Front Microbiol 5:355. https://doi.org/10.3389/fmicb.2014.00355

23. Castelle CJ, Brown CT, Anantharaman K, et al (2018) Biosynthetic capacity, metabolic variety and unusual biology in the CPR and DPANN radiations. Nat Rev Microbiol 16:629–645. https://doi.org/10.1038/s41579-018-0076-2

24. Biller SJ, Schubotz F, Roggensack SE, et al (2014) Bacterial Vesicles in Marine Ecosystems. Science 343:183–186. https://doi.org/10.1126/science.1243457

25. Schatz D, Vardi A (2018) Extracellular vesicles - new players in cell-cell communication in aquatic environments. Curr Opin Microbiol 43:148–154. https://doi.org/10.1016/j.mib.2018.01.014

26. Weitz JS (2016) Quantitative Viral Ecology: Dynamics of Viruses and Their Microbial Hosts. Princeton University Press

27. Colombet J, Billard H, Viguès B, et al (2019) Discovery of High Abundances of Aster-Like Nanoparticles in Pelagic Environments: Characterization and Dynamics. Frontiers in Microbiology 10:2376. https://doi.org/10.3389/fmicb.2019.02376

28. Sieburth JMcN, Smetacek V, Lenz J (1978) Pelagic ecosystem structure: Heterotrophic compartments of the plankton and their relationship to plankton size fractions 1. Limnology and Oceanography 23:1256–1263. https://doi.org/10.4319/lo.1978.23.6.1256

29. Hochella MF (2002) Nanoscience and technology: the next revolution in the Earth sciences. Earth and Planetary Science Letters 203:593–605. https://doi.org/10.1016/S0012-821X(02)00818-X

30. Santschi PH (2018) Marine colloids, agents of the self-cleansing capacity of aquatic systems: Historical perspective and new discoveries. Marine Chemistry 207:124–135. https://doi.org/10.1016/j.marchem.2018.11.003

31. Duda VI, Suzina NE, Polivtseva VN, Boronin AM (2012) Ultramicrobacteria: Formation of the concept and contribution of ultramicrobacteria to biology. Microbiology 81:379–390. https://doi.org/10.1134/S0026261712040054

32. Ghuneim L-AJ, Jones DL, Golyshin PN, Golyshina OV (2018) Nano-Sized and Filterable Bacteria and Archaea: Biodiversity and Function. Frontiers in Microbiology 9:1971. https://doi.org/10.3389/fmicb.2018.01971

33. Morris RM, Rappé MS, Connon SA, et al (2002) SAR11 clade dominates ocean surface bacterioplankton communities. Nature 420:806–810. https://doi.org/10.1038/nature01240

34. Rappé MS, Connon SA, Vergin KL, Giovannoni SJ (2002) Cultivation of the ubiquitous SAR11 marine bacterioplankton clade. Nature 418:630–633. https://doi.org/10.1038/nature00917

35. Dyson FJ (1999) Origins of life, Rev. ed. Cambridge University Press, Cambridge [England] ; New York

36. Gilbert W (1986) Origin of life: The RNA world. Nature 319:618–618. https://doi.org/10.1038/319618a0

37. Ikehara K (2016) Evolutionary Steps in the Emergence of Life Deduced from the Bottom-Up Approach and GADV Hypothesis (Top-Down Approach). Life 6:6. https://doi.org/10.3390/life6010006

38. Oparin AI (1959) Introductory Address. In: Oparin AI, Braunshteîn AE, Pasynskiî AG, Pavlovskaya TE (eds) The Origin of Life on the Earth. Pergamon, pp 1–3

39. Orgel LE (1968) Evolution of the genetic apparatus. Journal of Molecular Biology 38:381–393. https://doi.org/10.1016/0022-2836(68)90393-8

40. Preiner M, Asche S, Becker S, et al (2020) The Future of Origin of Life Research: Bridging Decades-Old Divisions. Life 10:20. https://doi.org/10.3390/life10030020

41. Shapiro R (2008) A Replicator Was Not Involved in the Origin of Life. IUBMB Life 49:173–176. https://doi.org/10.1080/713803621

42. Woese C (1998) The universal ancestor. PNAS 95:6854–6859. https://doi.org/10.1073/pnas.95.12.6854

43. Dass AV, Hickman-Lewis K, Brack A, et al (2016) Stochastic Prebiotic Chemistry within Realistic Geological Systems. ChemistrySelect 1:4906–4926. https://doi.org/10.1002/slct.201600829

44. Westall F, Hickman-Lewis K, Hinman N, et al (2018) A Hydrothermal-Sedimentary Context for the Origin of Life. Astrobiology 18:259–293. https://doi.org/10.1089/ast.2017.1680

45. Camprubí E, de Leeuw JW, House CH, et al (2019) The Emergence of Life. Space Sci Rev 215:56. https://doi.org/10.1007/s11214-019-0624-8

46. Forterre P, Gribaldo S (2007) The origin of modern terrestrial life. HFSP Journal 1:156–168. https://doi.org/10.2976/1.2759103

47. Peretó J (2005) INTERNATIONAL MICROBIOLOGY (2005) 8:23-31 www.im.microbios.org. ORIGIN OF LIFE 10

48. Baum DA (2015) Selection and the Origin of Cells. BioScience 65:678–684. https://doi.org/10.1093/biosci/biv063

49. Barr SC, Linke RA, Janssen D, et al (2003) Detection of biofilm formation and nanobacteria under long-term cell culture conditions in serum samples of cattle, goats, cats, and dogs. Am J Vet Res 64:176–182. https://doi.org/10.2460/ajvr.2003.64.176

50. Benzerara K, Menguy N, Guyot F, et al (2003) Nanobacteria-like calcite single crystals at the surface of the Tataouine meteorite. PNAS 100:7438–7442. https://doi.org/10.1073/pnas.0832464100

51. Cisar JO, Xu D-Q, Thompson J, et al (2000) An alternative interpretation of nanobacteria-induced biomineralization. PNAS 97:11511–11515. https://doi.org/10.1073/pnas.97.21.11511

52. Folk RL (1993) SEM imaging of bacteria and nannobacteria in carbonate sediments and rocks. Journal of Sedimentary Research 63:990–999. https://doi.org/10.1306/D4267C67-2B26-11D7-8648000102C1865D

53. Jones B, Peng X (2012) Amorphous calcium carbonate associated with biofilms in hot spring deposits. Sedimentary Geology 269–270:58–68. https://doi.org/10.1016/j.sedgeo.2012.05.019

54. Raoult D, Drancourt M, Azza S, et al (2008) Nanobacteria Are Mineralo Fetuin Complexes. PLOS Pathogens 4:e41. https://doi.org/10.1371/journal.ppat.0040041

55. Uwins PJR, Webb RI, Taylor AP (1998) Novel nano-organisms from Australian sandstones. American Mineralogist 83:1541–1550. https://doi.org/10.2138/am-1998-11-1242

56. Yaghobee S, Bayani M, Samiei N, Jahedmanesh N (2015) What are the nanobacteria? Biotechnology & Biotechnological Equipment 29:826–833. https://doi.org/10.1080/13102818.2015.1052761

57. Martel J, Young JD-E (2008) Purported nanobacteria in human blood as calcium carbonate nanoparticles. Proc Natl Acad Sci U S A 105:5549–5554. https://doi.org/10.1073/pnas.0711744105

58. McKay DS, Gibson EK, Thomas-Keprta KL, et al (1996) Search for past life on Mars: possible relic biogenic activity in martian meteorite ALH84001. Science 273:924–930. https://doi.org/10.1126/science.273.5277.924

59. Sillitoe null, Folk null, Saric null (1996) Bacteria as Mediators of Copper Sulfide Enrichment During Weathering. Science 272:1153–1155. https://doi.org/10.1126/science.272.5265.1153

60. Folk RL (1996) In defense of nannobacteria. Science 274:1288a. https://doi.org/10.1126/science.274.5291.1288a

61. Akernan KK, Kuronen I, Kajander EO (1993) Scanning Electron Microscopy of Nanobacteria - Novel Biofilm Producing Organisms in Blood. Scanning 15:2

62. Kajander EO, Kuronen I, Akerman KK, et al (1997) Nanobacteria from blood: the smallest culturable autonomously replicating agent on Earth. In: Instruments, Methods, and Missions for the Investigation of Extraterrestrial Microorganisms. SPIE, pp 420–428

63. Folk RL (1999) Nannobacteria and the precipitation of carbonate in unusual environments. Sedimentary Geology 126:47–55. https://doi.org/10.1016/S0037-0738(99)00031-7

64. Christian P, Von der Kammer F, Baalousha M, Hofmann Th (2008) Nanoparticles: structure, properties, preparation and behaviour in environmental media. Ecotoxicology 17:326–343. https://doi.org/10.1007/s10646-008-0213-1

65. Martel J, Young D, Young A, et al (2011) Comprehensive proteomic analysis of mineral nanoparticles derived from human body fluids and analyzed by liquid chromatography–tandem mass spectrometry. Analytical Biochemistry 418:111–125. https://doi.org/10.1016/j.ab.2011.06.018

66. Chen IA, Walde P (2010) From Self-Assembled Vesicles to Protocells. Cold Spring Harb Perspect Biol 2:a002170. https://doi.org/10.1101/cshperspect.a002170

67. Rasmussen S, Chen L, Nilsson M, Abe S (2003) Bridging nonliving and living matter. Artif Life 9:269–316. https://doi.org/10.1162/106454603322392479

68. Gill S, Forterre P (2016) Origin of life: LUCA and extracellular membrane vesicles (EMVs). International Journal of Astrobiology 15:7–15. https://doi.org/10.1017/S1473550415000282

69. Doyle LM, Wang MZ (2019) Overview of Extracellular Vesicles, Their Origin, Composition, Purpose, and Methods for Exosome Isolation and Analysis. Cells 8:E727. https://doi.org/10.3390/cells8070727

70. Gould SJ, Raposo G (2013) As we wait: coping with an imperfect nomenclature for extracellular vesicles. Journal of Extracellular Vesicles 2:20389. https://doi.org/10.3402/jev.v2i0.20389

71. EL Andaloussi S, Mäger I, Breakefield XO, Wood MJA (2013) Extracellular vesicles: biology and emerging therapeutic opportunities. Nat Rev Drug Discov 12:347–357. https://doi.org/10.1038/nrd3978

72. Koning RI, de Breij A, Oostergetel GT, et al (2013) Cryo-electron tomography analysis of membrane vesicles from Acinetobacter baumannii ATCC19606T. Research in Microbiology 164:397–405. https://doi.org/10.1016/j.resmic.2013.02.007

73. Milasan A, Tessandier N, Tan S, et al (2016) Extracellular vesicles are present in mouse lymph and their level differs in atherosclerosis. J Extracell Vesicles 5:31427. https://doi.org/10.3402/jev.v5.31427

74. Pérez-Cruz C, Delgado L, López-Iglesias C, Mercade E (2015) Outer-inner membrane vesicles naturally secreted by gram-negative pathogenic bacteria. PLoS One 10:e0116896. https://doi.org/10.1371/journal.pone.0116896

75. Biller SJ, McDaniel LD, Breitbart M, et al (2017) Membrane vesicles in sea water: heterogeneous DNA content and implications for viral abundance estimates. ISME J 11:394–404. https://doi.org/10.1038/ismej.2016.134

76. Prangishvili D, Holz I, Stieger E, et al (2000) Sulfolobicins, specific proteinaceous toxins produced by strains of the extremely thermophilic archaeal genus Sulfolobus. J Bacteriol 182:2985–2988. https://doi.org/10.1128/JB.182.10.2985-2988.2000

77. Soler N, Marguet E, Verbavatz J-M, Forterre P (2008) Virus-like vesicles and extracellular DNA produced by hyperthermophilic archaea of the order Thermococcales. Research in Microbiology 159:390–399. https://doi.org/10.1016/j.resmic.2008.04.015

78. Gaudin M, Gauliard E, Schouten S, et al (2013) Hyperthermophilic archaea produce membrane vesicles that can transfer DNA. Environmental Microbiology Reports 5:109–116. https://doi.org/10.1111/j.1758-2229.2012.00348.x

79. Ellen AF, Albers S-V, Huibers W, et al (2008) Proteomic analysis of secreted membrane vesicles of archaeal Sulfolobus species reveals the presence of endosome sorting complex components. Extremophiles 13:67. https://doi.org/10.1007/s00792-008-0199-x

80. Choi D-S, Kim D-K, Kim Y-K, Gho YS (2015) Proteomics of extracellular vesicles: Exosomes and ectosomes. Mass Spectrometry Reviews 34:474–490. https://doi.org/10.1002/mas.21420

81. Erdmann S, Tschitschko B, Zhong L, et al (2017) A plasmid from an Antarctic haloarchaeon uses specialized membrane vesicles to disseminate and infect plasmid-free cells. Nat Microbiol 2:1446–1455. https://doi.org/10.1038/s41564-017-0009-2

82. Harding C, Heuser J, Stahl P (1983) Receptor-mediated endocytosis of transferrin and recycling of the transferrin receptor in rat reticulocytes. Journal of Cell Biology 97:329–339. https://doi.org/10.1083/jcb.97.2.329

83. Pan B-T, Johnstone RM (1983) Fate of the transferrin receptor during maturation of sheep reticulocytes in vitro: Selective externalization of the receptor. Cell 33:967–978. https://doi.org/10.1016/0092-8674(83)90040-5

84. Yáñez-Mó M, Siljander PR-M, Andreu Z, et al (2015) Biological properties of extracellular vesicles and their physiological functions. J Extracell Vesicles 4:27066. https://doi.org/10.3402/jev.v4.27066

85. Bebelman MP, Smit MJ, Pegtel DM, Baglio SR (2018) Biogenesis and function of extracellular vesicles in cancer. Pharmacol Ther 188:1–11. https://doi.org/10.1016/j.pharmthera.2018.02.013

86. Simons M, Raposo G (2009) Exosomes--vesicular carriers for intercellular communication. Curr Opin Cell Biol 21:575–581. https://doi.org/10.1016/j.ceb.2009.03.007

87. Théry C, Ostrowski M, Segura E (2009) Membrane vesicles as conveyors of immune responses. Nat Rev Immunol 9:581–593. https://doi.org/10.1038/nri2567

88. Muralidharan-Chari V, Clancy JW, Sedgwick A, D'Souza-Schorey C (2010) Microvesicles: mediators of extracellular communication during cancer progression. Journal of Cell Science 123:1603–161. https://doi.org/10.1242/jcs.064386

89. Rilla K, Pasonen-Seppänen S, Deen AJ, et al (2013) Hyaluronan production enhances shedding of plasma membrane-derived microvesicles. Experimental Cell Research 319:2006–2018. https://doi.org/10.1016/j.yexcr.2013.05.021

90. Rilla K, Siiskonen H, Tammi M, Tammi R (2014) Chapter Five - Hyaluronan-Coated Extracellular Vesicles—A Novel Link Between Hyaluronan and Cancer. In: Simpson MA, Heldin P (eds) Advances in Cancer Research. Academic Press, pp 121–148

91. Villarroya-Beltri C, Baixauli F, Gutiérrez-Vázquez C, et al (2014) Sorting it out: Regulation of exosome loading. Seminars in Cancer Biology 28:3–13. https://doi.org/10.1016/j.semcancer.2014.04.009

92. Subra C, Laulagnier K, Perret B, Record M (2007) Exosome lipidomics unravels lipid sorting at the level of multivesicular bodies. Biochimie 89:205–212. https://doi.org/10.1016/j.biochi.2006.10.014

93. Llorente A, Skotland T, Sylvänne T, et al (2013) Molecular lipidomics of exosomes released by PC-3 prostate cancer cells. Biochim Biophys Acta 1831:1302–1309. https://doi.org/10.1016/j.bbalip.2013.04.011

94. Record M, Carayon K, Poirot M, Silvente-Poirot S (2014) Exosomes as new vesicular lipid transporters involved in cell-cell communication and various pathophysiologies. Biochim Biophys Acta 1841:108–120. https://doi.org/10.1016/j.bbalip.2013.10.004

95. Record M, Silvente-Poirot S, Poirot M, Wakelam MJO (2018) Extracellular vesicles: lipids as key components of their biogenesis and functions. J Lipid Res 59:1316–1324. https://doi.org/10.1194/jlr.E086173

96. Skotland T, Sagini K, Sandvig K, Llorente A (2020) An emerging focus on lipids in extracellular vesicles. Advanced Drug Delivery Reviews 159:308–321. https://doi.org/10.1016/j.addr.2020.03.002

97. Valadi H, Ekström K, Bossios A, et al (2007) Exosome-mediated transfer of mRNAs and microRNAs is a novel mechanism of genetic exchange between cells. Nat Cell Biol 9:654–659. https://doi.org/10.1038/ncb1596

98. Balaj L, Lessard R, Dai L, et al (2011) Tumour microvesicles contain retrotransposon elements and amplified oncogene sequences. Nat Commun 2:180. https://doi.org/10.1038/ncomms1180

99. Guescini M, Guidolin D, Vallorani L, et al (2010) C2C12 myoblasts release micro-vesicles containing mtDNA and proteins involved in signal transduction. Experimental Cell Research 316:1977–1984. https://doi.org/10.1016/j.yexcr.2010.04.006

100. Shader RI (2014) Cell-to-Cell Talk: Plasmids and Exosomes. Clinical Therapeutics 36:817–818. https://doi.org/10.1016/j.clinthera.2014.05.007

101. Thakur BK, Zhang H, Becker A, et al (2014) Double-stranded DNA in exosomes: a novel biomarker in cancer detection. Cell Res 24:766–769. https://doi.org/10.1038/cr.2014.44

102. Orench-Rivera N, Kuehn MJ (2016) Environmentally controlled bacterial vesicle-mediated export. Cellular Microbiology 18:1525–1536. https://doi.org/10.1111/cmi.12676

103. Forterre P (2017) THE ORIGIN, NATURE AND DEFINITION OF VIRUSES (AND LIFE): NEW CONCEPTS AND CONTROVERSIES. In: Evolutionary biology of the virome, adn impacts in human health and disease. Old Herborn University Foundation, Herborn, Germany, pp 15–26

104. Jalasvuori M, Mattila S, Hoikkala V (2015) Chasing the Origin of Viruses: Capsid-Forming Genes as a Life-Saving Preadaptation within a Community of Early Replicators. PLoS One 10:e0126094. https://doi.org/10.1371/journal.pone.0126094

105. Forterre P, Krupovic M (2012) The Origin of Virions and Virocells: The Escape Hypothesis Revisited. In: Witzany G (ed) Viruses: Essential Agents of Life. Springer Netherlands, Dordrecht, pp 43–60

106. Krupovic M, Koonin EV (2017) Multiple origins of viral capsid proteins from cellular ancestors. Proc Natl Acad Sci U S A 114:E2401–E2410. https://doi.org/10.1073/pnas.1621061114

107. Forterre P (2006) The origin of viruses and their possible roles in major evolutionary transitions. Virus Research 117:5–16. https://doi.org/10.1016/j.virusres.2006.01.010

108. Forterre P, Da Cunha V, Catchpole R (2017) Plasmid vesicles mimicking virions. Nat Microbiol 2:1340–1341. https://doi.org/10.1038/s41564-017-0032-3

109. Koonin EV (2009) Darwinian evolution in the light of genomics. Nucleic Acids Research 37:1011–1034. https://doi.org/10.1093/nar/gkp089

110. Weinbauer MG (2004) Ecology of prokaryotic viruses. FEMS Microbiology Reviews 28:127–181. https://doi.org/10.1016/j.femsre.2003.08.001

111. Koonin EV, Senkevich TG, Dolja VV (2006) The ancient Virus World and evolution of cells. Biology Direct 1:29. https://doi.org/10.1186/1745-6150-1-29

112. Bossart GD (2018) Emerging viruses in marine mammals. CAB Reviews 13:. https://doi.org/10.1079/PAVSNNR201813052

113. Weynberg KD (2018) Chapter One - Viruses in Marine Ecosystems: From Open Waters to Coral Reefs. In: Malmstrom CM (ed) Advances in Virus Research. Academic Press, pp 1–38

114. Kuhn JH, Wolf YI, Krupovic M, et al (2019) Classify viruses — the gain is worth the pain. Nature 566:318–320. https://doi.org/10.1038/d41586-019-00599-8

115. Mahmoudabadi G, Phillips R (2018) A comprehensive and quantitative exploration of thousands of viral genomes. Elife 7:e31955. https://doi.org/10.7554/eLife.31955

116. International Committee on Taxonomy of Viruses, King AMQ (2012) Virus taxonomy: classification and nomenclature of viruses: ninth report of the International Committee on Taxonomy of Viruses. Academic Press, London ; Waltham, MA

117. Baltimore D (1971) Expression of animal virus genomes. Bacteriol Rev 35:235–241. https://doi.org/10.1128/br.35.3.235-241.1971

118. Koonin EV (1991) The phylogeny of RNA-dependent RNA polymerases of positive-strand RNA viruses. J Gen Virol 72 (Pt 9):2197–2206. https://doi.org/10.1099/0022-1317-72-9-2197

119. Rohwer F (2003) Global Phage Diversity. Cell 113:141. https://doi.org/10.1016/S0092-8674(03)00276-9

120. Edwards RA, Rohwer F (2005) Viral metagenomics. Nat Rev Microbiol 3:504–510. https://doi.org/10.1038/nrmicro1163

121. Rohwer F, Thurber RV (2009) Viruses manipulate the marine environment. Nature 459:207–212. https://doi.org/10.1038/nature08060

122. Paez-Espino D, Eloe-Fadrosh EA, Pavlopoulos GA, et al (2016) Uncovering Earth's virome. Nature 536:425–430. https://doi.org/10.1038/nature19094

123. (2020) International Committee on Taxonomy Viruses. https://talk.ictvonline.org/taxonomy/. Accessed 20 May 2020

124. Simmonds P, Adams MJ, Benkő M, et al (2017) Virus taxonomy in the age of metagenomics. Nat Rev Microbiol 15:161–168. https://doi.org/10.1038/nrmicro.2016.177

125. Adriaenssens EM, Cowan DA (2014) Using Signature Genes as Tools To Assess Environmental Viral Ecology and Diversity. Applied and Environmental Microbiology 80:4470–4480. https://doi.org/10.1128/AEM.00878-14

126. STRAUSS JH, STRAUSS EG (2008) Subviral Agents. Viruses and Human Disease 345–368. https://doi.org/10.1016/B978-0-12-373741-0.50012-X

127. Nichols TA, Pulford B, Wyckoff AC, et al (2009) Detection of protease-resistant cervid prion protein in water from a CWD-endemic area. Prion 3:171–183. https://doi.org/10.4161/pri.3.3.9819

128. Mehle N, Gutiérrez-Aguirre I, Prezelj N, et al (2014) Survival and transmission of potato virus Y, pepino mosaic virus, and potato spindle tuber viroid in water. Appl Environ Microbiol 80:1455–1462. https://doi.org/10.1128/AEM.03349-13

129. Koonin EV, Dolja VV, Krupovic M (2015) Origins and evolution of viruses of eukaryotes: The ultimate modularity. Virology 479–480:2–25. https://doi.org/10.1016/j.virol.2015.02.039

130. Goodier JL, Kazazian HH (2008) Retrotransposons revisited: the restraint and rehabilitation of parasites. Cell 135:23–35. https://doi.org/10.1016/j.cell.2008.09.022

131. Kazazian HH (2004) Mobile elements: drivers of genome evolution. Science 303:1626–1632. https://doi.org/10.1126/science.1089670

132. Campillo-Balderas JA, Lazcano A, Becerra A (2015) Viral Genome Size Distribution Does not Correlate with the Antiquity of the Host Lineages. Frontiers in Ecology and Evolution 3:143. https://doi.org/10.3389/fevo.2015.00143

133. Cui J, Schlub TE, Holmes EC (2014) An Allometric Relationship between the Genome Length and Virion Volume of Viruses. Journal of Virology 88:6403–6410. https://doi.org/10.1128/JVI.00362-14

134. Fauquet CM, Mayo MA, Maniloff J, et al (2005) Virus Taxonomy: VIIIth Report of the International Committee on Taxonomy of Viruses. Academic Press

135. Duckworth D (1987) History and basic properties of bacterial viruses. In: Phage Ecology. John Wiley & Sons, New York, NY, USA, pp 1–44

136. Weitz JS, Li G, Gulbudak H, et al (2019) Viral invasion fitness across a continuum from lysis to latency†. Virus Evolution 5:. https://doi.org/10.1093/ve/vez006

137. Eisenreich W, Rudel T, Heesemann J, Goebel W (2019) How Viral and Intracellular Bacterial Pathogens Reprogram the Metabolism of Host Cells to Allow Their Intracellular Replication. Frontiers in Cellular and Infection Microbiology 9:42. https://doi.org/10.3389/fcimb.2019.00042

138. Suttle CA (2005) Viruses in the sea. Nature 437:356–361. https://doi.org/10.1038/nature04160

139. Suttle CA (2007) Marine viruses — major players in the global ecosystem. Nat Rev Microbiol 5:801–812. https://doi.org/10.1038/nrmicro1750

140. Sime-Ngando T, Colombet J (2009) [Virus and prophages in aquatic ecosystems]. Can J Microbiol 55:95–109. https://doi.org/10.1139/w08-099

141. Zeigler Allen L, McCrow JP, Ininbergs K, et al (2021) The Baltic Sea Virome: Diversity and Transcriptional Activity of DNA and RNA Viruses. mSystems 2:e00125-16. https://doi.org/10.1128/mSystems.00125-16

142. Coutinho FH, Silveira CB, Gregoracci GB, et al (2017) Marine viruses discovered via metagenomics shed light on viral strategies throughout the oceans. Nat Commun 8:15955. https://doi.org/10.1038/ncomms15955

143. Potapov SA, Tikhonova IV, Krasnopeev AY, et al (2019) Metagenomic Analysis of Virioplankton from the Pelagic Zone of Lake Baikal. Viruses 11:991. https://doi.org/10.3390/v11110991

144. Gregory AC, Zayed AA, Conceição-Neto N, et al (2019) Marine DNA Viral Macro- and Microdiversity from Pole to Pole. Cell 177:1109-1123.e14. https://doi.org/10.1016/j.cell.2019.03.040

145. Yang Q, Gao C, Jiang Y, et al (2019) Metagenomic Characterization of the Viral Community of the South Scotia Ridge. Viruses 11:95. https://doi.org/10.3390/v11020095

146. Al-Shayeb B, Sachdeva R, Chen L-X, et al (2020) Clades of huge phages from across Earth's ecosystems. Nature 578:425–431. https://doi.org/10.1038/s41586-020-2007-4

147. Paez-Espino D, Zhou J, Roux S, et al (2019) Diversity, evolution, and classification of virophages uncovered through global metagenomics. Microbiome 7:157. https://doi.org/10.1186/s40168-019-0768-5

148. Raoult D, Audic S, Robert C, et al (2004) The 1.2-Megabase Genome Sequence of Mimivirus. Science 306:1344–1350. https://doi.org/10.1126/science.1101485

149. Claverie J-M (2006) Viruses take center stage in cellular evolution. Genome Biology 7:110. https://doi.org/10.1186/gb-2006-7-6-110

150. Legendre M, Bartoli J, Shmakova L, et al (2014) Thirty-thousand-year-old distant relative of giant icosahedral DNA viruses with a pandoravirus morphology. Proc Natl Acad Sci U S A 111:4274–4279. https://doi.org/10.1073/pnas.1320670111

151. Philippe N, Legendre M, Doutre G, et al (2013) Pandoraviruses: amoeba viruses with genomes up to 2.5 Mb reaching that of parasitic eukaryotes. Science 341:281–286. https://doi.org/10.1126/science.1239181

152. Claverie J-M, Abergel C (2009) Mimivirus and its virophage. Annu Rev Genet 43:49–66. https://doi.org/10.1146/annurev-genet-102108-134255

153. Brandes N, Linial M (2019) Giant Viruses-Big Surprises. Viruses 11:E404. https://doi.org/10.3390/v11050404

154. Bobay L-M, Touchon M, Rocha EPC (2014) Pervasive domestication of defective prophages by bacteria. Proc Natl Acad Sci U S A 111:12127–12132. https://doi.org/10.1073/pnas.1405336111

155. Harrison E, Brockhurst MA (2017) Ecological and Evolutionary Benefits of Temperate Phage: What Does or Doesn't Kill You Makes You Stronger. Bioessays 39:. https://doi.org/10.1002/bies.201700112

156. Tomasz O, Agnieszka L, Bartosz R, et al (2017) Phage Life Cycles Behind Bacterial Biodiversity. Current Medicinal Chemistry 24:3987–4001

157. Redfield RJ, Soucy SM (2018) Evolution of Bacterial Gene Transfer Agents. Frontiers in Microbiology 9:2527. https://doi.org/10.3389/fmicb.2018.02527

158. Lang AS, Beatty JT (2007) Importance of widespread gene transfer agent genes in α-proteobacteria. Trends in Microbiology 15:54–62. https://doi.org/10.1016/j.tim.2006.12.001

159. Stanton TB (2007) Prophage-like gene transfer agents—Novel mechanisms of gene exchange for Methanococcus, Desulfovibrio, Brachyspira, and Rhodobacter species. Anaerobe 13:43–49. https://doi.org/10.1016/j.anaerobe.2007.03.004

160. Yen HC, Hu NT, Marrs BL (1979) Characterization of the gene transfer agent made by an overproducer mutant of Rhodopseudomonas capsulata. Journal of Molecular Biology 131:157–168. https://doi.org/10.1016/0022-2836(79)90071-8

161. Rapp BJ, Wall JD (1987) Genetic transfer in Desulfovibrio desulfuricans. Proc Natl Acad Sci U S A 84:9128–9130. https://doi.org/10.1073/pnas.84.24.9128

162. Humphrey SB, Stanton TB, Jensen NS (1995) Mitomycin C induction of bacteriophages from Serpulina hyodysenteriae and Serpulina innocens. FEMS Microbiol Lett 134:97–101. https://doi.org/10.1111/j.1574-6968.1995.tb07921.x

163. Eiserling F, Pushkin A, Gingery M, Bertani GY 1999 (2021) Bacteriophage-like particles associated with the gene transfer agent of Methanococcus voltae PS. Journal of General Virology 80:3305–3308. https://doi.org/10.1099/0022-1317-80-12-3305

164. Barbian KD, Minnick MFY 2000 (2021) A bacteriophage-like particle from Bartonella bacilliformis. Microbiology 146:599–609. https://doi.org/10.1099/00221287-146-3-599

165. Nagao N, Yamamoto J, Komatsu H, et al (2015) The gene transfer agent-like particle of the marine phototrophic bacterium Rhodovulum sulfidophilum. Biochemistry and Biophysics Reports 4:369–374. https://doi.org/10.1016/j.bbrep.2015.11.002

166. Tomasch J, Wang H, Hall ATK, et al (2018) Packaging of Dinoroseobacter shibae DNA into Gene Transfer Agent Particles Is Not Random. Genome Biology and Evolution 10:359–369. https://doi.org/10.1093/gbe/evy005

167. Matson EG, Thompson MG, Humphrey SB, et al (2005) Identification of Genes of VSH-1, a Prophage-Like Gene Transfer Agent of Brachyspira hyodysenteriae. Journal of Bacteriology 187:5885–5892. https://doi.org/10.1128/JB.187.17.5885-5892.2005

168. Fogg PCM, Westbye AB, Beatty JT (2012) One for All or All for One: Heterogeneous Expression and Host Cell Lysis Are Key to Gene Transfer Agent Activity in Rhodobacter capsulatus. PLOS ONE 7:e43772. https://doi.org/10.1371/journal.pone.0043772

169. Hynes AP, Mercer RG, Watton DE, et al (2012) DNA packaging bias and differential expression of gene transfer agent genes within a population during production and release of the Rhodobacter capsulatus gene transfer agent, RcGTA. Molecular Microbiology 85:314–325. https://doi.org/10.1111/j.1365-2958.2012.08113.x

170. Lang AS, Zhaxybayeva O, Beatty JT (2012) Gene transfer agents: phage-like elements of genetic exchange. Nat Rev Microbiol 10:472–482. https://doi.org/10.1038/nrmicro2802

171. Marrs B (1974) Genetic recombination in Rhodopseudomonas capsulata. Proc Natl Acad Sci U S A 71:971–973. https://doi.org/10.1073/pnas.71.3.971

172. Humphrey SB, Stanton TB, Jensen NS, Zuerner RL (1997) Purification and characterization of VSH-1, a generalized transducing bacteriophage of Serpulina hyodysenteriae. J Bacteriol 179:323–329. https://doi.org/10.1128/jb.179.2.323-329.1997

173. Bertani G (1999) Transduction-Like Gene Transfer in the MethanogenMethanococcus voltae. Journal of Bacteriology 181:2992–3002. https://doi.org/10.1128/JB.181.10.2992-3002.1999

174. Biers EJ, Wang K, Pennington C, et al (2008) Occurrence and expression of gene transfer agent genes in marine bacterioplankton. Appl Environ Microbiol 74:2933–2939. https://doi.org/10.1128/AEM.02129-07

175. Berglund EC, Frank AC, Calteau A, et al (2009) Run-off replication of host-adaptability genes is associated with gene transfer agents in the genome of mouse-infecting Bartonella grahamii. PLoS Genet 5:e1000546. https://doi.org/10.1371/journal.pgen.1000546

176. Grüll MP, Mulligan ME, Lang AS (2018) Small extracellular particles with big potential for horizontal gene transfer: membrane vesicles and gene transfer agents. FEMS Microbiology Letters 365:. https://doi.org/10.1093/femsle/fny192

177. Lang AS, Westbye AB, Beatty JT (2017) The Distribution, Evolution, and Roles of Gene Transfer Agents in Prokaryotic Genetic Exchange. Annual Review of Virology 4:87–104. https://doi.org/10.1146/annurev-virology-101416-041624

178. Westbye AB, Beatty JT, Lang AS (2017) Guaranteeing a captive audience: coordinated regulation of gene transfer agent (GTA) production and recipient capability by cellular regulators. Current Opinion in Microbiology 38:122–129. https://doi.org/10.1016/j.mib.2017.05.003

179. Hall JPJ, Brockhurst MA, Harrison E (2017) Sampling the mobile gene pool: innovation via horizontal gene transfer in bacteria. Philosophical Transactions of the Royal Society B: Biological Sciences 372:20160424. https://doi.org/10.1098/rstb.2016.0424

180. Québatte M, Dehio C (2019) Bartonella gene transfer agent: Evolution, function, and proposed role in host adaptation. Cell Microbiol 21:e13068. https://doi.org/10.1111/cmi.13068

181. Dombrowski N, Lee J-H, Williams TA, et al (2019) Genomic diversity, lifestyles and evolutionary origins of DPANN archaea. FEMS Microbiol Lett 366:. https://doi.org/10.1093/femsle/fnz008

182. Méheust R, Burstein D, Castelle CJ, Banfield JF (2019) The distinction of CPR bacteria from other bacteria based on protein family content. Nat Commun 10:4173. https://doi.org/10.1038/s41467-019-12171-z

183. Di Giulio M (2019) A qualitative criterion for identifying the root of the tree of life. Journal of Theoretical Biology 464:126–131. https://doi.org/10.1016/j.jtbi.2018.12.039

184. Di Giulio M (2019) The universal ancestor, the deeper nodes of the tree of life, and the fundamental types of primary cells (cellular domains). Journal of Theoretical Biology 460:142–143. https://doi.org/10.1016/j.jtbi.2018.10.020

185. Huber H, Hohn MJ, Rachel R, et al (2002) A new phylum of Archaea represented by a nanosized hyperthermophilic symbiont. Nature 417:63–67. https://doi.org/10.1038/417063a

186. Waters E, Hohn MJ, Ahel I, et al (2003) The genome of Nanoarchaeum equitans: Insights into early archaeal evolution and derived parasitism. PNAS 100:12984–12988. https://doi.org/10.1073/pnas.1735403100

187. Comolli LR, Baker BJ, Downing KH, et al (2009) Three-dimensional analysis of the structure and ecology of a novel, ultra-small archaeon. ISME J 3:159–167. https://doi.org/10.1038/ismej.2008.99

188. Baker BJ, Dick GJ (2013) Omic Approaches in Microbial Ecology: Charting the Unknown. Microbe Magazine 8:353–360

189. Baker BJ, Comolli LR, Dick GJ, et al (2010) Enigmatic, ultrasmall, uncultivated Archaea. PNAS 107:8806–8811. https://doi.org/10.1073/pnas.0914470107

190. Ghai R, Pašić L, Fernández AB, et al (2011) New abundant microbial groups in aquatic hypersaline environments. Sci Rep 1:135. https://doi.org/10.1038/srep00135

191. Narasingarao P, Podell S, Ugalde JA, et al (2012) De novo metagenomic assembly reveals abundant novel major lineage of Archaea in hypersaline microbial communities. ISME J 6:81–93. https://doi.org/10.1038/ismej.2011.78

192. Rinke C, Schwientek P, Sczyrba A, et al (2013) Insights into the phylogeny and coding potential of microbial dark matter. Nature 499:431–437. https://doi.org/10.1038/nature12352

193. Vavourakis CD, Ghai R, Rodriguez-Valera F, et al (2016) Metagenomic Insights into the Uncultured Diversity and Physiology of Microbes in Four Hypersaline Soda Lake Brines. Front Microbiol 7:211. https://doi.org/10.3389/fmicb.2016.00211

194. Kantor RS, Wrighton KC, Handley KM, et al (2013) Small genomes and sparse metabolisms of sediment-associated bacteria from four candidate phyla. mBio 4:e00708-00713. https://doi.org/10.1128/mBio.00708-13

195. Luef B, Frischkorn KR, Wrighton KC, et al (2015) Diverse uncultivated ultra-small bacterial cells in groundwater. Nat Commun 6:6372. https://doi.org/10.1038/ncomms7372

196. Lannes R, Olsson-Francis K, Lopez P, Bapteste E (2019) Carbon Fixation by Marine Ultrasmall Prokaryotes. Genome Biology and Evolution 11:1166–1177. https://doi.org/10.1093/gbe/evz050

197. Fuster M, Billard H, Mandart M, et al (2020) Trophic conditions influence widespread distribution of Aster-Like nanoparticles within aquatic environments. Microbial Ecology 80:741. https://doi.org/10.1007/s00248-020-01541-6

198. Chatterjee S, Yadav S (2019) The Origin of Prebiotic Information System in the Peptide/RNA World: A Simulation Model of the Evolution of Translation and the Genetic Code. Life 9:25. https://doi.org/10.3390/life9010025

199. Shirt-Ediss B, Murillo-Sánchez S, Ruiz-Mirazo K (2017) Framing major prebiotic transitions as stages of protocell development: three challenges for origins-of-life research. Beilstein J Org Chem 13:1388–1395. https://doi.org/10.3762/bjoc.13.135

200. Mukhanov VS, Rylkova OA, Sakhon EG, et al (2016) Transbiome invasions of femtoplankton. Contemp Probl Ecol 9:266–271. https://doi.org/10.1134/S1995425516030112

201. Sano E, Carlson S, Wegley L, Rohwer F (2004) Movement of viruses between biomes. Appl Environ Microbiol 70:5842–5846. https://doi.org/10.1128/AEM.70.10.5842-5846.2004

202. Reche I, D'Orta G, Mladenov N, et al (2018) Deposition rates of viruses and bacteria above the atmospheric boundary layer. ISME J 12:1154–1162. https://doi.org/10.1038/s41396-017-0042-4

203. Brown CT, Hug LA, Thomas BC, et al (2015) Unusual biology across a group comprising more than 15% of domain Bacteria. Nature 523:208–211. https://doi.org/10.1038/nature14486

204. Hug LA, Baker BJ, Anantharaman K, et al (2016) A new view of the tree of life. Nat Microbiol 1:1–6. https://doi.org/10.1038/nmicrobiol.2016.48

205. Parks DH, Rinke C, Chuvochina M, et al (2017) Recovery of nearly 8,000 metagenome-assembled genomes substantially expands the tree of life. Nat Microbiol 2:1533–1542. https://doi.org/10.1038/s41564-017-0012-7

206. R M, Df B (1995) Viral abundance in aquatic systems: a comparison between marine and fresh waters. Marine Ecology Progress Series 121:217–226. https://doi.org/10.3354/meps121217

207. Wommack KE, Colwell RR (2000) Virioplankton: Viruses in Aquatic Ecosystems. Microbiology and Molecular Biology Reviews 64:69–114. https://doi.org/10.1128/MMBR.64.1.69-114.2000

208. Wigington CH, Sonderegger D, Brussaard CPD, et al (2016) Re-examination of the relationship between marine virus and microbial cell abundances. Nat Microbiol 1:1–9. https://doi.org/10.1038/nmicrobiol.2015.24

209. Suttle CA (2013) Viruses: unlocking the greatest biodiversity on Earth. Genome 56:542–544. https://doi.org/10.1139/gen-2013-0152

210. Steward GF, Culley AI, Mueller JA, et al (2013) Are we missing half of the viruses in the ocean? ISME J 7:672–679. https://doi.org/10.1038/ismej.2012.121

211. Forterre P, Soler N, Krupovic M, et al (2013) Fake virus particles generated by fluorescence microscopy. Trends Microbiol 21:1–5. https://doi.org/10.1016/j.tim.2012.10.005

212. Soler N, Krupovic M, Marguet E, Forterre P (2015) Membrane vesicles in natural environments: a major challenge in viral ecology. ISME J 9:793–796. https://doi.org/10.1038/ismej.2014.184

213. Breitschwerdt EB, Sontakke S, Cannedy A, et al (2001) Infection with Bartonella weissii and Detection of Nanobacterium Antigens in a North Carolina Beef Herd. Journal of Clinical Microbiology 39:879–882. https://doi.org/10.1128/JCM.39.3.879-882.2001

214. Kajander EO, Çiftçioglu N (1998) Nanobacteria: An alternative mechanism for pathogenic intra- and extracellular calcification and stone formation. PNAS 95:8274–8279. https://doi.org/10.1073/pnas.95.14.8274

215. Domingues S, Nielsen KM (2017) Membrane vesicles and horizontal gene transfer in prokaryotes. Current Opinion in Microbiology 38:16–21. https://doi.org/10.1016/j.mib.2017.03.012

216. Schatz D, Rosenwasser S, Malitsky S, et al (2017) Communication via extracellular vesicles enhances viral infection of a cosmopolitan alga. Nat Microbiol 2:1485–1492. https://doi.org/10.1038/s41564-017-0024-3

217. Forterre P (2013) The virocell concept and environmental microbiology. ISME J 7:233–236. https://doi.org/10.1038/ismej.2012.110

218. Altan-Bonnet N (2016) Extracellular vesicles are the Trojan horses of viral infection. Current Opinion in Microbiology 32:77–81. https://doi.org/10.1016/j.mib.2016.05.004

219. Fuhrman JA (1999) Marine viruses and their biogeochemical and ecological effects. Nature 399:541–548. https://doi.org/10.1038/21119

220. Weitz JS, Wilhelm SW (2012) Ocean viruses and their effects on microbial communities and biogeochemical cycles. F1000 Biol Rep 4:17. https://doi.org/10.3410/B4-17

221. Record NR, Talmy D, Våge S (2016) Quantifying Tradeoffs for Marine Viruses. Frontiers in Marine Science 3:251. https://doi.org/10.3389/fmars.2016.00251

222. Middelboe M, Brussaard CPD (2017) Marine Viruses: Key Players in Marine Ecosystems. Viruses 9:302. https://doi.org/10.3390/v9100302

223. Zimmerman AE, Howard-Varona C, Needham DM, et al (2020) Metabolic and biogeochemical consequences of viral infection in aquatic ecosystems. Nat Rev Microbiol 18:21–34. https://doi.org/10.1038/s41579-019-0270-x

224. Suttle CA (1994) The significance of viruses to mortality in aquatic microbial communities. Microb Ecol 28:237–243. https://doi.org/10.1007/BF00166813

225. Fuhrman JA, Noble RT (1995) Viruses and protists cause similar bacterial mortality in coastal seawater. Limnology and Oceanography 40:1236–1242. https://doi.org/10.4319/lo.1995.40.7.1236

226. Bratbak G, Egge J, Heldal M (1993) Viral mortality of the marine alga Emiliania huxleyi (Haptophyceae) and termination of algal blooms. Mar Ecol Prog Ser 93:39–48. https://doi.org/10.3354/meps093039

227. Nagasaki K, Ando M, Itakura S, et al (1994) Viral mortality in the final stage of Heterosigma akashiwo (Raphidophyceae) red tide. Journal of Plankton Research 16:1595–1599. https://doi.org/10.1093/plankt/16.11.1595

228. Wilhelm SW, Suttle CA (1999) Viruses and Nutrient Cycles in the Sea: Viruses play critical roles in the structure and function of aquatic food webs. BioScience 49:781–788. https://doi.org/10.2307/1313569

229. Proctor L, Fuhrman J (1991) Roles of viral infection in organic particle flux. Mar Ecol Prog Ser 69:133–142. https://doi.org/10.3354/meps069133

230. Jover LF, Effler TC, Buchan A, et al (2014) The elemental composition of virus particles: implications for marine biogeochemical cycles. Nat Rev Microbiol 12:519–528. https://doi.org/10.1038/nrmicro3289

231. Thingstad TF (2000) Elements of a theory for the mechanisms controlling abundance, diversity, and biogeochemical role of lytic bacterial viruses in aquatic systems. Limnology and Oceanography 45:1320–1328. https://doi.org/10.4319/lo.2000.45.6.1320

232. Thingstad TF, Våge S, Storesund JE, et al (2014) A theoretical analysis of how strain-specific viruses can control microbial species diversity. PNAS 111:7813–7818. https://doi.org/10.1073/pnas.1400909111

233. Martiny JBH, Riemann L, Marston MF, Middelboe M (2014) Antagonistic coevolution of marine planktonic viruses and their hosts. Ann Rev Mar Sci 6:393–414. https://doi.org/10.1146/annurev-marine-010213-135108

234. Tf T, R L (1997) Theoretical models for the control of bacterial growth rate, abundance, diversity and carbon demand. Aquatic Microbial Ecology 13:19–27. https://doi.org/10.3354/ame013019

235. Winter C, Bouvier T, Weinbauer MG, Thingstad TF (2010) Trade-Offs between Competition and Defense Specialists among Unicellular Planktonic Organisms: the “Killing the Winner” Hypothesis Revisited. Microbiology and Molecular Biology Reviews 74:42–57. https://doi.org/10.1128/MMBR.00034-09

236. Maslov S, Sneppen K (2017) Population cycles and species diversity in dynamic Kill-the-Winner model of microbial ecosystems. Sci Rep 7:39642. https://doi.org/10.1038/srep39642

237. Paul JH (1999) Microbial gene transfer: an ecological perspective. J Mol Microbiol Biotechnol 1:45–50

238. Nasir A, Kim KM, Caetano-Anollés G (2017) Long-term evolution of viruses: A Janus-faced balance. Bioessays 39:. https://doi.org/10.1002/bies.201700026

239. Lindell D, Sullivan MB, Johnson ZI, et al (2004) Transfer of photosynthesis genes to and from Prochlorococcus viruses. Proc Natl Acad Sci U S A 101:11013–11018. https://doi.org/10.1073/pnas.0401526101

240. Ramisetty BCM, Sudhakari PA (2019) Bacterial "Grounded" Prophages: Hotspots for Genetic Renovation and Innovation. Front Genet 10:65. https://doi.org/10.3389/fgene.2019.00065

241. McDaniel LD, Young E, Delaney J, et al (2010) High frequency of horizontal gene transfer in the oceans. Science 330:50. https://doi.org/10.1126/science.1192243

242. Fogg PCM (2019) Identification and characterization of a direct activator of a gene transfer agent. Nat Commun 10:595. https://doi.org/10.1038/s41467-019-08526-1

243. Castelle CJ, Wrighton KC, Thomas BC, et al (2015) Genomic Expansion of Domain Archaea Highlights Roles for Organisms from New Phyla in Anaerobic Carbon Cycling. Current Biology 25:690–701. https://doi.org/10.1016/j.cub.2015.01.014

244. Anantharaman K, Brown CT, Hug LA, et al (2016) Thousands of microbial genomes shed light on interconnected biogeochemical processes in an aquifer system. Nat Commun 7:13219. https://doi.org/10.1038/ncomms13219

245. Wrighton KC, Castelle CJ, Varaljay VA, et al (2016) RubisCO of a nucleoside pathway known from Archaea is found in diverse uncultivated phyla in bacteria. ISME J 10:2702–2714. https://doi.org/10.1038/ismej.2016.53

246. Castelle CJ, Banfield JF (2018) Major New Microbial Groups Expand Diversity and Alter our Understanding of the Tree of Life. Cell 172:1181–1197. https://doi.org/10.1016/j.cell.2018.02.016

247. Deng L, Krauss S, Feichtmayer J, et al (2014) Grazing of heterotrophic flagellates on viruses is driven by feeding behaviour. Environmental Microbiology Reports 6:325–330. https://doi.org/10.1111/1758-2229.12119

248. Ortiz-Alvarez R, Casamayor EO (2016) High occurrence of *Pacearchaeota* and *Woesearchaeota* (Archaea superphylum DPANN) in the surface waters of oligotrophic high-altitude lakes: Archaeal occurrence in high-altitude lakes. Environmental Microbiology Reports 8:210–217. https://doi.org/10.1111/1758-2229.12370

249. Wurch L, Giannone RJ, Belisle BS, et al (2016) Genomics-informed isolation and characterization of a symbiotic Nanoarchaeota system from a terrestrial geothermal environment. Nat Commun 7:12115. https://doi.org/10.1038/ncomms12115

250. Benzerara K, Miller VM, Barell G, et al (2006) Search for Microbial Signatures within Human and Microbial Calcifications Using Soft X-Ray Spectromicroscopy: Journal of Investigative Medicine 54:367–379. https://doi.org/10.2310/6650.2006.06016

251. National Research Council (US) Steering Group for the Workshop on Size Limits of Very Small Microorganisms (1999) Size Limits of Very Small Microorganisms: Proceedings of a Workshop. National Academies Press (US), Washington (DC)

252. Liu Y, Smid EJ, Abee T, Notebaart RA (2018) Delivery of genome editing tools by bacterial extracellular vesicles. Microb Biotechnol 1751-7915.13356. https://doi.org/10.1111/1751-7915.13356

253. Pradeep Ram AS, Mari X, Brune J, et al (2018) Bacterial-viral interactions in the sea surface microlayer of a black carbon-dominated tropical coastal ecosystem (Halong Bay, Vietnam). Elementa: Science of the Anthropocene 6:13. https://doi.org/10.1525/elementa.276

254. Borrel G, Joblin K, Guedon A, et al (2012) Methanobacterium lacus sp. nov., isolated from the profundal sediment of a freshwater meromictic lake. International Journal of Systematic and Evolutionary Microbiology 62:1625–1629. https://doi.org/10.1099/ijs.0.034538-0

255. Kéraval B, Lehours AC, Colombet J, et al (2016) Soil carbon dioxide emissions controlled by an extracellular oxidative metabolism identifiable by its isotope signature. Biogeosciences 13:6353–6362. https://doi.org/10.5194/bg-13-6353-2016

256. Brussaard CPD (2004) Optimization of procedures for counting viruses by flow cytometry. Appl Environ Microbiol 70:1506–1513. https://doi.org/10.1128/AEM.70.3.1506-1513.2004

257. Manchenko GP (2003) Handbook of Detection of Enzymes on Electrophoretic Gels, CRC Press

258. Cisani G, Varaldo PE, Ingianni A, et al (1984) Inhibition of herpes simplex virus-induced cytopathic effect by modified hen egg-white lysozymes. Current Microbiology 10:35–40. https://doi.org/10.1007/BF01576045

259. Lee-Huang S, Maiorov V, Huang PL, et al (2005) Structural and Functional Modeling of Human Lysozyme Reveals a Unique Nonapeptide, HL9, with Anti-HIV Activity. Biochemistry 44:4648–4655. https://doi.org/10.1021/bi0477081

260. Engle EC, Manes SH, Drlica K (1982) Differential effects of antibiotics inhibiting gyrase. J Bacteriol 149:92–98. https://doi.org/10.1128/jb.149.1.92-98.1982

261. Dar MA, Sharma A, Mondal N, Dhar SK (2007) Molecular Cloning of Apicoplast-Targeted *Plasmodium falciparum* DNA Gyrase Genes: Unique Intrinsic ATPase Activity and ATP-Independent Dimerization of PfGyrB Subunit. Eukaryot Cell 6:398–412. https://doi.org/10.1128/EC.00357-06

262. Mackey BM, Miles CA, Parsons SE, Seymour DA (1991) Thermal denaturation of whole cells and cell components of Escherichia coli examined by differential scanning calorimetry. Journal of General Microbiology 137:2361–2374. https://doi.org/10.1099/00221287-137-10-2361

263. Mastronarde DN (2005) Automated electron microscope tomography using robust prediction of specimen movements. Journal of Structural Biology 152:36–51. https://doi.org/10.1016/j.jsb.2005.07.007

264. Chin C-S, Alexander DH, Marks P, et al (2013) Nonhybrid, finished microbial genome assemblies from long-read SMRT sequencing data. Nat Methods 10:563–569. https://doi.org/10.1038/nmeth.2474

265. Krumsiek J, Arnold R, Rattei T (2007) Gepard: a rapid and sensitive tool for creating dotplots on genome scale. Bioinformatics 23:1026–1028. https://doi.org/10.1093/bioinformatics/btm039

266. Altschul S (1997) Gapped BLAST and PSI-BLAST: a new generation of protein database search programs. Nucleic Acids Research 25:3389–3402. https://doi.org/10.1093/nar/25.17.3389

267. Quast C, Pruesse E, Yilmaz P, et al (2012) The SILVA ribosomal RNA gene database project: improved data processing and web-based tools. Nucleic Acids Research 41:D590–D596. https://doi.org/10.1093/nar/gks1219

268. Buchfink B, Xie C, Huson DH (2015) Fast and sensitive protein alignment using DIAMOND. Nat Methods 12:59–60. https://doi.org/10.1038/nmeth.3176

269. Hyatt D, Chen G-L, LoCascio PF, et al (2010) Prodigal: prokaryotic gene recognition and translation initiation site identification. BMC Bioinformatics 11:119. https://doi.org/10.1186/1471-2105-11-119

270. Aho K, Kajander EO (2003) Pitfalls in Detection of Novel Nanoorganisms. J Clin Microbiol 41:3460–3461. https://doi.org/10.1128/JCM.41.7.3460-3461.2003

271. King AMQ, Lefkowitz EJ, Mushegian AR, et al (2018) Changes to taxonomy and the International Code of Virus Classification and Nomenclature ratified by the International Committee on Taxonomy of Viruses (2018). Arch Virol 163:2601–2631. https://doi.org/10.1007/s00705-018-3847-1

272. Kajander EO, Ciftcioglu N, Aho K, Garcia-Cuerpo E (2003) Characteristics of nanobacteria and their possible role in stone formation. Urol Res 31:47–54. https://doi.org/10.1007/s00240-003-0304-7

273. Griffin S, Masood M, Nasim M, et al (2017) Natural Nanoparticles: A Particular Matter Inspired by Nature. Antioxidants 7:3. https://doi.org/10.3390/antiox7010003

274. Schulz F, Yutin N, Ivanova NN, et al (2017) Giant viruses with an expanded complement of translation system components. Science 356:82–85. https://doi.org/10.1126/science.aal4657

275. Abrahão J, Silva L, Silva LS, et al (2018) Tailed giant Tupanvirus possesses the most complete translational apparatus of the known virosphere. Nat Commun 9:749. https://doi.org/10.1038/s41467-018-03168-1

276. Häring M, Vestergaard G, Rachel R, et al (2005) Independent virus development outside a host. Nature 436:1101–1102. https://doi.org/10.1038/4361101a

277. Prangishvili D, Vestergaard G, Häring M, et al (2006) Structural and Genomic Properties of the Hyperthermophilic Archaeal Virus ATV with an Extracellular Stage of the Reproductive Cycle. Journal of Molecular Biology 359:1203–1216. https://doi.org/10.1016/j.jmb.2006.04.027

278. He L, Han X, Yu Z (2014) A Rare Phaeodactylum tricornutum Cruciform Morphotype: Culture Conditions, Transformation and Unique Fatty Acid Characteristics. PLoS ONE 9:e93922. https://doi.org/10.1371/journal.pone.0093922

279. Diao M, Sinnige R, Kalbitz K, et al (2017) Succession of Bacterial Communities in a Seasonally Stratified Lake with an Anoxic and Sulfidic Hypolimnion. Frontiers in Microbiology 8:2511. https://doi.org/10.3389/fmicb.2017.02511

280. Schindler DE, Scheuerell MD (2002) Habitat coupling in lake ecosystems. Oikos 98:177–189. https://doi.org/10.1034/j.1600-0706.2002.980201.x

281. Tokeshi M, Arakaki S (2012) Habitat complexity in aquatic systems: fractals and beyond. Hydrobiologia 685:27–47. https://doi.org/10.1007/s10750-011-0832-z

282. Takemon Y (1997) Management of Biodiversity in Aquatic Ecosystems: Dynamic Aspects of Habitat Complexity in Stream Ecosystems. In: Abe T, Levin SA, Higashi M (eds) Biodiversity: An Ecological Perspective. Springer, New York, NY, pp 259–275

283. Harvey E, Gounand I, Little CJ, et al (2017) Upstream trophic structure modulates downstream community dynamics via resource subsidies. Ecol Evol 7:5724–5731. https://doi.org/10.1002/ece3.3144

284. Dann LM, Smith RJ, Jeffries TC, et al (2017) Persistence, loss and appearance of bacteria upstream and downstream of a river system. Mar Freshwater Res 68:851. https://doi.org/10.1071/MF16010

285. Cho KH, Pachepsky YA, Oliver DM, et al (2016) Modeling fate and transport of fecally-derived microorganisms at the watershed scale: State of the science and future opportunities. Water Research 100:38–56. https://doi.org/10.1016/j.watres.2016.04.064

286. Baas Becking L, Nicolai E (1934) On the ecology of a Sphagnum bog. Blumea. Biodivers Evol Biogeogr Plants 1:10–45

287. Carlson R, Simpson J (1996) A coordinator's guide to volunteer lake monitoring methods., North American Lake Management Society

288. RE Carlson (1977) A trophic state index for lakes. Limnology and Oceanography 22:361–369

289. Martinet J, Guédant P, Descloux S (2016) Phytoplankton community and trophic status assessment of a newly impounded sub-tropical reservoir: case study of the Nam Theun 2 Reservoir (Lao PDR, Southeast Asia). Hydroécol Appl 19:173–195. https://doi.org/10.1051/hydro/2015006

290. Brussaard CPD (2004) Viral Control of Phytoplankton Populations-a Review1. J Eukaryotic Microbiology 51:125–138. https://doi.org/10.1111/j.1550-7408.2004.tb00537.x

291. Marie D, Rigaut-Jalabert F, Vaulot D (2014) An improved protocol for flow cytometry analysis of phytoplankton cultures and natural samples. Cytometry Part A 85:962–968. https://doi.org/10.1002/cyto.a.22517

292. Istvánovics V (2009) Eutrophication of Lakes and Reservoirs. In: Encyclopedia of Inland Waters. Elsevier, pp 157–165

293. Wu S, Zhou L, Zhou Y, et al (2020) Diverse and unique viruses discovered in the surface water of the East China Sea. BMC Genomics 21:441. https://doi.org/10.1186/s12864-020-06861-y

294. Tilman D (1995) Biodiversity: Population Versus Ecosystem Stability. Ecology 77:350–363. https://doi.org/10.2307/2265614

295. Loreau M (1998) Biodiversity and ecosystem functioning: A mechanistic model. Proc Natl Acad Sci USA 95:5632–5636. https://doi.org/10.1073/pnas.95.10.5632

296. Shade A, Jones SE, McMahon KD (2008) The influence of habitat heterogeneity on freshwater bacterial community composition and dynamics. Environ Microbiol 10:1057–1067. https://doi.org/10.1111/j.1462-2920.2007.01527.x

297. Eiler A, Bertilsson S (2004) Composition of freshwater bacterial communities associated with cyanobacterial blooms in four Swedish lakes. Environ Microbiol 6:1228–1243. https://doi.org/10.1111/j.1462-2920.2004.00657.x

298. Eiler A, Heinrich F, Bertilsson S (2012) Coherent dynamics and association networks among lake bacterioplankton taxa. ISME J 6:330–342. https://doi.org/10.1038/ismej.2011.113

299. Piovia-Scott J, Yang LH, Wright AN (2017) Temporal Variation in Trophic Cascades. Annu Rev Ecol Evol Syst 48:281–300. https://doi.org/10.1146/annurev-ecolsys-121415-032246

300. Fogg GE (1986) Review Lecture - Picoplankton. Proceedings of the Royal Society of London Series B Biological Sciences 228:1–30. https://doi.org/10.1098/rspb.1986.0037

301. Malone TC (1971) The Relative Importance of Nannoplankton and Netplankton as Primary Producers in Tropical Oceanic and Neritic Phytoplankton Communities1. Limnology and Oceanography 16:633–639. https://doi.org/10.4319/lo.1971.16.4.0633

302. Watson S, Kalff J (1981) Relationships between Nannoplankton and Lake Trophic Status. Can J Fish Aquat Sci 38:960–967. https://doi.org/10.1139/f81-129

303. Sime-Ngando T, Colombet J (2009) Virus et prophages dans les écosystèmes aquatiques. Canadian Journal of Microbiology 55:95–109

304. Christaki U, Courties C, Massana R, et al (2011) Optimized routine flow cytometric enumeration of heterotrophic flagellates using SYBR Green I. Limnology and Oceanography: Methods 9:329–339. https://doi.org/10.4319/lom.2011.9.329

305. Klindworth A, Pruesse E, Schweer T, et al (2013) Evaluation of general 16S ribosomal RNA gene PCR primers for classical and next-generation sequencing-based diversity studies. Nucleic Acids Research 41:e1. https://doi.org/10.1093/nar/gks808

306. Wang Y, Qian P-Y (2009) Conservative Fragments in Bacterial 16S rRNA Genes and Primer Design for 16S Ribosomal DNA Amplicons in Metagenomic Studies. PLOS ONE 4:e7401. https://doi.org/10.1371/journal.pone.0007401

307. Ihrmark K, Bödeker ITM, Cruz-Martinez K, et al (2012) New primers to amplify the fungal ITS2 region--evaluation by 454-sequencing of artificial and natural communities. FEMS Microbiol Ecol 82:666–677. https://doi.org/10.1111/j.1574-6941.2012.01437.x

308. Taib N, Mangot J-F, Domaizon I, et al (2013) Phylogenetic Affiliation of SSU rRNA Genes Generated by Massively Parallel Sequencing: New Insights into the Freshwater Protist Diversity. PLOS ONE 8:e58950. https://doi.org/10.1371/journal.pone.0058950

309. Kim M, Morrison M, Yu Z (2011) Evaluation of different partial 16S rRNA gene sequence regions for phylogenetic analysis of microbiomes. J Microbiol Methods 84:81–87. https://doi.org/10.1016/j.mimet.2010.10.020

310. Escudié F, Auer L, Bernard M, et al (2018) FROGS: Find, Rapidly, OTUs with Galaxy Solution. Bioinformatics 34:1287–1294. https://doi.org/10.1093/bioinformatics/btx791

311. Mahé F, Czech L, Stamatakis A, et al (2022) Swarm v3: towards tera-scale amplicon clustering. Bioinformatics 38:267–269. https://doi.org/10.1093/bioinformatics/btab493

312. Olejnik S, Algina J (2000) Measures of Effect Size for Comparative Studies: Applications, Interpretations, and Limitations. Contemporary Educational Psychology 25:241–286. https://doi.org/10.1006/ceps.2000.1040

313. Lymer D, Logue JB, Brussaard CPD, et al (2008) Temporal variation in freshwater viral and bacterial community composition. Freshwater Biology 53:1163–1175. https://doi.org/10.1111/j.1365-2427.2007.01882.x

314. Yannarell AC, Triplett EW (2005) Geographic and Environmental Sources of Variation in Lake Bacterial Community Composition. Applied and Environmental Microbiology 71:227–239. https://doi.org/10.1128/AEM.71.1.227-239.2005

315. Muylaert K, Van der Gucht K, Vloemans N, et al (2002) Relationship between Bacterial Community Composition and Bottom-Up versus Top-Down Variables in Four Eutrophic Shallow Lakes. Applied and Environmental Microbiology 68:4740–4750. https://doi.org/10.1128/AEM.68.10.4740-4750.2002

316. Tijdens M, Hoogveld HL, Kamst-van Agterveld MP, et al (2008) Population Dynamics and Diversity of Viruses, Bacteria and Phytoplankton in a Shallow Eutrophic Lake. Microb Ecol 56:29–42. https://doi.org/10.1007/s00248-007-9321-3

317. Jones EBG, Suetrong S, Sakayaroj J, et al (2015) Classification of marine Ascomycota, Basidiomycota, Blastocladiomycota and Chytridiomycota. Fungal Diversity 73:1–72. https://doi.org/10.1007/s13225-015-0339-4

318. Jobard M, Rasconi S, Sime-Ngando T (2010) Diversity and functions of microscopic fungi: a missing component in pelagic food webs. Aquat Sci 72:255–268. https://doi.org/10.1007/s00027-010-0133-z

319. Gleason FH, Kagami M, Lefevre E, Sime-Ngando T (2008) The ecology of chytrids in aquatic ecosystems: roles in food web dynamics. Fungal Biology Reviews 22:17–25. https://doi.org/10.1016/j.fbr.2008.02.001

320. Newton RJ, Jones SE, Eiler A, et al (2011) A Guide to the Natural History of Freshwater Lake Bacteria. Microbiology and Molecular Biology Reviews 75:14–49. https://doi.org/10.1128/MMBR.00028-10

321. Fahnenstiel GL, Sicko-Goad L, Scavia D, Stoermer EF (1986) Importance of Picoplankton in Lake Superior. Can J Fish Aquat Sci 43:235–240. https://doi.org/10.1139/f86-028

322. Jardillier L, Boucher D, Personnic S, et al (2005) Relative importance of nutrients and mortality factors on prokaryotic community composition in two lakes of different trophic status: Microcosm experiments. FEMS Microbiology Ecology 53:429–443. https://doi.org/10.1016/j.femsec.2005.01.011

323. Hugoni M (2013) Structure et activité des Archaea planctoniques dans les écosystèmes aquatiques. Université Blaise Pascal

324. Fuster M, Billard H, Bronner G, et al (2022) Occurrence and Seasonal Dynamics of ALNs in Freshwater Lakes Are Influenced by Their Biological Environment. Microb Ecol. https://doi.org/10.1007/s00248-022-01974-1

325. Grossart H, Massana R, McMahon KD, Walsh DA (2020) Linking metagenomics to aquatic microbial ecology and biogeochemical cycles. Limnol Oceanogr 65:. https://doi.org/10.1002/lno.11382

326. Tran PQ, Bachand SC, McIntyre PB, et al (2021) Depth-discrete metagenomics reveals the roles of microbes in biogeochemical cycling in the tropical freshwater Lake Tanganyika. ISME J 15:1971–1986. https://doi.org/10.1038/s41396-021-00898-x

327. Danczak RE, Johnston MD, Kenah C, et al (2017) Members of the Candidate Phyla Radiation are functionally differentiated by carbon- and nitrogen-cycling capabilities. Microbiome 5:112. https://doi.org/10.1186/s40168-017-0331-1

328. Anantharaman K, Brown CT, Burstein D, et al (2016) Analysis of five complete genome sequences for members of the class Peribacteria in the recently recognized Peregrinibacteria bacterial phylum. PeerJ 4:e1607. https://doi.org/10.7717/peerj.1607

329. Yuan Y, Gao M (2017) Jumbo Bacteriophages: An Overview. Front Microbiol 8:. https://doi.org/10.3389/fmicb.2017.00403

330. Boedeker C, Schüler M, Reintjes G, et al (2017) Determining the bacterial cell biology of Planctomycetes. Nat Commun 8:14853. https://doi.org/10.1038/ncomms14853

331. Jogler C, Glöckner FO, Kolter R (2011) Characterization of Planctomyces limnophilus and Development of Genetic Tools for Its Manipulation Establish It as a Model Species for the Phylum Planctomycetes. Appl Environ Microbiol 77:5826–5829. https://doi.org/10.1128/AEM.05132-11

332. Wiegand S, Jogler M, Jogler C (2018) On the maverick Planctomycetes. FEMS Microbiology Reviews 42:739–760. https://doi.org/10.1093/femsre/fuy029

333. Andrei A-Ş, Salcher MM, Mehrshad M, et al (2019) Niche-directed evolution modulates genome architecture in freshwater Planctomycetes. ISME J 13:1056–1071. https://doi.org/10.1038/s41396-018-0332-5

334. He X, McLean JS, Edlund A, et al (2015) Cultivation of a human-associated TM7 phylotype reveals a reduced genome and epibiotic parasitic lifestyle. Proc Natl Acad Sci USA 112:244–249. https://doi.org/10.1073/pnas.1419038112

335. Paez-Espino D, Sharon I, Morovic W, et al (2015) CRISPR Immunity Drives Rapid Phage Genome Evolution in Streptococcus thermophilus. mBio 6:e00262-15. https://doi.org/10.1128/mBio.00262-15

336. Downing JA, Watson SB, McCauley E (2001) Predicting Cyanobacteria dominance in lakes. Can J Fish Aquat Sci 58:1905–1908. https://doi.org/10.1139/f01-143

337. Tournié T, Lasserre P (1984) Microcalorimetric characterization of seasonal metabolic trends in marine microcosms. Journal of Experimental Marine Biology and Ecology 74:111–121. https://doi.org/10.1016/0022-0981(84)90080-7

338. Lasserre P, Tournié T (1984) Use of microcalorimetry for the characterization of marine metabolic activity at the water-sediment interface. Journal of Experimental Marine Biology and Ecology 74:123–139. https://doi.org/10.1016/0022-0981(84)90081-9

339. Naiman RJ, Melillo JM, Lock MA, et al (1987) Longitudinal Patterns of Ecosystem Processes and Community Structure in a Subarctic River Continuum. Ecology 68:1139–1156. https://doi.org/10.2307/1939199

340. Gustafsson L (1991) Microbiological calorimetry. Thermochimica Acta 193:145–171. https://doi.org/10.1016/0040-6031(91)80181-H

341. Ruiz T, Bec A, Danger M, et al (2018) A microcalorimetric approach for investigating stoichiometric constraints on the standard metabolic rate of a small invertebrate. Ecol Lett 21:1714–1722. https://doi.org/10.1111/ele.13137

342. Lemasson L, Pages J (1983) Utilisation de La méthode d'analyse par spectrométrie d'émission pour La détermination de 15N en écologie aquatique: Assimilation du nitrate par le phytoplancton en Mer de Banda (Indonésie). Journal of Experimental Marine Biology and Ecology 67:33–42. https://doi.org/10.1016/0022-0981(83)90133-8

343. Servais P, Becquevort S, Vandevelde F (2005) Comparaison de deux méthodes d'estimation du broutage des bactéries par les protozoaires en milieux aquatiques [Courte note]. rseau 11:631–639. https://doi.org/10.7202/705325ar

344. Perga M-E, Kainz M, Mazumder A (2008) Terrestrial carbon contribution to lake food webs: could the classical stable isotope approach be misleading? Can J Fish Aquat Sci 65:2719–2727. https://doi.org/10.1139/F08-172

Résumé

Face au changement global et notamment à l'augmentation de la température des eaux de surface (Whitehead *et al.*, 2009), il est devenu indispensable de comprendre et d'anticiper l'évolution des écosystèmes aquatiques. Le bon fonctionnement et l'évolution de ces écosystèmes ont toujours été intimement liés au fonctionnement du compartiment biologique et notamment microbien (Lalli and Parsons, 1997). Les avancées technologiques des dernières décennies ont permis de mettre en évidence un véritable réseau d'interactions microbiennes (Pomeroy *et al.,* 2007), intégrant une diversité jusqu'alors insoupçonnée d'entités sub-micrométriques pouvant avoir une importance fonctionnelle majeure (Mostajir *et al.,* 2012). Pour comprendre le fonctionnement global des écosystèmes aquatiques, il semble donc nécessaire de concentrer des efforts de recherche sur les plus petites fractions de taille, notamment sur les particules nanoplanctoniques appartenant au femtoplancton jusqu'alors sous-considérées (< 0.2 µm ou 200 nm).

Dans ce contexte, la découverte d'une nouvelle catégorie de particules organiques appartenant au femtoplancton, nommées « *Aster Like Nanoparticles* » (ALNs) (Colombet *et al.,* 2019), soulève de nombreuses questions et notamment celle de leur importance fonctionnelle au sein des écosystèmes aquatiques. L'objectif principal de cette thèse est donc d'approfondir nos connaissances sur les fonctionnalités des ALNs, en se focalisant particulièrement sur l'étude écologique de ces entités afin de pouvoir, à terme, expliquer leur présence et appréhender leurs interactions avec leur environnement physico-chimique et microbien. Pour cela, différentes échelles d'intégration seront considérées : de l'échelle écosystémique à l'échelle expérimentale, en conditions contrôlées.

Nos résultats ont, dans un premier temps, permis de mettre en évidence la présence des ALNs dans un large spectre d'habitats aux caractéristiques différentes (Fuster *et al.,* 2020). Ces résultats ont permis de prouver l'ubiquité des ALNs, capables de se développer dans des environnements physico-chimiques variés. Une étude complémentaire a permis de dresser la dynamique temporelle des ALNs dans différents écosystèmes aquatiques, suggérant que les ALNs sont un acteur majeur à intégrer dans les modèles de successions écologiques (Fuster *et al.,* 2022). Cette étude, menée dans trois lacs du Puy-de-Dôme, a permis de démontrer l'importance des paramètres biologiques dans la distribution des ALNs, et notamment l'importance potentielle des procaryotes. Finalement, des études en microcosmes ont permis de confirmer l'importance des procaryotes, avec des résultats montrant un développement jusqu'à 20 fois plus important des ALNs en présence d'une forte concentration de procaryotes. De façon générale, nos résultats ont démontré l'importance des ALNs en tant que nouveaux acteurs dans les écosystèmes aquatiques, d'une part par leur dynamique écosystémique marquée et, d'autre part, par leurs interactions avec les procaryotes, principaux régulateurs des flux de matière et d'énergie. Les ALNs sont donc de nouvelles entités planctoniques qu'il faudra désormais prendre en compte dans l'étude des écosystèmes aquatiques. Enfin, l'ensemble de nos résultats soulève des perspectives de recherche sur la nature et l'écologie des ALNs et leur place dans les schémas évolutifs du monde organique.